

REGULATION OF SNARE-DEPENDENT FUSION IN AN *IN VITRO* SYSTEM

A thesis submitted to the
FACULTY OF BIOMEDICAL AND LIFE SCIENCES

For the degree of
DOCTOR OF PHILOSOPHY

By

Veronica Aran-Ponte

Division of Biochemistry and Molecular Biology
Institute of Biomedical and Life Sciences
University of Glasgow
February 2009

Abstract

Glucose homeostasis depends on the ability of insulin to stimulate glucose uptake into both muscle and adipose tissue by promoting the translocation of glucose transporters (GLUT4) from intracellular sites to the plasma membrane (PM). In individuals with Type 2 diabetes the ability of insulin to stimulate glucose transport is impaired. The incidence of Type 2 diabetes is increasing worldwide, highlighting the need to understand the molecular basis of insulin-stimulated glucose uptake. GLUT4 translocation is a specialised example of vesicular trafficking.

Within the context of vesicle trafficking, all eukaryotic cells contain a common set of conserved components responsible for the execution of membrane fusion. Central to this machinery are members of the SNARE (soluble NSF attachment protein receptor) family of proteins. The process of SNARE-mediated membrane fusion needs to be tightly regulated and the SNARE proteins are partially responsible for the specificity in communication between eukaryotic subcellular organelles. Other proteins such as the Sec1p/ Munc18 (SM) proteins were shown to be essential for SNARE-mediated membrane fusion. Several methods were used to test the ability of SNARE proteins to drive membrane fusion, and one of the most important methods described to date is the *in vitro* fusion assay used in this study.

The first topic addressed in this thesis was related to the molecular interactions between the regulatory SM protein Munc18c and the SNARE proteins VAMP2 and syntaxin 4. The use of pull-down assays revealed the novel fact that Munc18c interacts not only with the t-SNARE syntaxin 4 but also with the v-SNARE VAMP2 *via* its SNARE motif. The SM:v-SNARE interaction was disrupted by the presence of syntaxin 4 revealing that these two SNARE proteins compete for binding to Munc18c. Next, the role of Munc18c in membrane fusion driven by four different versions of syntaxin 4 plus SNAP23 and VAMP2 liposomes, was investigated using the well-characterised *in vitro* fusion assay. Results suggested that Munc18c negatively regulates SNARE-mediated membrane fusion by inhibiting the formation of SNARE complexes. Interestingly, deletion of the first 36 amino acids of syntaxin 4 was not sufficient to suppress Munc18c negative regulation of fusion indicating that this inhibition might involve other interactions apart from the short N-terminal peptide of syntaxin 4. Finally, the role of phosphorylation in SNARE complex formation was assessed using several techniques such as site-directed mutagenesis, pull-down assays and radiolabelling studies. Data obtained revealed that both syntaxin 4 and

Munc18c become phosphorylated *in vitro* by a recombinant cytoplasmic insulin receptor kinase (CIRK). Munc18c phosphorylated by CIRK was unable to bind syntaxin 4 *in vitro*. Furthermore, phosphomimetic mutations were also introduced on both proteins and pull-down assays indicated that phosphorylated Munc18c is unable to interact with both syntaxin 4 and VAMP2, whereas phosphomimetic mutations in syntaxin 4 did not affect the interaction with its cognate SNARE proteins and Munc18c. These results were very useful to further understand and confirm the importance of phosphorylation in SNARE complex formation.

Collectively, these data suggest that Munc18c acts through different modes of interaction with its cognate SNARE proteins, and support a model in which Munc18c negatively regulates SNARE complex formation. However, this regulation might also be dependent on other factors such as phosphorylation upon insulin signalling.

Table of Contents

Abstract	2
Abbreviations	13
Chapter 1	18
1 Introduction	18
1.1 The importance of membrane trafficking	19
1.1.1 The secretory and endocytic pathways	19
1.1.2 Membrane fusion.....	20
1.2 SNARE proteins	21
1.2.1 Syntaxins	22
1.2.2 SNAP25 family	23
1.2.3 VAMP family	24
1.2.4 The SNARE hypothesis	24
1.2.5 Common structural features of SNARE proteins	25
1.2.6 Classification of SNAREs.....	26
1.2.7 The different locations of SNARE proteins	27
1.2.8 SNAREs: The minimal machinery for fusion	28
1.2.9 SNARE-mediated membrane fusion regulation.....	32
1.3 Glucose transport.....	38
1.3.1 Types of glucose transporters.....	38
1.3.2 GLUT4.....	39
1.3.3 Insulin action and GLUT4 trafficking	39
1.3.4 SNARE-mediated GLUT4 fusion with the plasma membrane.....	42
1.3.5 Regulation of GLUT4 fusion	44
1.3.6 Diabetes.....	48
1.3.7 Relationship between GLUT4 trafficking and Diabetes.....	49
1.4 Aims of this thesis	50
Chapter 2	51
2 Materials and Methods	51
2.1 Materials	52
2.1.1 <i>Escherichia coli</i> (<i>E. coli</i>) strains	56
2.1.2 Primary antibodies	56
2.1.3 General solutions	57
2.2 Methods	58
2.2.1 Molecular Biology.....	58
2.2.2 Biochemical Methods	64
2.2.3 <i>In vitro</i> fusion studies	68
2.2.4 M18c protein purification	72
2.2.5 Cytoplasmic Insulin Receptor (tyrosine) Kinase - “CIRK”	73
2.2.6 Immunoprecipitation using anti-phosphotyrosine agarose	74
Chapter 3	76
3 <i>In vitro</i> studies of Munc18c binding modes to cognate SNARE proteins	76
3.1 Introduction.....	77
3.2 Aims of this chapter	78
3.3 Results	78
3.3.1 M18c interaction with non-syntaxin SNAREs.....	78
3.3.2 M18c interacts with the SNARE motif of VAMP2.....	80
3.3.3 GST-Sx 4 displaces GST-VAMP2 from His ₆ -M18c in a dose dependent manner	81

3.3.4	GST-VAMP2 is not able to displace GST-Sx 4 from His ₆ -M18c	83
3.3.5	The importance of the GST tags present in both VAMP2 and Sx 4 in the competing assay results	84
3.3.6	M18c and Sx 4 different modes of interaction	86
3.4	Discussion	91
Chapter 4.....		94
4	Negative regulation of Sx 4/SNAP23/VAMP2-mediated fusion by Munc18c <i>in vitro</i>	94
4.1	Introduction.....	95
4.1.1	The N-terminal domain of Sx 4.....	96
4.2	Aims of this chapter	100
4.3	Results	100
4.3.1	Expression and purification of t-SNARE complexes	100
4.3.2	Reconstitution of recombinant t-SNAREs into liposomes	105
4.3.3	VAMP2 expression, purification and reconstitution into liposomes.....	109
4.3.4	<i>In vitro</i> fusion assays using reconstituted liposomes.....	110
4.3.5	Effects of the addition of M18c directly into the <i>in vitro</i> fusion assay	115
4.4	Discussion.....	135
Chapter 5.....		137
5	The consequences of Syntaxin 4 and Munc18c phosphorylation on the regulation of SNARE complex formation	137
5.1	Introduction.....	138
5.2	Aims of this chapter	139
5.3	Results	140
5.3.1	Sx 4 phosphomimetic mutants	140
5.3.2	Munc18c phosphomimetic mutant Y521E	149
5.3.3	The Recombinant Cytoplasmic Insulin Receptor Kinase (CIRK)	158
5.3.4	Phosphorylation of endogenous M18c in response to insulin.....	170
5.4	Discussion.....	172
Chapter 6.....		177
6	Discussion	177
Appendix.....		185
Supplementary figures for chapter 4:.....		185
Supplementary figures for chapter 5:.....		199
References.....		203
Publications.....		215

List of Figures

Chapter 1

Figure 1.1 The secretory and endocytic pathways	20
Figure 1.2 Model of the OPEN and CLOSED conformation of syntaxins	23
Figure 1.3 Schematic representation of the SNARE hypothesis	25
Figure 1.4 General comparison between domains of different SNARE proteins	26
Figure 1.5 The different locations of mammalian SNAREs within the cell	28
Figure 1.6 Hypothetical model of the SNARE core complex.....	30
Figure 1.7 Ribon representation of M18a, Sx 1A and the complex formed by them.....	34
Figure 1.8 Diagram of the GLUT protein family	38
Figure 1.9 Schematic model of both PI3K dependent and independent pathways	42

Chapter 3

Figure 3.1 M18c interacts specifically with the non-syntaxin SNARE VAMP2.....	79
Figure 3.2 His ₆ -M18c binds the SNARE motif of GST-VAMP2	81
Figure 3.3 GST- Sx 4 displaces GST-VAMP2 from His ₆ -M18c.	82
Figure 3.4 GST-VAMP2 is not able to displace GST-Sx 4 from His ₆ -M18c.....	83
Figure 3.5 Untagged versions of both VAMP2 and Sx 4, when used in the competition experiments, give the same results as their tagged versions	85
Figure 3.6 CLUSTALW multiple sequence alignment between Vps45p and M18c	87
Figure 3.7 SDS-PAGE analysis of His ₆ -M18cF119A protein purification	88
Figure 3.8 A hydrophobic pocket mutation in His ₆ -M18c disrupts its binding to SNARE proteins <i>in vitro</i>	90

Chapter 4

Figure 4.1 The predicted two modes of interaction between M18c and Sx 4.....	97
Figure 4.2 Quantifications of the amount of M18c bound to either N- (A) or C-tagged versions (B) of cytosolic Sx 4 (Figure taken from Dr Fiona Brandie, University of Glasgow)	99
Figure 4.3 Purified Sx 4/SNAP23 t-SNARE complex from <i>E.coli</i> lysates	101
Figure 4.4 Purification of Sx 4 NΔ36/SNAP23 complex from <i>E.coli</i>	102

Figure 4.5 Purification of Sx 4 OPEN NΔ36/SNAP23 complex from <i>E.coli</i>	103
Figure 4.6 Purification of Sx 4 OPEN/SNAP23 complex from <i>E.coli</i>	104
Figure 4.7 Schematic representation of the different Sx 4 constructs used in this study.	105
Figure 4.8 Schematic representation of the incorporation of SNARE proteins into liposomes (kindly given by Prof James A. McNew, Rice University).....	107
Figure 4.9 Reconstitution of recombinant SNAREs into liposomes	108
Figure 4.10 Purification and reconstitution of VAMP2 into liposomes	109
Figure 4.11 Fusion assay model (Prof James A. McNew, Rice University, USA).....	111
Figure 4.12 <i>In vitro</i> fusion assays of liposomes containing either full-length Sx 4/SNAP23 (A) or Sx 4 NΔ36/SNAP23 (B) or Sx 4 OPEN/SNAP23 (C) or Sx 4 OPEN NΔ36/SNAP23 (D) with liposomes containing VAMP2	114
Figure 4.13 His ₆ -M18c protein purification.....	116
Figure 4.14 His ₆ -M18c inhibits SNARE-mediated membrane fusion <i>in vitro</i> in a dose dependent manner.....	119
Figure 4.15 Proteoliposomes used for fusion assays with M18c	120
Figure 4.16 <i>In vitro</i> fusion of wild-type Sx 4/SNAP23 with VAMP2 vesicles (pre-docked or not) in the presence and in the absence of His ₆ -M18c	123
Figure 4.17 <i>In vitro</i> fusion of Sx 4 NΔ36/SNAP23 with VAMP2 vesicles (pre-docked overnight or not) in the presence and in the absence of His ₆ -M18c.....	125
Figure 4.18 <i>In vitro</i> fusion of Sx 4 NΔ36/SNAP23 liposomes with VAMP2 liposomes (pre-docked or not) in the presence or in the absence of His ₆ -M18c for 2 h.....	127
Figure 4.19 <i>In vitro</i> fusion of Sx 4 OPEN/SNAP23 with VAMP2 vesicles (pre-docked overnight or not) in the presence and in the absence of M18c.....	129
Figure 4.20 <i>In vitro</i> fusion of Sx 4 OPEN NΔ36/SNAP23 with VAMP2 vesicles (pre-docked overnight and not docked) in the presence and in the absence of M18c	131
Figure 4.21 <i>In vitro</i> fusion of Sx 4 OPEN NΔ36/SNAP23 with VAMP2 vesicles (pre-docked overnight or not) in the presence and in the absence of M18c for 2 h	133
Figure 4.22 Quantifications of the percentages of fusion inhibited by M18c when added at the same time as the SNARE liposomes or added after pre-incubation of SNAREs	134

Chapter 5

Figure 5.1 Purification of Sx 4 phosphomimetic mutants	142
Figure 5.2 Far UV CD spectra of the cytosolic domains of wild-type Sx 4, Y115E, Y251E and Y115E/Y251E.....	144
Figure 5.3 Near UV CD spectra of wild-type GST-Sx 4 and Sx 4 Y115E, Sx4 Y251E, and Y115E/Y251E	145
Figure 5.4 Binding of His ₆ -M18c to GST-Sx 4 wild-type (WT), Sx 4 Y115E, Sx 4 Y251E and Sx 4Y115E/Y251E.....	146
Figure 5.5 Binding of His ₆ -SNAP23 to GST-Sx 4 wild-type (WT), Sx 4 Y115E, Sx 4 Y251E and Sx 4 Y115E/Y251E.....	148
Figure 5.6 M18cY521E protein purification.....	150
Figure 5.7 Comparison between wild-type M18c and M18cY521E.....	151
Figure 5.8 Far UV CD spectra of wild-type M18c (blue) and mutant M18cY521E (red).....	152
Figure 5.9 Tryptophan fluorescence spectra of His ₆ -M18c and His ₆ -M18c Y521E.....	154
Figure 5.10 Pull-down assay of the different versions of cytosolic GST-Sx4 with both wild-type His ₆ - M18c and His ₆ -M18cY521E	155
Figure 5.11 GST pull-down of GST-VAMP2 and His ₆ - M18cY521E.....	157
Figure 5.12 SDS-PAGE analysis of recombinant CIRK	159
Figure 5.13 Autoradiography studies using M18c and Sx 4/SNAP23 complex which were pre-incubated with CIRK	160
Figure 5.14 M18c and Sx 4 phosphorylation by CIRK	161
Figure 5.15 M18c phosphorylation by CIRK using different amounts of CIRK and different times of incubation	163
Figure 5.16 M18c phosphorylated by CIRK loses affinity for Sx 4 <i>in vitro</i>	166
Figure 5.17 Pull-down assay of GST- VAMP2 and M18c phosphorylated by CIRK	167
Figure 5.18 Negative-ion ESI-MS of phosphorylated M18c.....	169
Figure 5.19 Negative-ion ESI-MS of non-phosphorylated M18c.....	170
Figure 5.20 Endogenous M18c undergoes insulin-stimulated tyrosine phosphorylation.....	171

Appendix

Figure I (chapter 4, figure 4.12) Raw fluorescence data from <i>in vitro</i> fusion assays of liposomes containing either full-length Sx 4/SNAP23 (A) or Sx 4 NΔ36/SNAP23 (B) or Sx 4 OPEN/SNAP23 (C) or Sx 4 OPEN NΔ36/SNAP23 (D) with liposomes containing VAMP2	187
Figure II (chapter 4, figure 4.16) Raw fluorescence data from <i>in vitro</i> fusion of wild-type Sx 4/SNAP23 with VAMP2 vesicles (pre-docked and not docked) in the presence and in the absence of His ₆ -M18c	189
Figure III (chapter 4, figure 4.17) Raw fluorescence data from <i>in vitro</i> fusion of Sx 4 NΔ36/SNAP23 with VAMP2 vesicles (pre-docked overnight or not) in the presence and in the absence of His ₆ -M18c	191
Figure IV (chapter 4, figure 4.18) Raw fluorescence data from <i>in vitro</i> fusion of Sx 4 NΔ36/SNAP23 liposomes with VAMP2 liposomes (pre-docked or not) in the presence or in the absence of His ₆ -M18c for only 2 h	193
Figure V (chapter 4, figure 4.19) Raw fluorescence data from <i>in vitro</i> fusion of Sx 4 OPEN/SNAP23 with VAMP2 vesicles (pre-docked overnight and not docked) in the presence and in the absence of M18c	195
Figure VI (chapter 4, figure 4.20) Raw fluorescence data <i>in vitro</i> fusion of Sx 4 OPEN NΔ36/SNAP23 with VAMP2 vesicles (pre-docked overnight and not docked) in the presence and in the absence of M18c	197
Figure VII (chapter 4, figure 4.21) Raw fluorescent data from <i>in vitro</i> fusion of Sx 4 OPEN NΔ36/SNAP23 with VAMP2 vesicles (pre-docked overnight or not) in the presence and in the absence of M18c for 2 h.....	199
Figure VIII Positive-ion ESI-MS/MS of Peptide 1 (residues Thr 519- Arg 526).....	199
Figure IX Positive-ion ESI-MS/MS spectrum of the phosphorylated peptide 2 (residues Thr 519-Lys 527) of M18c.....	200
Figure X Sequences of the phosphorylated tryptic peptides 1 and 2 from M18c	201

Acknowledgements

There are a number of people I would like to thank for helping me to make this project possible. Firstly, I am very thankful to my supervisor Prof Gwyn W Gould, for being a great supervisor, always willing to help and encourage me throughout my studies. I will always be grateful for the opportunity to work in his lab. Secondly, thanks to Diabetes UK for funding this project. I would also like to thank collaborator Dr Nia Bryant for her scientific advice and for always being helpful and friendly (and of course, for saving my overnight cultures from death!).

I would like to thank everybody in lab 241 (past and present) for their moral support, friendship and happy tea breaks. Special thanks to Dr Scott Shanks, Dr Lindsay Carpp and Dr Amber Yu for technical advice and friendship. Thanks to Dr Fiona Brandie for introducing me into the world of *in vitro* fusion assays, for her technical advice and collaboration. Special thanks to best pals Marion Struthers and Dr Becky McCann for being such wonderful friends and trip companions (we will always be the three musketeers☺). Thanks to “curly” Chris, for being so kind in helping me with the French press torture machine! Thanks to Clare Miller for informing me of the latest football scores and for being so friendly. Thanks to Dr Ian Salt for his help and comments on this thesis. Thanks must also go to, Dr Sharon Kelly and Prof James Milner-White for their assistance with CD analysis and modelling studies.

Outside the lab I would like to thank my friends from all over the world for making my life so special and for listening to my moans on the phone. I specially thank Alvaro for all his moral support, patience, invaluable scientific advice and love. And finally, I don't have enough words to thank my family for always believing in me and giving me support to achieve my goals in life.

Muito Obrigada, Muchas Gracias, Thank you very much!!!

Dedication

To Mum: the most intelligent, loving and brave woman I have ever met in my life
To my brother Jose Carlos for all his love and support
In memory of Dad

Declaration

I declare that the work presented in this thesis has been carried out by myself, unless otherwise stated. It is entirely of my own composition and has not, in whole or in part, been submitted for any other degree.

Veronica Aran-Ponte

February 2009

Abbreviations

AEBSF	4-(2-Aminoethyl)benzenesulphonyl fluoride
APS	Ammonium persulfate
ADP	Adenosine diphosphate
Amp	Ampicillin
ATP	Adenosine 5'-triphosphate
~	Approximately
β -cell	Beta cell
bp	Base pairs
DMSO	Dimethylsulphoxide
DNA	Deoxyribonucleic acid
DNase	Deoxyribonuclease
dNTP	Deoxynucleoside (5')-triphosphate
DOPS	1,2-dioleoyl phosphatidylserine
DTT	Dithiothreitol
<i>E. coli</i>	<i>Escherichia coli</i>
ECL	Enhanced chemiluminescence
EDTA	Ethylenediaminetetraacetic acid
ER	Endoplasmic reticulum

g	Gram
<i>g</i>	Gravitational force
GDP	Guanosine diphosphate
GLUT	Glucose transporter
GST	Glutathione S-transferase
GSV	GLUT4 storage vesicle
GTP	Guanosine-5'-triphosphate
h	Hour
HAc	Acetic acid
HCl	Hydrochloric acid
HEPES	2-[4-(2-Hydroxyethyl)-1-piperazine]ethanesulfonic acid
His ₆	six-histidine residue tag
HRP	Horseradish peroxidase
IgG	Immunoglobulin G
IP	Immunoprecipitation
IPTG	Isopropyl- β -D-Thiogalactopyranoside
IRS	Insulin receptor substrate
L	Litre
μ	Micro

Kan	Kanamycin
kb	Kilobase
kDa	Kilodalton
M	Molar
mA	Milliamp
mg	Milligram
ml	Millilitre
min	Minute(s)
M18c	Munc18c
MWCO	Molecular Weight Cut-Off
n	Nano
NBD-DPPE	(N-(7-nitro-2,1,3-benzoxadiazol-4-yl)-1,2-dipalmitoyl phosphatidylethanolamine
NSF	N-ethylmaleimide sensitive factor
Ni-NTA	Nickel-nitrilotriacetic acid
OD ₆₀₀	Optical density at 600 nm
OG	n-octyl- β -D-glucopyranoside
KOAc	Potassium acetate
KOH	Potassium hydroxide
PAGE	Polyacrylamide gel electrophoresis

PBS	Phosphate buffered saline
PBS-T	0.1 % Tween-20 in PBS
PCR	Polymerase chain reaction
<i>Pfu</i>	<i>Pyrococcus furiosus</i>
PH	Pleckstrin homology domain
PI3K	Phosphatidylinositol 3-kinase
PIP ₂	Phosphatidylinositol 4,5-bisphosphate
PIP ₃	Phosphatidylinositol 3,4,5-triphosphate
PKB	Protein kinase B
PKC	Protein kinase C
PM	Plasma membrane
PMSF	Phenylmethylsulfonyl fluoride
POPC	Palmitoyl oleoyl phosphatidyl choline
PrA	Protein A
Rhodamine-DPPE	N-(Lissamine rhodamine B sulfonyl)-1,2-dipalmitoyl phosphatidylethanolamine
rpm	Rotations per minute
<i>S. cerevisiae</i>	<i>Saccharomyces cerevisiae</i>
SDS	Sodium dodecyl sulfate
SDS-PAGE	Sodium dodecyl sulfate polyacrylamide gel electrophoresis

SM	<u>Sec1/Munc18</u>
SNAP	Soluble NSF attachment protein
SNAP25	25 kDa synaptosome-associated protein
SNAP23	23 kDa synaptosome-associated protein
SNARE	soluble NSF attachment protein receptor
Sx 4	Syntaxin 4
TAE	Tris-acetate EDTA
<i>Taq</i>	<i>Thermus aquaticus</i>
TEM	Transmission Electron Microscopy
TEMED	N, N, N', N' , - tetramethyl ethylene diamine
Tris	2-Amino-2-(hydroxymethyl)-1,3-propanediol
t-SNARE	target SNARE
TGN	<i>Trans</i> -Golgi network
Tris	Tris(hydroxymethyl)aminoethane
Tween 20	Polyoxyethylene sorbitan monolaurate
VAMP	Vesicle associated membrane protein
v/v	volume/volume ratio
v-SNARE	vesicle SNARE
w/v	weight/volume ratio

Chapter 1

1 Introduction

1.1 The importance of membrane trafficking

The plasma membrane (PM) is a structured bilayer of phospholipids, cholesterol and protein molecules which serves as a barrier between the cell and the extracellular environment. The selective permeability of the membrane allows only lipophilic molecules in or out of the cell. Other molecules can only cross the cell membrane if specific transporters are involved. This process allows the PM to maintain a stable internal environment.

Eukaryotic cells are compartmentalised into different membrane-bound organelles containing specific proteins and lipids. In order to maintain homeostasis of these organelles, membrane trafficking is essential. Cells require two main trafficking pathways to maintain cellular integrity: the secretory and endocytic pathways.

1.1.1 The secretory and endocytic pathways

More than 30 years ago, it was demonstrated that newly synthesised secretory proteins pass through several membrane-enclosed organelles such as the endoplasmic reticulum (ER), the Golgi complex, and secretory granules on their way to the PM where vesicles finally fuse releasing their contents extracellularly (Palade, 1975). This process corresponds to the secretory pathway, which is also known as exocytosis. There are two types of secretory pathway: constitutive and regulated. The first pathway delivers proteins to the PM from the Golgi apparatus. In the second pathway, both soluble and integral membrane proteins are initially stored in secretory vesicles for later release. These vesicles accumulate at the target membrane in preparation for fusion, until triggered to fuse in response to extracellular signals. This regulated exocytic pathway is found mainly in cells specialised for secreting products such as hormones, neurotransmitters, or digestive enzymes (van Vliet *et al.*, 2003).

In the endocytic pathway, defined regions of the PM invaginate to form endocytic vesicles, which pinch off to form intracellular vesicles, so allowing molecules to be internalised and then transported to the early endosome where sorting occurs. Many of the endocytosed molecules end up in lysosomes, where they are degraded. Endocytosed molecules can also be recycled to the PM (*e.g.* recycling receptors) or transported to the *Trans*-Golgi network (TGN) *via* the late endosomes (van Vliet *et al.*, 2003). Figure 1.1 summarises the secretory and endocytic pathways.

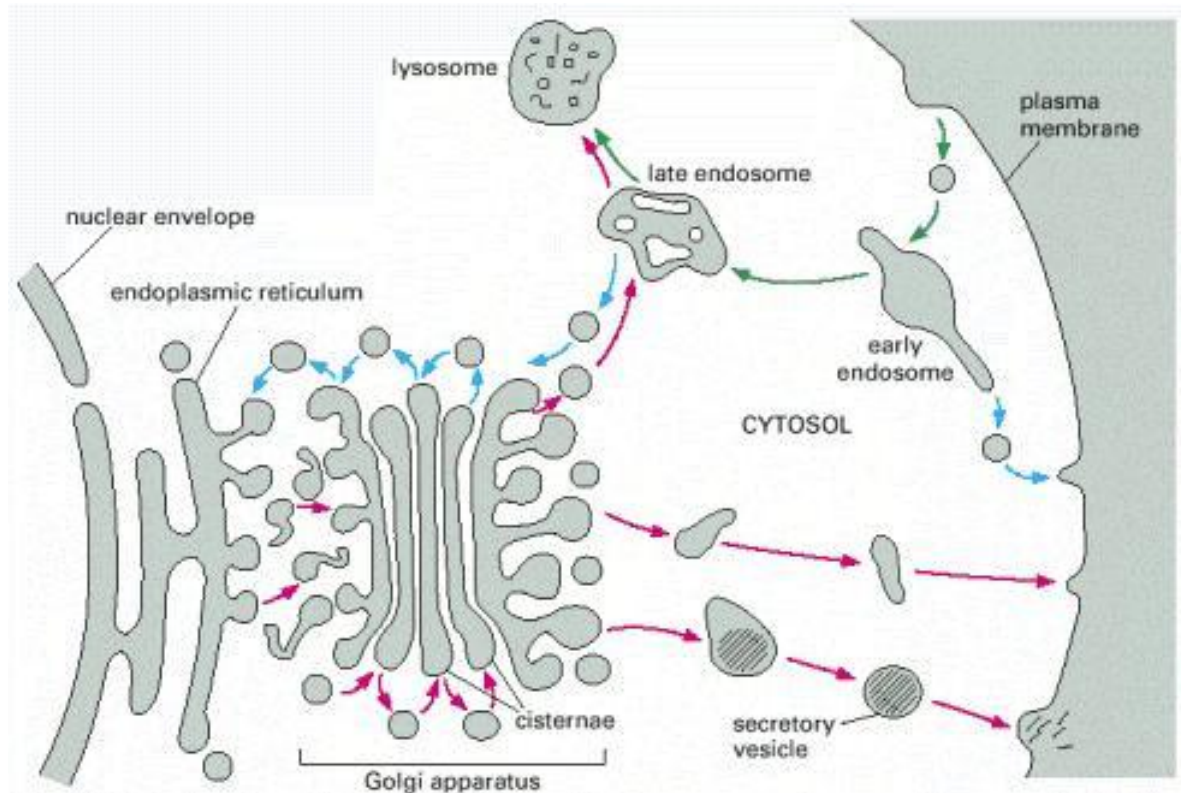


Figure 1.1 The secretory and endocytic pathways

The red arrows correspond to the biosynthetic-secretory pathway where protein molecules are transported from the ER to the PM. They can also be transported *via* late endosomes to lysosomes (where molecules are digested). Green arrows correspond to the endocytic pathway where a portion of the PM is invaginated and pinched off generating a membrane-bounded vesicle termed endosome. Molecules are packed in these vesicles and delivered to the early endosomes and then to lysosomes *via* late endosomes. Blue arrows correspond to the retrieval pathways. For example, some endocytosed molecules are retrieved from early endosomes and returned to the cell surface for recycling; Other molecules are retrieved from the late endosome and recycled to the Golgi apparatus, and finally, some are retrieved from the Golgi apparatus and returned to the ER.

Figure taken from the book *Molecular Biology of the Cell*, fourth edition, 2002.

1.1.2 Membrane fusion

In all trafficking pathways, vesicles bud from a “donor” compartment by a process that allows incorporation of cargo into the forming vesicles. These vesicles are then targeted to a specific “acceptor” compartment, into which they release their cargo upon fusion of their limiting membranes. The proper function of vesicle targeting and fusion is crucial for maintenance of cellular integrity, normal growth, and for intercellular signalling events, such as neurotransmission and insulin signalling.

Membrane fusion occurs when two separate lipid bilayers come close together and fuse to become one lipid bilayer. Fusion can be homotypic (occurs when similar compartments fuse) or heterotypic (when different compartments fuse). The mechanism of membrane

fusion is thought to occur *via* an intermediate stage before complete fusion. This stage is called hemifusion, which occurs when the apposing monolayers merge, however the distal monolayers do not (Chernomordik and Kozlov, 2005). After hemifusion, a fusion stalk is formed which then develops into a fusion pore, resulting in the complete membrane fusion of the two bilayers (Chernomordik and Kozlov, 2005).

Membrane fusion is not a simple process to achieve since the energy barrier resulting from the close apposition of two membranes needs to be overcome. The main candidates that help to overcome this energy barrier are the SNARE (soluble *N*-ethylmaleimide-sensitive factor attachment protein receptor) proteins, which are assisted by tethering factors and other regulatory molecules. Interestingly, SNARE-mediated membrane fusion was shown to transit through a hemifusion intermediate (Xu *et al.*, 2005).

1.2 SNARE proteins

SNARE proteins are the main protein mediators of membrane fusion events. Their finding was a result of studies using both genetic and biochemical approaches which sought to define proteins involved in membrane trafficking. The identification of NSF (N-ethylmaleimide-Sensitive Factor), a protein that is present in cytosolic or membrane bound forms (Glick and Rothman, 1987) and its requirement for membrane fusion (Beckers *et al.*, 1989; Diaz *et al.*, 1989; Malhotra *et al.*, 1988) together with the identification of its partner called α -SNAP (Soluble NSNF Association Protein) (Clary *et al.*, 1990), led scientists to the discovery of SNARE proteins. An affinity column containing both NSF and α -SNAP was used to isolate proteins from brain lysates capable of binding to these proteins. This resulted in the identification of three membrane associated “SNAP receptors” - proteins subsequently known as SNARE proteins (Sollner *et al.*, 1993b). Further studies revealed the interesting observation that “SNAP receptors” comprised one type of protein present in the synaptic vesicle (v-SNARE) and another type in the PM (t-SNARE).

The SNARE proteins identified by this study were the v-SNARE VAMP, a member of the synaptobrevin family present on the synaptic vesicle, and the t-SNAREs SNAP25 (synaptosomal protein of 25 kDa) and Syntaxin 1A (Sx 1A) present in the presynaptic PM. These are the most thoroughly characterized SNARE proteins and are described in sections 1.2.1, 1.2.2 and 1.2.3.

In the years since these proteins were identified, much research has established that these SNARE proteins interact to form a so-called SNARE complex, which acts to drive fusion of membranes. The structure of this complex is discussed further below. It is now equally clear that the proteins purified from brain by virtue of their binding to NSF and α -SNAP are examples of families of similar proteins. Genome sequencing projects have established that SNAP receptors exist in all species and across phyla. In addition, higher eukaryotes have evolved more SNAREs. Of these SNARE proteins there were more syntaxins in all the genomes than the other types of SNARE-coils (Bock *et al.*, 2001). Before elaborating further on the mechanism and function of SNARE proteins, the individual families of SNAP-receptors (syntaxin, VAMP and SNAP-families) will first be described.

1.2.1 Syntaxins

Syntaxins were first identified as 35 kDa proteins present in the nervous system concentrated to the PM of pre-synaptic neurons (Bennett *et al.*, 1992), but since then many homologues have been identified in many phyla. There are currently 15 syntaxins in mammals and 8 in yeast which localise to different intracellular compartments and are cytoplasmically oriented (Hong, 2005; Teng *et al.*, 2001).

Mammalian syntaxins contain 288-301 amino acids and are attached to membranes *via* highly hydrophobic trans-membrane domains at the extreme carboxyl terminus (Bennett *et al.*, 1993). Apart from this C-terminal domain, syntaxins contain a SNARE motif (discussed in more depth in section 1.2.5) and an N-terminal domain. This N-terminal region is conserved in all isoforms which are localised at the PM such as syntaxins 1A, 2, 3 and 4 (Bennett *et al.*, 1993; Bock *et al.*, 1996; Wong *et al.*, 1998). Nuclear magnetic resonance (NMR) spectroscopy analysis of neuronal Sx 1A revealed the N-terminal peptide as an autonomously folded region comprising three anti-parallel helices (termed Habc domain) connected *via* a flexible linker to the SNARE motif (also called H3 domain) (Fernandez *et al.*, 1998). Interestingly, this Habc domain can fold over the C-terminus of the protein containing the SNARE motif, making several contacts with the H3 domain (Dulubova *et al.*, 1999; Misura *et al.*, 2000). This confers syntaxin the ability to flip between 2 different conformations: “open” and “closed” (Figure 1.2), which is an important regulatory step in the formation of the SNARE core complex (Dulubova *et al.*, 1999), since syntaxins need to adopt an open conformation to form SNARE complexes (Sutton *et al.*, 1998). This ability was observed in other syntaxins such as yeast syntaxins

Sso1p, which is functionally homologous to Sx 1A and also contain a similar N-terminal domain (Fiebig *et al.*, 1999). Recently, the closed conformation of Sx 1A was shown to stimulate the initiation of the synaptic vesicle fusion reaction (Gerber *et al.*, 2008).

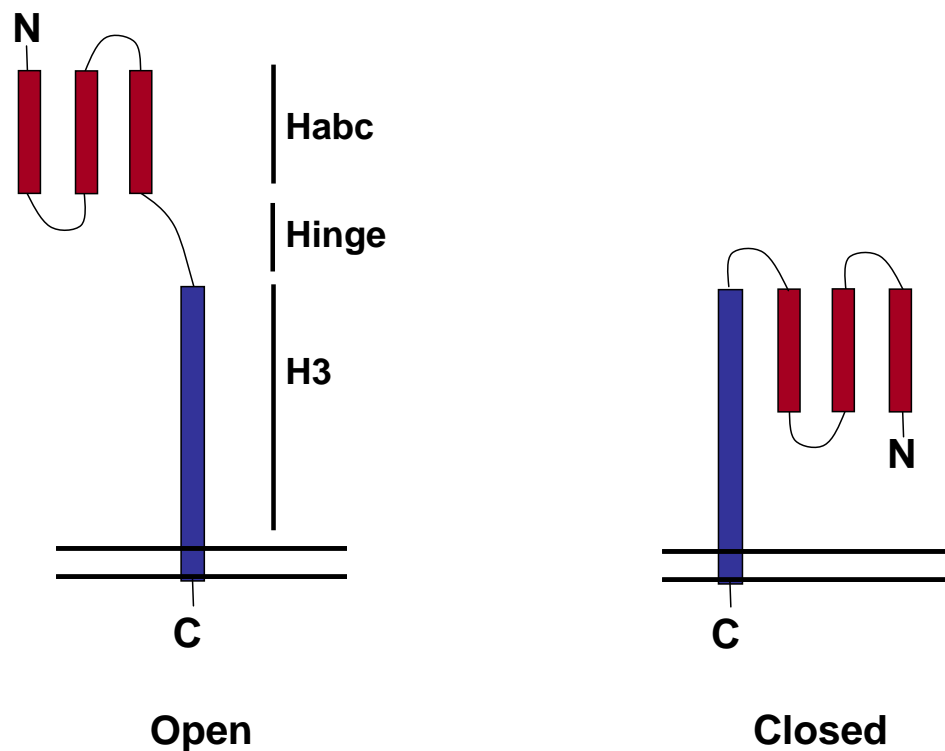


Figure 1.2 Model of the OPEN and CLOSED conformation of syntaxins

This model was based on the model described by Dulubova and colleagues, which suggests that Sx 1A adopts two different conformations (Dulubova *et al.*, 1999). The N-terminal domain, also known as Habc domain, is shown. This terminal autonomously folds and contains three α -helices arranged in parallel (highlighted in red) (Fernandez *et al.*, 1998). The SNARE motif, also called H3 domain, is highlighted in blue and the hinge region that connects the SNARE motif to the N-terminal domain, is also shown. In the closed conformation, the Habc domain folds back into the SNARE motif (Dulubova *et al.*, 1999; Misura *et al.*, 2000). Figure made by Prof. Gwyn W. Gould.

1.2.2 SNAP25 family

The first SNARE protein from the SNAP family to be characterised was SNAP25 which is present in neurons and neuroendocrine cells (Oyler *et al.*, 1989). Later, another three members of the SNAP25 family were identified and described as SNAP23, SNAP29 and SNAP47 (Holt *et al.*, 2006; Ravichandran *et al.*, 1996; Steegmaier *et al.*, 1998), which

unlike SNAP25, are ubiquitously expressed. These SNARE proteins are thought to be directed to the targeted membranes post-translationally and most of them are peripheral membrane proteins. SNAREs like SNAP25, 23 and 29 do not contain trans-membrane domains and, unlike VAMP and synaxins, contain two SNARE motifs, which participate in the formation of the SNARE core complex. SNAP25 and SNAP23 were shown to be palmitoylated *in vivo* at cysteine residues located in the linker region which connects their two coiled-coil domains helping these proteins to attach to membranes (Lane and Liu, 1997; Vogel and Roche, 1999). SNAP29, unlike SNAP25 and SNAP23 is not palmitoylated and associates with membranes *via* its direct interaction with syntaxins (Steggmaier *et al.*, 1998).

1.2.3 VAMP family

VAMP (vesicle associated membrane proteins) or synaptobrevins were first described as integral membrane components of synaptic vesicles (Trimble *et al.*, 1988). They are small conserved proteins of ~120 amino acids which contain a proline-rich amino terminus, a highly charged internal region, and a hydrophobic carboxyl-terminal domain (trans-membrane domain) which anchors the protein to the membrane and, like the syntaxin family, a SNARE motif of ~70 amino acids (Trimble *et al.*, 1988).

The mammalian VAMP subfamily contains seven members: VAMP1 (synaptobrevin 1), VAMP2 (synaptobrevin 2), VAMP3 (cellubrevin), VAMP4, VAMP5 (myobrevin), VAMP7 (tetanus toxin insensitive), and VAMP8 (endobrevin) (Hong, 2005). VAMP1 is present primarily in neurons, whereas other VAMP isoforms are more ubiquitously expressed (Lin and Scheller, 2000). VAMP proteins are localised to several sites and one isoform can be present in multiple intracellular compartments, such as VAMP2 which is present both in neurons and in GLUT4-containing vesicles (Volchuk *et al.*, 1995). Other examples that show overlapping in trafficking steps include VAMP5 and 7 which are both present at the PM. However, VAMP7 is also localised in late endosomes and lysosomes (Advani *et al.*, 1999; Zeng *et al.*, 1998).

1.2.4 The SNARE hypothesis

The identification of the SNARE proteins gave rise to the SNARE hypothesis which stated that the formation of a complex consisting of v-SNAREs on the vesicle and t-SNAREs on the target membrane mediates docking of the membranes leading to membrane fusion

(Sollner *et al.*, 1993a). Although this hypothesis has been widely accepted in the field, some studies have suggested that membrane docking can occur in the absence of SNAREs and that SNAREs are promiscuous *in vitro* (Gagescu, 2000). However, reconstitution of yeast SNAREs into liposomes in several possible combinations have confirmed the specificity in SNARE pairing and fusion (McNew *et al.*, 2000).

Figure 1.3 shows a simple schematic representation of the SNARE hypothesis.

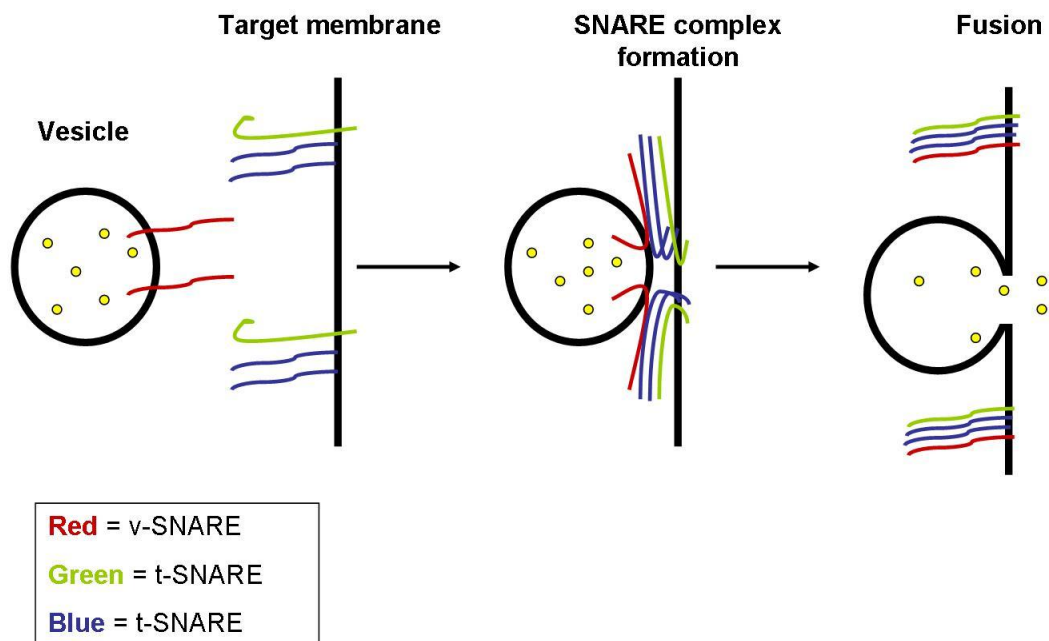


Figure 1.3 Schematic representation of the SNARE hypothesis

v- and t-SNAREs present in opposite membranes (v- on the vesicle and t- on the target membrane) come into close proximity which favours the formation of SNARE complexes, that will eventually drive membrane fusion by overcoming the energy barrier for fusion.

1.2.5 Common structural features of SNARE proteins

The majority of SNARE proteins have a C-terminal membrane-spanning region (apart from SNAP25 family), an N-terminal domain and a region characterised by a heptad-repeats of approximately 60-70 amino acids referred to as the SNARE motif (Hong, 2005). This region is common to all SNAREs and it is critical for SNARE complex formation and important for fusion specificity (Paumet *et al.*, 2004). Monomeric SNARE proteins present unstructured SNARE motifs, nevertheless upon SNARE complex formation these SNARE motifs associate forming helical SNARE core complexes (Antonin *et al.*, 2002; Fasshauer *et al.*, 1997). The SNARE core complex is described in detail in section 1.2.8.1.

Figure 1.4 shows a general comparison of overall structure of SNARE proteins.

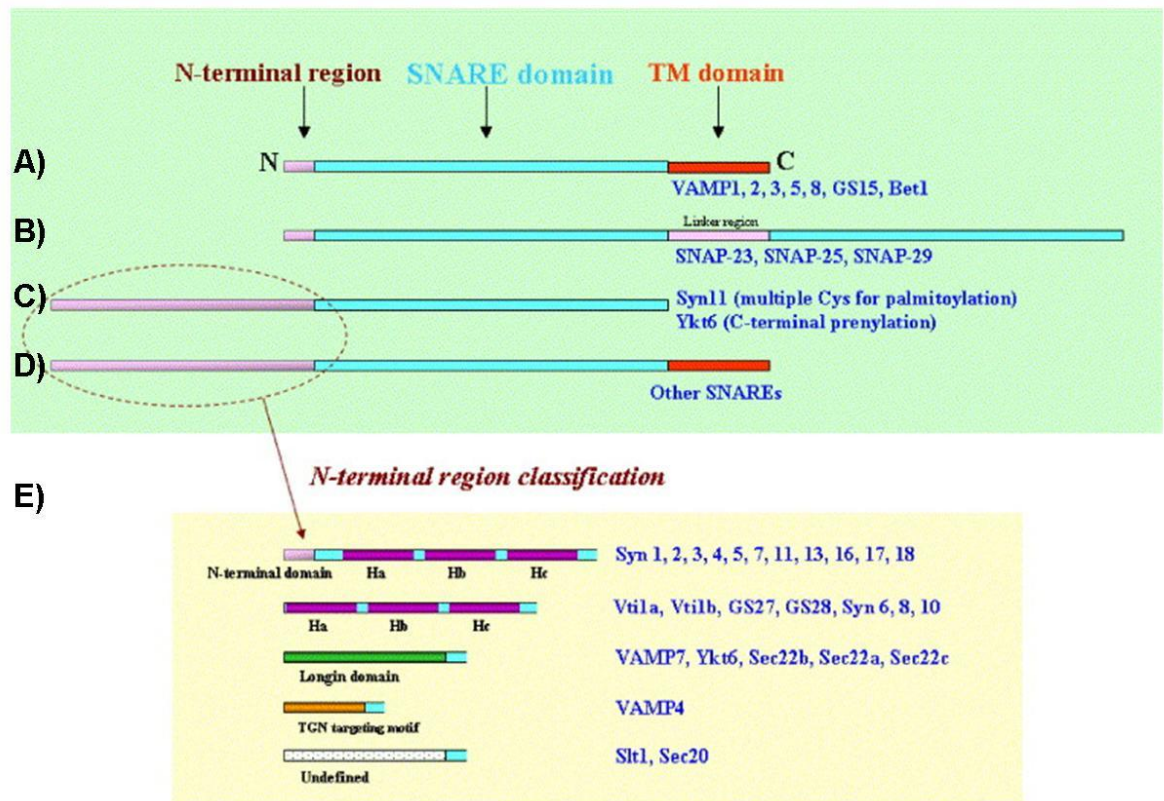


Figure 1.4 General comparison between domains of different SNARE proteins

(A) Proteins from the VAMP family have a short N-terminal region (pink), one SNARE domain (light blue) and a C-terminal trans-membrane domain which anchors VAMP to the vesicle membrane (red). (B) Members from the SNAP25 family are composed of two SNARE domains connected by a linker (pink) that is post-translationally modified by addition of palmitate groups to conserved central cysteine residues. (C) Some SNAREs that do not possess trans-membrane domains (Syntaxin 11 and Yky6); (D) Most of syntaxins contain a C-terminal trans-membrane region (red), a SNARE motif (light blue) and a N-terminal domain which is autonomously folded (pink). (E) Comparisons between the N-terminal domains of different SNARE proteins (This figure was taken and adapted from Hong, 2005)

1.2.6 Classification of SNAREs

SNARE proteins used to be classified according to their preferred localisation inside the cell. This could be either on the vesicle (v-SNARE) or at the target membrane (t-SNARE). However, this classification can not easily be applied when v- and t-SNAREs are present in the same compartment (*i.e.* homotypic fusion). This led scientists to further classify SNAREs according to their structure. Since the four-helix bundle structure of the SNARE complex is well conserved among the SNARE family, SNAREs were re-classified as Q- or

R-SNAREs (see below) taking in consideration the most highly conserved residues at the centre of the fusion complex (*i.e.* SNARE motifs) (Fasshauer *et al.*, 1998).

1.2.6.1 Q-SNAREs

Q-SNAREs correspond to SNARE proteins that provide a glutamine to the formation of the central layer of the SNARE complex (also called ionic 0 layer). Examples come from the Sx 1A and SNAP25 homologues (Fasshauer *et al.*, 1998). In addition, this group of SNAREs have been further classified into Qa, Qb and Qc SNAREs according to their position in the SNARE complex. Syntaxins form part of the Qa subgroup, the SNAP25 homologues are part of the Qb (corresponds to the N-terminal SNARE motif of SNAP25 family) and Qc (corresponds to the C-terminal SNARE motif of the SNAP25 family) subgroups (Hong, 2005).

1.2.6.2 R-SNAREs

Since all proteins from the synaptobrevin family share a common structure, the observation of an arginine common to the central residue within the SNARE domain of these proteins suggested their new classification as R-SNAREs (Fasshauer *et al.*, 1998). Since all rules have exceptions, the exceptions in these cases are yeast Bet1p (which provides a serine the central layer) and leech synaptobrevin (which provides a lysine to the layer) (Fasshauer *et al.*, 1998).

1.2.7 The different locations of SNARE proteins

To date, 21 SNARE proteins have been found in yeast and over 35 in mammals. They are usually found in specific cellular compartments within the cell. This indicates that their localisation might influence their function and specificity in membrane trafficking (Chen and Scheller, 2001). The SNARE proteins can be found at the PM (facing the cytosol), or on intracellular vesicles and organelles (figure 1.5).

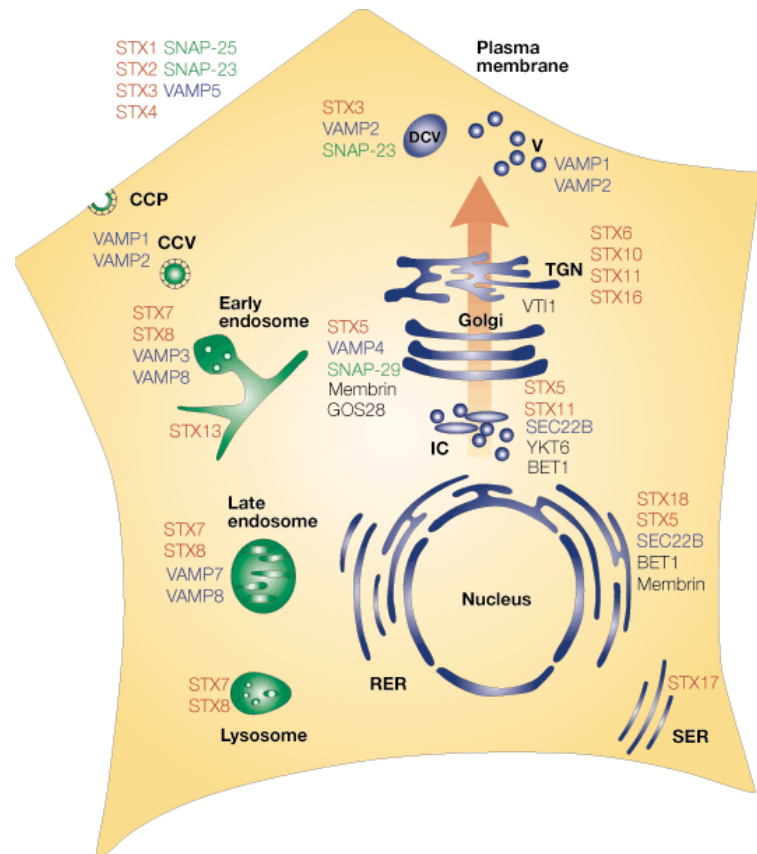


Figure 1.5 The different locations of mammalian SNAREs within the cell

The different locations of mammalian SNAREs are depicted. Red = Syntaxin family; Blue = VAMP family; Green = SNAP-25 family; black = others (Taken from Chen and Scheller, 2001).

1.2.8 SNAREs: The minimal machinery for fusion

SNARE proteins were shown to be the minimal machinery that mediates membrane fusion *in vitro* (Weber *et al.*, 1998). The cytoplasmic domains of SNAREs self-assemble into a rod-like SNARE complex (Sutton *et al.*, 1998) stimulating the docking of vesicles to target membranes, and the use of artificial lipid bilayers has confirmed that SNARE pairing triggers membrane fusion (Weber *et al.*, 1998).

1.2.8.1 The SNARE core complex

Sx 1A, SNAP25 and VAMP2 were the proteins originally identified as SNAP-receptors (see above in section 1.2). Subsequent studies have shown that these proteins form a highly stable complex, resistant to proteases and SDS and also resistant to cleavage by clostridial

neurotoxin (Hayashi *et al.*, 1994; Poirier *et al.*, 1998a). This structure (and its relatives comprised of other cognate SNARE proteins) has been termed the core complex.

The SNARE complex is a parallel four-stranded helical bundle (Poirier *et al.*, 1998b) where one helix is contributed from syntaxin, two helices from the SNAP25 family and the other helix from the VAMP family. This four helices bundle contains a central layer termed “zero-layer” of interaction between one R- and three Q- hydrophilic residues forming the core of the SNARE complex (hence the R-SNARE and Q-SNARE nomenclature outlined previously) (Sutton *et al.*, 1998). Although this well characterised SNARE complex comes from neurones, comparisons of sequences, length and positions of some interacting layers of SNARE proteins that act in other tissues suggest that the major hallmarks of the neuronal SNARE complex are conserved for all SNAREs (Antonin *et al.*, 2002).

Circular dichroism (CD) analysis have indicated that, apart from syntaxin, SNARE proteins are unstructured and that SNARE complex formation is associated with an increase in α -helicity and thermal stability of the complex (Fasshauer *et al.*, 1997). The change from unstructured monomers to a tightly packed ternary complex is a favourable process that helps to overcome energy barriers for membrane fusion (Fasshauer *et al.*, 1997). Figure 1.6 shows a general model of the SNARE complex.

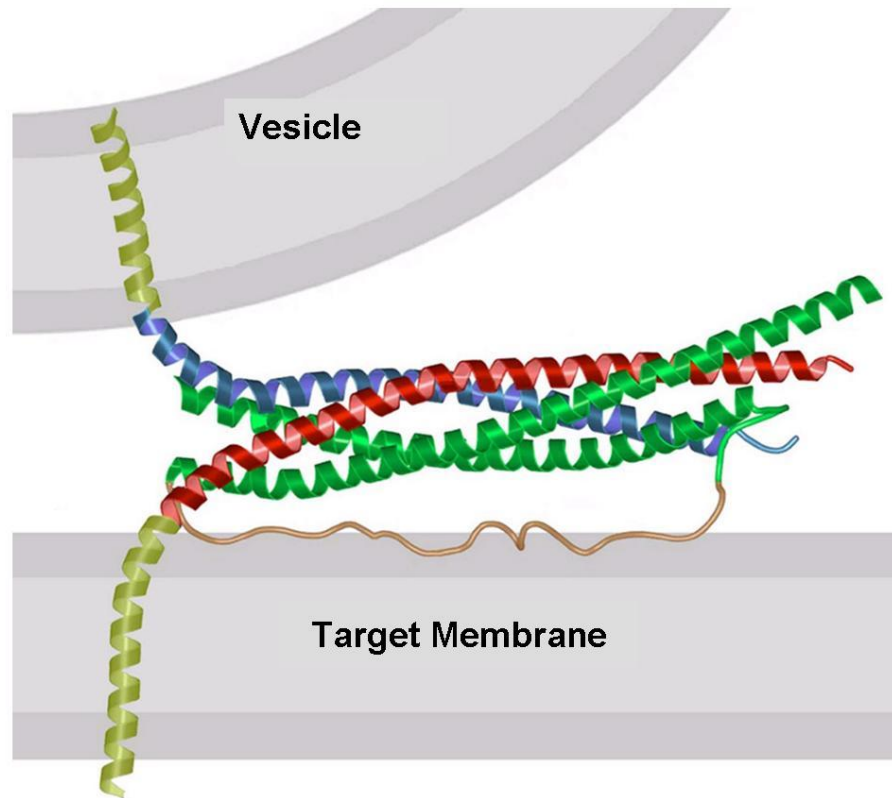


Figure 1.6 Hypothetical model of the SNARE core complex

Adaptation of the hypothetical model of the synaptic fusion complex based on the X-ray crystal structure at 2.4 Å resolution containing Sx 1A, VAMP2 and SNAP25 made by Sutton and colleagues (Sutton *et al.*, 1998). Sx 1A is shown in red; VAMP2 is shown in blue; SNAP25 is shown in green. The trans-membrane domains of VAMP2 (vesicle) and Sx 1A (target membrane) are shown in yellow. The overall structure shows 4 α -helices highly twisted and parallel to each other forming a bundle.

1.2.8.2 *In vitro* fusion assay

The ability of SNAREs to form a highly ordered and energetically favourable complex led to the suggestion that the formation of the SNARE complex may be sufficient to overcome the energy barrier to fuse two lipid bilayers. In an effort to test this hypothesis, Rothman and colleagues used a liposome fusion assay that was first described by Struck and colleagues (Struck *et al.*, 1981). Reconstitution experiments using purified recombinant SNARE proteins have shown that they act as fusogens promoting the fusion of two different populations of liposomes: one containing reconstituted v- and the other reconstituted t-SNAREs (Weber *et al.*, 1998). Such experiments offer conclusive evidence that SNAREs constitute the basic membrane fusion apparatus. However, this SNARE-mediated liposome fusion occurs at a much slower rate than vesicle fusion *in vivo*,

suggesting that in the cell additional factors are employed to accelerate the rate of fusion (Weber *et al.*, 1998).

Although, *in vitro* fusion can be mediated by one SNARE complex, where each SNARE protein is separately reconstituted into liposomes, *in vivo* each exocytic event between vesicles and membranes are thought to involve more than one set of SNARE proteins. Interestingly, SNARE proteins are able to form clusters suggesting that more than one complex of SNARE proteins might be necessary for SNARE-mediated membrane fusion. A model was proposed where a cluster of three t-SNAREs is positioned opposite to a cluster of three v-SNAREs, then the complexes form originating a fusion pore which is composed of three VAMP2 trans-membrane domains, and three syntaxin trans-membrane domains (Hua and Scheller, 2001). This hypothesis was later confirmed when native brain SNARE complexes were isolated from bovine brain detergent extract (and also recombinant neuronal SNARE complexes were generated) and these SNARE complexes were analysed using negative stain transmission electron microscopy since this method is a useful tool to visualise SNARE bundles (Rickman *et al.*, 2005). This study identified oligomers of SNARE protein complexes which acquire forms of star shaped bundles containing 3 or 4, but also up to 6 SNARE complexes (Rickman *et al.*, 2005). The oligomeric appearance that the SNARE bundles acquire could be a result of the interaction of the SNARE trans-membrane domains (Laage *et al.*, 2000). Apart from the trans-membrane domain, the SNARE motif was shown to be also important for the formation of SNARE clusters *in vivo* (Sieber *et al.*, 2006).

The liposome fusion assay has been a very important tool to unravel two of the major functions of SNARE proteins, the first being their role as mediators of membrane fusion and the second being the fact that SNAREs helps to confer specificity to membrane fusion (McNew *et al.*, 2000; Weber *et al.*, 1998). The latter function was doubted when experiments using recombinant purified SNAREs indicated that they can pair promiscuously *in vitro* (Gagescu, 2000). In contrast, when purified SNAREs were tested in the liposome fusion assay, the formation of *trans*-SNARE complexes was mostly restricted to specific v- and t-SNARE combinations (McNew *et al.*, 2000). For example, in yeast, of the 300 different combinations of SNARE proteins tested using *in vitro* fusion assays, only nine mediate fusion (Shen *et al.*, 2007).

Fidelity in membrane fusion *in vivo* is not such a simple process to achieve. It requires other regulatory mechanisms to ensure that specific pairs of t- and v-SNAREs will

participate in specific fusion reactions at different intracellular locations. Thus, further specificity is provided by other proteins. These include tethering proteins that link the apposing membranes prior to SNARE complex formation, Rab family of GTPases which promote the initial association of two membranes and Sec1/Munc18 (SM) proteins which still have a controversial function (Hong, 2005).

1.2.9 SNARE-mediated membrane fusion regulation

SNARE proteins alone are not the sole mediators of membrane fusion. The fact that they are sufficient to catalyse membrane fusion events *in vitro* does not mean that under physiological conditions they are similarly sufficient. Fusion is a very rapid process where several factors need to work in concert to maintain membrane fusion control and specificity.

1.2.9.1 Sec1/Munc18 (SM) proteins

Sec1/Munc18 (SM) proteins play an important role in the process of membrane fusion control. The UNC-18 gene was originally identified through studies performed in *C. elegans* (Brenner, 1974), but homologues have now been described in all organisms examined. For example, a temperature-sensitive mutation in the *SEC1* gene (*sec1-1*) induced an accumulation of intracellular vesicles demonstrating that this gene is important for vesicle exocytosis in yeast (Novick and Schekman, 1979). In *Drosophila*, the Rop protein was shown to be homologous to the products of the *S. cerevisiae* *SLY1* and *SEC1* genes (Salzberg *et al.*, 1993). Subsequent studies have revealed that all intracellular membrane fusion events involve a Munc18 homologue (Dulubova *et al.*, 1999).

SM proteins are hydrophilic proteins of around 60-70 kDa which can be present in the cytosol or attached to membranes *via* their high affinity interaction with syntaxins. Four SM proteins in yeast (*i.e.* Sly1p, Vps45p, Vps33p and Sec1p) and seven SM proteins in mammals (*i.e.* Munc18a, Munc18b, and Munc18c, VPS33A, VPS33B, VPS45, and SLY1) have been identified (Hong, 2005). Munc18a (also termed n-Sec1 or Munc18-1), b (also termed Munc18-2) and c (also termed Munc18-3) are functionally homologous to yeast Sec1p and act at the PM. Munc18a (M18a) was found to be predominantly expressed in the brain (Hata *et al.*, 1993), whereas the Munc18b (M18b) and c (M18c) isoforms appeared to be more ubiquitously expressed throughout different tissues (Tellam *et al.*, 1995). VPS33A and VPS33B correspond to yeast Vps33p and function in the endocytic pathway. VPS45

and SLY1 correspond to yeast Vps45p and Sly1p, respectively, and are involved in trafficking at the *trans*- and *cis*-faces of the Golgi apparatus (Hong, 2005).

Different trafficking events are thought to involve specific SM isoforms. For example, in mice lacking M18a, synaptic transmission is abolished even with the presence of other SM isoforms such as M18b and M18c (Verhage *et al.*, 2000). Thus, one SM protein cannot compensate the loss of another. Null mutations in other isoforms were shown to cause a reduction in vesicle exocytosis, suggesting that SM proteins are essential, not only in mammals, but also in different organisms (Cowles *et al.*, 1994; Harrison *et al.*, 1994).

It is known that SM proteins are binding partners of syntaxins, and one of the best Syntaxin/SM interactions studied to date is the one formed by Sx 1A/M18a, which were shown to form a tight complex (Pevsner *et al.*, 1994a; Pevsner *et al.*, 1994b). A detailed study performed by Misura and colleagues solved the crystal structure of this interaction showing that M18a “holds” Sx 1A when this syntaxin is in a “closed” conformation, thereby preventing Sx 1A from forming SNARE complexes (Misura *et al.*, 2000). Figure 1.7, shows the three-dimensional structure of the complex between Sx 1A/M18a and also the structures of M18a and Sx1A separately. Both the Habc and H3 regions of Sx 1A interact with M18a which forms a central cavity which is formed by domains 1 and 3 (Misura *et al.*, 2000). These two domains provide the binding surfaces for Sx 1A. Nevertheless, domain 1 contributes more contacts and generates a larger contact area than domain 3, contacting Sx 1A *via* the Habc, H3 and the following C-terminal extended region of H3 (Misura *et al.*, 2000).

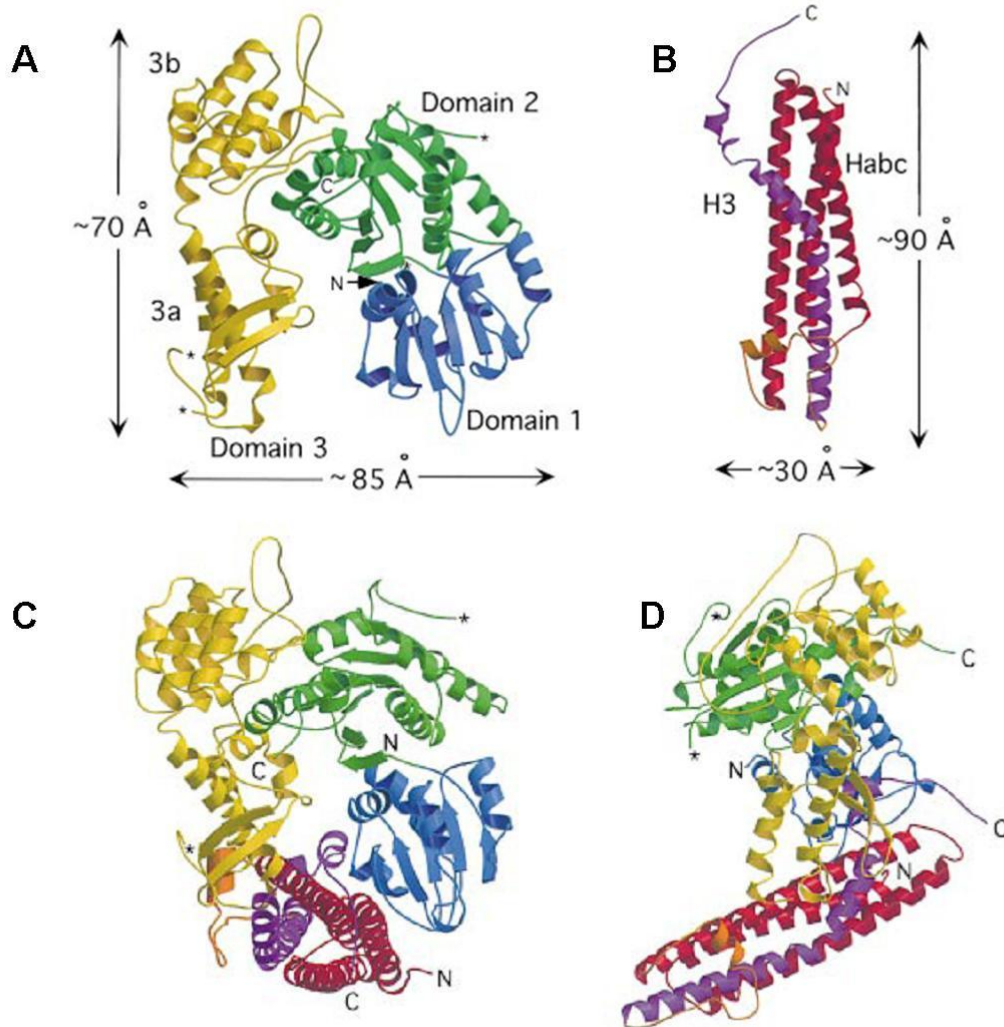


Figure 1.7 Ribbon representation of M18a, Sx 1A and the complex formed by them (A) Ribbon representation of the M18a structure. Neuronal M18a is an arch-shaped molecule with a central cavity (~ 15 Å wide). Its peptide chain can be divided into three domains: domain 1 (blue), domain 2 (green) and domain 3 (yellow). (B) Ribbon diagram of Sx 1A showing Habc domain (red), the Habc/H3 linker (orange) and H3 region (purple). (C) and (D) Ribbon representation of the M18a/Sx 1A complex. (C) View looking down the long Sx 1A helices (D) Similar figure as c but rotated 90° . Figure adapted from Misura and colleagues (Misura *et al.*, 2000).

Interestingly, one of the possible regulators of the formation of Sx 1A/M18a complex is protein kinase C (PKC). This kinase phosphorylates both Ser 306 and Ser 313 (located in domain 3, near the contact area for Sx 1A) of M18a inhibiting formation of the Sx 1A/M18a complex, however if the complex is already formed, these sites can no longer be phosphorylated (Fujita *et al.*, 1996). Other kinases were also shown to be involved in SM/syntaxin interactions (see more details in chapter 5).

It is controversial whether SM proteins play a positive or a negative role in membrane fusion events. This subject is addressed in more detail in chapter 4.

1.2.9.2 NSF and SNAP

NSF and α -SNAP proteins are important regulators of SNARE-mediated membrane fusion. Once membrane fusion is achieved, SNARE proteins remain as a complex in the same membrane (*cis*-SNARE complex). In order to recycle these SNAREs for further rounds of fusion, disassembly of these *cis*-complexes is required and this is performed by the action of α -SNAP and NSF. Three α -SNAP molecules bind to the centre of the *cis*-SNARE core complex, and these molecules recruit the hexameric NSF forming a transient 20 S complex, which then stimulates the ATPase activity of NSF (Hohl *et al.*, 1998; Marz *et al.*, 2003; Wimmer *et al.*, 2001). NSF only binds SNARE complexes in the presence of α -SNAP and uses ATP hydrolysis to disassemble the SNARE complexes (Hayashi *et al.*, 1995). The use of temperature-sensitive NSF mutants in *Drosophila* has shown that the inactivation of NSF causes the accumulation of SNARE complexes and a block in synaptic transmission (Littleton *et al.*, 1998).

1.2.9.3 Rab proteins

Ras-associated binding (Rab) proteins are small GTPases (20-29 kDa) of the Ras superfamily which are ubiquitously expressed and cycle between the cytosol and different membranes (Bock *et al.*, 2001). They form the largest family of membrane trafficking proteins, with the number of isoforms varying depending on the species analysed. There are 11 Rabs in budding yeasts, 29 in *Caenorhabditis elegans* and *Drosophila melanogaster*, and more than 60 in humans and mice (Fukuda, 2008). Because several organelles contain multiple Rabs, they might help in the regulation of membrane transport specificity (Zerial and McBride, 2001).

Rab proteins can exist in two different states: a GDP-bound inactive state and a GTP-bound active state. The switch between these two states is controlled by two classes of enzymes: guanine nucleotide exchange factors (GEF, which stimulates the binding of GTP) and GTPase-activating proteins (GAP, which accelerate hydrolysis of the bound GTP to GDP). When Rab is active, it promotes vesicle trafficking through the interaction with specific effector molecules (Fukuda, 2008). Rab effectors bind specifically to the GTP-bound conformation of Rab proteins (Novick and Zerial, 1997). These proteins

undergo a membrane insertion and extraction cycle, for example a GDP dissociation inhibitor (GDI) is responsible for maintaining the Rab protein in the cytosol and also to deliver Rabs to their specific membrane compartments, whereas a GDI displacement factor (GDF) is needed to maintain membrane attachment (Dirac-Svejstrup *et al.*, 1997; Pfeffer *et al.*, 1995; Shisheva *et al.*, 1999).

Several membrane trafficking steps have been shown to require the function of Rab proteins, which are believed to be involved in the initial contact between vesicles and membranes (tethering and docking) (Pfeffer and Aivazian, 2004). For example, in mammals, Rab10 and Rab4 have been implicated in the regulation of GLUT4 trafficking (Sano *et al.*, 2007; Vollenweider *et al.*, 1997). AS160 (Akt substrate of 160 kDa) was also shown to contribute to the regulation of GLUT4 trafficking since it is a substrate of the insulin-dependent kinase Akt (Larance *et al.*, 2005; Sano *et al.*, 2003; Zeigerer *et al.*, 2004) and serve as a Rab-GAP for Rab10 (Miinea *et al.*, 2005), Rab8a and Rab14 (Ishikura *et al.*, 2007). Interestingly, siRNA directed against Rab10 in adipocytes was shown to cause inhibition of GLUT4 translocation (Sano *et al.*, 2007). Another example of Rab involved in membrane trafficking is the function of the the Rab GTPase Sec4p, which is thought to control the final stage of the exocytic pathway in yeast (Novick *et al.*, 2006).

1.2.9.4 The Exocyst

In *S. cerevisiae*, a protein complex termed the “exocyst” was identified at sites of vesicle fusion (TerBush *et al.*, 1996). The components of the exocyst were initially identified as products of yeast *sec* genes, but mammalian homologues were later identified indicating its importance in all eukaryotes (Kee *et al.*, 1997; TerBush *et al.*, 1996; TerBush and Novick, 1995). The yeast exocyst complex consists of eight components: Sec3, Sec5, Sec6, Sec8, Sec10, Sec15, Exo70, and Exo84 (TerBush and Novick, 1995). An example of a mammalian homologue is Exo70 in 3T3-L1 adipocytes. It was shown that TC10 activation (a component of the PI-3-kinase independent pathway) stimulates Exo70 translocation to the PM in response to insulin and that Exo70 assembles in a complex that includes Sec6 and Sec8 at the PM (Inoue *et al.*, 2003). Interestingly, when a mutant version of Exo70 was over-expressed in adipocytes, insulin-stimulated glucose uptake was inhibited and also the extracellular exposure of the GLUT4 protein (Inoue *et al.*, 2003). Later, Sec6 and Sec8 were also shown to translocate to the PM of adipocytes, and their over-expression in adipocytes caused an increase in insulin-stimulated glucose transport (Ewart *et al.*, 2005).

These data collectively indicate that the exocyst complex is an important regulator in targeting vesicles to their proper site of fusion.

1.2.9.5 Tomosyn

Tomosyn is a 130 kDa cytoplasmic protein that was identified in neurons as a binding partner of Sx 1A (Fujita *et al.*, 1998). It is a ubiquitously expressed protein which was also identified in 3T3-L1 adipocytes (Widberg *et al.*, 2003). It has three splice variants referred to as m (original)-, b (big one)-, and s (small one)-Tomosyn (Yokoyama *et al.*, 1999).

Tomosyn has a coiled-coil VAMP2-like region in its C-terminal domain and a N-terminal containing WD repeats (also known as Trp-Asp or WD40 repeat) (Fujita *et al.*, 1998). The VAMP2-like region was shown to be necessary for its interaction with Sx 1A and for complex formation with Sx 1A and SNAP25 resembling a typical SNARE core complex (Yokoyama *et al.*, 1999). The crystal structure of this complex was resolved at a 2.0-Å resolution and showed that it is very similar to the structure of the neuronal complex, however the surface residues are different and the tomosyn complex is less stable since it is not SDS resistant (Pobbati *et al.*, 2004). This study also demonstrated that when the R-SNARE domain of tomosyn was pre-bound to the binary complex Sx 1A/SNAP25, this prevented VAMP2 binding to binary complex and *vice versa* (Pobbati *et al.*, 2004). Since M18a also associates with Sx 1A, tomosyn was shown to have the ability to dissociate M18a from Sx 1A (Fujita *et al.*, 1998). Interestingly, over-expression of tomosyn in PC12 cells resulted in a strong abrogation of exocytosis which could be a result of competition with VAMP2 in the formation of SNARE complexes (Fujita *et al.*, 1998). Tomosyn was proposed to be a negative regulator of synaptic transmission and this was confirmed in *C.elegans*, since tomosyn null mutants increased levels of neurotransmitter release (Dybbs *et al.*, 2005). Although a negative role was proposed, a positive role was also detected in other studies as knock-down of tomosyn in neurons and pancreatic β -cells caused a decrease in regulated exocytosis (Baba *et al.*, 2005; Cheviet *et al.*, 2006).

Tomosyn was also identified in adipocytes where the isoform expressed is b-Tomosyn (Yokoyama *et al.*, 1999). Tomosyn binds Sx 4 and SNAP23 and the VAMP2-like domain in tomosyn was shown to be responsible for the interaction with Sx 4 (Widberg *et al.*, 2003). Although in neurons tomosyn was shown to compete with M18a for binding to Sx 1A (Fujita *et al.*, 1998), in adipocytes M18c and tomosyn were shown to bind simultaneously to Sx 4 (Widberg *et al.*, 2003). In addition, over-expression of M18c and

tomosyn inhibited insulin-stimulated GLUT4 translocation to a similar extent indicating a negative role in GLUT4 translocation (Widberg *et al.*, 2003).

1.3 Glucose transport

Mammalian cells need glucose as an energy source. Glucose transporters (GLUTs) are a family of integral membrane proteins responsible for facilitating glucose transport through membranes. GLUTs contain 12 predicted membrane spanning helices with both the amino and carboxyl terminus exposed to the cytosol as can be seen in figure 1.8 (Bryant *et al.*, 2002). There are thirteen known mammalian isoforms of glucose transporters and each glucose transporter has different regulatory properties, transport kinetics, and a specific role in glucose uptake in various tissues in order to maintain whole body glucose homeostasis efficiently.

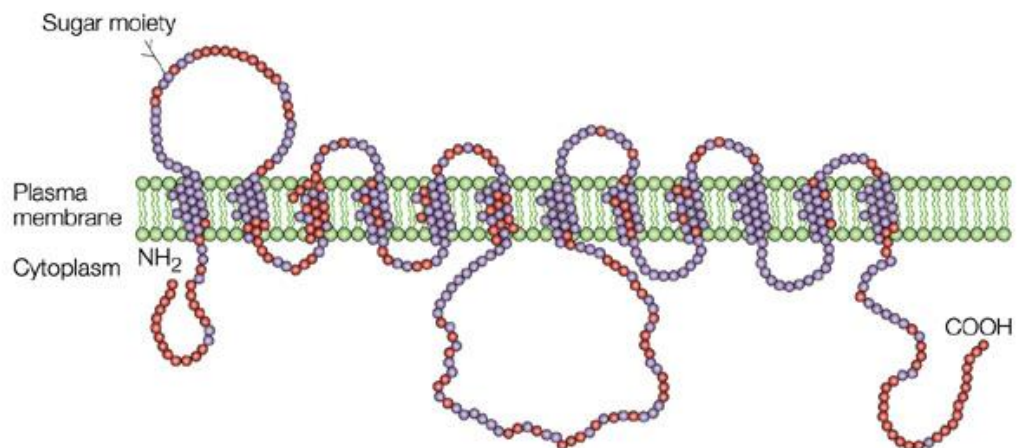


Figure 1.8 Diagram of the GLUT protein family

GLUT proteins are thought to span the membrane 12 times with both amino- and carboxyl-ends oriented into the cytosol. This figure shows the homologous regions between GLUT1 and GLUT4. In red, are residues that are only present in GLUT4. Figure taken from Bryant and colleagues (Bryant *et al.*, 2002).

1.3.1 Types of glucose transporters

As mentioned above, there are thirteen mammalian glucose transporters which can be grouped into three different classes based on sequence similarities: class I (the main glucose transporters GLUT1-4), class II (fructose transporters GLUT5, GLUT7, GLUT9

and GLUT11), and class III (GLUT6, 8, 10, 12, and the *myo*-inositol transporter HMIT1) (Joost and Thorens, 2001). Class III are atypical members of the GLUT family.

GLUT1 is the most ubiquitously distributed isoform, however it is expressed at high levels in endothelial and epithelial-like barriers of the brain, eye, peripheral nerve, placenta and lactating mammary gland (Mueckler, 1994). GLUT2 expression occurs mainly in kidney, intestinal absorptive epithelial cells, liver, pancreas and brain (Mueckler, 1994; Thorens, 1992). GLUT3 is expressed mainly in neurons (restricted to nervous tissue in mouse), however it has also been detected in other human tissues such as placenta, liver and kidney (Gould *et al.*, 1992; Kayano *et al.*, 1988; Nagamatsu *et al.*, 1992). GLUT4 expression is highest in the insulin sensitive tissues including adipose tissue, skeletal and cardiac muscle (James *et al.*, 1989). GLUT1 and GLUT4 are both present in the insulin-sensitive tissues, however GLUT1 is distributed between intracellular compartments and the PM under basal conditions, whereas GLUT 4 is distributed in intracellular compartments in the basal state and in response to insulin it moves dramatically to the PM (Slot *et al.*, 1991a; Slot *et al.*, 1991b).

1.3.2 GLUT4

More than 25 years ago, it was demonstrated that adipocytes contain an intracellular pool of glucose transporters which move ('translocate') to the plasma membrane in response to insulin stimulation (Cushman and Wardzala, 1980; Suzuki and Kono, 1980). This movement of glucose transporters was also observed in muscle (Hirshman *et al.*, 1990) and heart cells (Watanabe *et al.*, 1984). In 1988, a unique insulin-sensitive glucose transport protein was identified (James *et al.*, 1988) and in 1989 several studies using molecular cloning indicated that this protein was indeed a facilitative glucose transporter termed GLUT4 (Bell *et al.*, 1989; Birnbaum, 1989; Charron *et al.*, 1989; Kaestner *et al.*, 1989; Leysens *et al.*, 1989).

1.3.3 Insulin action and GLUT4 trafficking

One of the major effects of insulin stimulation is to increase the number of GLUT4 molecules at the cell surface of adipose, muscle and cardiac tissue by inducing the movement of GLUT4-containing vesicles to the plasma membrane, where they dock and fuse (Rodnick *et al.*, 1992; Slot *et al.*, 1991a; Slot *et al.*, 1991b). GLUT4 vesicles constantly recycle between intracellular compartment(s) and the plasma membrane,

mediated by slow exocytosis and rapid endocytosis (Li *et al.*, 2001; Satoh *et al.*, 1993). In these tissues, electron microscopy studies identified that different intracellular sites have a proportion of GLUT4, including endosomes and TGN (Rodnick *et al.*, 1992; Slot *et al.*, 1991a; Slot *et al.*, 1991b). To further determine the sites of GLUT4 intracellular localisation in the presence or absence of insulin, several approaches were taken. Analysis of the co-localisation of GLUT4 with the transferrin (TfR) receptor suggested that a proportion of the intracellular GLUT4 is localised to the early endosomal recycling system in basal adipocytes, however a larger proportion is present in a separate, TfR-negative compartment (Livingstone *et al.*, 1996). A similar result was observed in muscle cells where the presence of at least two internal GLUT4 pools was observed (one derived from an endosomal recycling compartment, and the other coming from a separate GLUT4 storage pool) (Aledo *et al.*, 1997). Furthermore, a population of small vesicles (50 nm diameter) which are highly insulin sensitive were identified as GLUT4 storage vesicles (GSVs) (Hashiramoto and James, 2000; Kandror and Pilch, 1996; Ramm *et al.*, 2000). These GSVs translocate to the PM in response to insulin (Bryant *et al.*, 2002).

The insulin signalling pathways play an important role in the stimulation of glucose uptake by insulin since the insulin receptor is capable of generating multiple intracellular signals to regulate glucose transport and absorption into cells. The insulin receptor contains 2 disulphide linked heterodimers, corresponding to 2 α extracellular subunits and 2 β intracellular subunits, which span the membrane and contain an intrinsic tyrosine kinase activity (Gual *et al.*, 2005). Upon insulin binding to the α subunit of the receptor, tyrosine autophosphorylation of the β subunit occurs which in turn recruits and phosphorylates several substrates including the insulin receptor substrate proteins (IRS1, 2, 3, and 4). These phosphorylated proteins activate different signalling pathways including those involved in the regulation of GLUT4 trafficking in response to insulin (Gual *et al.*, 2005).

Two signalling pathways were shown to mediate the insulin-stimulated translocation of GLUT4 in fat and muscle cells. One is *via* phosphatidylinositol 3'-kinase (PI3K) activation and the other is independent of PI3K.

1.3.3.1 The PI3K dependent pathway of GLUT4 translocation

Upon tyrosine phosphorylation, IRS proteins, particularly IRS1 and IRS2, interact with the p85 regulatory subunit of PI3K, leading to the activation of its catalytic subunit (p110) and its targeting to the PM. On the cytosolic leaflet of the PM, PI3K generates the lipid product

phosphatidylinositol 3,4,5-trisphosphate (PIP₃) from phosphatidylinositol 4,5-bisphosphate (PIP₂). Subsequently, PIP₃ recruits and activates pleckstrin homology (PH) domain-containing proteins, including the Ser/Thr kinase phosphoinositide-dependent kinase 1 (PDK1), which in turn phosphorylates and activates the serine/threonine kinase PKB (also called Akt) (Alessi *et al.*, 1997). Subsequently, PKB phosphorylates the Rab-GTPase activating protein (Rab-GAP)AS160 (Kane *et al.*, 2002), which was shown to be important in GLUT4 trafficking (see below) (Larance *et al.*, 2005; Sano *et al.*, 2003; Zeigerer *et al.*, 2004). Furthermore, a constitutively active form of PKB, caused an enhancement of glucose transport and an increase in GLUT4 localisation at the PM when expressed in 3T3-L1 adipocytes (Kohn *et al.*, 1998; Kohn *et al.*, 1996).

The importance of this pathway has also been demonstrated by the use of pharmacological inhibitors such as wortmannin and also by over-expression of a dominant-interfering mutant p85 regulatory subunit of PI3K, which all inhibit GLUT4 translocation (Cheatham *et al.*, 1994; Okada *et al.*, 1994).

1.3.3.2 The PI3K independent pathway of GLUT4 translocation

Although activation of the PI3K dependent pathway is crucial in insulin signal transduction, other studies have indicated that additional signalling pathways might be also important, and that these pathways operate independently of PI3K.

In the PI3K independent pathway, the insulin receptor causes the tyrosine-phosphorylation of the c-Cbl proto-oncogene (Ribon and Saltiel, 1997). In 3T3-L1 adipocytes, both the insulin receptor and c-Cbl are capable of interacting with Cbl-associated protein (CAP) which contains a Src homology 3 domain (Ribon *et al.*, 1998). Upon insulin stimulation, the Cbl-CAP complex is formed and translocates to lipid raft domains in the PM (*i.e.* microdomains containing lipids and proteins), mediated by the interaction of the N-terminal of CAP with the protein flotillin (Baumann *et al.*, 2000). When phosphorylated CAP/c-Cbl are present in these lipid raft domains, Cbl recruits the adapter protein CrkII and the guanine nucleotide exchange factor C3G which in turn stimulates the GTPase activity of TC10 (a Rho family small G-protein) since this protein is in close proximity (Chiang *et al.*, 2001). This pathway is thought to be important to promote GLUT4 translocation since over-expression of either TC10 or CAP mutants reduces insulin-stimulated GLUT4 translocation in adipocytes (Baumann *et al.*, 2000; Chiang *et al.*, 2001; Watson *et al.*, 2001). However, other studies have argued the relevance of c-Cbl/TC10,

since siRNA mediated depletion of several components in this pathway had no effect on insulin-stimulated glucose transport in 3T3-L1 adipocytes (Mitra *et al.*, 2004). Further work is required to clearly elucidate the role of this additional pathway in regulating cell surface GLUT4 levels.

Figure 1.9 summarises the PI3K dependent and independent signalling pathways.

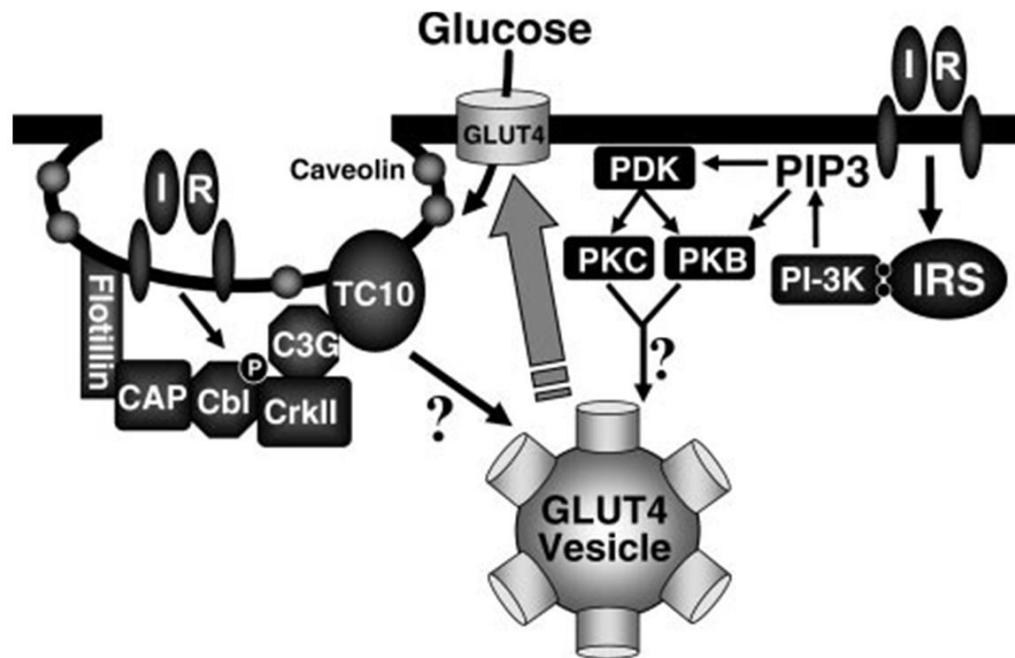


Figure 1.9 Schematic model of both PI3K dependent and independent pathways

Insulin activates the insulin receptor which stimulates the tyrosine phosphorylation of the IRS family of docking proteins (IRS1 and IRS2). These proteins subsequently engage PI3K, activate it and localise it to the PM generating the lipid products PIP₃ from PIP₂. PIP₃ then stimulates the kinase activity of PDK and also interacts with protein kinase B (PKB) to make it a more efficient substrate. In addition, PDK can phosphorylate and activate the atypical protein kinase C (PKC). Activation of these proteins are thought to stimulate GLUT4 translocation (Watson and Pessin, 2001). Another pathway operates independently of PI3K. In this case, the insulin receptor can tyrosine phosphorylate Cbl-CAP complex due to its localisation (recruitment) to the lipid raft domains in response to insulin (mediated by the interaction of the N-terminal of CAP with the protein flotillin). Activated Cbl recruits the CrkII/C3G complex into the lipid raft environment, where C3G can stimulate the GTPase activity of TC10, subsequently promoting GLUT4 translocation (Watson and Pessin, 2001). Figure taken from Watson and Pessin, 2001.

1.3.4 SNARE-mediated GLUT4 fusion with the plasma membrane

After the discovery that SNARE proteins mediate synaptic exocytosis, studies in a range of other systems sought to identify which SNAREs were involved in other trafficking events, such as the insulin-dependent fusion of GLUT4 vesicles with the surface of adipocytes and muscle cells. In the case of GLUT4-mediated membrane fusion, the SNARE proteins identified were Syntaxin 4 (Sx 4) and SNAP23 at the PM, and VAMP2 in the vesicle membrane. These proteins are described below.

1.3.4.1 Syntaxin 4

Sx 4 is an important t-SNARE expressed in several tissues including heart, spleen, kidney, muscle and adipocytes (Bennett *et al.*, 1993; Volchuk *et al.*, 1996) and is involved in the regulation of GLUT4 vesicle trafficking (Tellam *et al.*, 1997). Sx 4 function has been confirmed by several studies such as the introduction of anti-Sx 4 monoclonal antibodies into 3T3-L1 adipocytes causing the inhibition of insulin-stimulated GLUT4 translocation and by the establishment of knockout mice in which the expression of Sx 4 was partially or completely ablated both globally and in defined tissues (Tellam *et al.*, 1997; Volchuk *et al.*, 1996).

The importance of Sx 4 in insulin resistance was demonstrated when Sx 4-knockout mice was generated, resulting in early embryonic lethality (Yang *et al.*, 2001). On the other hand, heterozygous knockout mice developed normally, but exhibited impaired glucose tolerance with a 50 % reduction in whole-body glucose uptake resulting in insulin resistance (Yang *et al.*, 2001). This defect is caused by a 50 % reduction in skeletal muscle glucose transport, showing that GLUT4 translocation in response to insulin was reduced in skeletal muscle. In contrast, in adipose tissue and liver, heterozygous knockout mice displayed normal insulin-stimulated glucose uptake and metabolism (Yang *et al.*, 2001). These results indicate that down-regulation of Sx 4 expression leads to an impairment of insulin-stimulated GLUT4 translocation in skeletal muscle.

1.3.4.2 SNAP23

SNAP25 is present mostly in the brain, which indicated the existence of SNAP25 homologues involved in membrane fusion in other tissues. Thus, a yeast two-hybrid screen of a human B lymphocyte cDNA library were used to identify non-neuronal components of

the SNARE complex that were able to interact with Sx 4 (Ravichandran *et al.*, 1996). A cDNA was isolated that encoded a 211 amino-acid protein with approximate molecular weight of 23 kDa being 59 % identical and 79 % similar to SNAP25 at the amino acid level. This protein, SNAP23, is ubiquitously expressed in human tissues and the membrane-proximal region of Sx 4 was shown to be required for SNAP23 association (Ravichandran *et al.*, 1996).

The involvement of SNAP23 in the GLUT4 trafficking machinery was confirmed when 3T3-L1 adipocytes were microinjected with anti-SNAP23 antibodies and when permeabilised adipocytes were incubated with a SNAP23 synthetic peptide (comprising 24 amino acids from the C-terminus) (Rea *et al.*, 1998). These two approaches inhibited insulin-stimulated GLUT4 translocation to the cell surface, whereas GLUT1 trafficking remained unaffected so providing compelling evidence that SNAP23 was involved in GLUT4 trafficking to the cell surface (Rea *et al.*, 1998).

1.3.4.3 VAMP2

Immunoblotting studies on low density microsomes (LDM) from rat adipocytes (which are rich in GLUT4 vesicles), identified VAMP2 as a component of the GLUT4 vesicles (Cain *et al.*, 1992). Subcellular fractionation has shown that, in response to insulin, this v-SNARE also translocates to the PM (Cain *et al.*, 1992). Adipocytes, apart from expressing VAMP2, were shown to express another v-SNARE called cellubrevin (Volchuk *et al.*, 1995) and these two proteins co-localise with GLUT4 (Martin *et al.*, 1996). Nevertheless, only VAMP2 was shown to be specifically involved in the insulin-dependent translocation of GLUT4 since the majority of cellubrevin is present in endosomes, whereas VAMP2 was found predominantly co-localised with GLUT4 in the GSVs (Martin *et al.*, 1996). This finding was confirmed by other studies where permeabilised 3T3-L1 adipocytes were treated with botulinum neurotoxin D (which cleaves VAMP2) or were transfected with either recombinant soluble VAMP2 fused to a GST tag or synthetic peptides comprising different VAMP2 domains. These approaches generated in all cases a similar result: a reduction in the ability of insulin to stimulate translocation of GLUT4 vesicles to the PM (Cheatham *et al.*, 1996; Martin *et al.*, 1998).

1.3.5 Regulation of GLUT4 fusion

Surface plasmon resonance analysis demonstrated that VAMP2, Sx 4, and SNAP23 form a ternary complex which is SDS-resistant (Rea *et al.*, 1998). This was also confirmed by other studies which showed that these proteins could form a complex both *in vitro* and *in vivo* (Kawanishi *et al.*, 2000; St-Denis *et al.*, 1999).

Several factors might be involved in the formation of the Sx 4/SNAP23/VAMP2 complex involved in GLUT4 fusion with the PM. The main candidate which has been the centre of attention of several studies is the SM protein Munc18c, which was shown to bind Sx 4 with high affinity (Tellam *et al.*, 1997). Other proteins, notably synip and tomosyn, may also be involved.

1.3.5.1 Munc18c and its interaction with Syntaxin 4

The mammalian SM protein Munc18c (M18c) is a ubiquitously expressed protein involved in the regulation of GLUT4 fusion with the PM in muscle and adipocytes (Tellam *et al.*, 1997; Tellam *et al.*, 1995). M18c binds to Sx 4 *in vitro* (Tellam *et al.*, 1997), but its role, like that of M18a in neurons, is controversial.

Negative and positive regulatory effects have been attributed to M18c. Binding assays demonstrated that M18c inhibit the binding of Sx 4 to VAMP2 suggesting a negative role of this SM protein in the regulation of GLUT4 trafficking (Tellam *et al.*, 1997). When M18c was over-expressed in 3T3-L1 adipocytes, an inhibition of GLUT4 translocation to the PM occurred (Tamori *et al.*, 1998; Thurmond *et al.*, 1998), whereas translocation of GLUT1, which is also expressed in adipocytes, was not abolished by M18c over-expression (Tamori *et al.*, 1998). Interestingly, increased expression of full-length Sx 4 rescues the inhibition observed by over-expression of the M18c (Thurmond *et al.*, 2000). Another group reported that tetracycline-repressible transgenic mice that over-expressed M18c in skeletal muscle, adipose tissue, and pancreas resulted in insulin resistance and impaired insulin secretion (Spurlin *et al.*, 2003). This was reversed by tetracycline administration or by the simultaneous over-expression of Sx 4 *in vivo* (Spurlin *et al.*, 2003). Together these data suggest that this SM protein has a negative regulatory role in GLUT4 trafficking, and may act stoichiometrically with Sx 4.

A positive role in GLUT4 trafficking was also suggested for M18c, since this SM protein was shown to be necessary for GLUT4 fusion. For example, microinjection of M18c peptides, which disrupted binding to Sx 4, inhibited the fusion of endogenous GLUT4 vesicles with the PM in 3T3-L1 adipocytes (Thurmond *et al.*, 2000). Later, other studies showed that homozygotic disruption of the M18c gene by homologous recombination producing M18c knockout (KO) mice, resulted in early embryonic lethality (Kanda *et al.*, 2005; Oh *et al.*, 2005), however heterozygous KO mice had normal viability (Oh *et al.*, 2005). Also, when compared to wild-type (WT), heterozygous mice displayed significantly decreased insulin sensitivity and more than 50 % reduction in skeletal muscle insulin-stimulated GLUT4 translocation (Oh *et al.*, 2005).

Different studies suggested that Munc18 proteins share a similar overall structure in which the cytosolic portion of syntaxins mediate binding with Munc18 proteins. One of the first studies on the structural interactions between M18c/Sx 4 utilised a yeast two-hybrid assay and protein-protein interaction analysis in order to reveal that the N-terminal 139 amino acids of M18c (Domain 1) was sufficient for its interaction with Sx 4 (Grusovin *et al.*, 2000). In Sx 4, the N-terminal 29 amino acids of Sx 4 was shown to be necessary for the interaction with M18c (Latham *et al.*, 2006). The crystal structure of the M18c/Sx 4 N-peptide complex interaction was determined (Hu *et al.*, 2007) and agreed with the N-terminal binding modes observed in yeast syntaxins Sed5p and Tlg2p and their respective SM proteins (Bracher and Weissenhorn, 2002; Carpp *et al.*, 2006; Latham *et al.*, 2006; Yamaguchi *et al.*, 2002). This binding mode requires syntaxins to be in a open conformation where the short N-terminal peptide is free to interact with a hydrophobic pocket on the surface of domain I in the SM protein (Bracher and Weissenhorn, 2002; Carpp *et al.*, 2006; Hu *et al.*, 2007). This interaction *via* the N-terminal region of syntaxins would allow SM proteins to associate to them before complex assembly and also after complex assembly. However, the role of M18c in GLUT4 translocation and fusion is therefore still controversial.

1.3.5.2 Munc18c and Syntaxin 4 phosphorylation in response to Insulin

The requirement for M18c inactivation in order to allow GLUT4 fusion with the PM has been suggested by several studies (Araki *et al.*, 1997; Kanda *et al.*, 2005; Thurmond *et al.*, 2000). Interestingly, insulin was shown to be able to induce the dissociation of M18c from Sx 4 in 3T3-L1 adipocytes (Thurmond *et al.*, 1998). The use of pervanadate treatment, phosphotyrosine-specific antibodies, [³²P]orthophosphate incorporation and mass

spectrometric analysis have confirmed that M18c undergoes tyrosine phosphorylation (Oh and Thurmond, 2006; Schmelzle *et al.*, 2006). Residues Y219 and Y521 were shown to become tyrosine phosphorylated (Oh and Thurmond, 2006; Schmelzle *et al.*, 2006; Umahara *et al.*, 2008) and the consequence of tyrosine phosphorylation was the dissociation of M18c from Sx 4 in a time frame consistent with GLUT4 translocation (Umahara *et al.*, 2008). This data agrees with other studies which suggested that over-expression of M18c markedly decreases GLUT4 exocytosis (Khan *et al.*, 2001; Tamori *et al.*, 1998; Thurmond *et al.*, 1998). This decrease could be a consequence of Sx 4 sequestration by M18c, thus inhibiting the formation of the Sx 4/VAMP2/SNAP23 complex.

1.3.5.3 Synip

In 1999, a new Sx 4 interacting protein was isolated from 3T3-L1 adipocytes using a yeast two-hybrid cDNA library cytosolic where the domain of Sx 4 was used as bait (Min *et al.*, 1999). The protein identified was termed Synip and it is specifically expressed in insulin sensitive tissues that are involved in glucose transport and specifically interacts with Sx 4 (Min *et al.*, 1999). Sx 4 binding to SNAP23 was not affected by interaction with Synip, whereas VAMP2 interaction is affected, which indicates that the presence of Synip might perturb the formation of SNARE complexes (Min *et al.*, 1999). Interestingly, this resembles the tomosyn-Sx 4 interaction described in section 1.2.9.5, which also interferes with SNARE complex formation (Widberg *et al.*, 2003). Synip was shown to be insulin sensitive and its insulin sensitivity is conferred by the N-terminal half of synip, whereas Sx 4 interacts with the C-terminal and this region is responsible for GLUT4 translocation (Min *et al.*, 1999). Analysis performed in pancreatic β HC-9 Cells, revealed that insulin secretion from these cells is negatively regulated by the over-expression of Synip (Saito *et al.*, 2003). Another study reported that insulin stimulation induces a decrease in Sx 4-Synip association indicating that insulin might be necessary to release the inhibitory effect of Synip over SNARE complex formation (Yamada *et al.*, 2005). In addition, this dissociation occurred *via* the classical insulin-signalling pathway, since Synip was shown to be phosphorylated *in vitro* (on residue serine 99) by Akt/PKB in response to insulin (Yamada *et al.*, 2005). Although this observation was contested by another group which substituted the Synip serine residue to alanine (S99A) and its over-expression in adipocytes resulted in no inhibition of GLUT4 translocation (Sano *et al.*, 2005), a more recent study has confirmed that the mutant Synip S99A, when over-expressed in 3T3-L1 adipocytes, does indeed inhibit insulin-stimulated GLUT4 translocation (Okada *et al.*, 2007).

In summary, Synip may function to repress GLUT4 vesicle fusion and insulin stimulation is responsible to release Synip from Sx 4 *via* activation of Akt/PKB-mediated Synip phosphorylation. Recently, a co-expression system was generated using pGEX6p-1 and pET28a to efficiently co-express the recombinant complex formed by Sx 4 and the C-terminal of Synip, in order to improve the *in vitro* strategies to further analyse this interaction (Tian *et al.*, 2008).

1.3.6 Diabetes

Insulin is secreted by the β -cells of the pancreatic islets of Langerhans and, as mentioned previously, stimulates glucose uptake into tissues, and also helps the body to store extra glucose in muscle, adipose, and liver cells (Leibiger and Berggren, 2008). Type 2 diabetes mellitus is a lifelong disease that develops when the normal amount of insulin secreted by the pancreas is unable to maintain normal levels of blood glucose. To overcome this and maintain glycaemia, the pancreas secretes additional insulin. When the tissues are resistant to or do not respond to even high levels of insulin, glucose accumulates in the blood resulting in high blood glucose or Type 2 diabetes. Thus, to develop Type 2 diabetes, two defects must co-exist: insulin resistance and inability to increase β -cell production of insulin sufficiently (Kahn *et al.*, 2006). Diabetic patients can have higher than normal blood insulin levels due to peripheral insulin resistance. Then, eventually fasting hyperglycemia develops as inhibition of hepatic gluconeogenesis declines. In Type 1 diabetes, the immune system attacks the insulin-producing β -cells in the pancreas, which then produces little or no insulin (Leibiger and Berggren, 2008).

In recent years, the number of obese and sedentary people has increased and the combination of both conditions has been proposed to contribute dramatically to the increase in insulin resistance and Type 2 diabetics (Kahn *et al.*, 2006; Zimmet *et al.*, 2001). Interestingly, this has been observed in not only mature adults but also young people (Banerji, 2002). However, Type 2 diabetes is associated with additional health problems apart from hyperglycaemia. People who are insulin resistant typically have an imbalance in their blood lipids (Saltiel, 2001). They have an increased level of triglycerides and a decreased level of HDL “good” cholesterol. Imbalances in triglycerides and HDL cholesterol increase the risk of developing heart disease (Saltiel, 2001). These findings have heightened awareness of insulin resistance and its impact on health.

Insulin resistance can be a result of environmental and genetic factors (Zimmet *et al.*, 2001). It has already been attributed to defects in insulin signal transduction, alterations in insulin receptor expression, metabolic abnormalities, changes in the expression of genes or proteins that are influenced by insulin, defects in glucose transport and several other causes still to be confirmed (Saltiel, 2001). Although Type 2 diabetes has been extensively studied, the importance of alterations in GLUT4 vesicle trafficking to the PM in generating insulin resistance is still incompletely understood.

1.3.7 Relationship between GLUT4 trafficking and Diabetes

Type 2 diabetes is a polygenic disease involving polymorphisms in several genes, including those encoding proteins involved in insulin signalling, insulin secretion and intermediary metabolism (Stern, 2000). The proper clearance of glucose from the bloodstream is mediated by the glucose transporter GLUT4. Thus, the inability to translocate GLUT4 to the cell surface of muscle and adipose tissue can result in insulin resistance (Olson and Pessin, 1996). Several studies performed in obese and lean subjects have shown a direct relation between Type 2 diabetes and a decrease in insulin stimulated glucose transport (Hirshman *et al.*, 1990; Klip *et al.*, 1990).

Skeletal muscle is responsible for approximately 80 % of postprandial glucose uptake, and GLUT4 heterozygous knockout mice were shown to develop muscle insulin resistance and diabetes (Stenbit *et al.*, 1997). However, GLUT4-null mice in muscle, cardiac and adipose tissue showed that functional GLUT4 protein is not required for maintaining normal glycaemia (Katz *et al.*, 1995; Stenbit *et al.*, 1997).

Proteins that are involved in the GLUT4 trafficking machinery were also shown to be important in the maintenance of whole body glucose homeostasis. M18c and Sx 4 play an important role in this mechanism. The importance of M18c in the processes that generate insulin resistance was confirmed when M18c heterozygous knockout mice were produced. These mice showed impaired insulin sensitivity leading to severe glucose intolerance (Oh *et al.*, 2005).

A better knowledge of the role of SNAREs and other components in the fusion of GLUT4 vesicles with the PM is fundamental for the comprehension of the molecular mechanisms underlying insulin resistance. Furthermore, the study of SM proteins is also important for the understanding of insulin action and the identification of new proteins involved in the

membrane fusion reactions. Therefore, this research could bring new insights on the mechanisms that generate Type 2 Diabetes.

1.4 Aims of this thesis

The main aim of this study was to investigate the function of the SM protein M18c and to examine the molecular interactions of this protein with the SNAREs (Sx 4, SNAP23 and VAMP2) involved in GLUT4 trafficking. The results obtained in this work are divided into three chapters described as follows.

In chapter 3, Pull-down assays using recombinant SNARE proteins were performed to assess their interactions with recombinant M18c. Understanding how M18c interacts with SNARE proteins is important to further understand its function.

In chapter 4, the fusion between v- and t-SNAREs was assessed in the presence and in the absence of M18c. *In vitro* fusion assays were set up containing Sx 4 constructs which were co-expressed with SNAP23 and reconstituted into synthetic liposomes in order to test their ability to fuse *in vitro* with VAMP2 liposomes. The effect of M18c on SNARE-mediated membrane fusion and how the short N-terminal peptide region of Sx 4 mediates its interaction with M18c were investigated.

Finally in chapter 5, the effects of M18c phosphorylation on its interaction with Sx 4, SNAP23 and VAMP2 *in vitro* were investigated. Since M18c and Sx 4 were shown to become tyrosine phosphorylated in response to insulin, this might be an important regulatory factor in the fusion of GLUT4 vesicles with the PM of muscle and adipose tissue.

Chapter 2

2 Materials and Methods

2.1 Materials

Materials used in this study were of high quality and were obtained from the following suppliers (all other materials were obtained from Sigma):

Ambion, Austin, USA

Nuclease-free water

Amersham Pharmacia Biotech, Little Chalfont, Buckinghamshire, UK

Glutathione Sepharose 4B

Horseradish peroxidase (HRP)-conjugated donkey anti-rabbit IgG antibody

Horseradish peroxidase (HRP)-conjugated sheep anti-mouse IgG antibody

Phosphorus-32 (370 MBq/ml, 10 mCi/ml)

Anachem Ltd., Luton, Bedfordshire, UK

30 % acrylamide/bisacrylamide

Avanti polar lipids, Alabaster, USA

1,2-dioleoyl phosphatidylserine (DOPS)

1-palmitoyl-2-oleoyl phosphatidylcholine (POPC)

N-(Lissamine rhodamine B sulfonyl)-1,2-dipalmitoyl phosphatidylethanolamine

(rhodamine-DPPE)

(N-(7-nitro-2,1,3-benzoxadiazol-4-yl)-1,2-dipalmitoyl phosphatidylethanolamine

(NBD-DPPE)

Bio-Rad Laboratories Ltd, Hemel Hempstead, Hertfordshire, UK

Biobeads

Bradford protein assay reagent

Eco-Pac disposable chromatography columns

N, N, N',N'-tetramethylethylenediamine (TEMED)

Calbiochem, Beeston, Nottingham, UK

4-(2-aminoethyl) benzenesulfonyl fluoride (AEBSF)

Fisher Scientific Ltd, Loughborough, Leicestershire, UK

Ammonium persulphate

Calcium chloride (CaCl₂)

Diaminoethane tetra-acetic acid, Disodium salt (EDTA)

Disodium hydrogen orthophosphate (Na₂HPO₄)

Glycerol

Glycine

N-2-hydroxyethylpiperazine-N'-2-ethanesulphonic acid (HEPES)

Hydrochloric acid (HCl)

Isopropanol

Methanol

Magnesium Chloride (MgCl₂)

Potassium Chloride (KCl)

Potassium dihydrogen orthophosphate (KH_2PO_4)

Sodium chloride (NaCl)

Sodium dihydrogen orthophosphate dehydrate ($\text{NaH}_2\text{PO}_4 \cdot 2(\text{H}_2\text{O})$)

Sodium dodecyl sulphate, SDS ($\text{NaC}_{12}\text{H}_{25}\text{SO}_4$)

Formedium Ltd, Norwich, UK

Micro agar

Tryptone

Yeast extract

Invitrogen Ltd, Paisley, UK

BL21 (DE3) *E. coli* cells

PCRII-TOPOTM TA cloning kit

SOC Media

TOP10 *E. coli* cells

Kodak Ltd, Hemel Hempstead, Hertfordshire, UK

X-ray film

Melford Labs Ltd, Suffolk, UK

Dithiothreitol (DTT)

Terrific broth

Yorkshire Bioscience Ltd, Heslington, York, UK

All oligonucleotide primers

New England Biolabs (UK) Ltd, Hitchin, Hertfordshire, UK

Pre-stained broad range protein marker (6-175 kDa)

T4 DNA ligase

Premier Brands UK, Knighton, Adbaston, Staffordshire, UK

Marvel powdered milk

Princeton Separations, Adelphia, NJ

Chymotrypsin (Bovine) Sequencing Grade Modified

Promega, Southampton, UK

Deoxynucleotides (dNTPs)

Pfu DNA polymerase (2-3 units/ μ l)

Pfu polymerase 10x Reaction Buffer (200 mM Tris-HCl (pH 8.8 at 25 °C), 100 mM KCl, 100 mM $(\text{NH}_4)_2\text{SO}_4$, 20 mM Mg SO_4 , 1.0 % Triton X-100 and 1 mg/ml nuclease-free BSA).

Taq DNA polymerase

Restriction enzymes

Wizard[®] Plus SV Minipreps DNA Purification Kit

Qiagen, Crawley, West Sussex, UK

Nickel NTA-agarose (Ni-NTA agarose)

Qiagen gel purification kit

Roche, Basel, Switzerland

Agarose

Complete™ and complete™ EDTA-free Protease Inhibitor Tablets

Schleicher & Schuell, Dassel, Germany

Nitrocellulose membrane (pore size: 0.45 μM)

Spectrum laboratories, Inc., Netherlands

Float-a-lyzer, 3 ml 10000 kDa MWCO

2.1.1 *Escherichia coli* (*E. coli*) strains

All bacterial strains used are modifications of *E. coli*.

TOP10 *F*⁺ *mcrA* Δ(*mrr-hsdRMS-mcrBC*) φ80*lacZ*ΔM15
Δ*lacX74 recA1 ara*Δ139 Δ (*ara-leu*)7697 *galU galK*
rpsL (Str^R) *endA1 nupG*

BL21 (DE3) *F*⁺ *ompT hsdS_B(r_B⁻m_B⁻) gal dcm* (DE3)

2.1.2 Primary antibodies

Rabbit polyclonal to Syntaxin 4 and rabbit polyclonal to SNAP23 were both purchased from Synaptic Systems (Gottingen, Germany).

Rabbit polyclonal to Munc18c and rabbit polyclonal to VAMP2 were both purchased from Abcam (Cambridge, UK).

Mouse monoclonal [PT-66] to phosphotyrosine (coupled to agarose) was purchased from Abcam (Cambridge, UK)

Mouse monoclonal to phosphotyrosine was purchased from Cell Signalling Technology, Inc. (MA, USA)

2.1.3 General solutions

A200	25 mM HEPES, 200 mM KCl, 10 % (w/v) glycerol, 2 mM DTT pH 7.4
DNA loading buffer	40 % (w/v) Ficoll, 0.25 % bromophenol blue
Coomassie Brilliant Blue solution	0.25 g Coomassie Brilliant blue R250 in H ₂ O: Methanol: Glacial Acetic Acid (4.5:4.5:1 v/v/v)
Destain Solution	5 % (v/v) methanol, 10 % (v/v) glacial acetic acid
HIS-purification buffer	100 mM HEPES, 200 mM KCL, 5 mM imidazole, 2 mM β -mercaptoethanol pH 8.0
GST-purification buffer	25 mM HEPES, 400 mM KCl, 10 % (v/v) glycerol, 2 mM β -mercaptoethanol, 1 % Triton X-100, complete protease inhibitors (1/50 ml) pH 7.4
Phosphate buffered saline (PBS)	136 mM NaCl, 10 mM NaH ₂ PO ₄ , 2.5 mM KCL, 1.8 mM KH ₂ PO ₄ pH 7.4
PBS-T	PBS, 0.1 % (v/v) Tween-20
SDS-PAGE electrode buffer	25 mM Tris base, 190 mM glycine, 0.1 % (w/v) SDS
SDS-PAGE sample buffer	93 mM Tris-HCl (pH 6.8), 1 mM sodium EDTA, 10 % (w/v) glycerol, 2 % (w/v) SDS, 0.002 % (w/v) bromophenol blue and 20 mM dithiothreitol
SOC media	2 % (w/v) Tryptone, 0.5 % (w/v) Yeast extract, 20 mM glucose, 20 mM MgSO ₄ , 10 mM NaCl, 2.5 mM KCL, 10 mM MgCl ₂

TAE	40 mM Tris-acetate, 1 mM EDTA (pH 7.8)
Terrific broth	1.2 % (w/v) Tryptone, 2.4 % (w/v) Yeast extract, 0.4 % (v/v) glycerol, 2.3 % (w/v) KH ₂ PO ₄ , 12.5 % (w/v) K ₂ HPO ₄
Transfer buffer	192 mM glycine, 25 mM Tris base, 20 % (v/v) methanol
2 YT medium	1.6 % (w/v) tryptone, 1 % (w/v) yeast extract, 0.5 % (w/v) NaCl

2.2 Methods

2.2.1 Molecular Biology

2.2.1.1 DNA amplification by PCR (polymerase chain reaction)

PCR reactions were performed in order to amplify the DNA of interest. Primers (forward and reverse) were designed containing the appropriate restriction sites. Small thin-walled PCR tubes were used and the following general protocol was followed:

Nuclease-free water	40 µl
10x DNA polymerase buffer (containing 20 mM MgSO ₄)	5 µl
Template DNA (50-100 ng)	1 µl
Forward primer (10 pmol/µl)	1 µl
Reverse primer (10 pmol/µl)	1 µl
dNTP mix (10 mM each dCTP, dGTP, dATP, dTTP)	1 µl
<i>Pfu</i> DNA polymerase (2-3u/µl)	1 µl
Total volume	50 µl

To minimise the possibility of pipetting errors, a master mix containing water, buffer, dNTPs, primers and template DNA was prepared in a single tube, which was then

aliquoted into individual tubes. *Pfu* DNA Polymerase was added last. All reactions were set up on ice.

The general thermal cycle conditions are outlined below:

95 °C	2 min	} 25 cycles
94 °C	30 sec	
55 °C	30 sec	
72 °C	2 min/kb	
72 °C	10 min	
4 °C	Hold	

The melting temperatures of the primers were taken in consideration in order to choose the most suitable annealing temperature. The optimal annealing temperature is generally 5 °C lower than the lowest melting temperature of the primers. So, the 55 °C value was variable. After the thermal cycling was finished, an aliquot of the PCR mixture was run on an agarose gel (as outlined in section 2.2.1.3) to check if the correct sized DNA product was obtained.

2.2.1.2 Site-directed mutagenesis

This method was used in order to introduce defined base-pair changes at specific locations within a target DNA sequence. The QuickChange® protocol (Stratagene) was followed. Primers containing the appropriate mutation(s) were designed containing the desired mutation in the centre of the primer. The plasmid DNA template used was generally purified using a Wizard® Plus Miniprep Kit. The reactions were set up according to the recipe below:

Nuclease-free water	40 μ l
10x DNA polymerase buffer (with MgSO ₄)	5 μ l
Template DNA (5 - 50 ng)	1 μ l
Forward primer (10 pmol/ μ l)	1 μ l
Reverse primer (10 pmol/ μ l)	1 μ l
dNTP mix (10 mM each dCTP, dGTP, dATP, dTTP)	1 μ l
<i>Pfu</i> DNA polymerase	1 μ l
Total volume	50 μ l

The tubes were flick mixed and spun briefly in a microfuge prior to thermal cycling. The cycling conditions used for site-directed mutagenesis were as follows:

95 °C	1 min	} 18 cycles
94 °C	30 sec	
55 °C	30 sec	
68 °C	1 min/kb	
68 °C	10 min	
4 °C	Hold	

Upon the end of the reaction above, tubes were transferred to ice in order to cool down the mixture prior to the addition of 1 μ l of *Dpn I* (10 units/ μ l). The reaction was then incubated for 1 h at 37 °C in order to cut the methylated, non-mutated parental DNA template. A small aliquot of the mixture, 5 μ l, was transformed into TOP10 *E.coli* competent cells. The plasmids were isolated from single colonies and the mutations were confirmed by DNA sequencing as outlined in section 2.2.1.10.

2.2.1.3 Agarose gel electrophoresis

Agarose gels were usually made containing 1 % agarose in TAE buffer (1.5 g of agarose in 150 ml of TAE) and placed in a 250 ml glass bottle. Solution was melted in a microwave until all agarose was properly dissolved. The mix was allowed to cool down to 50-60 °C before addition of 20 μ l ethidium bromide. Following a quick mix, solution was poured

into a horizontal gel plate which was adequately sealed with tape at both ends and an appropriate comb was also inserted. The agarose gel was left to set for 25 min at room temperature. Comb and tape were removed and gel was then transferred into a DNA gel tank.

In order to run the DNA samples into the gel, 6 x DNA load dye was added to each sample. 1 kb or 100 bp DNA ladder (chosen accordingly to the product size) was loaded into the gel's first lane to distinguish the sizes of the DNA fragments. All the DNA samples were run alongside the marker. Electrophoresis was performed at 90 volts for approximately 40 min. Each DNA gel was photographed in order to keep a record of it and analyse the results.

2.2.1.4 DNA gel extraction and purification

In order to extract the DNA band of interest, agarose gels were firstly examined under UV light and a clean scalpel blade was used to excise the correct DNA band. The excised gel band was then transferred into a sterile 1.5 ml microcentrifuge tube and the product was purified using the QIAGEN gel extraction kit. The manufacturer's instructions were carefully followed. In a typical experiment, the gel slice was dissolved in 600 μ l QC buffer at 50 °C until the agarose gel was totally dissolved. Then, 200 μ l of isopropanol was added to the tube and the solution was then placed into a QIASpin column. The latter was spun at 14,000 xg for 1 min, then 750 μ l of Buffer PE (containing ethanol) was added to column in order to wash it. After centrifugation, the flow-through was discarded. To make sure all ethanol was removed, the column was centrifuged for an extra 1 min. Finally, the column was placed into a 1.5 ml microcentrifuge tube and 30 μ l of nuclease-free water was added to the centre of the column and allowed to incubate for 1 min at room temperature. The column was spun for 1 min at 14,000 xg in order to collect the DNA. DNA was usually stored at - 20 °C.

2.2.1.5 Restriction digestion

Usually, a pair of enzymes was selected to cut plasmid or PCR product. Enzymes were chosen depending on the restriction sites of interest. The buffer used in the reaction was selected according to its compatibility with the enzymes. Both enzymes usually retained 75-100 % activity in the buffer chosen.

The restriction digestion mixture typically contained:

DNA (0.5 - 1 µg)	5 µl
10x Buffer	2 µl
Restriction enzyme 1	1 µl
Restriction enzyme 2	1 µl
Nuclease free water	11 µl

Samples were mixed and tubes spun briefly prior to incubation at 37 °C for 3 h. After digestion was completed, products were analysed using agarose gel electrophoresis as outlined in section 2.2.1.3.

2.2.1.6 TA cloning

Taq polymerase possesses a terminal transferase activity which is able to add a single deoxyadenosine (A) to the 3'-ends of PCR products. This makes cloning of PCR products directly into a linearized cloning vector possible. The vector selected for this study was the pCR®2.1-TOPO® (Invitrogen) which contains overhanging 3' deoxythymidine (T) residues allowing the PCR inserts to ligate efficiently. So in order to clone the desired PCR product into pCR®2.1-TOPO® vector (Invitrogen), incubations were set up as outlined below:

Gel purified DNA	10 µl
10x Mg free Buffer	1 µl
MgCl ₂	0.6 µl
<i>Taq</i> polymerase	0.4 µl
dNTPs	0.4 µl

Reactions were mixed by gently flicking the tubes and briefly centrifuged before incubation at 72 °C for 20 min in a thermocycler.

TA cloning into vector pCR2.1 was performed using the TOPO TA Cloning Kit (Invitrogen). 2 µl of the reaction above (*i.e.* *Taq* treated PCR product) was mixed with 0.5 µl of pCR2.1-TOPO vector in a sterile tube and incubated for 5 min at room temperature. The reaction was stopped by addition of 5 µl of salt solution. The whole reaction was used to transform chemically competent TOP10 cells as outlined in section 2.2.1.8.

2.2.1.7 DNA ligation

After performing successful restriction digestions of destination vector and vector containing insert, gel purified vector and insert were ligated using a standard ligation protocol. The vector and insert were mixed usually at a ratio of 1:3 respectively. The complementary overhangs of the vector and PCR product were ligated under the action of T4 DNA ligase. Reactions included T4 ligase, 10 x ligase buffer and sterile water. Ligations were incubated at 16 °C overnight (or 3 h at room temperature) to allow the T4 ligase to join the 5' phosphate and the 3'-hydroxyl groups of the double stranded DNA molecules. The following morning the whole ligation mixture was used to transform TOP10 cells as outlined in section 2.2.1.8.

2.2.1.8 Transformation of *E.coli* cells

Chemically competent cells (usually containing 50 µl / tube) were stored at - 80 °C until use. Transformation was carried out by firstly defrosting cells on ice for 15 min. For each transformation, the amount of plasmid DNA varied from 3-10 µl. After DNA addition, the mixture was further incubated for 15 min on ice. Cells were heat shocked for 45 seconds and then chilled on ice for 1 min. Tubes were removed from ice and 250 µl of SOC media was added into the tube. The mix was incubated at 37 °C for 1 h with shaking. Cells were then plated onto agar plates containing the appropriate antibiotic for selection and incubated overnight at 37 °C.

2.2.1.9 Small scale DNA preparation from *E.coli* (miniprep)

Single bacterial colonies were picked from 2YT agar plates to inoculate sterile universal tubes containing 5 ml of 2YT and appropriate antibiotics and grown overnight at 37 °C with shaking. DNA purification was carried out using the Wizard[®] Plus Minipreps DNA Purification Kit following the manufactures instructions. In order to produce a cleared lysate, the 5 ml cultures were firstly pelleted by centrifuging the tubes for 5 min at 3000 xg. The cell pellet was resuspended in 250 µl cell resuspension solution and transferred to a sterile 1.5 ml eppendorf tube. Following resuspension, cells were lysed by the addition of 250 µl cell lysis solution and tube was inverted 4 times to mix contents. Then, 10 µl of alkaline protease solution was added and tube was once again mixed by inversion. The mixture was incubated at room temperature for 5 min. 350 µl of neutralization solution was added and quickly mixed. The tube was then centrifuged at 14,000 xg in a microfuge for

10 min. The cleared lysate was added to a Wizard Plus spin column and centrifuged at 14,000 xg in order to bind plasmid DNA. The column was washed as per manufacturer's protocol. Finally, plasmid DNA was eluted from the column in 100 µl of nuclease-free water which was added into the centre of the column and incubated for 1 min prior to collection of the DNA into a sterile eppendorf tube by centrifugation at 14,000 xg for 1 min. DNA concentration was assessed using a spectrophotometer set at 260 nm and the DNA was usually stored at - 20 °C.

2.2.1.10 DNA sequencing

All DNA constructs obtained in this study were carefully analysed by DNA sequencing in order to ensure that all sequences were correct. DNA samples were sent to Dundee University for sequencing analysis.

2.2.2 Biochemical Methods

2.2.2.1 SDS-PAGE

The standard protocol for sodium dodecyl sulphate polyacrylamide gel electrophoresis (SDS-PAGE) was followed in order to separate proteins according to their size. The Bio-Rad mini-PROTEAN III gel apparatus were used. In this study, the percentage of acrylamide of the resolving gel varied from 10-15 % depending on the molecular weight of the protein analysed. Apart from acrylamide, the resolving gel contained Tris-HCL (pH 8.8), 10 % (w/v) SDS, 10 % (w/v) ammonium persulphate and TEMED. Usually 5 ml of the resolving gel was poured into the gel apparatus, then overlaid with 1 ml of 100 % isopropanol and allowed to set at room temperature. The stacking gel was prepared using the same components as the resolving gel, however at different concentrations and the stacking gel Tris-HCL buffer was used at pH 6.8. After the resolving gel was set, the isopropanol was removed and the stacking gel was then applied on the top of the resolving gel. Either a 10 or 15 well comb was inserted at the top and the gel was allowed to polymerise at room temperature.

Protein samples were then resuspended in SDS-PAGE sample buffer and placed in a bench heat block to boil for 5 min at 95 °C. Tubes were flick mixed and briefly centrifuged before loading the samples into the gel lanes. Samples were loaded adjacent to a broad-range (6-175 kDa) pre-stained molecular weight marker. Gels were run in SDS-PAGE electrode

buffer, at a voltage of 85 volts through the stacking gel which was then increased to 130 volts through the resolving gel. Gels were electrophoresed until the pre-stained broad range markers had adequately separated.

2.2.2.2 Immunoblot Analysis

Proteins were transferred from SDS-PAGE onto nitrocellulose membranes where they were probed using specific antibodies. This was achieved by firstly carefully transferring the gel into a sandwich like arrangement. Polyacrylamide gel, membrane and other components were sandwiched in the following order from bottom to top: a sponge pad, a whatman 3 mm filter paper, nitrocellulose paper (0.45 μ M pore size), electrophoresed gel, a whatman 3 mm filter paper and finally a sponge pad. All these components were soaked in transfer buffer prior to assemble. The sandwich was then put into a cassette and placed into a Bio-Rad mini trans-blot tank filled with transfer buffer. A constant current of 250 mA was applied to transfer proteins for 2 h and a 50 mA current for overnight transfers.

After protein transfer, non-specific binding sites on the membrane were blocked by incubating the latter with 5 % (w/v) non-fat dried milk (made up in PBS-T) for at least 30 min with shaking at room temperature. The membrane was exposed to primary antibody appropriately diluted in 1 % (w/v) non-fat dried milk (made up in PBS-T) for at least 1h. After incubation, membrane was washed three times with PBS-T for 30 min. After washes, the membrane was exposed to the secondary antibody (IgG HRP conjugate) at a 1:2000 dilution performed in 5 % (w/v) non-fat dried milk (made up in PBS-T). Incubation with the secondary antibody usually lasted 50 min and was performed at room temperature with shaking. The membrane was finally washed over 20 min, first with PBS-T and last with high salt PBS-T to avoid any possible antibody background. Protein bands were then visualised using lab made enhanced chemiluminescence (ECL). Equal volumes of ECL reagents 1 and 2 were mixed and membrane immersed into this mix for exact 1 min. The membrane was wrapped with cling film and ECL excess was removed before placing the membrane in a light proof cassette. In the dark room, membrane was exposed to Kodak X-ray film at appropriate exposure times and the films were developed using a X-OMAT automatic processor.

2.2.2.3 Coomassie Blue staining of SDS-PAGE

In order to visualise protein bands from polyacrylamide gel electrophoresis, a Coomassie Blue stain solution was produced using the components mentioned in section 2.1.3. The polyacrylamide gels were soaked in this solution for at least 1h at room temperature while shaking. After incubation, the Coomassie Blue stain was removed and the excess stain was then eluted with destain solution (section 2.1.3) until the protein bands were clearly visualised.

2.2.2.4 Recombinant protein expression and purification

A single *E.coli* colony was picked from a fresh selective agar plate and used to inoculate a 2YT overnight culture containing the appropriate antibiotics (either 50 µg/ml in the case of Kan and 100 µg/ml in the case of Amp). Bacteria were grown overnight at 37 °C with shaking at 250 rpm. The next day, 50 ml of the overnight culture was spun at 3000 xg for 10 min and the resulting pellet was used to inoculate fresh 1L cultures of terrific broth (TB) medium containing appropriate antibiotics.

TB cultures were grown at 37 °C with shaking at 250 rpm until the optical density (OD) at 600 nm was ranging between 0.6-0.8. At this stage, protein production was induced by the addition of Isopropyl-β-D-Thiogalactopyranoside (IPTG). The concentration added varied between 0.2 - 1 mM depending on the protein (see figure legends for details). Protein production was typically induced for 4 h at 37 °C or overnight at 22 °C. Cells were then harvested in a Beckman Coulter Allegra X-12R centrifuge for 30 min at 3,270 xg. Cell pellets were resuspended in the appropriate buffer and either processed for purification immediately or stored at - 80 °C.

Frozen cell pellets were thawed on ice. Proteins were purified according to their tags, being at either the N- or C-terminus. The two tags utilised in this study were GST and Hexa-HIS (HIS). Cell pellets containing GST-tagged proteins were resuspended in GST-purification buffer (containing complete protease inhibitor cocktail and 1 mM PMSF) and HIS-tagged proteins were resuspended in HIS-purification buffer (containing EDTA-free complete protease inhibitor tablet and 1 mM PMSF). Lysozyme was added to the resuspended cells to a final concentration of 1 mg/ml and the mixture was incubated at 4 °C for 30 min on a rotator. Cells were then sonicated for 6 x 20 sec periods with 20 sec intervals on ice, using a Sanyo Soniprep 150 sonicator, set at an amplitude of 15 microns. DNA was digested by

the addition of *DNase I* (10 µg/ml) for 30 min at 4 °C. The lysate was then clarified by centrifugation in a pre-cooled Beckman JA-20 rotor for 1 h at 48,400 xg at 4 °C. Glutathione sepharose or Ni-NTA agarose was added to the clarified lysate (0.5 ml glutathione sepharose and 0.25 ml Ni-NTA agarose per 1L original culture). To bind glutathione sepharose, the mix was incubated overnight at 4 °C and to bind Ni-NTA agarose, the mix was usually incubated for 2 h. Incubations were always carried out at 4 °C with constant rotation.

Lysates containing beads were then transferred into a chromatography column pre-equilibrated in wash buffer in order to start the washes. Glutathione sepharose was washed 3 times with 50 ml of PBS + 1 % Triton (pH 7.4), followed by 3 times with 50 ml of PBS + 0.5 M NaCl (pH 7.4), and finally three times with 50 ml of PBS (pH 7.4). Protein was eluted from the beads by either incubating the beads for 5 min with 50 mM Tris, 15 mM reduced glutathione pH 8.0 (to keep the GST-tag) or incubation with thrombin in PBS pH 7.4 for 4 h at room temperature (to cleave the GST tag from the protein).

Ni-NTA agarose was washed five times with 50 ml wash buffer which contained 100 mM HEPES, 200 mM KCl, 10 % glycerol (v/v) and 15 mM imidazole pH 8.0. The protein was eluted by incubating the beads with the HIS elution buffer containing 100 mM HEPES, 200 mM KCl and 500 mM imidazole pH 8.0 for usually 5 min. Typically, this step was repeated 4 times in order to elute as much protein as possible from the beads.

Protein concentrations were analysed as outlined in section 2.2.2.5.

2.2.2.5 Analysis of protein concentration

The Bio-Rad Bradford protein assay reagent was used to determine the concentration of solubilised protein. This is a dye-binding assay in which a color change of a dye occurs in response to different protein concentrations. Bovine serum albumin (0.5 - 10 µg) was used as the standard. The amount of sample assayed varied within the linear range of the standard. Assays were set up in duplicate, in 1 cm path length disposable cuvettes, according to the manufactures instructions and absorbance measured in a spectrophotometer set to 595 nm. Protein concentrations were calculated using a curve derived from the standard values.

2.2.2.6 Pull-down assays

Usually 5 µg of GST-tagged or HIS-tagged proteins were incubated with 10 µl glutathione sepharose or Ni-NTA agarose in binding buffer (20 mM HEPES, 150 mM Potassium acetate, 1 mM MgCl₂, 0.05 % Tween 20, pH 7.4) in a total volume of 200 µl for at least 1.5 h at 4 °C with constant rotation. Beads were washed 3 times with 1 ml binding buffer in order to remove unbound protein. Beads were harvested by centrifugation in a bench microfuge at 4,500 xg at 4 °C for 2 min. 5 µg of HIS-tagged proteins (for glutathione beads) or 5 µg of GST-tagged proteins (for Ni-NTA agarose) plus binding buffer were added to each tube up to a total volume of 500 µl. Tubes were placed on a rotator for overnight incubation at 4 °C. The following day, 20 µl sample was removed from each tube in order to examine protein input. Unbound protein was then removed by washing the beads 3 times with 1ml binding buffer plus 0.2 % fish skin gelatin, followed by 3 washes with 1 ml of binding buffer plus 5 % (w/v) glycerol and finally 4 washes with 1 ml of binding buffer alone. After the final wash, all remaining supernatant was carefully removed and 15 µl of 1 x SDS-PAGE sample buffer (containing 20 mM DTT) was added to the beads and samples were boiled at 95 °C for 5 min. After centrifugation at 20,345 xg for 5 min, the supernatant was removed and analysed by SDS-PAGE and/or immunoblotting.

2.2.3 In vitro fusion studies

2.2.3.1 Purification of full-length SNARE proteins

The full-length SNARE proteins necessary to form SNARE complexes were purified by means of a GST-tag (Syntaxin 4 / SNAP23) or a HIS-tag (VAMP2) attached to the proteins. Full length VAMP2 was a generous gift from Dr Fiona Brandie, thus purification of this protein was not performed in this thesis. However, t-SNARE complexes were purified as described below.

The different versions of the full-length His₆-Sx 4 (Wt Sx4, Sx 4 NΔ36, Sx 4 OPEN, Sx 4 OPEN NΔ36) were co-expressed with SNAP23-GST in the same BL21 (DE3) *E. coli* cells. They were usually transformed by mixing 50 ng of SNAP23 DNA with 100 ng of Sx 4 DNA into the same BL21 (DE3) cells (except for Sx 4 open, where 200 ng of Sx 4 was transformed). Cells containing both plasmids were selected on dual antibiotic plates since SNAP23 is expressed from a Kan resistant vector (pET41) and the different versions of Sx

4 are expressed from Amp resistant vectors (pQE30). A single colony was used to inoculate an overnight 2 YT culture containing 500 µg/ml ampicillin and 50 µg/ml kanamycin. The following day, the overnight culture was centrifuged at 3,000 xg for 10 min, the supernatant removed, and the pellets were used to inoculate each litre of TB cultures (usually 16 L of TB were used to obtain a satisfactory protein yield) containing 200 µg Amp and 50 µg Kan, which were grown at 37 °C with shaking at 250 rpm. An additional 100 µg Amp was added each hour until cells reached an OD₆₀₀ of ~ 0.6. Then, the t-SNARE complex protein expression was induced with 1 mM IPTG. Cells were grown overnight at 25 °C with shaking at 250 rpm (for approximately 16 h).

The following day, purification proceeded taking advantage of the GST-tag on the N-terminus of SNAP23. Cells were then harvested in a Beckman Coulter Allegra X-12R centrifuge for 30 min at 4 °C at 3,270 xg. Buffer A200 containing protease inhibitors (1 tablet/ 50 ml) was used to resuspend the cell pellets followed by the addition of ¼ volume 20 % Triton X-100. At this stage the resuspended pellets could either be stored at -80 °C prior to use, or could be used straight away to continue protein purification. To achieve cell lysis, cells were passed twice through a French press set at 950 psi. Insoluble matter was removed by centrifugation in a Beckman JA-20 rotor at 48,400 xg for 1 h at 4 °C. After a cell lysate was obtained, 5 ml of glutathione sepharose (pre-equilibrated in lysis buffer) was added and incubation occurred overnight at 4 °C. The following morning, lysate-containing beads were divided into 50 ml tubes and centrifuged at 500 xg for 5 min. The supernatant was removed and each tube containing beads were resuspended in 5 ml of a buffer containing 25 mM HEPES, 300 mM KCl A200, 1 % (v/v) Triton X-100, 10 % (v/v) glycerol and 10 mM β-mercaptoethanol. Solutions were mixed and all were applied to a Bio-Rad Eco-pac disposable chromatography column. 200 ml of this buffer was used to wash the beads inside the column (approximately 8 washes). The Triton was then exchanged for n-octyl-β-d-glucopyranoside (OG) by washing the column 10 times with 15 mls of buffer A200 + 1 % (w/v) OG. After final wash, beads were resuspended in 4 ml A200 containing 1 % (w/v) OG plus 125 units of thrombin. Both ends of the column were sealed with the provided caps and beads were incubated on a rotator for 4 h at room temperature in order to elute the protein. At the end of the 4 h, thrombin action was inhibited by the addition of 2 mM AEBSF. The eluted sample was let to flow through the column into a 15 ml corning tube. Then, another 2 ml of elution buffer was added to the column in order to elute any extra protein still left on the beads. The column was placed on a roller for further 10 min and a second elution was obtained. The eluates were aliquoted into 510 µl samples, snap frozen in liquid nitrogen and stored at - 80 °C until use.

2.2.3.2 Preparation of lipid stocks

The phospholipids for both v- and t-SNARES consisted of a mixture of POPC and DOPS, however the v-SNARE lipids also contained two head group-labelled fluorescent lipids. For t-SNARE liposomes, a 15 mM lipid stock containing a mixture of 85 mol % POPC and 15 mol % DOPS was prepared in chloroform. For v-SNARE liposomes, the final concentration was 3 mM and contained a mix of 82 mol % POPC, 15 mol % DOPS, 1.5 mol % NBD-DPPE and 1.5 mol % rhodamine-DPPE. This stock was also made up in chloroform.

2.2.3.3 SNARE protein reconstitution into liposomes

In order to reconstitute t- and v-SNAREs into liposomes, 100 μ l of 15 mM unlabelled lipid stock (for t-SNARE liposomes) and 500 μ l of 3 mM labelled lipid stock (for v-SNARE liposomes) were placed at the bottom of 12 x 75 mm glass test tubes. Tubes were carefully placed under a stream of Nitrogen for 15 min inside the fume hood to dry the lipids. After 15 min, tubes were placed inside a vacuum desiccator for 30 min in order to further remove any remaining traces of chloroform. Purified t- or v-SNAREs (500 μ l) containing 1 % OG, as outlined in section 2.2.3.1, were added to each tube. The lipid film was totally resuspended with the protein by vortexing for 15 min.

After the lipid film was completely mixed with the proteins, 1 ml of buffer A200 + 1 mM DTT was added drop-wise to each tube while vortexing it in order to dilute the detergent below its critical micellar concentration. The samples were then transferred into 3 ml Float-a-Lyzers with a MWCO of 10,000 pre-equilibrated in dialysis buffer in order to remove detergent monomers from samples. Dialysers containing samples were floated in 4 L of buffer A200 containing 1 mM DTT plus 4 g of Bio-Beads. Dialysers in buffer were left stirring in the cold room overnight. Samples were collected in the following day, and placed at the bottom of a SW60 tube on ice for subsequent separation using gradient centrifugation.

2.2.3.4 Gradient preparation and proteoliposome recovery

A three step density gradient was used to separate proteoliposomes from unincorporated protein. Proteoliposomes were recovered by floatation on a histodenz gradient. In order to achieve this, an appropriate mass of histodenz was first mixed with A200 buffer to give

rise to solutions containing histodenz at 80 % (w/v) and 30 % (w/v). 1 mM DTT was then added to each solution just before starting the experiment. An equal volume of 80 % histodenz was mixed with the recovered dialysate to produce a 40 % histodenz mixture. This was overlaid with 1.5 ml of 30 % histodenz. Finally, 250 μ l of glycerol free A200 was added carefully to the top of the previous layer. Tubes were then transferred to an ultracentrifuge. A SW60 rotor was used to centrifuge samples for 4 h at 46,000 rpm (\sim 372,000 $\times g$) at 4 °C. Proteoliposomes float to the 0 % (i.e. glycerol free A200) / 30 % histodenz interface (due to their lipid content) and free protein remains in the 40 % layer. After centrifugation, tubes were placed on ice and 400 μ l of proteoliposomes were recovered from the top of the gradient and transferred into a 1.5 ml tube. Proteoliposomes were stored at -80 °C.

2.2.3.5 Characterisation of v- and t-SNARE liposomes

Protein content and lipid recovery were characterised by different methods. Lipid recovery was analysed by scintillation counting [3 H]DPPC in the recovered sample compared to the input lipid stocks. Protein content was analysed by SDS-PAGE.

2.2.3.6 *In vitro* fusion assay

Fusion assays were performed in which 5 μ l of fluorescently labelled donor (v-SNARE liposome) was mixed with 45 μ l of unlabelled acceptor (t-SNARE liposome). t- and v-liposomes were mixed in a well of a 96 well microtitre plate, on ice. As a control, the t-SNARE liposomes were pre-incubated with 3 μ l of purified VAMP2 mutant lacking the trans-membrane domain. This version of VAMP2 is known to act as a dominant negative inhibitor of fusion (Weber *et al.*, 1998). Incubation was performed on ice for 10 min. Then, the v-SNARE liposomes were added and the microtitre plate was either incubated overnight at 4 °C or placed directly into the fluorescent plate reader.

The microtitre plate was warmed to 37 °C by placing it inside the pre-warmed Fluostar Optima, BMB labtech plate reader and incubated for 5 min before starting the fusion measurements. Fluorescence was measured at 2 min intervals for 2 h with the excitation filter set to 485 nm and the emission filter set at 520 nm. After 2 h, the plate was removed and 10 μ l of 2.5 % (w/v) n-dodecylmaltoside was added to the wells containing liposomes and mixed, and the fluorescence was recorded for further 40 min at 2 min intervals.

2.2.3.7 KaleidaGraph analysis

A graphing and analysis programme called KaleidaGraph (Synergy Software) was used in order to analyse the data obtained from the Fluorescence reader. Raw fluorescence data was transferred to this software and it was plotted against time. This was then normalised to percentage of maximal detergent signal and the latter was plotted against time.

2.2.4 M18c protein purification

His₆-M18c was expressed from vector pQE30 in M15 *E. coli* co-expressing the chaperone GroEL. Cells containing both plasmids were selected on dual antibiotic plates since GroEL is Kan resistant and pQE30His₆-M18c is Amp resistant. A single colony was used to inoculate an overnight 2 YT culture containing 500 µg/ml Amp and 50 µg/ml Kan. The following day, the overnight culture was centrifuged at 2,000 xg for 10 min, the supernatant removed, and the pellets were used to inoculate each 1 L of TB cultures containing 200 µg Amp and 50 µg Kan. These cultures were grown at 37 °C with shaking at 250 rpm. Usually 10 L of TB were used to obtain a satisfactory M18c protein yield. His₆-M18c expression was induced overnight at 22 °C by adding 0.2 mM IPTG when cells reached an OD₆₀₀ of ~ 0.6. Cells were grown overnight with shaking at 250 rpm (for approximately 16 h).

In the following day, purification proceeded taking advantage of the HIS tag on the N-terminus of M18c. Cells were then harvested in a Beckman Coulter Allegra X-12R centrifuge for 30 min at 3,270 xg. A purification buffer described as A400 were made containing 25 mM HEPES, 400 mM KCl, 10 % (v/v) Glycerol, 1mM β-mercaptoethanol, 5 mM imidazole pH 8.0 and EDTA-free protease inhibitors (1 tablet/ 50ml). This buffer was used to resuspend the cell pellets. At this stage the resuspended pellets could either be stored at -80 °C or could be used straight away to continue protein purification.

Lysozyme was added to the resuspended cells to a final concentration of 1 mg/ml and the mixture was incubated for 30 min on a rotator at 4 °C. To achieve cell lysis, cells were sonicated for 6 x 20 sec periods with 20 sec intervals on ice. Sonications were performed using a Sanyo Soniprep 150 sonicator, set at an amplitude of 15 microns. DNA was then digested by the addition of *DNase I* (10 µg/ml) for 30 min at 4 °C. The lysate was then clarified by centrifugation in a pre-cooled Beckman JA-20 rotor for 1 hour at 48,400 xg at 4 °C, and 3 ml of Ni-NTA agarose (pre-equilibrated in A400 buffer) was added, mixed and

incubated for 2 h at 4 °C with constant rotation. Lysate-containing beads were divided into 50 ml tubes and centrifuged at 500 xg for 5 min. The supernatant was removed and each tube containing beads were resuspended in 5 ml of buffer A400 containing 15 mM imidazole and applied to a Bio-Rad Eco-pac disposable chromatography column. 200 ml of A400 (+15 mM imidazole) was used to wash the column (approximately 8 washes). This was followed by a further wash in 200 ml of A200 containing 15 mM imidazole, 20 mM MgCl₂ and 5 mM ATP Na-salt (MgCl₂ and ATP were added to the buffer in order to wash off any GroEL that may co-express with M18c).

Protein was then eluted in A200 plus 500 mM imidazole at pH 7.4. The amount of elution buffer corresponded to the amount of beads used. So, for 3 ml Ni-NTA beads, 3ml elution buffer was added. After 15 min incubation with the beads, the eluted sample was allowed to flow through the column into a 15 ml corning tube. This step was repeated 4 times to increase the chances of obtaining as much protein as possible from the beads. The eluates were aliquoted into 200 µl samples, snap frozen in liquid nitrogen and stored at - 80 °C until use.

2.2.5 Cytoplasmic Insulin Receptor (tyrosine) Kinase - “CIRK”

2.2.5.1 CIRK activation

The cytoplasmic insulin receptor kinase (CIRK) consists of amino acids 941-1343 of the β-subunit of the insulin receptor and it was expressed and purified from Baculovirus-infected Sf9 cells by Melanie Cobb (Prof Lienhard lab, Dartmouth medical school, USA). In order to activate this receptor, first one vial containing 1 ml CIRK was thawed on ice and diluted with an equal volume of buffer A (4 mM ATP (Na-salt), 5 mM MnCl₂, 100 mM HEPES pH 7.5, sterilised before use). After incubation at 30 °C for 30 min, CIRK was diluted 10-fold into buffer B (1 mM DTT, 10 % glycerol, 50 mM HEPES pH 7.5). At this stage, CIRK was activated, the concentration was 0.37 mg / ml and the specific activity was 46 nmol/ min/ mg. The solution was then divided into several tubes (50 µl aliquots), snap-frozen in liquid nitrogen and finally stored at - 80 °C.

2.2.5.2 Proteins phosphorylation by CIRK

In an eppendorf tube, autophosphorylated CIRK and the recombinant protein of interest were mixed and made up to a final volume of 50 µl in filter sterilised buffer C (50 mM

HEPES pH 7.5, 4 mM MnCl₂, 0.2 mM freshly made DTT, 100 μM ATP Na-salt).

Samples were incubated at 30 °C in a water bath, and the time of incubation varied from 30 to 150 min. After the reaction was finished, phosphorylated protein was tested in pull-downs.

2.2.5.3 Stoichiometry of protein phosphorylation in response to CIRK

Stoichiometry of phosphorylation was determined by phosphorylating the protein of interest with [γ -³²P]ATP of known specific activity. Protein plus CIRK made up to a final volume of 50 μl in buffer C, were incubated with 6 μCi [γ -³²P]ATP at 30 °C in a pre-warmed water bath and the time of incubation varied depending on the protein studied (from 30 to 150 min). The labelled protein was then isolated and analysed by gel electrophoresis. The control was repeating the solution above without CIRK. After electrophoresis, SDS-PAGE gels were stained with Coomassie Blue as described in section 2.2.2.3, destained and dried. Gels were then exposed to a X-ray film in a cassette with no intensifying screen for different times ranging from 24 h to 72 h, at room temperature.

The stoichiometry of protein phosphorylation was calculated by measuring counts per min (cpm) from a given sample. The cpm of the analysed proteins were determined by excising the dried gel band corresponding to each of the proteins, placing them in vials and measuring cpm using a scintillation counter programmed to measure phosphorus-32. Knowing the molecular weight of the molecule, the amount of protein loaded and the cpm obtained, it is possible to calculate an estimate of the percentage of the protein that is phosphorylated.

2.2.6 Immunoprecipitation using anti-phosphotyrosine agarose

Fully differentiated 3T3-L1 adipocytes were kindly given by Dr Rebecca McCann in order to perform immunoprecipitation experiments using anti-phosphotyrosine agarose (anti-PTyr).

Two different 10-cm dishes containing differentiated adipocytes were incubated with 10 ml of pre-warmed serum-free media for 2 h. Cells were stimulated with and without 150 nM insulin for 5 min. Plates were washed twice with 5 ml ice-cold HPFE buffer (25 mM HEPES, 10 mM, sodium pyrophosphate, 50 mM sodium fluoride and 10 mM EDTA pH 7.4). Cells were solubilised by adding 5ml of HPFE buffer containing 1 % (v/v) Thesit plus

protease inhibitors, gently scraped off the plate with a cell scraper, then triturated. Both lysates were placed in 15 ml corning tubes on ice for 20 min. Lysates were spin at 50,000 xg in an ultracentrifuge at 4 °C for 1 h at 4 °C.

Meanwhile, an aliquot of anti-PTyr-Agarose (50 μ l) was mixed with 1ml of HPFE/Thesit. This mix was centrifuged for 30 seconds at 9,300 xg , then supernatant was removed and discarded. This step was repeated twice before resuspension in 50 μ l HPFE/Thesit.

When the ultracentrifuge stopped, tubes were removed carefully and fat residues were gently aspirated off the top of the tubes. The supernatant, which contains the solubilised proteins, were decanted into clean tubes and divided into 1 ml aliquots. These aliquots were stored at - 80 °C until use.

To one 1 ml basal aliquot, 25 μ l of anti-PTyr-agarose was added and tube was sealed with Nescofilm. The same was done to the 1 ml of insulin-treated lysate. Tubes were rotated in the cold room for 3 h, then spun at 9,300 xg for 30 seconds. Supernatants were removed and frozen at - 80 °C. Beads were gently mixed with 1ml HPFE/Thesit plus protease inhibitors and spun at 9,300 xg for 30 seconds. The supernatants were aspirate off and this step was repeated twice more. However, in the final wash, beads were resuspended in HPFE buffer containing 0.1 % Thesit instead of 1 %. This reduced detergent wash was performed to reduce the non-ionic detergent in the sample. Thus, after this final spin, the supernatant was aspirated off and beads were resuspended in 40 μ l of 1 x SDS-PAGE buffer containing 20 mM DTT. Samples were boiled for 5 min at 95 °C. Samples were spun for 30 seconds at 9,300 xg and supernatant was carefully removed and placed into fresh tubes. This contains the immunoprecipitated proteins released from the PTyr agarose. 25 μ l samples were run on a SDS-PAGE and probed with anti-PTyr antibody and anti-M18c antibody.

Chapter 3

3 *In vitro* studies of Munc18c binding modes to cognate SNARE proteins

3.1 Introduction

Among several proteins that interact with syntaxins, members of the Sec1p/Munc18 family have been shown to bind with high affinity and are proposed to be important regulators of syntaxin function. Different SM proteins show high sequence homology suggesting a similar structure. However, the mechanisms of interaction between SM proteins and syntaxins appear to differ. The neuronal syntaxin known as Sx 1A is one of the best characterised syntaxins to date. As mentioned in the introduction (section 1.2.1), Sx 1A has the ability to switch between two different conformations, “open” and “closed” (Dulubova *et al.*, 1999). It was thought that the SM protein M18a was only able to bind Sx 1A in the closed conformation preventing this syntaxin from forming SNARE complexes (Misura *et al.*, 2000). However, recent data indicates that M18a is also able to bind open Sx 1A and Sx 1A assembled in SNARE complexes (Burkhardt *et al.*, 2008; Khvotchev *et al.*, 2007).

In recent years, several studies have focussed their attention in identifying which regions in both SM and syntaxins are important for their interaction. The crystal structure of M18a in complex with Sx 1A revealed the SM protein as an arch-shaped molecule containing three different domains, which form a central cavity that cradles Sx 1A in its closed conformation (Misura *et al.*, 2000) (see introduction, figure 1.7C and D). On the other hand, the crystal structure of the yeast SM protein Sly1p in complex with a short N-terminal peptide of Sed5p revealed that these two proteins interact in a different way (Bracher and Weissenhorn, 2002). Sly1p was shown to also be a three-domain arch-shaped molecule, but in contrast to the M18A/Sx 1A interaction, the Sed5p N-terminal peptide inserts into a hydrophobic pocket on the outer face of domain I on Sly1p. Interestingly, residues 1-139, which are part of domain I in M18c (similar to M18a domains; figure 1.7A), were also shown to interact with Sx 4 in pull-down and yeast two-hybrid binding assays (Grusovin *et al.*, 2000). Apart from Sed5p/Sly1p, this N-terminal mode of interaction was subsequently observed between Sx 1A, Sx 4, Sx 5, Sx 16, Tlg2p and their respective SM proteins M18a, M18c, mVps45p and Vps45p (Burkhardt *et al.*, 2008; Carpp *et al.*, 2006; Dulubova *et al.*, 2003; Dulubova *et al.*, 2002; Hu *et al.*, 2007; Khvotchev *et al.*, 2007).

SM protein interaction with SNARE complexes has been observed in both yeast and mammalian systems. In neuronal cells, M18a was shown to interact directly with the assembled neuronal SNARE complex formed by Sx1A/SNAP25/VAMP2 (Dulubova *et al.*, 2007). Another study has reported that M18c, apart from directly binding to monomeric Sx

4, also binds to the assembled Sx4/SNAP23/VAMP2 SNARE complex (Latham *et al.*, 2006). In yeast, the relationship between the SM protein Sly1p and the syntaxin Sed5p, which are essential for ER to Golgi vesicular transport, were also studied. Interestingly, the binding of Sly1p to Sed5p not only allows the efficient formation of SNARE complexes, but also prevents non-specific SNARE complex formation (Peng and Gallwitz, 2002).

The sole interaction with syntaxins is unlikely to be the only way by which SM proteins regulate membrane fusion, since interactions with non-syntaxin SNAREs could also be important. For example, in yeast, the SM protein Vps45p not only binds directly to its cognate syntaxin, Tlg2p, but also binds to the assembled SNARE complex and the v-SNARE Snc2p (Carpp *et al.*, 2006). Interestingly, Sly1p is also able to interact with the non-syntaxin SNARE proteins Bet1p, Bos1p, Sft1p and Gos1p (Peng and Gallwitz, 2004). Together, all these data indicate that SM proteins might not only regulate the SNARE complex assembly/disassembly through interaction with syntaxins, but also *via* their interaction with v-SNAREs.

3.2 Aims of this chapter

In this study, I have examined the molecular interactions of the SNARE proteins Sx 4 and VAMP2 with the SM protein M18c, which are all involved in GLUT4 trafficking. Several pull-down assays using recombinant proteins were performed to demonstrate the novel finding that M18c not only binds to the t-SNARE Sx 4, but also binds to the v-SNARE VAMP2. Also, to confirm whether M18c utilise a pocket mode of interaction similar to the one captured by Sly1p/Sed5p crystal structure and by Tlg2p/Vps45p, sequence comparison analysis and site-directed mutagenesis studies were carried out.

3.3 Results

3.3.1 M18c interaction with non-syntaxin SNAREs

Recently, it has been demonstrated that SM proteins are able to interact with non-syntaxin SNARE proteins. Since this finding was observed in yeast, we decided to carry out similar studies using proteins that mediate fusion of GLUT4 vesicles with the PM in muscle and fat cells. In order to check if an interaction occurs between the SM protein M18c and the v-SNARE VAMP2, pull-down assays were performed in which recombinant expressed proteins containing the cytosolic domains of the GST-tagged proteins Sx 4, VAMP2,

VAMP4 and VAMP8 were first immobilised on glutathione sepharose and then incubated with recombinant His₆-M18c. As control proteins we used soluble GST, and the v-SNAREs VAMP4 (found in the TGN but also in early endosome compartments) and VAMP8 (which was shown to play a role in the PM retrieval of GLUT4 (Williams and Pessin, 2008)). After extensive washing, proteins bound to the GST beads were assessed by immunoblotting using α -M18c antibody.

As shown in figure 3.1, His₆-M18c binds to GST-fusion proteins harbouring the cytosolic domains of Sx 4 (amino acid residues 1-273) and VAMP2 (amino acid residues 1-92), but not those harbouring the unrelated VAMP4 and VAMP8.

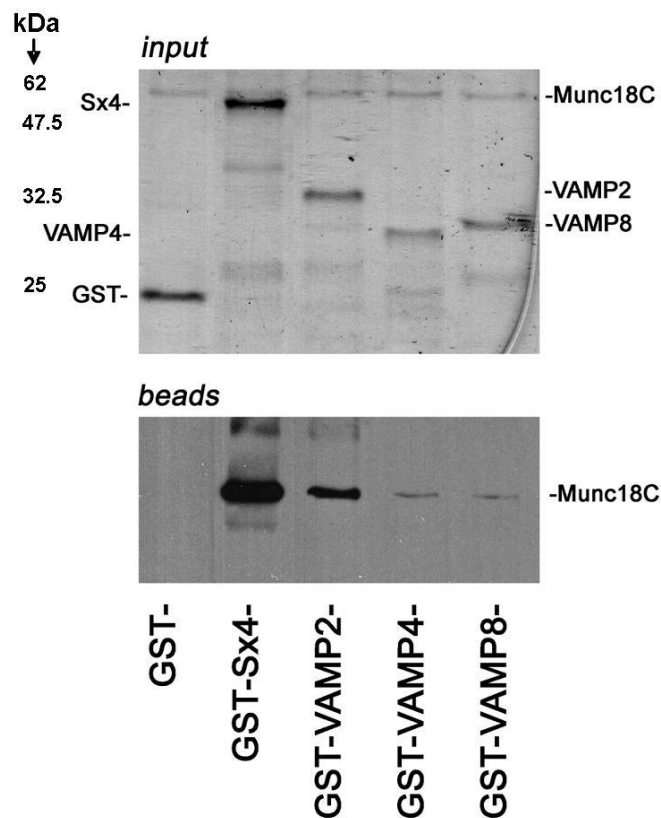


Figure 3.1 M18c interacts specifically with the non-syntaxin SNARE VAMP2

Pull-down assay was performed where 5 μ g of either recombinant GST, or GST fused to the cytosolic domain of Sx 4, VAMP2, VAMP4 or VAMP8 were firstly immobilised on glutathione Sepharose. Beads were then incubated overnight at 4 $^{\circ}$ C with 5 μ g of His₆-tagged M18c in a final volume of 500 μ l. 4 % of each mixture was removed to assess protein input. After extensive washing, bound proteins were eluted, resolved by SDS-PAGE and immunoblot analysis was carried out to determine which of the GST proteins M18c had bound to (for a more detailed protocol, see section 2.2.2.6). Upper panel represents a Coomassie stained gel of the GST-fusion proteins/Munc18c inputs (4 % of the total input); lower panel shows immunoblot analysis with α -M18c antibody used to determine bound M18c (~ 67 % of the final sample was loaded into the gel).

3.3.2 M18c interacts with the SNARE motif of VAMP2

Since His₆-M18c was able to bind cytosolic GST-VAMP2, we then sought to examine which region of VAMP2 was important for its interaction with M18c. The SNARE motif of the yeast v-SNAREs Snc2p and Bet1p/Bos1p/Gos1p were shown to be important for their interaction with Vps45p and Sly1p respectively (Carpp *et al.*, 2006; Peng and Gallwitz, 2004). VAMP2 is a small protein comprising 116 amino acids. It contains a short N-terminal region of 30 amino acids prior to the SNARE motif (Figure 3.2A). To determine whether this region was required for M18c binding, a truncated version of VAMP2 was generated. A construct containing cytosolic VAMP2, in which all of the N-terminus was deleted (VAMP2Δ) leaving only the SNARE domain, was cloned into the vector pGEX4T-1. Cytosolic VAMP2Δ was generated by PCR using pGEX-VAMP2 as template. Primers used to amplify desired sequence were:

VAMP2Δ Forward: 5' GGA TCC AGA CTG CAG CAG ACC CAG 3'

VAMP2Δ Reverse: 5' GAA TTC TTA CAT CTT GAG GTT TTT CCA 3'

Cytosolic VAMP2Δ (30-92) was cloned between the *Bam*HI and *Eco*RI sites in pGEX4T-1. Truncated VAMP2 was then expressed in *E.coli* as a GST fusion protein and it was tested for its ability to bind His₆- M18c. Pull-down assays were performed in which set amounts of recombinant GST, GST- Sx 4, GST-VAMP2 and GST-VAMP2Δ were immobilised on glutathione sepharose beads before overnight incubation with His₆- M18c. After extensive washing, bound protein was analysed by Western blot using an antibody against M18c.

Panel C in Figure 3.2 demonstrates that the VAMP2 SNARE motif accounts for the M18c-VAMP2 interaction since VAMP2 lacking the amino terminus retained the ability to efficiently bind M18c *in vitro*.

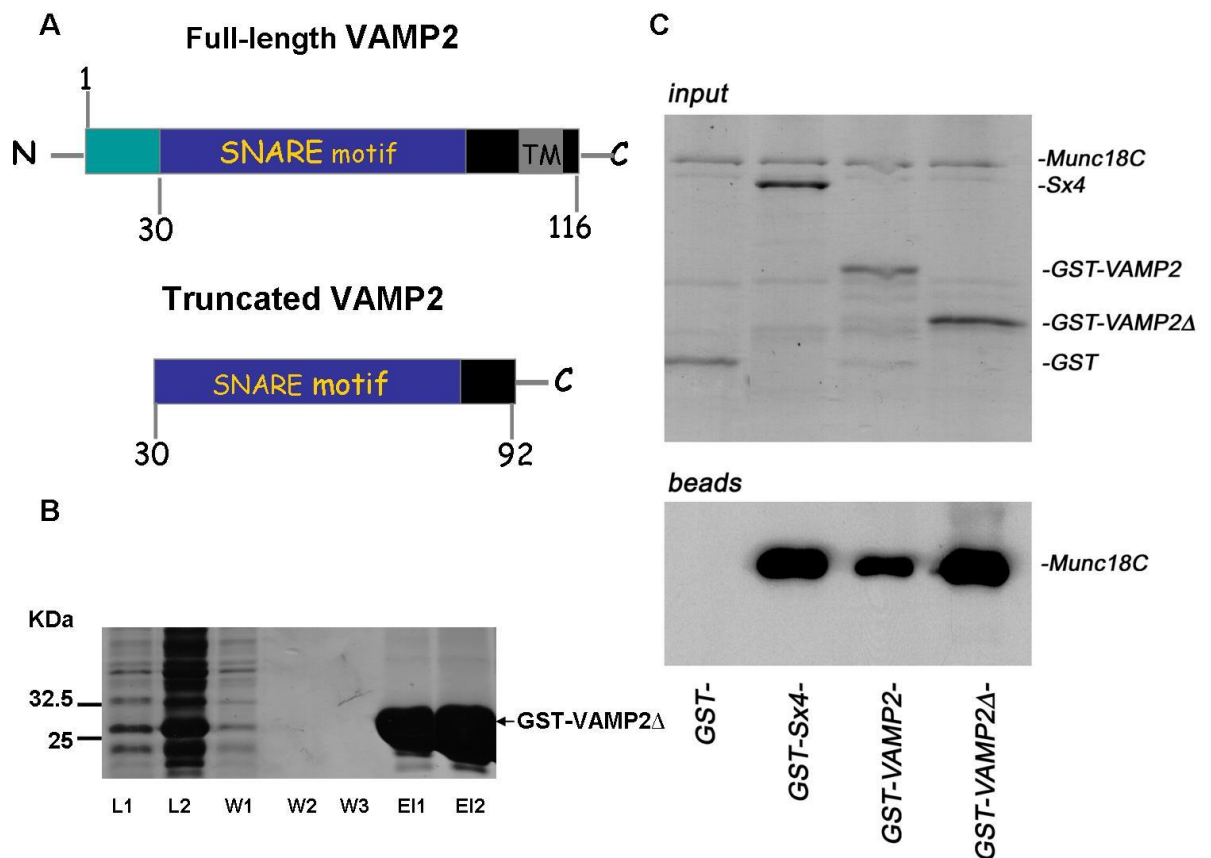


Figure 3.2 His₆-M18c binds the SNARE motif of GST-VAMP2

(A) Schematic diagram comparing full-length VAMP2 with cytosolic VAMP2 harbouring only the SNARE motif (VAMP2 Δ) which was used to map M18c binding. (B) A mutant of VAMP2 lacking the first 30 amino acids was generated by PCR and expressed as an N-terminal GST-fusion protein from vector pGEX4T-1 in BL21 (DE3) *E.coli* cells. Protein production was induced overnight at 24 °C by adding 0.5 mM IPTG. Protein purification was carried out as outlined in section 2.2.2.4. Lower panel shows VAMP2 Δ resolved by SDS-PAGE and visualised by staining with Coomassie Blue. The figure shows the purity of the pre-spin Lysate (L1), post-spin lysate (L2), wash 1 (W1), wash 2 (W2), wash 3 (W3) and protein samples (10 μ l) eluted using 15 mM Reduced Glutathione (E11, E12). (C) Pull-down assay was performed to test the ability of His₆-M18c to bind to GST-VAMP2 Δ using the same protocol as described in figure 3.1. Upper panel represents a Coomassie stained gel of the GST-fusion proteins/ His₆-M18c inputs (4 % of the total input); lower panel shows immunoblot analysis with α -M18c antibody used to determine bound His₆-M18c (~ 67 % of the final sample was loaded into the gel). This result was confirmed by repeating this experiment several times.

3.3.3 GST-Sx 4 displaces GST-VAMP2 from His₆-M18c in a dose dependent manner

Since we observed that both GST-VAMP2 and GST-Sx 4 interact with His₆-M18c, we sought to determine whether the binding sites of either protein could overlap. Thus, a set amount of His₆-M18c was immobilised on Ni²⁺-nitrilotriacetic acid-agarose (Ni-NTA agarose) before overnight incubation with GST-VAMP2. After extensive washing,

increasing amounts of GST-Sx 4 were added to beads containing both His₆-M18c and GST-VAMP2. Then, after several washes with binding buffer, the bound material was analysed by 12 % SDS-PAGE followed by immunoblot analysis using antibody against VAMP2. The unrelated yeast syntaxin Tlg2p was used as a negative control.

Figure 3.3 shows the result of a typical competition assay. Whilst GST-Sx 4 was able to displace GST-VAMP2 from His₆-M18c in a dose-dependent manner, the unrelated PrA-Tlg2p was not. This data indicates that GST-VAMP2 is specifically displaced from His₆-M18c by GST-Sx 4.

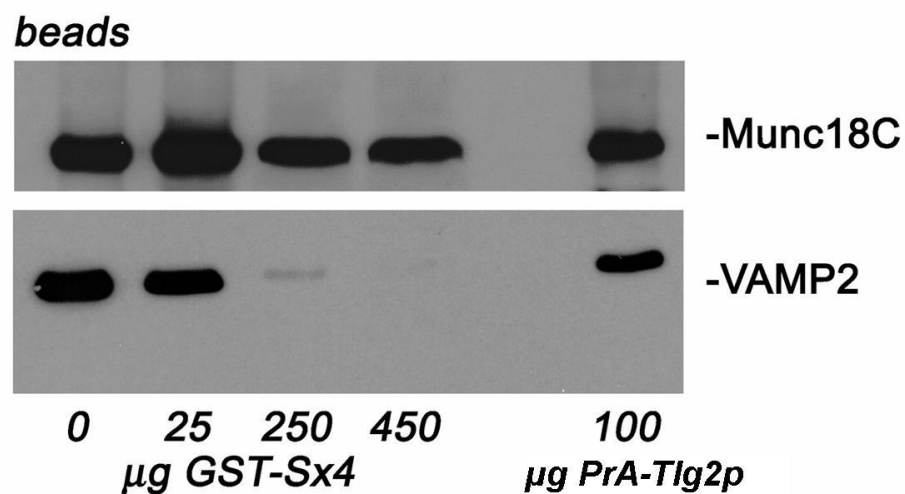


Figure 3.3 GST- Sx 4 displaces GST-VAMP2 from His₆-M18c.

Pull-down assay was performed in which 5 μg of M18c was immobilised on Ni-NTA agarose and incubated overnight with 10 μg of GST-VAMP2. This pre-formed complex was then incubated with increasing concentrations of GST-Sx 4 or the unrelated yeast syntaxin PrA-Tlg2p as a negative control. PrA-Tlg2p was generously given by Dr Lindsay Carpp. Upper panel shows immunoblot analysis using α-M18c antibody to determine levels of M18c immobilised on the beads (~ 33 % of final sample). Lower panel shows immunoblot analysis using α-VAMP2 antibody to determine the amount of VAMP2 that remained bound to the beads (~ 67 % of the final sample was loaded). A typical experiment is shown.

3.3.4 GST-VAMP2 is not able to displace GST-Sx 4 from His₆-M18c

The ability of VAMP2 to displace bound GST-Sx 4 from His₆-M18c was also investigated. A similar approach was taken as in section 3.3.3. Firstly, GST-Sx 4 and His₆-M18c were immobilised on Ni-NTA agarose, and then increasing amounts of GST-VAMP2 were added in order to displace GST-Sx 4 from His₆-M18c.

Figure 3.4 shows that increasing amounts of GST-VAMP2 are not able to displace GST-Sx 4 from His₆-M18c.

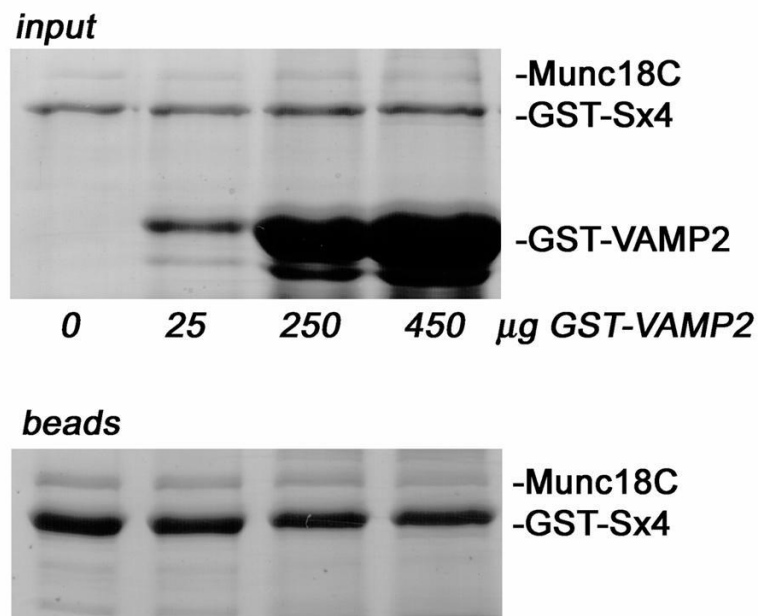


Figure 3.4 GST-VAMP2 is not able to displace GST-Sx 4 from His₆-M18c.

Pull-down assay was performed in which 5 µg of His₆-M18c was immobilised on Ni-NTA agarose and incubated overnight with 10 µg of GST-Sx 4. GST-Sx 4/His₆-M18c complexes were recovered on Ni-NTA agarose and increasing amounts of GST-VAMP2 were added to attempt to displace GST-Sx 4 from His₆-M18c. The upper panel shows 4 % of total protein input which was analysed by SDS-PAGE followed by Coomassie Blue staining. The lower panel shows the amount of GST-Sx 4 that remained bound to the beads. This was also analysed by Coomassie staining (~ 67 % of final sample was analysed). This figure represents data from a typical result, repeated three times.

3.3.5 The importance of the GST tags present in both VAMP2 and Sx 4 in the competing assay results

Since both Sx 4 and VAMP2 were recombinantly expressed from *E.coli* as GST-fusion proteins, this raised some doubts: could the GST-tags in each protein affect their interaction with each other, thus affecting the competition assay results? In order to answer this question, a similar approach as before was taken, however this time both VAMP2 and Sx 4 GST-tags were thrombin cleaved prior to their addition into the pull-down assays. In order to cleave the fusion proteins from their GST tags, after performing protein purification as outlined in section 2.2.2.4, VAMP2 and Sx 4 were eluted from the beads by incubating the beads with thrombin in PBS for 4 h at room temperature. Then, a similar approach to sections 3.3.3 and 3.3.4 was taken, however this time using VAMP2 and Sx 4 lacking the GST tags.

Figure 3.5 shows a typical set of results. As it can be seen, cleaved VAMP2 is not able to displace Sx 4 from His₆-M18c (A). In contrast, cleaved Sx 4 is able to displace VAMP2 from His₆-M18c (B). This result confirms that the VAMP2 and Sx 4 GST tags present in the previous competing experiments did not contribute to the results obtained.

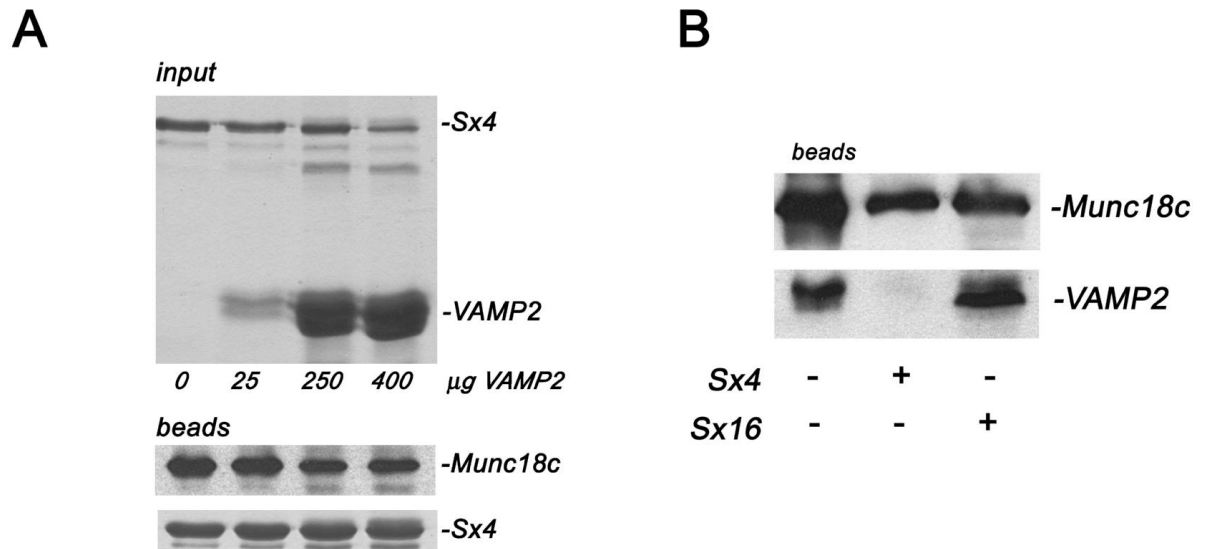


Figure 3.5 Untagged versions of both VAMP2 and Sx 4, when used in the competition experiments, give the same results as their tagged versions

(A) 5 μg of M18c was immobilised on Ni-NTA agarose and incubated overnight at 4 °C with an excess (10 μg) of Sx 4 cytosolic domain. After extensive washing, the M18c/Sx 4 complex was incubated with increasing amounts of cytosolic VAMP2. The upper panel shows a Coomassie Blue stained gel of the input proteins, the lower panel shows an immunoblot of the beads probed with anti-M18c (control), or stained with Coomassie Blue to show the levels of Sx 4 which remained bound to the beads. (B) Again, 5 μg of M18c was immobilised on Ni-NTA agarose followed by overnight incubation with an excess (10 μg) of cytosolic VAMP2. After extensive washing, the M18c/VAMP2 complex was subsequently incubated alone or with 250 μg of cytosolic Sx 4 or (as a control) 250 μg Sx 16 cytosolic domain (amino acid residues 1-269), as indicated. Upper panel represents the result of an immunoblot analysis using anti-M18c to show levels of M18c which remained bound to the beads and lower panel shows also an immunoblot analysis to determine the amount of VAMP2 that remained bound to the beads.

3.3.6 M18c and Sx 4 different modes of interaction

As mentioned previously in section 3.1, the function of SM proteins is controversial, since their mode of binding to their cognate syntaxins varies depending on the organism and pathway studied. Interestingly, several studies performed using both yeast and mammalian proteins, have identified a hydrophobic pocket on the outer face of domain I of the SM protein. A hydrophobic pocket was identified in the crystal structure of Sly1p in complex with the N-terminal 45 residues of Sed5p (Bracher and Weissenhorn, 2002) and mutations performed in the hydrophobic pocket of yeast Vps45p also identified that this region is important for binding the short N-terminal peptide in Tlg2p (Carpp *et al.*, 2006).

3.3.6.1 Alignment of M18c against Vps45p

Yeast Vps45p interacts with Tlg2p *via* two different modes: with monomeric Tlg2p and with cis-SNARE complexes *in vivo* (Bryant and James, 2003). This interaction is mediated by the N-terminal region in Tlg2p in a similar manner to the Sly1p/Sed5p crystal structure (Dulubova *et al.*, 2002). Tlg2p/Vps45p binding occurs *via* a hydrophobic pocket in Vps45p which consists of residues L137, L140, A141, V153 and V156. The mutation of Sly1p L137 to an arginine disrupts Sly1p/Sedp5p binding (Peng and Gallwitz, 2004) and Dr Bryant's laboratory observed that the mutation of Vps45p L117 to an arginine also disrupts the binding of Vps45p to Tlg2p (Carpp *et al.*, 2006). Therefore, sequence comparison between yeast Vps45p and mouse M18c was performed to identify which residue in M18c corresponds to the residue L117 in the Vps45p sequence.

Figure 3.6 shows a CLUSTALW multiple sequence alignment between Vps45p and M18c indicating residue F119 (M18c) in alignment with L117 (Vps45p). This residue was also identified by another research group in 2006, which by performing sequence alignments of M18c in comparison to Sly1p, have also identified a N-terminal hydrophobic pocket on M18c corresponding to residues F119, I122, C126, I130 and C133. In their study, residue L137 in yeast Sly1p corresponded to residue F119 in M18c (Bracher and Weissenhorn, 2002; Latham *et al.*, 2006).

```

Vps45p      YLVERIENEQREVSRHLRCLVYVKPTEETLQHLLRELRNP---RYGEYQIFFSNIVSKSQ 116
Munc18c     TVIENIYKN-REPVRQMKALYFISPTPKSVDCFLRDFGSKSEKKYKAAYIYFTDFCPDSL 118
           :*:.*  ::  **  *:::.*  :::.*  :::  :*:  .  :*  *:*:::  ..*

Vps45p      LERLAESDDLEAVTKVEEIFQDFFILNQDLFSFDLQPREFLSN-----KLVWSEGGLTKC 171
Munc18c     FIKIKAS-CSKSIRRCKEINISFIPQESQVYTLDVDPDAFYCYSPDPSNASRKEVMEAM 177
           :::  *  :::  :  :**  .*:  :::  :*:  :  .  :  .  *  :

```

Figure 3.6 CLUSTALW multiple sequence alignment between Vps45p and M18c

Vps45p sequence from *S. cerevisiae* and M18c sequence from mouse were aligned using Clustalw software. The hydrophobic residue L117 in Vps45p corresponds to the hydrophobic residue F119 in M18c and both are highlighted in red. Sequence alignments between different SM proteins were also performed by other research groups confirming the importance of residue F119 M18c (Hu *et al.*, 2007; Latham *et al.*, 2006).

3.3.6.2 Generation of His₆-M18cF119A

In order to assess the importance of residue F119 in the formation of the Sx 4/M18c complex, the highly hydrophobic amino acid phenylalanine was changed to the less hydrophobic residue alanine by site-directed mutagenesis. The F119A mutation was introduced into the M18c sequence using pQE30-M18c as template and mutation was performed as outlined in section 2.2.1.2. Primers were designed taking in consideration melting temperature, length and GC content of the primer. Primers used were (letters in bold refer to original codon and underlined refer to mutated codon):

M18c sequence: 5' TGT CCT GAC AGT CTC **TTT** AAC AAG ATT AAA GCA 3'

F119A Forward: 5' TGT CCT GAC AGT CTC GCT AAC AAG ATT AAA GCA 3'

F119A Reverse: 5' TGC TTT AAT CTT GTT AGC GAG ACT GTC AGG ACA 3'

Successful mutation was confirmed by DNA sequencing of both strands.

His₆-M18cF119A was expressed, similarly to wild-type M18c, in M15 *E. coli* cells that also co-expressed the chaperone protein GroEL in order to increase M18cF119A solubility. During His₆-M18cF119A protein purification, low levels of IPTG were used (0.2 mM) and protein expression was induced at 22 °C overnight as outlined in section 2.2.4 as these conditions were empirically determined to give better levels of expression. His₆-M18cF119A was purified using Ni-NTA agarose.

A typical purification is shown in figure 3.7.

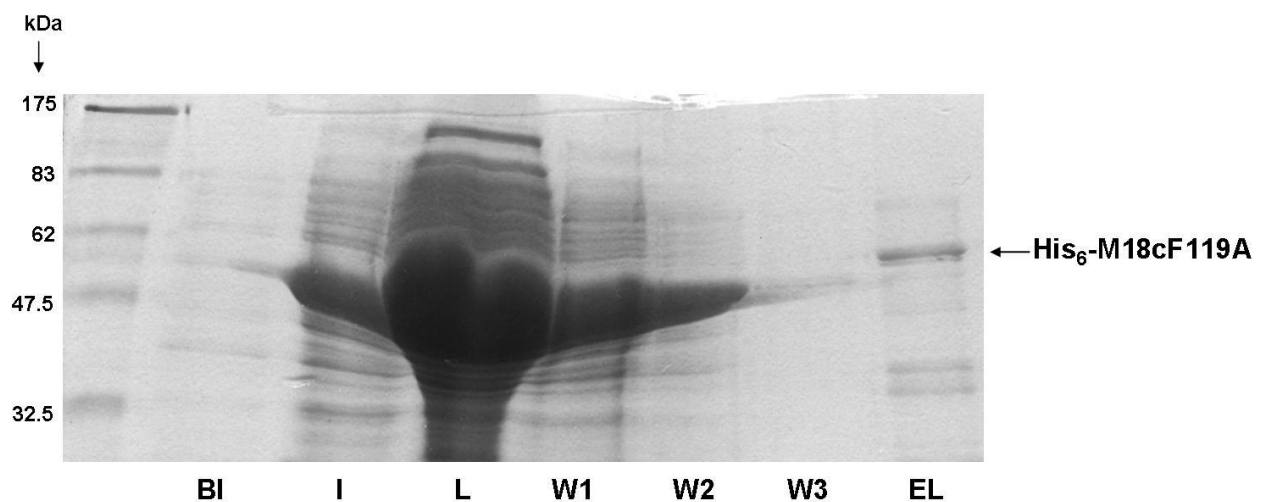


Figure 3.7 SDS-PAGE analysis of His₆-M18cF119A protein purification

His₆-M18cF119A was expressed from vector pQE30 in M15 *E. coli* expressing the chaperone GroEL. Expression was induced by adding 0.2 mM IPTG and incubation was carried out overnight at 22 °C. The figure shows several samples taken during the process of protein purification which were run on a 12 % SDS-PAGE gel and stained with Coomassie Blue as outlined in sections 2.2.2.1 and 2.2.2.3 respectively. The positions of the molecular weight markers are shown on the left. The first lane corresponds to a sample before induction (BI) followed by a sample after induction (I), sample from the lysate (L), wash 1 (W1), wash 2 (W2), wash 3 (W3) and fraction eluted (10 μl) using 500 mM imidazole (EL).

3.3.6.3 The effects of the M18c “hydrophobic pocket” mutation on its binding to both GST-Sx 4 and GST-VAMP2

In order to test whether the F119A mutation in M18c could affect its binding to either GST-Sx 4 or GST-VAMP2, pull-down experiments were carried out in which set amounts of the GST-Sx 4 recombinant proteins and GST-VAMP2 were immobilised on glutathione sepharose beads before incubation with His₆-M18cF119A. GST alone was used as a negative control in the pull-downs. Both N- and C-terminally tagged versions of Sx 4 were used in order to assess if the tag's position could cause any difference in binding to His₆-M18cF119A (GST tag at the N-terminus could block binding *via* the N-terminal domain of Sx 4 in contrast to the C-terminally tag version as shown in chapter 4, section 4.1.1). The N-terminal tag could favour an interaction *via* the closed conformation of Sx 4, whereas the C-terminal tag could favour an interaction *via* the open conformation of Sx 4 (Aran *et al.*, 2009).

The result of a typical experiment is shown in figure 3.8. GST-fusion proteins harbouring the cytosolic domains of N- and C-terminally tagged Sx 4 and VAMP2 efficiently bound wild-type His₆-M18c. In contrast, these proteins were unable to bind His₆-M18cF119A.

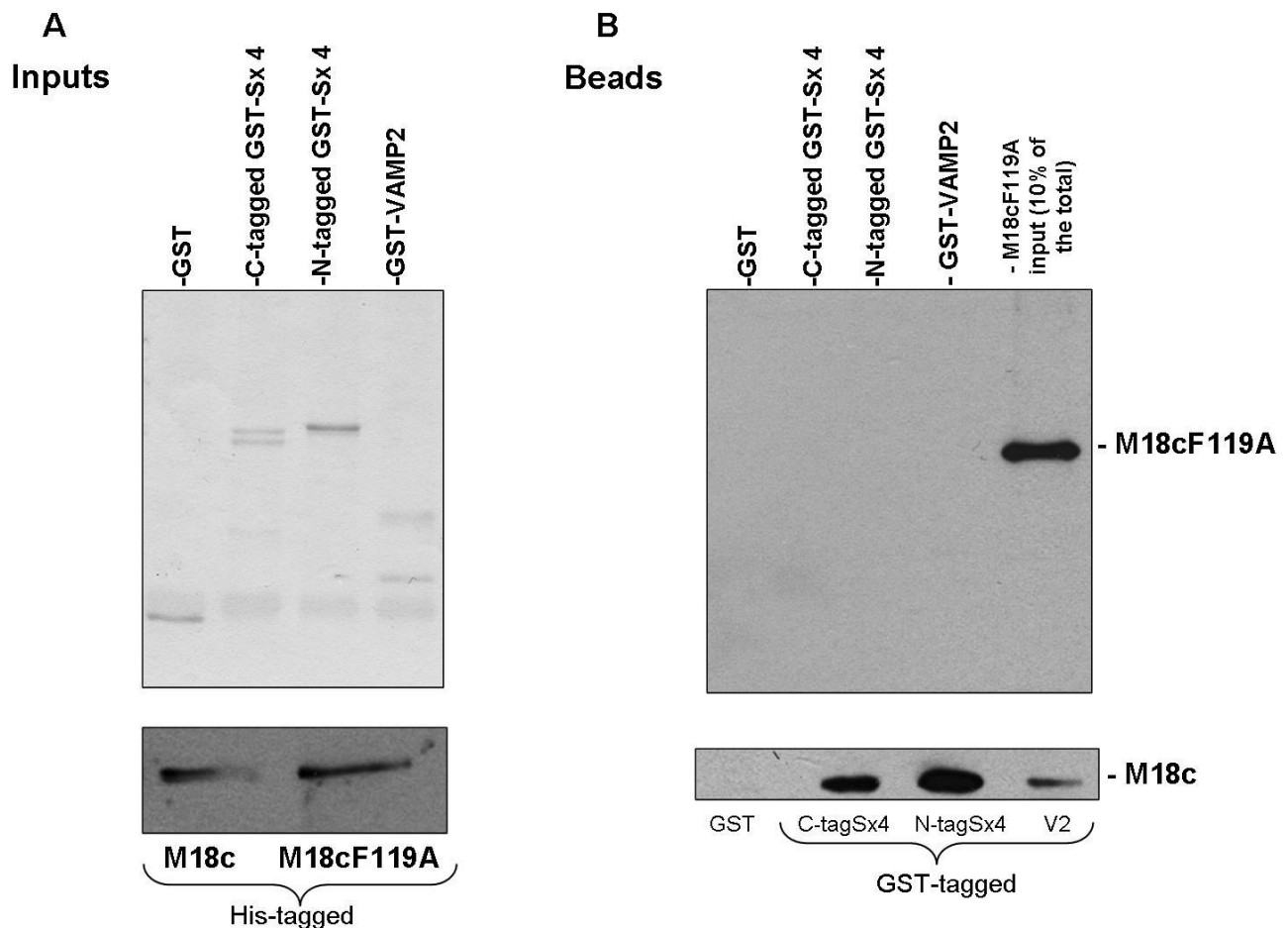


Figure 3.8 A hydrophobic pocket mutation in His₆-M18c disrupts its binding to SNARE proteins *in vitro*

Pull-down assays were performed where 5 μ g of either recombinant GST, or GST fused to the cytosolic domain of Sx 4 (C-tagged), Sx 4 (N-tagged) and VAMP2 were firstly immobilised on glutathione Sepharose. Beads were then incubated overnight at 4 $^{\circ}$ C with either 5 μ g of His₆-tagged M18c or 5 μ g of His₆-tagged M18cF119A in a final volume of 500 μ l. 4 % of each mixture was removed to assess protein input. After extensive washing, bound proteins were eluted by boiling beads with 15 μ l of 1 x sample buffer (+ 20 mM DTT), resolved by SDS-PAGE and immunoblot analysis were carried out to determine which of the GST proteins His₆-M18c or His₆-M18cF119A had bound to. **(A)** Upper panel represents a Coomassie stained gel of the GST-fusion proteins (4 % of the total input); lower panel shows immunoblot analysis with α -M18c antibody used to determine 5 % of total His₆-M18c and His₆-M18cF119A used in the pull-downs. **(B)** Upper panel shows immunoblot analysis with α -M18c antibody used to determine bound His₆-M18cF119A (80 % of the total final sample was tested); lower panel also shows an immunoblot analysis using α -M18c antibody in order to determine bound wild-type His₆-M18c (80 % of the total final sample was tested). This experiment was repeated with similar results.

3.4 Discussion

The interaction between syntaxins and SM proteins has been proposed as a potential regulatory step in the process of SNARE-mediated membrane fusion. Despite all the research performed in this area, the interaction of SM protein with non-syntaxin members was an unknown event until Peng and Gallwitz demonstrated that v- SNARE proteins could also interact with SM proteins in yeast (Peng and Gallwitz, 2004). The results presented in this chapter have reinforced this finding by demonstrating that the SM protein M18c, apart from binding Sx 4, also interacts specifically with VAMP2 *in vitro* (figure 3.1). During the course of this work, an interaction between VAMP2/M18a was also reported (Shen *et al.*, 2007). Nevertheless, the M18c/VAMP2 interaction has not been previously identified, providing new insight into the mechanism by which SM functions in muscle and adipose tissue.

M18c binding to VAMP2 does not require the short N-terminal peptide of VAMP2, since cytosolic GST-VAMP2 only harbouring the SNARE motif was still able to interact with His₆-M18c (figure 3.2). This result indicates that unlike Sx 4, M18c does not require the short N-terminal peptide of VAMP2 to interact. Furthermore, data presented in this chapter also demonstrated that Sx 4 can displace VAMP2 from His₆-M18c (figure 3.3 and 3.5B). In contrast, VAMP2 was unable to displace Sx 4 from His₆-M18c (figure 3.4 and 3.5A). An explanation for this could be that upon Sx 4/M18c binding, a conformational change in M18c occurs, which in consequence disrupts M18c binding to VAMP2. In fact, the two binding modes by which Sx 4 interacts with M18c (“open” and “closed”) suggest that affinity between these two proteins is strong and it could be higher than M18c/VAMP2 affinity. Moreover, the immunoblots performed to demonstrate that M18c binds VAMP2 (figure 3.1), also indicate that the amount of His₆-M18c which were recovered on GST-VAMP2 beads were smaller than that recovered on the GST-Sx 4 beads.

The “bridging hypothesis” by Peng and Gallwitz argues that the binding of specific v- and t-SNAREs on opposite membranes could involve SM proteins regardless of whether it is bound to syntaxin or not (Peng and Gallwitz, 2004). Thus, data presented here could serve as an indicator that the bridging theory could occur since both the v-SNARE VAMP2 and the t-SNARE Sx 4, which are present in opposite membranes, interact with M18c. Unfortunately, there was not enough time to perform careful and detailed investigation on whether M18c could bridge VAMP2 and Sx 4 interaction. Nevertheless, this interaction

might be very transient since Sx 4 displaces VAMP2 from His₆-M18c *in vitro* (figure 3.3 and 3.5B).

The other subject addressed in this chapter was the hydrophobic pocket mode of interaction between M18c and Sx 4. This N-terminal mode of interaction between syntaxins and SM proteins has been shown to be conserved from yeast to mammals with the determination of the structure of both the yeast Sly1p/Sed5p and the mammalian M18c/Sx 4 N-peptide complex (Bracher and Weissenhorn, 2002; Hu *et al.*, 2007). The hydrophobic residue L117 in yeast Vps45p was shown to be an important residue mediating Tlg2p/Vps45p interaction (Carpp *et al.*, 2006). Our alignment studies between M18c and Vps45p revealed that residue F119 corresponded to residue L117 in Vps45p (figure 3.6). Therefore, a mutant was generated by changing a phenylalanine to an alanine in residue F119. This mutation prevented both Sx 4 and VAMP2 binding to M18c (figure 3.8). Unfortunately, it was not possible to perform circular dichroism (CD) to analyse if the conformation of His₆-M18cF119A was affected by the mutation since the high levels of GroEL co-purified with recombinant His₆-M18cF119A could affect the CD measurements. Thus, a change in the overall structure of the mutant version of M18c could be the reason for the results obtained, although another group has also confirmed that mutation of F119 to glutamic acid disrupts binding of M18c to Sx 4 (Latham *et al.*, 2006). Structural analysis have also confirmed that the Sx 4 N-terminal residue L8 is important in mediating Sx 4 interaction with the hydrophobic pocket on the outer face of domain I in M18c and mutation of this residue (L8) to Lysine disrupts Sx 4 binding to M18c (Hu *et al.*, 2007; Latham *et al.*, 2006). In yeast, hydrophobic pocket mutations in Sed5p and Vps45p also prevented interaction with their respective syntaxins (Bracher and Weissenhorn, 2002; Carpp *et al.*, 2006). In contrast to data obtained in this chapter, Vps45p L117A mutant was shown to interact with the v-SNARE Snc2p (Carpp *et al.*, 2006). Figure 3.8B shows that His₆-M18c F119A was not able to interact with GST-VAMP2. This result indicates that, if His₆-M18c F119A protein is properly folded, there might be some sort of connection between the SNARE motif of VAMP2 and the hydrophobic region in the N-terminal of M18c.

In summary, the data presented in this chapter indicate that the SM protein M18c has two SNARE partners. These SNARE proteins correspond to the PM SNARE Sx 4 and the GLUT4 vesicle SNARE VAMP2 (Brandie *et al.*, 2008). However, Sx 4 showed a strong affinity to M18c, since it can displace VAMP2 from M18c but VAMP2 cannot do the same (Brandie *et al.*, 2008). The Sx 4/M18c affinity might involve two modes of

interaction, one being the interaction *via* the short N-terminal peptide in Sx 4, which inserts into a hydrophobic pocket in M18c, and one *via* the closed conformation of Sx 4 which is predicted to be similar to Sx 1A/M18a crystal structure (D'Andrea-Merrins *et al.*, 2007; Misura *et al.*, 2000). The His₆-M18c F119A mutant reinforced the existence of an N-terminal mode of interaction since this mutation abolished interaction to Sx 4. Therefore, this pocket mode of interaction could allow SM proteins not only to bind to monomeric syntaxins but also to SNARE complexes. All the different modes of interaction between SM and SNARE proteins might play an active role in the regulation of SNARE complex formation.

Chapter 4

4 Negative regulation of Sx 4/SNAP23/VAMP2-mediated fusion by Munc18c *in vitro*

4.1 Introduction

The role of SM proteins in membrane fusion has recently become the centre of attention in several studies in cell biology. While the SNARE proteins were shown to have a more defined role, the precise function of SM proteins has not yet been unravelled. However it is known that SM proteins might regulate positively or negatively SNARE function depending on the trafficking pathway and organism studied. In chapter 3, the novel finding that M18c not only binds Sx 4 but also binds VAMP2 was described. In this chapter, another approach was taken to determine how SM proteins interact with SNAREs. SNAREs were reconstituted into synthetic liposomes in order to perform *in vitro* fusion assays. This technique is an invaluable tool to study SNARE-mediated membrane fusion *in vitro*.

The fusion assay performed in this study was first described by Struck and colleagues (Struck *et al.*, 1981). It is a very useful tool to study the fusogenic properties of SNARE proteins, which were shown to promote spontaneous fusion of liposomes (Schuette *et al.*, 2004; Weber *et al.*, 1998; Zhang *et al.*, 2004). The fluorescence resonance energy transfer (FRET) capability between a donor fluorescent lipid and a nonfluorescent acceptor lipid can be measured, giving an indication of the levels of liposome fusion. When fusion occurs, FRET decreases due to an increase in the distance between fluorescent probes. Details on this technique are described in sections 2.2.3.2, 2.2.3.3, 2.2.3.4 and 4.3.4.

The v-SNARE VAMP2 present in GLUT4 vesicles forms an SDS-resistant complex with the t-SNAREs Sx 4 and SNAP23 which are present in the PM of muscle cells and adipocytes (Rea *et al.*, 1998). *In vitro* fusion studies performed in our lab have confirmed this finding since these proteins were shown to catalyse fusion when reconstituted in synthetic liposomes (Brandie *et al.*, 2008). Fusion facilitated by these SNAREs is subjected to multiple levels of regulation *in vivo* and the SM protein M18c is thought to participate in this regulatory process. Studies performed with SM proteins present in other organisms such as yeast, indicated some clues into the possible role of M18c.

The importance of the yeast SM protein Sec1p in the regulation of post-Golgi secretion have given further insights into the SM function. Sec1p binds with low affinity to the yeast syntaxin Sso1p and with higher affinity to both the t-complex formed by Sso1p and Sec9c, and to the SNARE ternary complex Sso1p/Sec9c/Snc2p (Scott *et al.*, 2004). *In vitro* fusion studies using these proteins revealed that Sec1p directly stimulates Sso1p/Sec9c/Snc2p-

mediated membrane fusion *in vitro* (Scott *et al.*, 2004). In neuronal cells, a similar result was observed. M18a was shown to be able to strongly stimulate fusion mediated by the t-SNAREs Sx 1A/SNAP25 with the v-SNARE VAMP2 (Shen *et al.*, 2007). Stimulation occurred not only *via* interaction with the t-SNAREs, but also *via* interaction with v-SNAREs (Shen *et al.*, 2007).

It is unclear how SM proteins might stimulate some fusion reactions, but some research groups have identified a small peptide at the N-terminal region of syntaxins as the binding site for SM proteins (Bracher and Weissenhorn, 2002; Carpp *et al.*, 2006; Dulubova *et al.*, 2003; Dulubova *et al.*, 2002; Hu *et al.*, 2007; Rickman *et al.*, 2007). The N-terminal region of Sx 4 will be described in the following section.

4.1.1 The N-terminal domain of Sx 4

As previously described in section 1.2.1, most syntaxins contain an independently folded N-terminal domain which is an important regulatory region in these proteins. This domain contains a short N-terminal peptide followed by a three-helix bundle called the Habc domain similar to Sx 1A (Fernandez *et al.*, 1998). The N-terminal region of Sx 4 was shown to be necessary for its interaction with M18c (Latham *et al.*, 2006). This SM protein can interact with Sx 4 alone (Hu *et al.*, 2003), VAMP2 (Brandie *et al.*, 2008) and also with the binary (Sx 4/SNAP23) and ternary SNARE complexes (Sx 4/SNAP23/VAMP2) (Latham *et al.*, 2006). It is already established that the neuronal SM protein M18a binds Sx 1A when the latter is in the closed conformation (Misura *et al.*, 2000; Yang *et al.*, 2000) and also when Sx 1A is in the open conformation (*via* the N-terminal peptide region in Sx 1A) (Burkhardt *et al.*, 2008; Khvotchev *et al.*, 2007; Rickman *et al.*, 2007). Sx 4 also uses its short N-terminal peptide to bind a hydrophobic region in M18c (Hu *et al.*, 2007; Latham *et al.*, 2006), however it is not certain if Sx 4 also adopts a closed conformation, such as that reported for Sx 1A. Furthermore, modeling studies based on the crystal structure of Sx 1A in complex with M18a (Misura *et al.*, 2000), have shown that the M18a/Sx 1A complex has a high sequence homology to M18c/Sx 4 (D'Andrea-Merrins *et al.*, 2007). The regions of intramolecular interactions between the Habc domain and the SNARE motif (H3 domain) of Sx 4 were found to be highly conserved between the two different syntaxins (D'Andrea-Merrins *et al.*, 2007). This could suggest that Sx 4, like Sx 1A, could adopt a closed conformation. Figure 4.1 shows two different modes of interaction for Sx 4/M18c. Figure 4.1A shows the hypothetical model of M18c binding Sx 4 in the closed conformation (D'Andrea-Merrins *et al.*, 2007), whereas figure 4.1B shows

the interaction between the N-terminal peptide of Sx 4 and the hydrophobic region (already described in chapter 3) in the outer face of domain I in M18c.

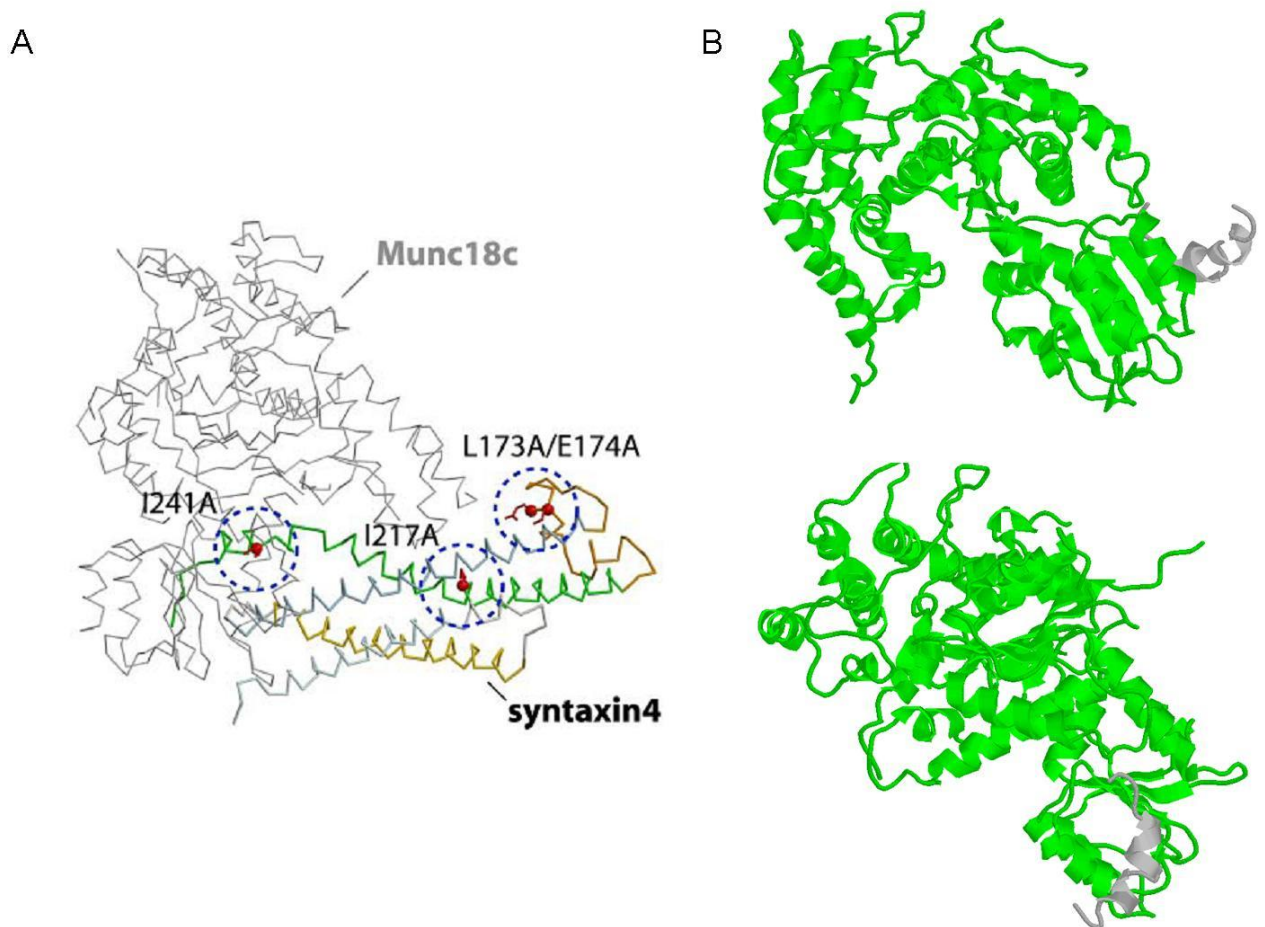


Figure 4.1 The predicted two modes of interaction between M18c and Sx 4.

(A) Figure A was taken from D'Andrea-Merrins and colleagues work (D'Andrea-Merrins *et al.*, 2007). Using a ClustalW alignment, the complex M18c (grey)/Sx4 was modeled directly into the crystal structure of M18a/Sx 1A (D'Andrea-Merrins *et al.*, 2007). The helical Habc domains (Ha- pale blue, Hb- gold, Hc- cyan), the SNARE motif (green), and the linker region which connects the SNARE motif with the Habc domain (orange), are shown. When Sx 4 is in the open conformation, the Habc domain is moved away from the SNARE motif leaving it free to participate in the SNARE core complex. *In vitro*, this is achieved by mutating residues L173A/E174A in the hinge region of Sx 4 (Aran *et al.*, 2009; D'Andrea-Merrins *et al.*, 2007). I241A and I217A mutations were shown to be also important, since they reduce affinity for M18c (D'Andrea-Merrins *et al.*, 2007). (B) Using the Rasmol software, models of M18c (green) interacting with the first 36 amino acids (grey) from the N-terminus of Sx 4 were obtained based on previous described models (Hu *et al.*, 2007) and designed by Prof James Milner-White (University of Glasgow). The model on the top panel shows M18c as an arch shaped molecule binding the 36 amino acids of the helical Sx 4 short N-terminal region. The lower panel represents the same figure from a different perspective, showing the M18c hydrophobic region (composed of β sheets) present on the outer face of domain I, where the short peptide inserts.

In our lab, Dr Fiona Brandie has generated mutant versions of cytosolic Sx 4. These versions were: Sx 4 lacking the short N-terminal peptide (Sx 4 N Δ 36); Sx 4 locked in the open conformation, which was obtained by introducing two point mutations at the hinge region (L173A, E174A); and Sx 4 in the open conformation but lacking the 36 amino acids from the N-terminus (Sx 4 open N Δ 36). These mutants were compared to the wild-type form of Sx 4 in their ability to bind M18c *in vitro*. These constructs contained a GST tag at either the C- or the N- terminal region in order to compare if the position of the bulky GST moiety could affect M18c/Sx 4 interaction. Indeed, the GST tag affected the results (Aran *et al.*, 2009). When syntaxin was tagged with GST at the N-terminus, this affected the pocket-mode of binding and favoured a different interaction not previously described. This interaction was independent of the binding *via* the short N-terminal peptide. As can be seen in figure 4.2A, M18c is able to bind the mutant lacking the short N-terminal peptide, whereas both open mutants (full-length and N Δ 36) exhibit a dramatic reduction in the levels of bound M18c compared to the full-length cytosolic Sx 4. Nevertheless, figure 4.2B shows that by changing the tag to the C-terminus, the short N-terminal peptide becomes “free” to interact with M18c *via* the hydrophobic pocket mode of interaction. In this case, deletion of the N-terminal peptide in the open and wild-type Sx 4 versions results in a dramatic reduction in binding (Aran *et al.*, 2009). These data supports the idea that when Sx 4 is tagged at the C-terminus, the cytosolic domain of Sx 4 predominantly adopts an open conformation or transits easily from a closed to an open form. In contrast, when Sx 4 is tagged at the N-terminus it might adopt a different conformation which could be related to the closed conformation observed for Sx 1A. *In vitro* fusion assays using these mutants are a very useful tool to understand the function of the N-terminal peptide in the process of SNARE assembly and to define the importance of M18c in the regulation of Sx 4/SNAP23/VAMP2-mediated membrane fusion.

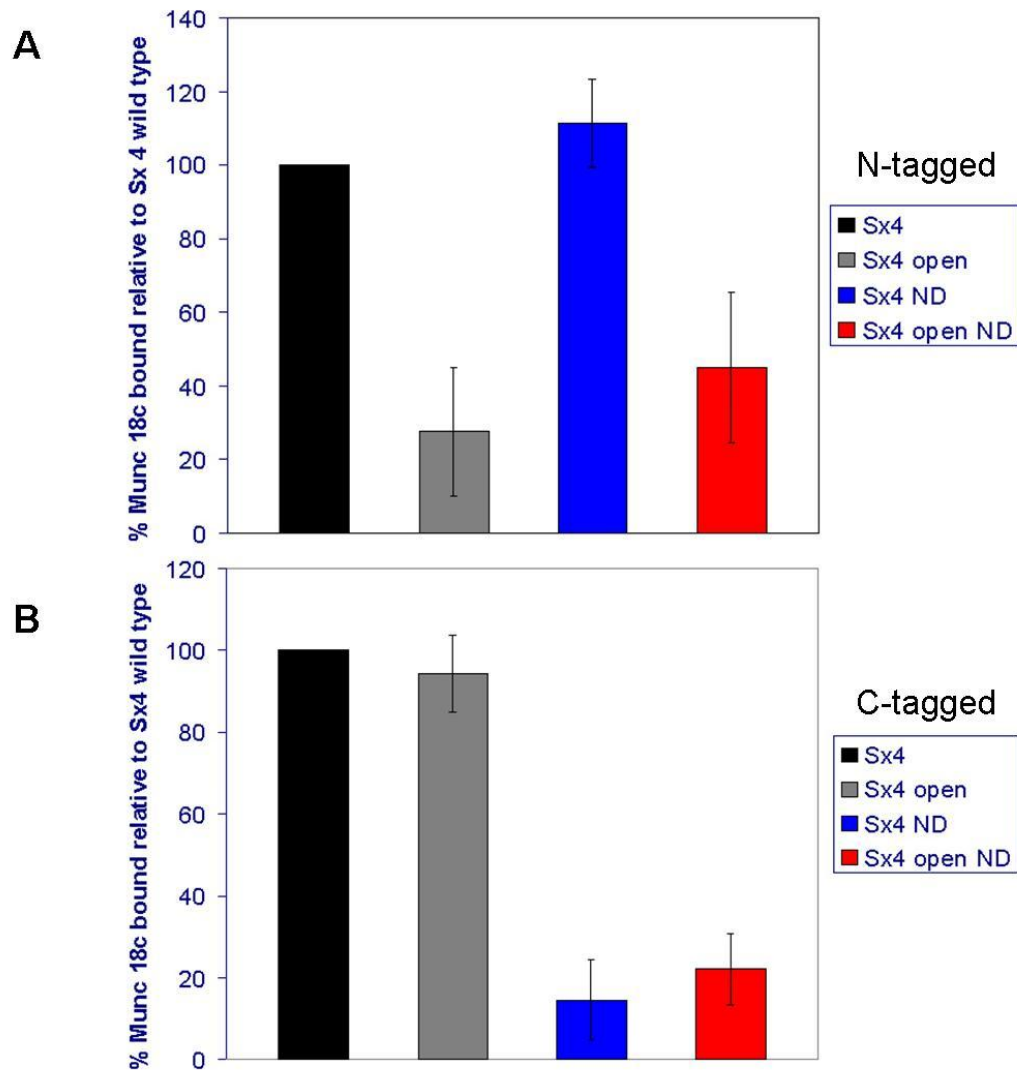


Figure 4.2 Quantifications of the amount of M18c bound to either N- (A) or C-tagged versions (B) of cytosolic Sx 4 (Figure taken from Dr Fiona Brandie, University of Glasgow) (A) The N-terminally tagged versions of Sx 4 (GST- Sx 4, GST-Sx 4 L173A/E174A (OPEN), GST-Sx 4 Δ N36 (ND) and GST-Sx 4 OPEN ND) were incubated with His₆-M18c and the results are shown as a percentage of bound M18c relative to wild-type Sx 4. (B) The C-terminally tagged Sx 4 versions were incubated with His₆-M18c and again, the results are shown as a percentage of bound M18c relative to wild-type Sx 4. Figure taken from Dr Fiona Brandie (University of Glasgow).

4.2 Aims of this chapter

The aims of this chapter were to generate full-length Sx 4 constructs containing the following changes: an N-terminal peptide truncation (N Δ 36) and open form (L173A/E174A) also lacking the N-terminal peptide. The original construct containing the full-length open form of Sx 4 was made by Dr Fiona Brandie (University of Glasgow). These constructs were generated in order to co-express them with SNAP23 and to test their ability to fuse *in vitro* with VAMP2. Previously in our lab, Dr Fiona Brandie has shown that M18c is able to bind to the extreme N-terminus of Sx 4 *in vitro* (Aran *et al.*, 2009). Hence, these mutants when used in the *in vitro* fusion assay may reveal further details about the mechanism of action of M18c.

4.3 Results

4.3.1 Expression and purification of t-SNARE complexes

Full-length SNARE complexes were expressed and purified as described in section 2.2.3.1. Full-length Sx 4 constructs containing the following changes: N-terminal peptide truncation (N Δ 36), Sx 4 locked in the OPEN conformation (*i.e.* containing mutations L173A/E174A) and Sx 4 OPEN N Δ 1-36 were generated in this study. Recombinant wild-type Sx 4 in complex with SNAP23 was obtained from Dr Fiona Brandie. A typical protein purification of wild-type Sx 4/SNAP23 is shown in figure 4.3.

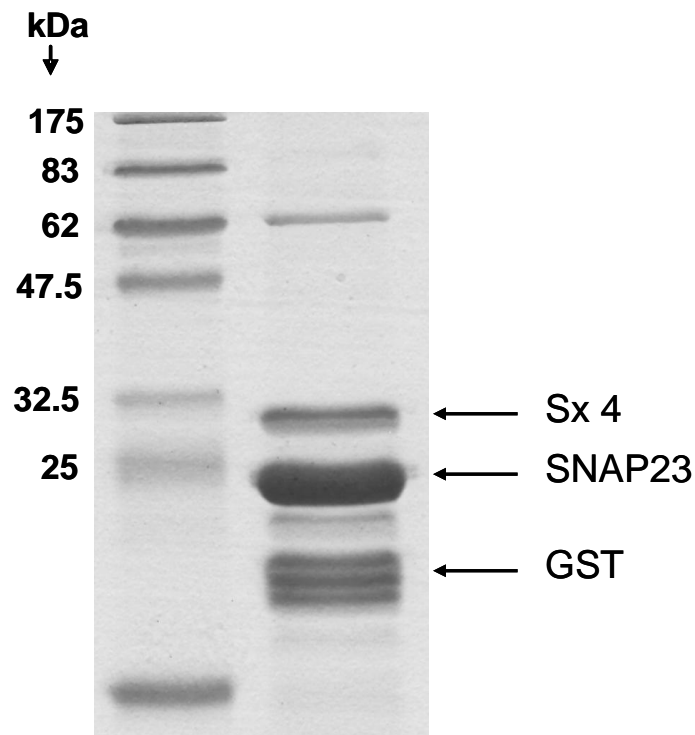


Figure 4.3 Purified Sx 4/SNAP23 t-SNARE complex from *E.coli* lysates

Dr Fiona Brandie has expressed Sx 4 and SNAP23-GST in BL21 (DE3) *E. coli* cells, purified the complex and samples from the eluted fractions were used in this chapter. Complete details on how wild-type Sx 4/SNAP23 heterodimer was expressed and purified are described in section 2.2.3.1. The purity of the proteins was assessed on a 15 % SDS-PAGE followed by Coomassie Blue staining as outlined in sections 2.2.2.1 and 2.2.2.3. The figure shows the recovered cleaved complex after 4 h of thrombin cleavage (5 μ l). Positions of the molecular weight markers are shown on the left of the gel.

4.3.1.1 Generation of Sx 4 N Δ 36 and Sx 4 “OPEN” (L173A/E174A) N Δ 36 to co-express with SNAP23

The wild-type and open forms of Sx 4 lacking amino acids 1-36 were cloned into the vector pQE30. Sx 4 N Δ 36 and Sx 4 OPEN N Δ 36 were generated by PCR using pQE30 Sx 4 (full-length) as template for the wild-type Sx 4 N Δ 36 and pQE30 Sx 4 (full-length L173A/E174A) as template for Sx 4 OPEN N Δ 36. Primers used to amplify desired sequences were:

Sx 4 N Δ 36 Forward: 5' GGT ACC CCG GAC GAC GAG TTC TTC CAG AAG 3'

Sx 4 N Δ 36 Reverse: 5' AAG CTT TTA TCC AAC GGT TAT GGT GAT GC 3'

Both versions of Sx 4 were cloned between the *KpnI* and *HindIII* sites in pQE30. After successful cloning, pQE30 Sx 4 N Δ 36 and pQE30 Sx 4 OPEN N Δ 36 were co-transformed with pET41a SNAP23 into *E. coli* BL21 (DE3) cells. Both plasmids were transformed by mixing 50 ng of SNAP23 DNA with 100 ng of either pQE30 Sx 4 N Δ 36 or pQE30 Sx 4 OPEN N Δ 36 DNA in the same *E. coli* cells. Cells containing both plasmids were selected on dual antibiotic plates since SNAP23 is expressed from a kan resistant vector (pET41) and the different versions of Sx 4 are expressed from amp resistant vectors (pQE30). Selected colonies were used to start protein purification which is described in detail in section 2.2.3.1. Both t-SNARE complexes were successfully purified and samples from each step were analysed by SDS-PAGE, followed by Coomassie blue staining, as shown in figures 4.4 and 4.5.

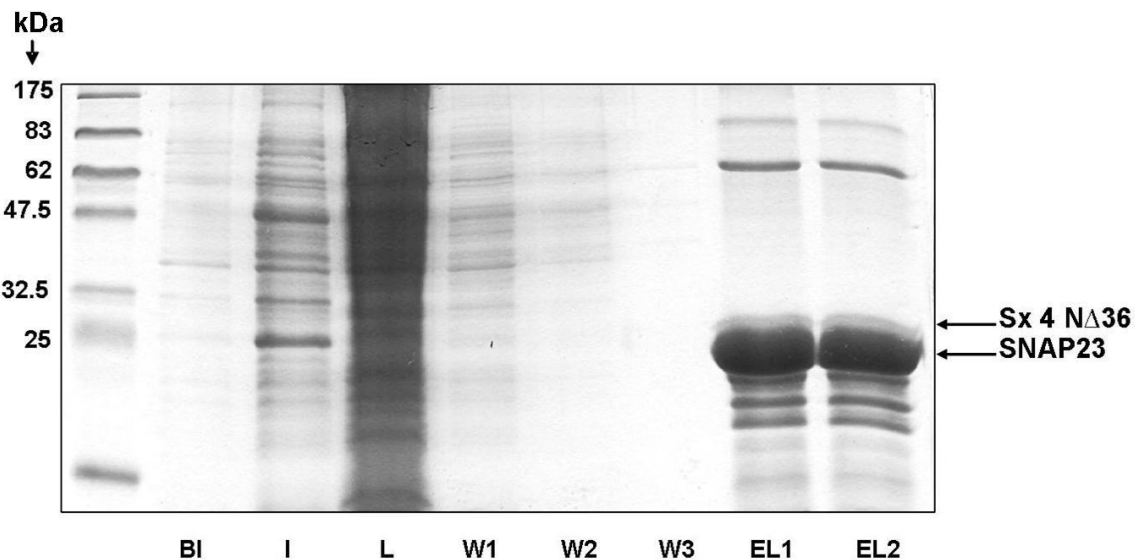


Figure 4.4 Purification of Sx 4 N Δ 36/SNAP23 complex from *E. coli*

Full-length His₆-Sx 4 N Δ 36 and SNAP23-GST were co-expressed in BL21 (DE3) *E. coli* cells. Expression was induced overnight (~16 h) by adding 1 mM IPTG and incubation was carried out at 25 °C. The complex was purified taking advantage of the GST tag attached to the N-terminus of SNAP23 and this tag was cleaved at the end of the purification by incubation with thrombin for 4 h at room temperature. The figure shows several samples taken during the process of protein purification which were run on a 12 % SDS-PAGE gel and stained with Coomassie Blue as outlined in sections 2.2.2.1 and 2.2.2.3. The positions of the molecular weight markers are shown on the left. The first lane corresponds to a sample before induction (BI) followed by a sample after induction (I), sample from the lysate (L), wash 1 (W1), wash 2 (W2), wash 3 (W3) and 3 μ l of eluted fractions (EL1 and EL2).

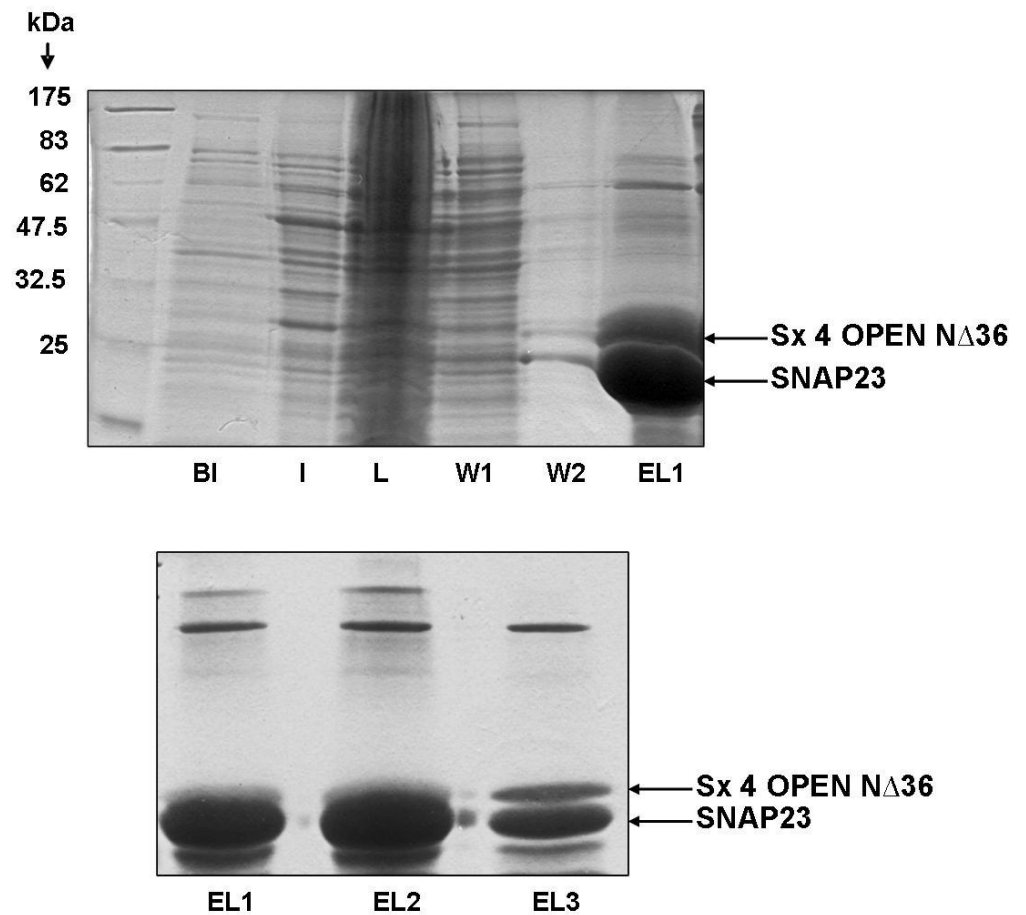


Figure 4.5 Purification of Sx 4 OPEN N Δ 36/SNAP23 complex from *E.coli*

Full-length His₆-Sx 4 OPEN N Δ 36 and SNAP23-GST were co-expressed in BL21 (DE3) *E.coli* cells. Expression was induced overnight (~16 h) by adding 1 mM IPTG and incubation was carried out at 25 °C. The complex was purified taking advantage of the GST tag attached to the N-terminus of SNAP23 and this tag was cleaved at the end of the purification by incubation with thrombin for 4 h at room temperature. The figure shows several samples taken during the process of protein purification which were run on a 12 % SDS-PAGE gel and stained with Coomassie Blue. The positions of the molecular weight markers are shown on the left. The first lane corresponds to a sample before induction (BI) followed by a sample after induction (I), sample from the lysate (L), wash 1 (W1), wash 2 (W2) and 5 μ l of eluted fraction (EL1). Molecular weight markers are shown on the left. Lower figure shows more elutions and 2 μ l of EL1, EL2 and EL3 were run on a 15 % SDS-PAGE in order to better resolve the upper band corresponding to Sx 4 OPEN N Δ 36, which due to the lack of 36 amino acids, it runs very close to SNAP23.

4.3.1.2 Generation of full-length Sx 4 “OPEN” (L173A/E174A) in complex with SNAP23

The construct containing full length Sx 4 OPEN (pQE30 Sx 4 L173A/E174A) was made by Dr Fiona Brandie (University of Glasgow). However, in her work the co-expression of this protein with SNAP23 was not achieved due to the poor solubility of Sx 4 OPEN. Therefore, in this study Sx 4 OPEN/SNAP23 expression and purification conditions were

optimised in order to obtain enough quantities of this t-complex to reconstitute into liposomes and therefore perform *in vitro* fusion assays. In order to achieve this, SNAP23 and Sx 4 OPEN plasmids were co-transformed into the same BL21 (DE3) *E. coli* cells by mixing 50 ng of SNAP23 DNA with 200 ng of Sx 4 OPEN DNA (for wild-type versions only 100 ng was necessary). Cells containing both plasmids were selected on dual antibiotic plates (amp/kan) and these colonies were used to start protein purification which is described in detail in section 2.2.3.1.

The t-SNARE complex Sx 4 OPEN/SNAP23 was purified and samples from each step were analysed by SDS-PAGE, followed by Coomassie blue staining, as shown in figure 4.6.

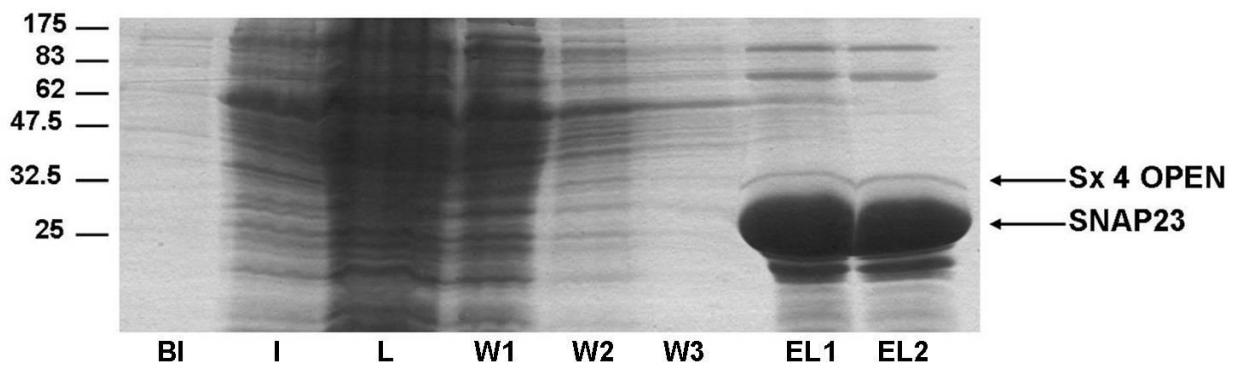


Figure 4.6 Purification of Sx 4 OPEN/SNAP23 complex from *E.coli*

Full-length His₆-Sx 4 OPEN and SNAP23-GST were co-expressed in BL21 (DE3) *E.coli* cells. Expression was induced overnight (~16 h) by adding 1 mM IPTG and incubation was carried out at 24 °C. The complex was purified taking advantage of the GST tag attached to the N-terminus of SNAP23 and this tag was cleaved by incubation with thrombin for 4 h at room temperature. The figure shows several samples taken during the process of protein purification which were run on a 15 % SDS-PAGE gel and stained with Coomassie Blue as outlined in sections 2.2.2.1 and 2.2.2.3 respectively. The positions of the molecular weight markers are shown on the left. The first lane corresponds to a sample before induction (BI) followed by a sample after induction (I), sample from the lysate (L), wash 1 (W1), wash 2 (W2), wash 3 (W3) and 3 µl of eluted fractions (EL1 and EL2). Molecular weight markers are shown on the left. This result is from a typical Sx 4 OPEN/SNAP23 protein purification.

In summary, figure 4.7 shows a schematic representation of all Sx 4 constructs used in this study which were purified alongside SNAP23 according to the protocol described in section 2.2.3.1.

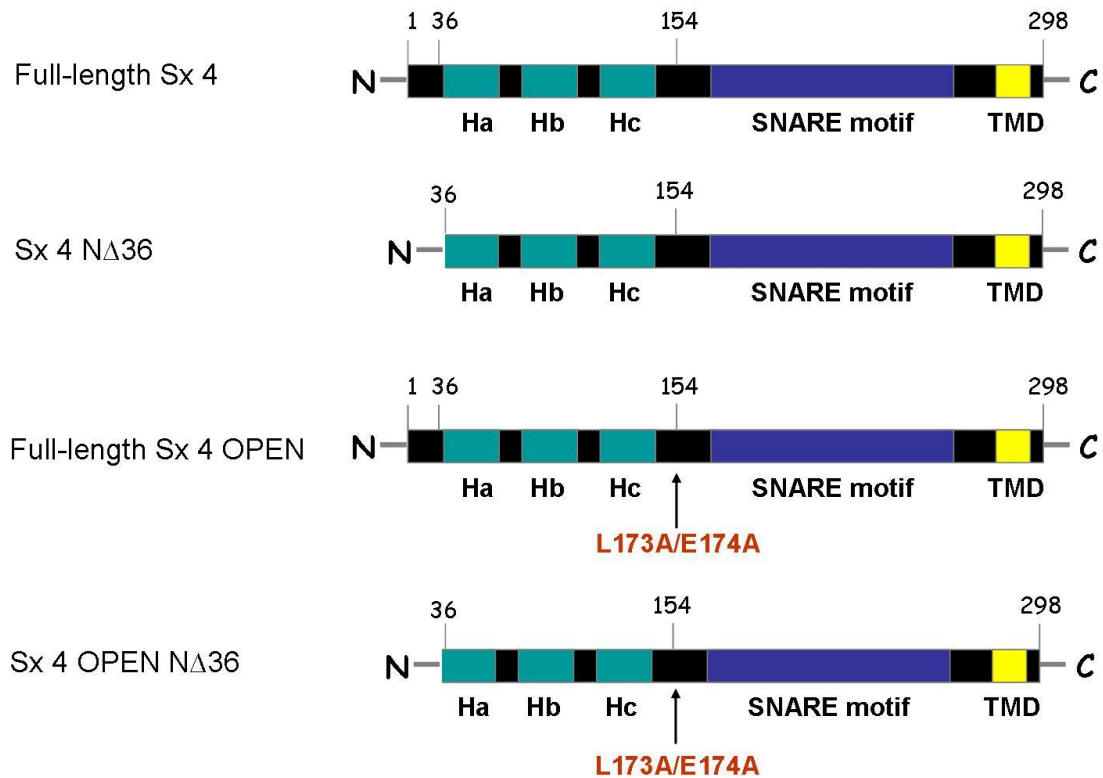


Figure 4.7 Schematic representation of the different Sx 4 constructs used in this study. The figure shows 4 schematic representations of wild-type Sx 4 and the Sx 4 mutants generated in this study. Full-length Sx 4 corresponds to amino acids 1-298 of the Sx 4 sequence. Sx 4 N Δ 36 corresponds to Sx 4 lacking the first 36 amino acids from the N-terminal region. Full-length Sx 4 OPEN contains the mutations L173A/E174A which were shown to prevent Sx 4 for adopting the closed conformation (Aran *et al.*, 2009; D'Andrea-Merrins *et al.*, 2007). Sx 4 OPEN N Δ 36 also contains the L173A/E174A mutation, however it also lacks the first 36 amino acids from the N-terminal region.

4.3.2 Reconstitution of recombinant t-SNAREs into liposomes

All t-complexes purified in this study show that the levels of SNAP23 and Sx 4 were not equimolar in the eluted fractions (figures 4.3, 4.4, 4.5 and 4.6). The usual protein concentration of the eluted samples ranged from 1 mg/ml to 5 mg/ml. Concentrations were estimated using the Bio-Rad protein assay as described in section 2.2.2.5. Although SNAP23 levels contribute much more in terms of protein concentration, this is not a major

problem for reconstitution into liposomes since SNAP23 does not contain a trans-membrane domain. In addition, recombinant SNAP23 purified from *E. coli* cells does not possess palmitate groups. This means that SNAP23 needs to be in complex with Sx 4, which contains a trans-membrane domain, in order to be reconstituted into liposomes. Therefore, it is very important to have enough recombinant Sx 4 for Sx 4/SNAP23 reconstitution to occur.

In order to reconstitute SNARE proteins into liposomes, first the lipid mixtures were prepared as outlined in section 2.2.3.2. Briefly, the labelled donor vesicles contained a quenched mixture of fluorescent phospholipids and the unlabelled acceptor vesicles were not fluorescent labelled. Lipids were dried under nitrogen and resuspended in a solution containing either the v-SNAREs (fluorescent donor vesicles) or t-SNAREs (non-fluorescent acceptor vesicles) in the presence of OG, which helps to incorporate the trans-membrane domains of SNAREs into the liposome membranes. A complete description on the SNARE reconstitution technique is outlined in section 2.2.3.3 and a schematic representation is shown in figure 4.8.

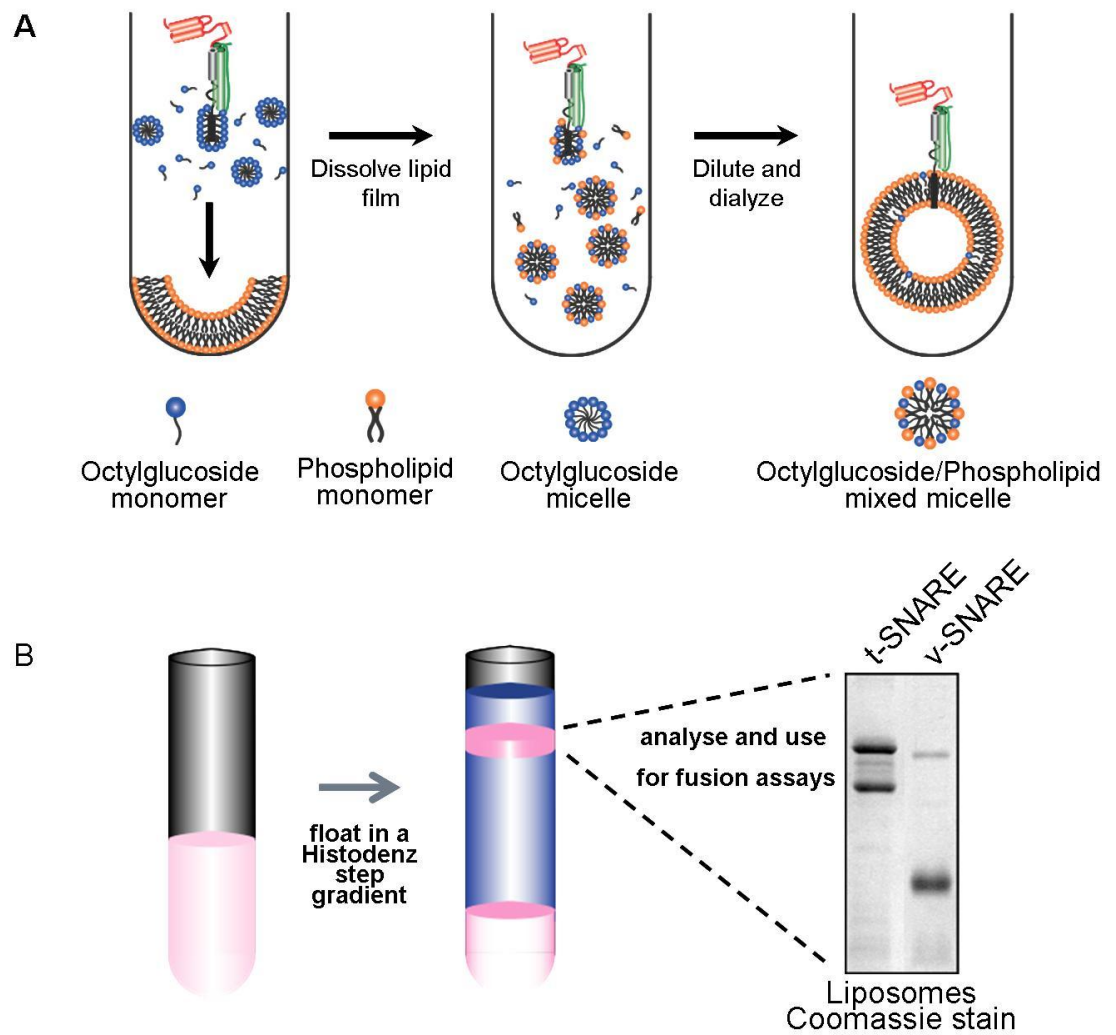


Figure 4.8 Schematic representation of the incorporation of SNARE proteins into liposomes (kindly given by Prof James A. McNew, Rice University)

This schematic model shows how v- and t- SNAREs are reconstituted into vesicles (**A**) Dried phospholipids were mixed with protein in the presence of the detergent octyl- β -d glucopyranoside (OG). The OG monomer and the phospholipid monomer are represented in blue and orange respectively. After rapid dilution below the critical micellar level of the detergent by addition of 1.5 ml of buffer A200, solution is placed into a float-a-lyser to dialyze overnight in order to remove any free OG monomers still present in the solution. After dialysis, the octylglucoside/phospholipid mixed micelle is formed. (**B**) The resulting proteoliposomes can then be isolated by flotation in a Histodenz density gradient. After ultracentrifugation for 4 h at $\sim 372,000$ xg, proteoliposomes float to the top layer of the sample due to their high lipid content. Recovered proteoliposomes can be assessed by analysing 10 μ l on a SDS-PAGE followed by Coomassie Blue staining. Unincorporated protein remains at the bottom of the tube. Complete details on SNARE reconstitution and proteoliposome recovery are outlined in sections 2.2.3.3 and 2.2.3.4 respectively.

Purified SNARE proteins shown in figures 4.3, 4.4, 4.5 and 4.6 were successfully reconstituted into liposomes (figure 4.9). Immunoblot analysis using anti-Sx 4 shows the Sx 4 levels present in each complex before reconstitution (figure 4.9; left panel). This was performed in order to reconstitute the 4 different complexes at similar quantities into their respective liposomes. The resulting different versions of reconstituted Sx 4 in complex with SNAP23 were resolved by SDS-PAGE and can be seen in figure 4.9 (right panel).

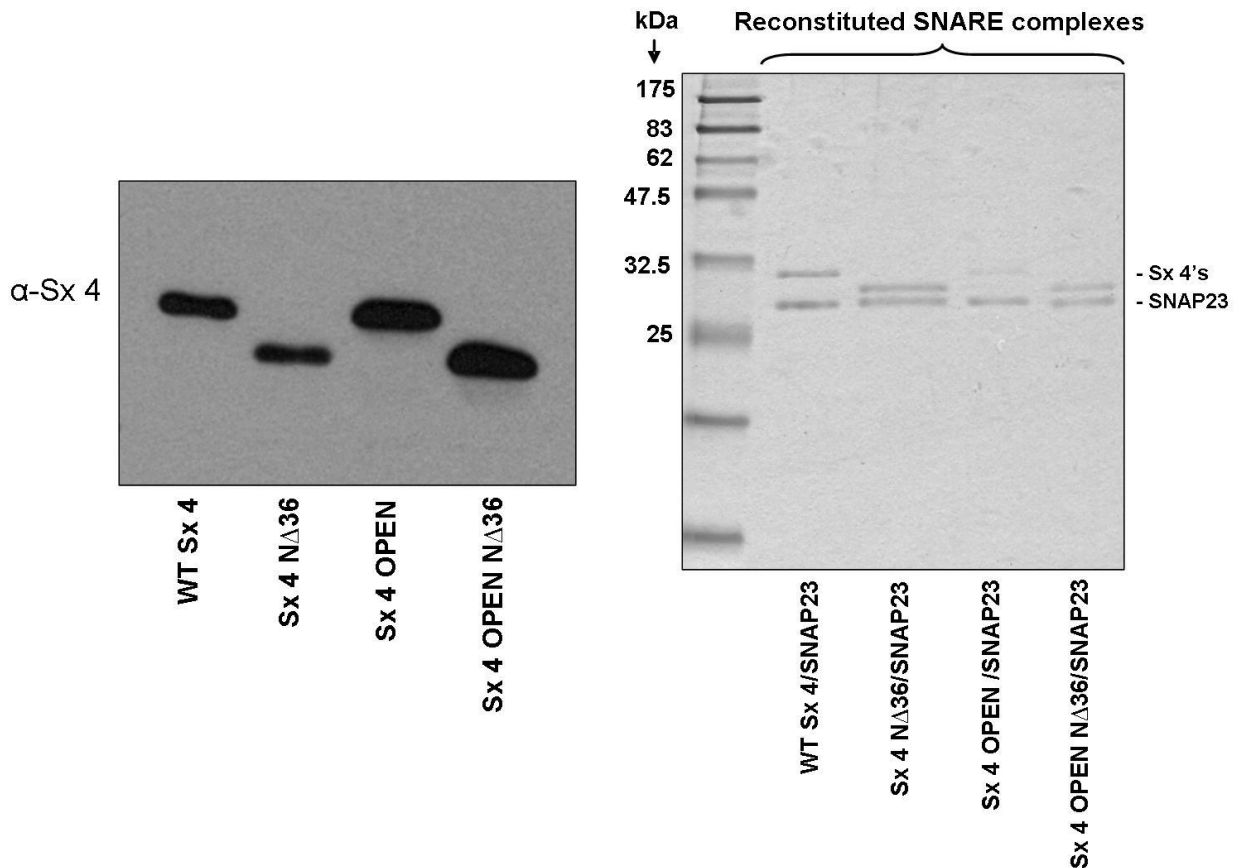


Figure 4.9 Reconstitution of recombinant SNAREs into liposomes

Purified t-SNARE complexes were successfully reconstituted into synthetic liposomes. Left panel shows an immunoblot analysis using anti-Sx 4 antibody performed to check levels of recombinant Sx 4 (complexed with SNAP23) before reconstitution. Using the program Image J, it was possible to calculate the differences in quantities between each t-SNARE complex. After reconstitution, 10 μ l of reconstituted t-SNARE liposomes were separated on a 15 % SDS-PAGE gel and stained with Coomassie Blue as outlined in sections 2.2.2.1 and 2.2.2.3 respectively. Positions of the molecular weight markers are shown. Data from a typical set of reconstitutions is shown.

4.3.3 VAMP2 expression, purification and reconstitution into liposomes

Full-length C-terminally tagged VAMP2 was expressed as a Hexa-HIS-tagged protein in BL21 (DE3) cells and purified by Dr Fiona Brandie (University of Glasgow). pET-VAMP2FL-myc-HIS was a kind gift from Giampietro Schiavo (London, UK).

VAMP2 was successfully reconstituted into liposomes as shown in figure 4.10. Samples taken before (lane 1) and after (lane 2) reconstitution are shown. Lane 3 represents a sample of soluble recombinant VAMP2 lacking the trans-membrane domain (VAMP2 Δ TMD) which was used as an inhibitor of fusion in the controls for *in vitro* fusion assays.

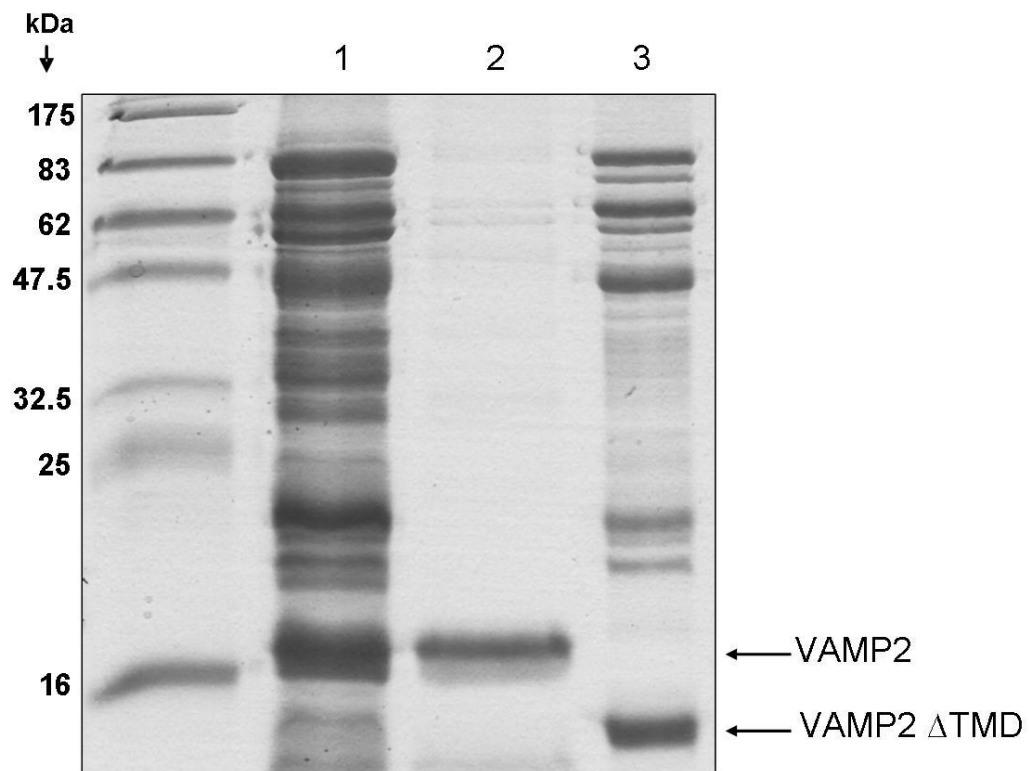


Figure 4.10 Purification and reconstitution of VAMP2 into liposomes

Full-length VAMP2 (lane1, 10 μ l) purified by Dr Fiona Brandie was reconstituted into liposomes (lane 2, 10 μ l). Cytoplasmic VAMP2 (*i.e.* lacking the trans-membrane domain-VAMP2 Δ TMD) which is used as an inhibitor of *in vitro* fusion, is shown in lane 3 (10 μ l). Samples were separated on a 15 % SDS-PAGE gel and stained with Coomassie blue. Positions of the molecular weight markers are shown on the left. This is a result of a typical VAMP2 reconstitution experiment.

4.3.4 *In vitro* fusion assays using reconstituted liposomes

After the SNARE proteins shown in figures 4.9 and 4.10 were successfully reconstituted into their appropriate liposomes, a series of different *in vitro* fusion assays were carried out using these proteoliposomes. These assays were performed in order to investigate if mutations in Sx 4 could affect the fusion rates, either positively or negatively.

Figure 4.11 shows a schematic representation of the principle of the *in vitro* fusion assay. Briefly, the fusion reactions were set up on a microtitre plate on ice. One well was used to add the fusion reaction and a second well was used for the fusion control reaction. The fusion reaction mixtures are set up at approximately 1:1 v-SNARE:t-SNARE molar ratio which represents the addition of approximately 10 times more volume of t-SNARE vesicles than v-SNARE in each reaction. Fusion assays containing the wild-type Sx 4/SNAP23, Sx 4 N Δ 36/SNAP23, Sx 4 OPEN/SNAP23 and Sx 4 OPEN N Δ 36/SNAP23 t-SNARE complexes were performed in which 5 μ l of fluorescently labelled donor VAMP2 liposomes were mixed with 45 μ l of unlabelled acceptor t-complexes. As a control, the t-SNARE liposomes were pre-incubated for 10 min with 3 μ l of VAMP2 lacking the transmembrane domain (VAMP2 Δ TMD) which is known to act as a dominant negative inhibitor of fusion. The plate was incubated for 10 min on ice followed by the addition of 5 μ l of VAMP2 liposomes (VAMP2 liposomes are shown in figure 4.10). To the “fusion” well, 3 μ l of buffer A200 (glycerol free) was added instead. NBD fluorescence was then measured at 2 min intervals for 2 h before addition of 10 μ l of 2.5 % dodecylmaltoside, and measurements proceeded for further 40 min. Raw data was collected and normalised to maximum detergent signal (see Appendix, figure I). Rate of fusion was then measured as a percentage of the maximum NBD fluorescence (100 %).

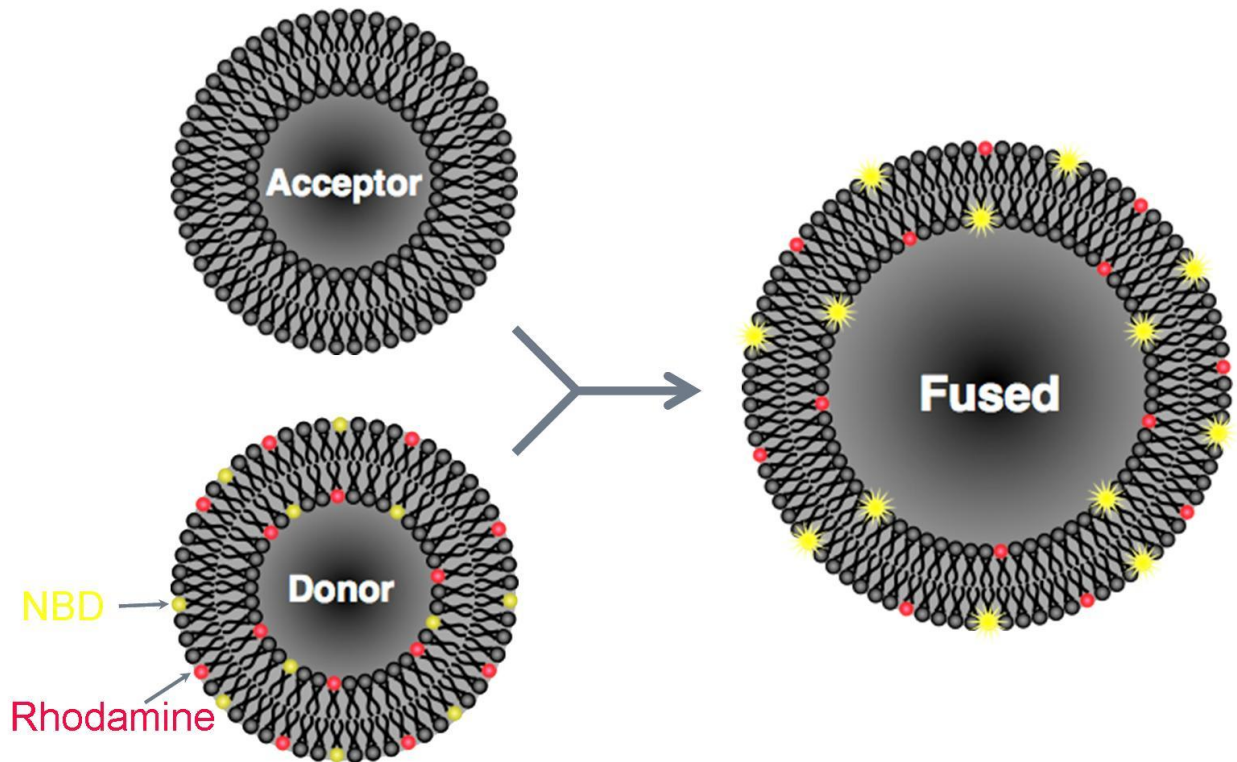


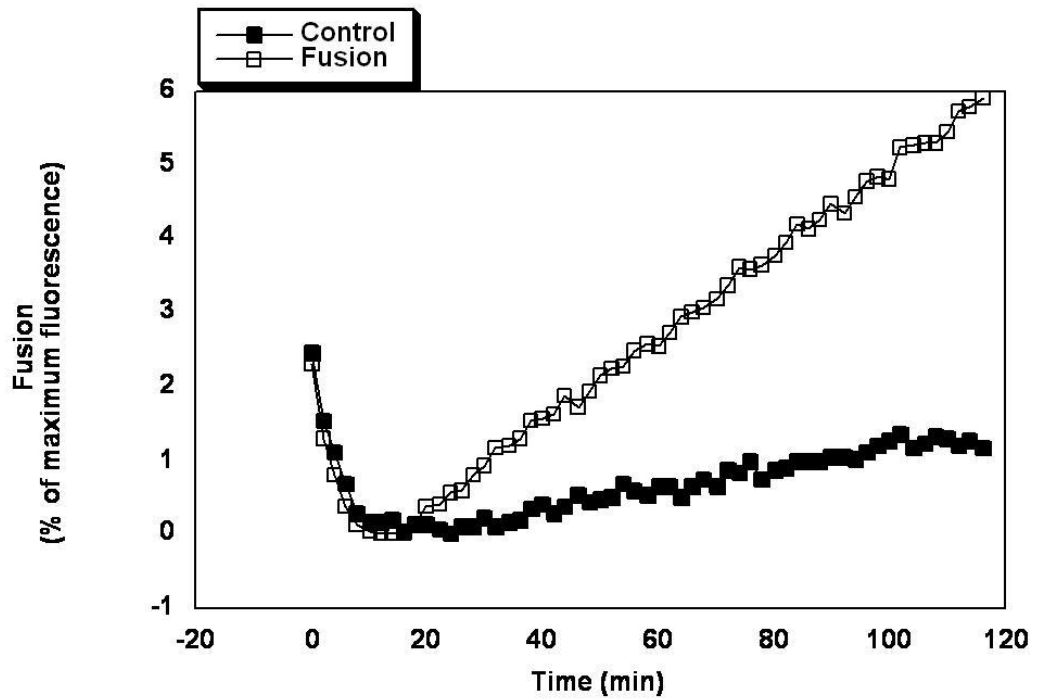
Figure 4.11 Fusion assay model (Prof James A. McNew, Rice University, USA)

The fusion assay model takes advantage of two different labelled lipids, one labelled with rhodamine (pink spheres) and one labelled with NBD (yellow spheres). A quenched mixture of these fluorescent labelled lipids is present in the same membrane (donor) which will contain the reconstituted v-SNARE proteins. The acceptor vesicles (acceptor) are not labelled and will contain the reconstituted t-SNARE proteins. When both acceptor and donor vesicles are mixed at 37 °C, these vesicles fuse. When NBD and rhodamine are in close proximity, excitation of NBD leads to an energy transfer to the rhodamine fluorophore in a process known as fluorescent resonance energy transfer (FRET), which is dependent on the distance between the 2 fluorophores. Upon fusion, a decrease in quenching (due to the decrease in proximity of the two fluorophores) occurs, which leads to an increase in the overall NBD fluorescence which can be measured using a fluorescence plate reader. Complete details on this technique are outlined in section 2.2.3.6.

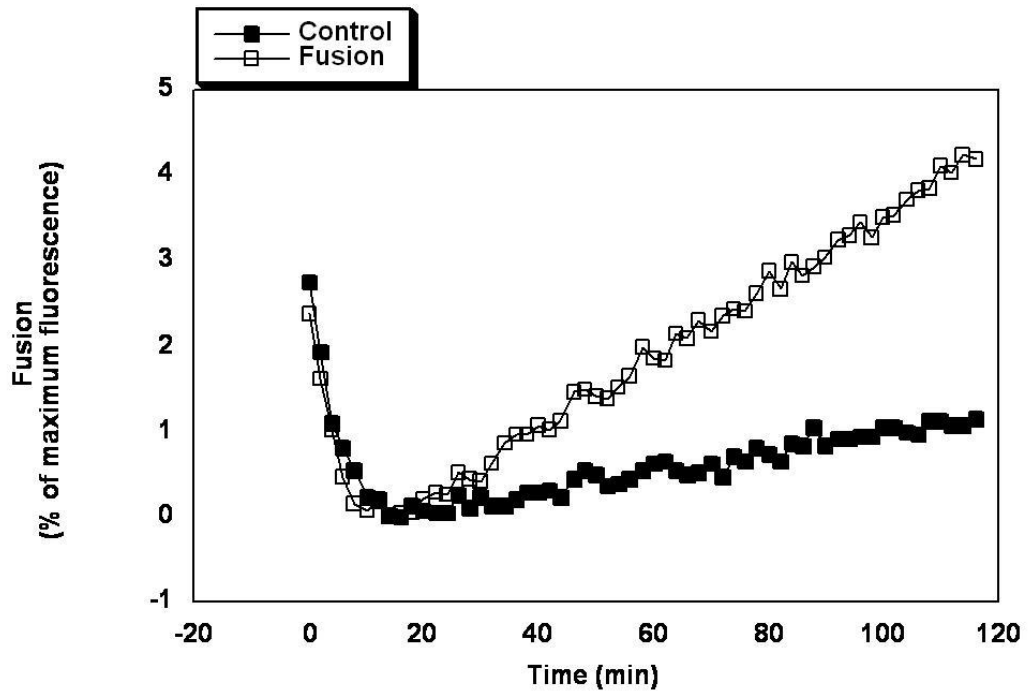
Figure 4.12 shows the successful fusion of the four different t-SNARE complexes with their respective v-SNARE VAMP2 vesicles. Results obtained confirm that, as expected, t-complex containing wild-type Sx 4 liposomes fuse with VAMP2 liposomes (figure 4.12A). The removal of the short N-terminal peptide in both open (figure 4.12D) and wild-type (figure 4.12B) Sx 4 mutants did not inhibit fusion. The t-complex containing the full-length open version of Sx 4 was also shown to be able to fuse with VAMP2 liposomes (figure 4.12C). Differences in the rates of fusion observed between all 4 different fusions

might be due to the subtly different levels of t-SNARE complexes reconstituted into liposomes (figure 4.9).

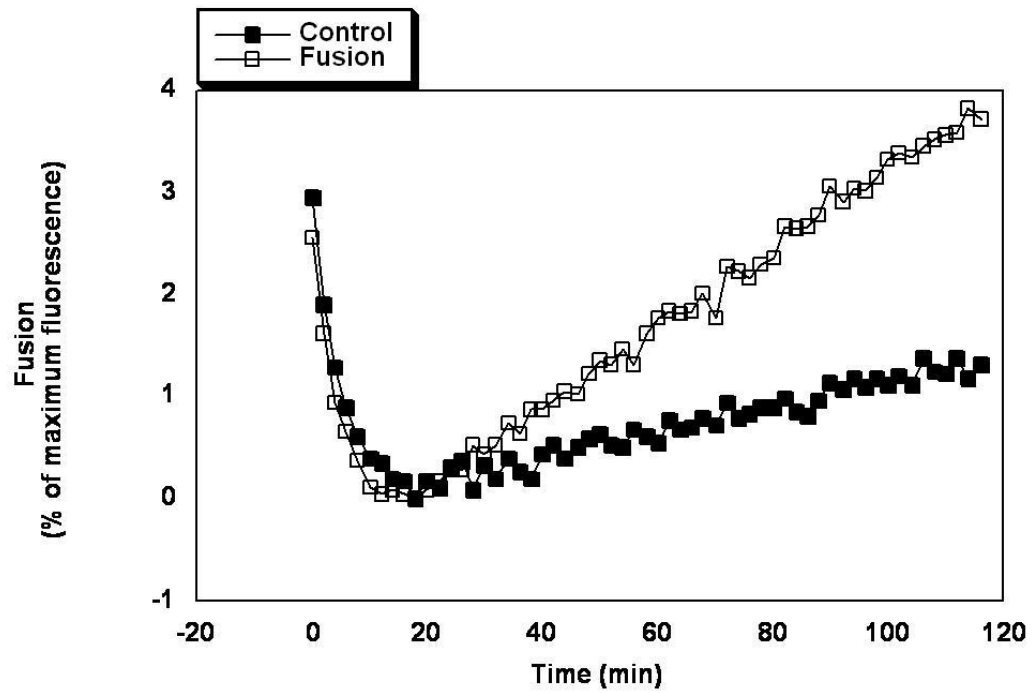
A



B



C



D

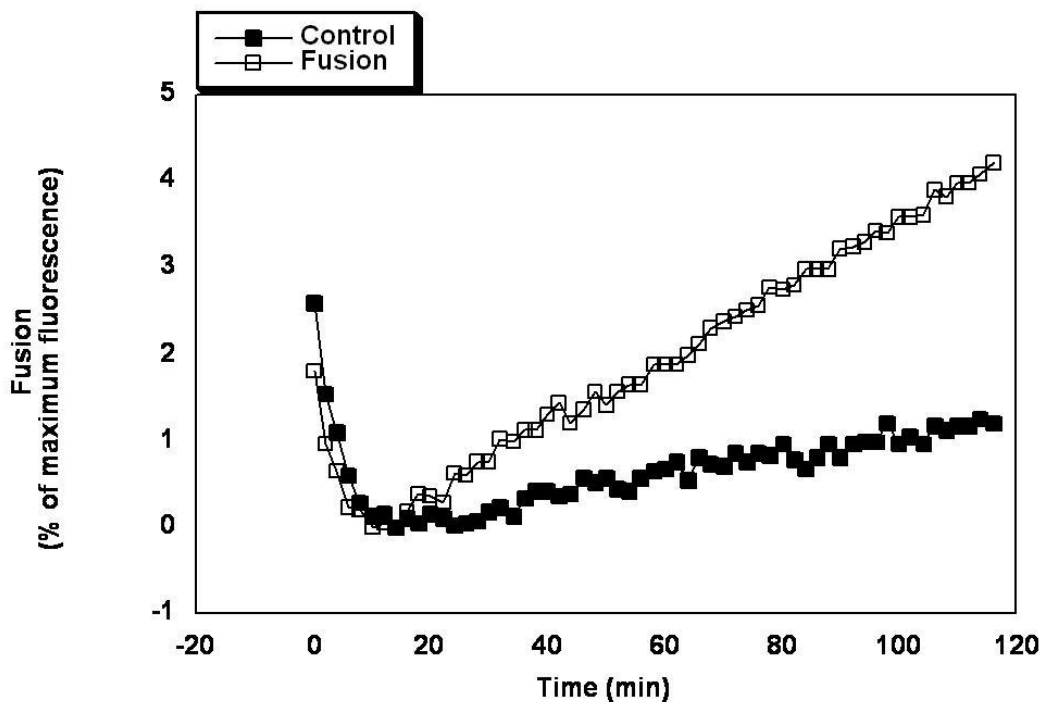


Figure 4.12 *In vitro* fusion assays of liposomes containing either full-length Sx 4/SNAP23 (A) or Sx 4 N Δ 36/SNAP23 (B) or Sx 4 OPEN/SNAP23 (C) or Sx 4 OPEN N Δ 36/SNAP23 (D) with liposomes containing VAMP2

In all fusion assays A, B, C and D shown, 5 μ l of fluorescently labelled donor VAMP2 liposomes were mixed with 45 μ l of unlabelled acceptor t-complexes being either wild-type (A) or Sx 4 N Δ 36/SNAP23 (B) or Sx 4 OPEN/SNAP23 (C) or Sx 4 OPEN N Δ 36/SNAP23 (D). To all 4 fusion assays, 3 μ l of buffer A200 (fusion reaction; open squares) or 3 μ l of cytoplasmic VAMP2 (negative control; filled squares) were added. Note that the soluble VAMP2 was pre-incubated with the t-complex in order to block VAMP2 liposome fusion. Fusions between the two vesicle populations (t- and v-SNAREs) in A, B, C and D were monitored by first placing the 96 well plate (where the proteoliposomes were mixed) inside the fluorescence reader. Before starting the fusion measurements, the plate was incubated inside the reader for 5 min at 37 $^{\circ}$ C to try to avoid the drop in the fluorescence intensity observed in all 4 fusion reactions above (see first 10 min). This drop is the result of the shift from 4 $^{\circ}$ C to 37 $^{\circ}$ C at the beginning of each fusion. Fluorescence was then measured at 2 min intervals for 2 h with the excitation filter set to 485 nm and the emission filter set at 520 nm. After 2 h, the plate was removed and 10 μ l of 2.5 % (w/v) n-dodecylmaltoside was added to the wells containing liposomes and mixed (this produces a maximum detergent signal represented by 100 % in the raw graphs of A, B, C and D, see appendix, figure I) and the fluorescence was recorded for further 40 min at 2 min intervals. A graphing and analysis programme called KaleidaGraph (Synergy Software) was used in order to analyse the data obtained from the Fluorescence reader. Raw fluorescence was normalised to maximum detergent signal (100 %) and plotted against time in minutes (see appendix, figure I). The levels of fusion were determined as a percentage of the maximum signal of NBD emission. The detailed protocol is described in section 2.2.3.6 and 2.2.3.7.

These figures show a typical result from the *in vitro* fusions mediated by the different versions of Sx 4/SNAP23 with VAMP2, repeated 3 times for all complexes.

4.3.5 Effects of the addition of M18c directly into the *in vitro* fusion assay

The role of SM proteins in SNARE-mediated membrane fusion has also been investigated through the use of *in vitro* fusion assays, which confirms the valuable tool of these types of experiments. Previous studies have shown that SM proteins possess a stimulatory effect over SNARE-mediated liposome fusion. Examples are M18a on Sx 1A/SNAP25/VAMP2 fusion and Sec1p on Sso1p/Sec9p/Snc2p fusion (Scott *et al.*, 2004; Shen *et al.*, 2007). Since the effect of M18c over Sx 4/SNAP23/VAMP2 fusion has not been previously analysed, experiments were carried out to investigate the effect of M18c addition to fusion assays containing the t-SNARE complex Sx 4/SNAP23 and the v-SNARE VAMP2.

4.3.5.1 M18c protein expression and purification

His₆-M18c was expressed in M15 *E. coli* cells that also co-expressed the chaperone protein GroEL in order to increase M18c solubility. Low levels of IPTG were used (0.2 mM) and protein expression was induced at 22 °C overnight as outlined in section 2.2.4 as these conditions were empirically determined to give better levels of expression. His₆-M18c was purified using Ni-NTA agarose as described in section 2.2.4.

A typical purification is shown in figure 4.13. M18c was successfully purified and protein concentration was determined as described in section 2.2.2.5. Recombinant His₆-M18c was used in the *in vitro* fusion assays described in sections 4.3.5.4 and 4.3.5.5.

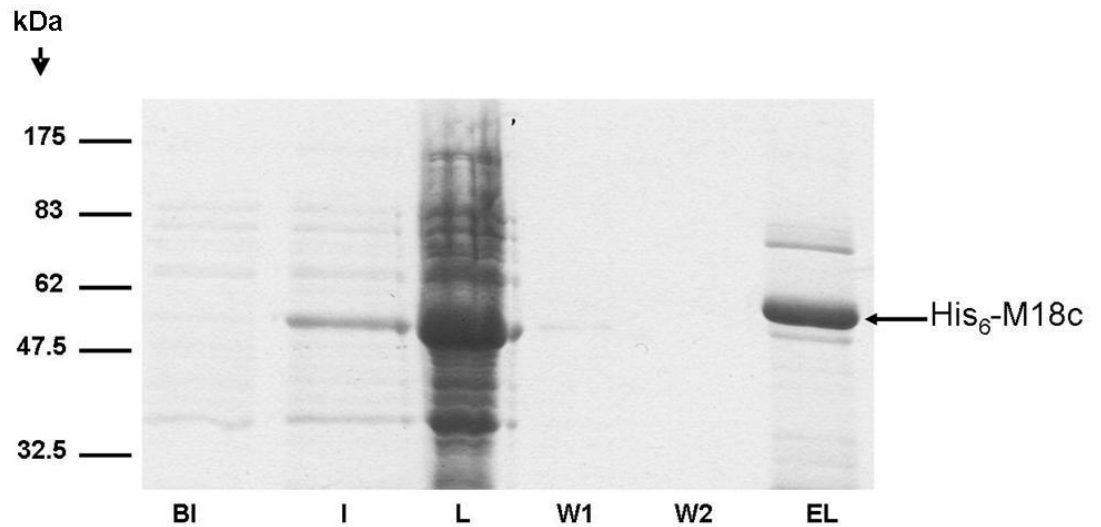


Figure 4.13 His₆-M18c protein purification

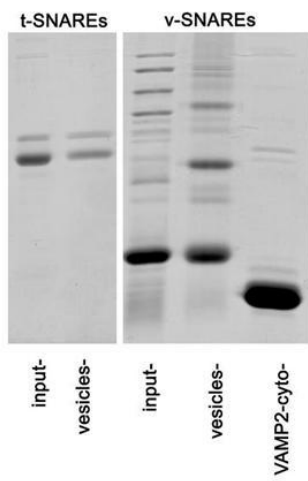
His₆-M18c was expressed from vector pQE30 in M15 *E.coli* cells co-expressing the chaperone GroEL. Expression was induced by adding 0.2 mM IPTG and incubation was performed overnight at 22 °C. The figure shows several samples taken during the process of protein purification which were run on a 10 % SDS-PAGE gel and stained with Coomassie Blue as outlined in sections 2.2.2.1 and 2.2.2.3 respectively. The positions of the molecular weight markers are shown on the left. The first lane corresponds to a sample before induction (BI) followed by a sample after induction (I), sample from the lysate (L), wash 1 (W1), wash 2 (W2) and fraction eluted (8 µl) using 500 mM imidazole (EL).

4.3.5.2 Effects of adding M18c into the fusion assay mediated by wild-type Sx 4/SNAP23/VAMP2

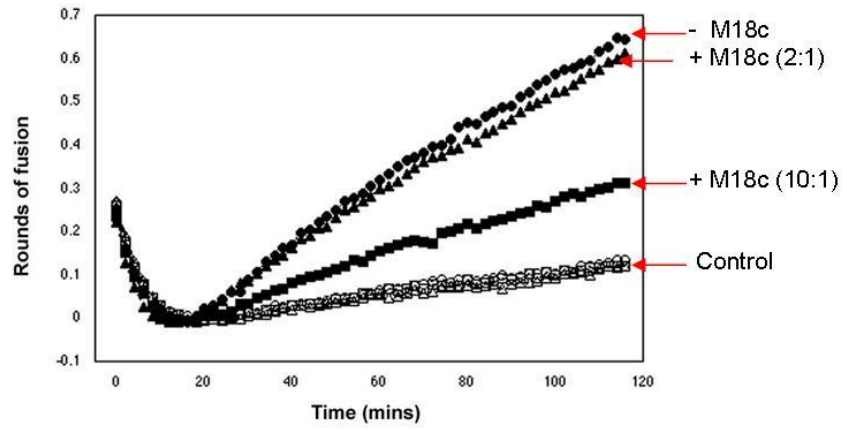
In order to test how His₆-M18c affect wild-type Sx 4/SNAP23/VAMP2-mediated membrane fusion *in vitro*, two different experimental protocols were performed in collaboration with Dr Fiona Brandie (University of Glasgow).

In the first, His₆-M18c was added directly to the fusion assays at molar ratios of either 2:1 or 10:1 M18c: t-SNARE. This resulted in a dose-dependent inhibition of liposome fusion catalysed by wild-type Sx 4/SNAP23 and VAMP2 (Figure 4.14B) (Brandie *et al.*, 2008). Importantly, when an equivalent amount of M18a, a neuronal SM protein that does not bind to Sx 4, is added to the same assay, no effect on fusion is observed (unpublished; data from Prof James A McNew, Rice University). In the second protocol, recombinant His₆-M18c was pre-bound to the t-SNARE complexes prior to reconstitution into liposomes (equimolar amounts of both proteins were used). The result was that the reconstitution of pre-bound M18c/Sx4/SNAP23 into liposomes completely abolished fusion when mixed with VAMP2 liposomes at 37 °C (Figure 4.14C).

A



B



C

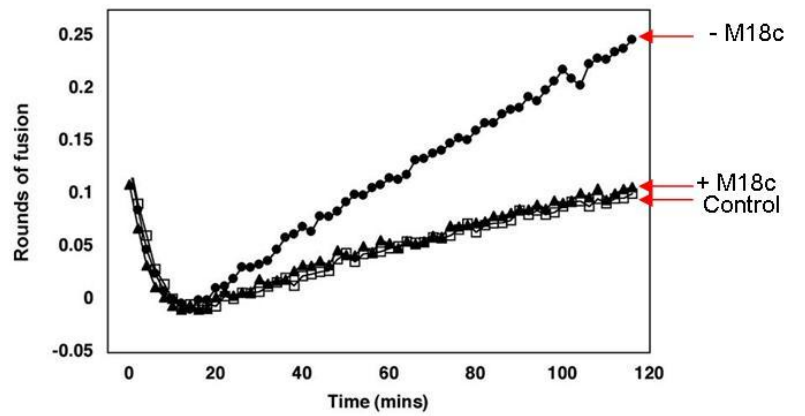


Figure 4.14 His₆-M18c inhibits SNARE-mediated membrane fusion *in vitro* in a dose dependent manner

(A) Purified t-SNARE complex, consisting of Sx 4/SNAP23 (input, 2 μ l), along with reconstituted t-SNARE complexes (vesicles, 10 μ l) were separated on a 12 % SDS-PAGE gel and stained with Coomassie Blue. Purified v-SNARE protein (input, 2 μ l) and reconstituted VAMP2 (vesicles, 10 μ l) and the cytoplasmic domain of VAMP2 (VAMP2-cyto, 2 μ l) were separated on a 15 % SDS-PAGE gel and also stained with Coomassie Blue. These proteins were used for the *in vitro* fusion assay. (B) Before addition of M18c to the assays, recombinant His₆-M18c was dialysed overnight against glycerol free A200 buffer. M18c was added directly to the fusion assay containing the mixture of t- and v-SNAREs and incubation occurred at 4 °C overnight. Fusion between the two vesicle populations in the absence (filled circles) and presence of M18c at two different ratios to Sx 4/SNAP23 (2:1, filled triangles, 10:1, filled squares) was monitored by measuring NBD fluorescence at 535 nm every 2 min. As a control, fluorescence was monitored in each population in the presence of 2 μ l of VAMP2-cyto (open circles, open triangles and open squares respectively). The raw Fluorescence was normalised to maximal detergent signal after addition of n-dodecylmaltoside (DM). Using a program called kaleidagraph, the percentage of maximal DM fluorescence was converted to “rounds of fusion” or fold lipid dilution by a calibration curve which is derived from the absorbance of dilutions of the two head group labeled lipids. (C) In this experiment, a different approach was taken. Equimolar amounts of M18c (dialysed against A200 buffer) and t-SNARE complex were pre-mixed overnight at 4 °C. As a control, the same amount of t-SNARE was mixed overnight at 4 °C with A200 buffer instead of M18c. OG was added to maintain the concentration at 1 %. Reconstitution into liposomes was then carried out as outlined in section 2.2.3.3. Fusion was monitored between vesicles containing t-SNAREs alone (filled circles) and t-SNAREs pre-mixed with M18c (filled triangles) with v-SNARE vesicles. As a control, fusion was also monitored between vesicles containing t-SNAREs alone and v-SNARE vesicles in the presence of VAMP2-cyto (open squares). This figure shows a typical result obtained (Brandie *et al.*, 2008).

4.3.5.3 Reconstitution of SNARE proteins containing Sx 4 in the wild-type and mutant forms to use in the assays with M18c

Data from Dr Fiona Brandie (University of Glasgow) has shown that deletion of the N-terminal 36 residues of Sx 4 significantly reduced M18c binding (Aran *et al.*, 2009) (figure 4.2). Thus, Sx 4 lacking this short N-terminal peptide in the open and wild-type forms were generated as described in section 4.3.1.1. Since it was observed that M18c negatively regulates membrane fusion *in vitro* (figure 4.14), the different Sx 4 constructs were again reconstituted together with SNAP23 (figure 4.15) and fusion assays were performed again in the presence and in the absence of His₆-M18c. Figure 4.12 shows that these new constructs, when reconstituted into liposomes, are capable of mediating membrane fusion together with VAMP2 vesicles.

Figure 4.15 shows the levels of the reconstituted SNARE proteins used in the *in vitro* fusion experiments with M18c.

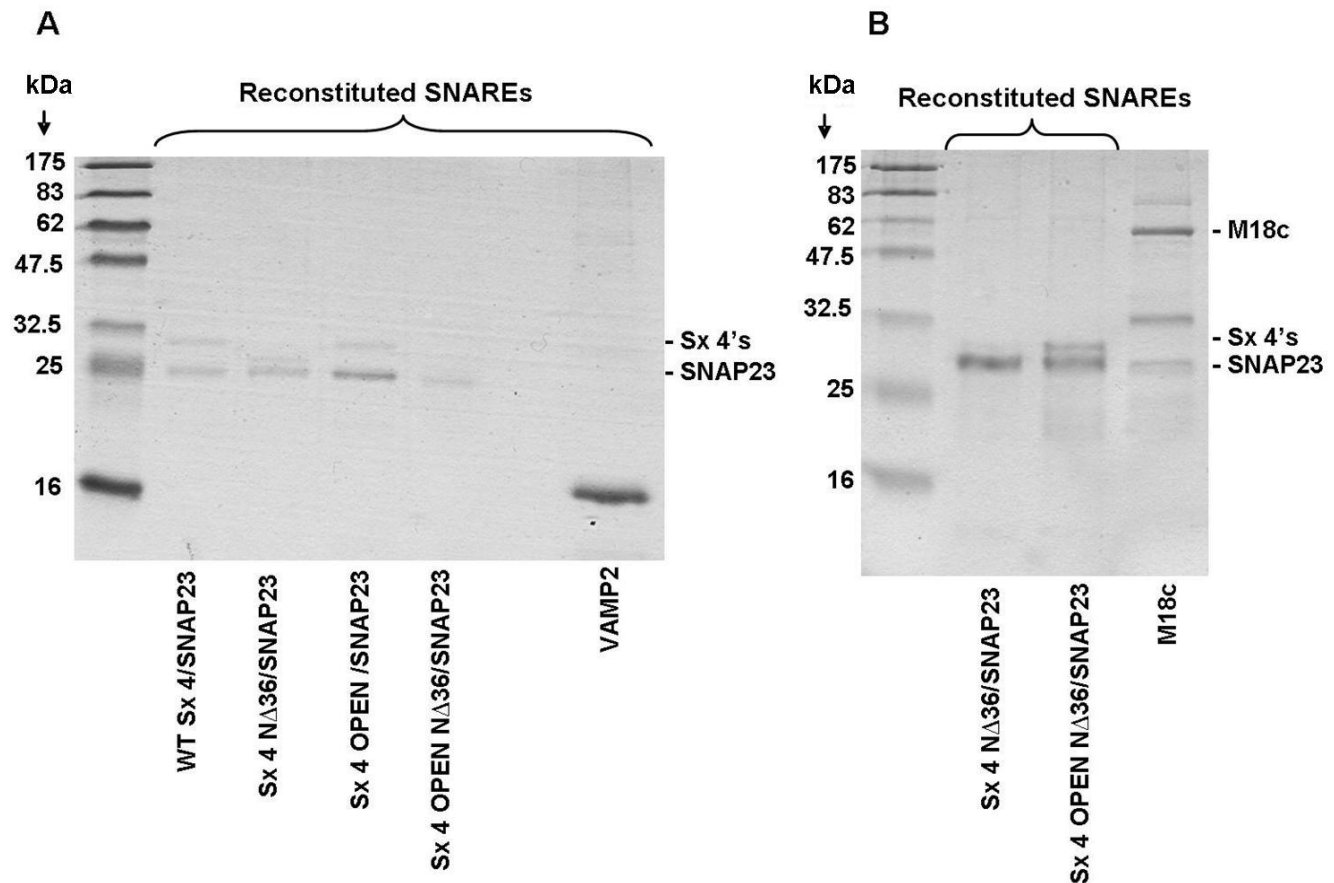


Figure 4.15 Proteoliposomes used for fusion assays with M18c

(A) Approximately similar amounts of purified t-SNARE complexes were successfully reconstituted into synthetic liposomes. VAMP2 was also reconstituted. After reconstitution, 10 μ l of reconstituted t-SNARE liposomes and VAMP2 liposomes were separated on a 15 % SDS-PAGE gel and stained with Coomassie Blue as outlined in sections 2.2.2.1 and 2.2.2.3. (B) Due to the poor levels of the reconstituted t-complexes containing Sx 4 N Δ 36/SNAP23 and Sx 4 OPEN N Δ 36/SNAP23, another reconstitution was performed as shown. 1 μ g of M18c (used in the assays) is also shown. Positions of the molecular weight markers are shown.

4.3.5.4 Consequences of adding M18c into the fusion assays mediated by either wild-type Sx 4/SNAP23 or Sx 4 N Δ 36/SNAP23 with VAMP2

Figure 4.14B shows that M18c inhibits SNARE-mediated membrane fusion in a dose dependant manner, however it is not known whether this inhibition occurs *via* the first 36 amino acids present at the N-terminus of Sx 4 or not. Thus, in this section M18c was directly added to the fusion assays of both wild-type Sx 4/SNAP23/VAMP2 and Sx 4 N Δ 36/SNAP23/VAMP2. In each set of fusions, measurements were made in the absence (filled triangles) and in the presence of M18c (empty triangles) at a 4:1 molar ratio to Sx 4/SNAP23. The controls in the presence (open squares) and in the absence of M18c (filled

circles) contained 3 μ l of VAMP2 Δ TMD which was pre-incubated with the t-complex prior to addition of both VAMP2 liposomes and M18c. The difference between sets A and B is that in set A M18c was added directly to the fusion assay containing the mixture of t- and v-SNAREs and the mixtures were incubated overnight before starting the fluorescence measurements. In set B, v- and t-SNARE vesicles were mixed at the same time as set A, however they were allowed to pre-dock overnight at 4 °C before addition of M18c. This was performed since it was already observed that pre-incubation of liposomes at 4 °C allows SNARE assemblies to accumulate (Shen *et al.*, 2007). After M18c was added, incubation with the v- and t-SNAREs proceeded for 2 h before starting measurements. In summary, in set A vesicles were not allowed to pre-dock while in set B, vesicles were allowed to dock before addition of M18c. This approach is useful to check if M18c influences SNARE complex formation and to test if deleting the 36 amino acids from Sx 4 abolishes M18c inhibition.

Figure 4.16 shows that M18c inhibits, almost totally (approximately 78 % inhibition), the fusion between vesicles that were not allowed to form trans-SNARE complexes before M18c addition (figure 4.16A). The fusion of vesicles that were allowed to pre-dock overnight, were much less affected (approximately 20 % inhibition) by M18c addition (figure 4.16B). These results indicate that the formation of the ternary complex formed by Sx 4/SNAP23/VAMP2 prior to addition of M18c abolishes M18c inhibition.

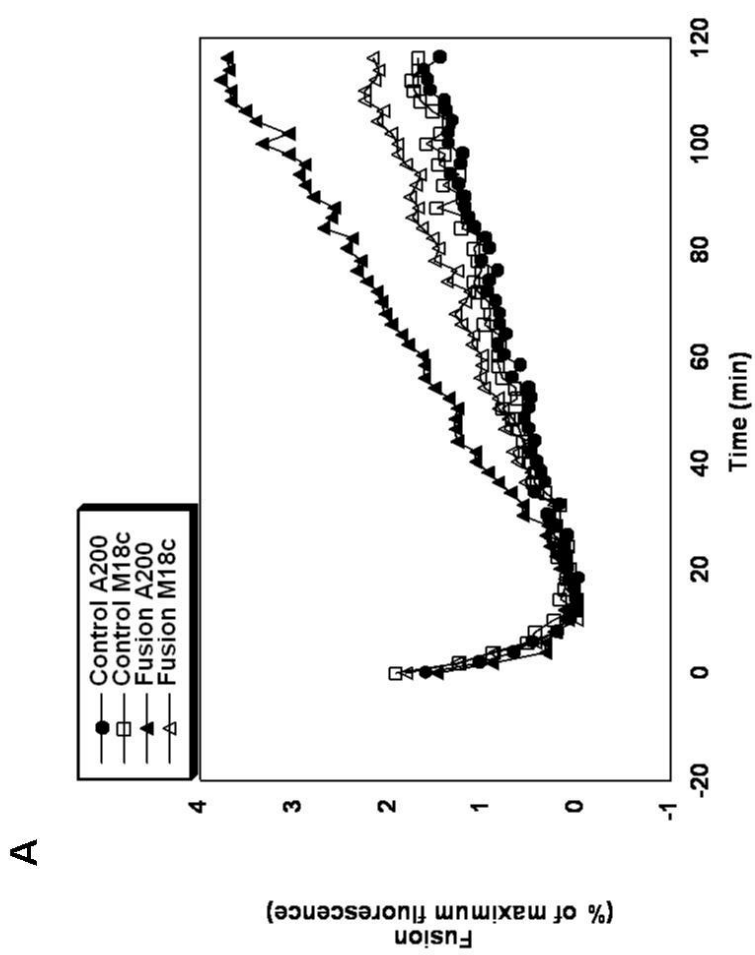
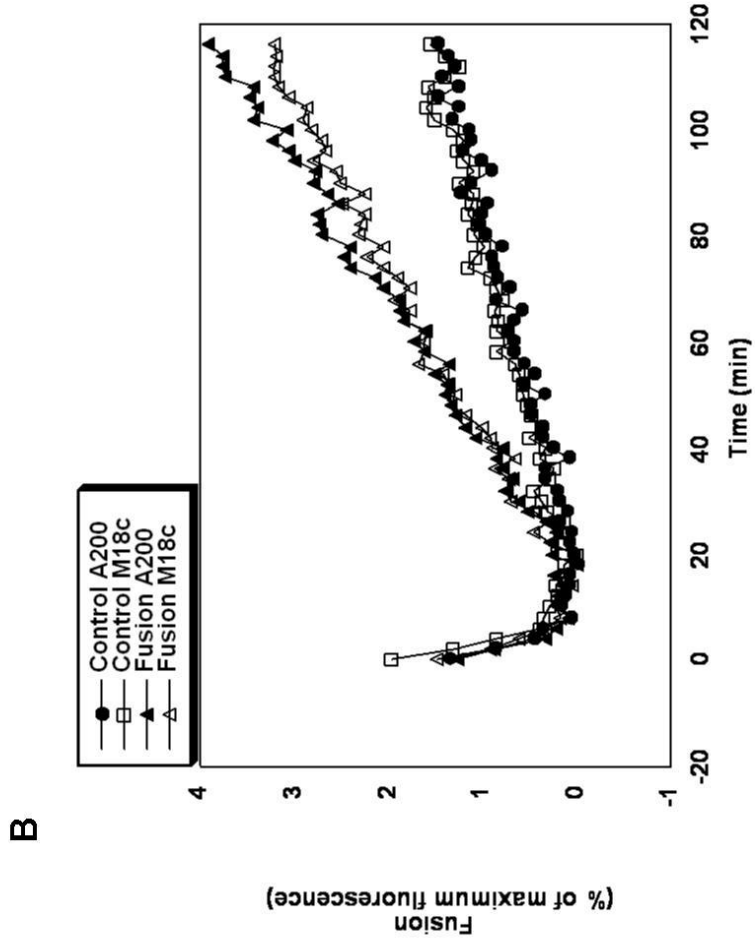


Figure 4.16 *In vitro* fusion of wild-type Sx 4/SNAP23 with VAMP2 vesicles (pre-docked or not) in the presence and in the absence of His₆-M18c

(A) 5 μ l of v- and 45 μ l of t- SNARE liposomes were mixed inside a well and incubated at 4 °C with M18c overnight at a molar ratio of 4:1 M18c to Sx 4/SNAP23 (open triangles). In another well, instead of M18c, an equal volume A200 buffer was added (filled triangles). To block the formation of trans-SNARE complexes (negative controls), the cytoplasmic domain of VAMP2 (VAMP2 Δ TMD) was added to the t-complex and incubated for 10 min before the addition of VAMP2 vesicle in the presence and in the absence of M18c (open squares and filled circles respectively). (B) In this experiment the liposomes were NOT pre-incubated overnight with M18c. So, 5 μ l of v- and 45 μ l of t- SNARE liposomes were pre-mixed and incubated at 4 °C overnight thus allowing the trans-SNARE complex to form. In the following day, M18c was added to the pre-assembled liposomes at a molar ratio of 4:1 M18c to Sx 4/SNAP23 and incubated for 2 h at 4 °C (open triangles). For the controls, A200 buffer was added instead of M18c (filled triangles). As negative controls, VAMP2 Δ TMD was added to separate reactions containing either A200 buffer (filled circles) or M18c (open squares). Fluorescence was measured at 2 min intervals for 2 h with the excitation filter set to 485 nm and the emission filter set at 520 nm and it was temperature dependent (37 °C). After 2 h, 10 μ l of 2.5 % (w/v) n-dodecylmaltoside was added to the wells containing liposomes and mixed, and the fluorescence was recorded for further 40 min at 2 min intervals. The raw data normalised to 100 % detergent signal for A and B is shown in the appendix (figure II). Graphs A and B show levels of fusion as a percentage of the maximum NBD emission plotted against time in min. This figure shows a typical result obtained after several fusion assays.

In figure 4.17 instead of wild-type Sx 4, a shorter version lacking the 36 amino acids from the N-terminus was used. Results show that M18c negatively affects the fusion of vesicles that were not allowed to form trans-SNARE complexes (approximately 63 % inhibition), in contrast to the vesicles that were allowed to pre-dock overnight at 4 °C, which were not significantly affected (figures 4.17A and 4.17B respectively). These data indicate that the formation of the ternary complex formed by Sx 4 Δ 36/SNAP23/VAMP2 prior to addition of M18c abolishes M18c inhibition. Deletion of the short N-terminal peptide in Sx 4 does not seem to influence the result when compared to its wild-type version (figures 4.17 and 4.16 respectively).

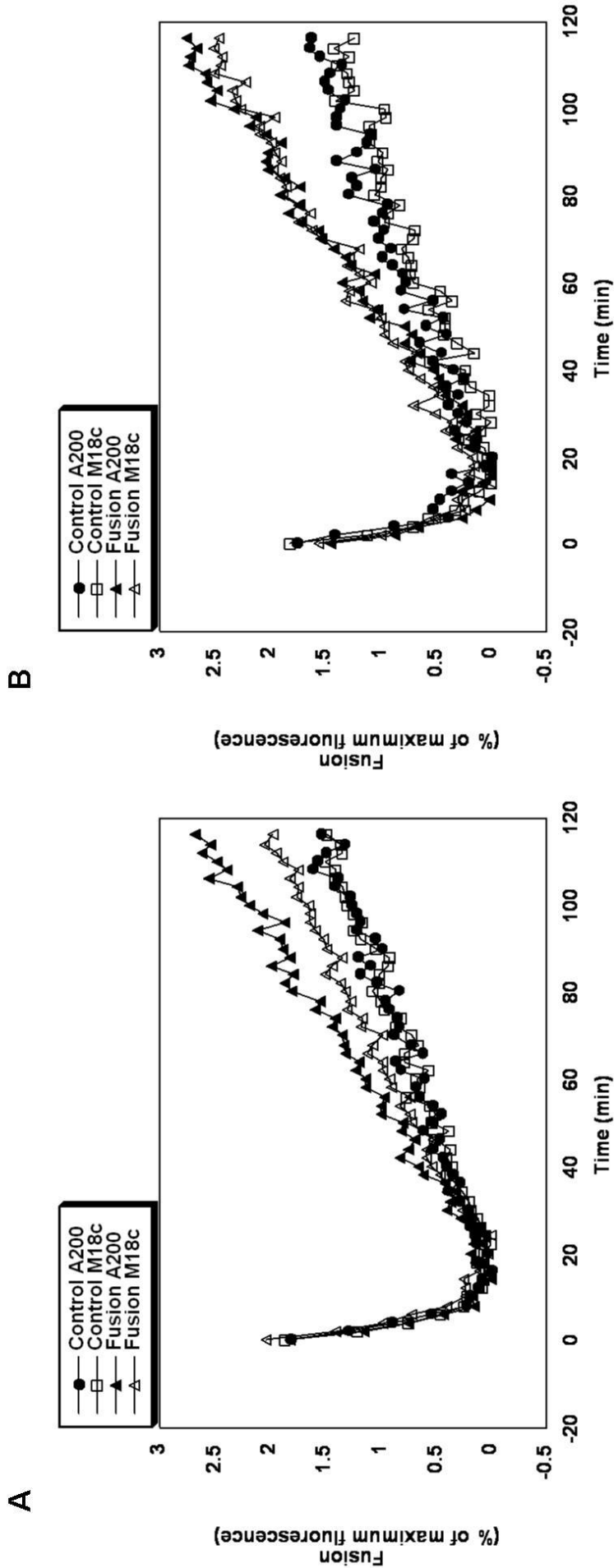


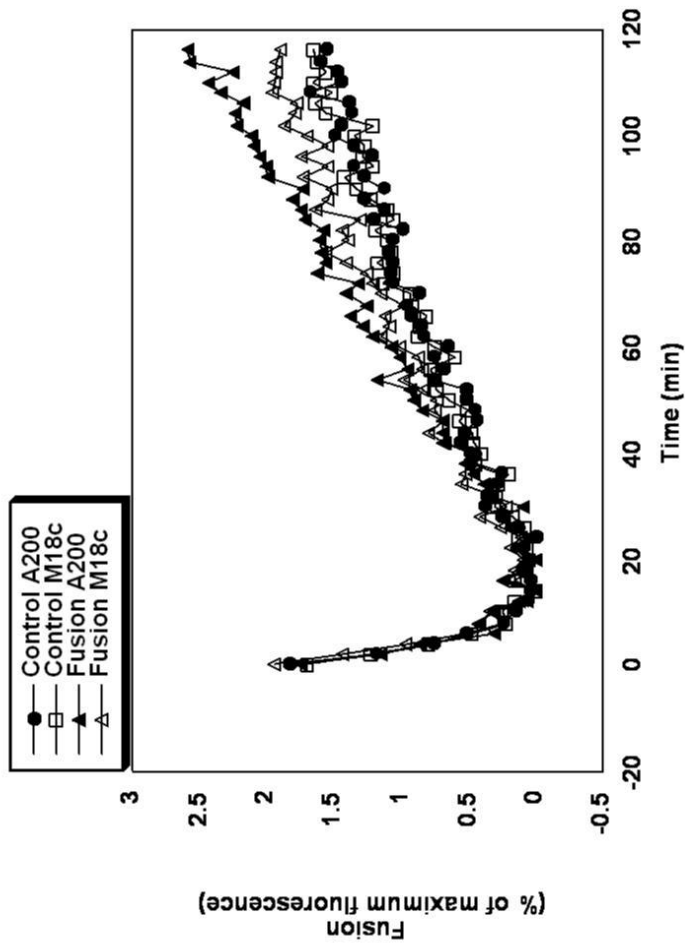
Figure 4.17 *In vitro* fusion of Sx 4 N Δ 36/SNAP23 with VAMP2 vesicles (pre-docked overnight or not) in the presence and in the absence of His₆-M18c

In this fusion assay, the same protocol described in figure 4.16 was followed, but instead of using reconstituted t-complexes containing wild-type Sx 4, a shorter version lacking the 36 amino acids from the N-terminus was used. Figure 4.15A shows reconstituted Sx 4 N Δ 36/SNAP23 and VAMP2 used in this assay. The raw data normalised to 100 % detergent signal for A and B is shown in the appendix (figure III). Graphs A and B show levels of fusion as a percentage of the maximum NBD emission plotted against time in minutes. In A and B, filled circles correspond to control with cytoplasmic VAMP2 plus A200 buffer, open squares represent control with cytoplasmic VAMP2 plus M18c (1:4 molar ratio M18c to Sx 4 N Δ 36/SNAP23), filled triangles correspond to fusion in the presence of A200 buffer and finally open triangles correspond to fusion in the presence of M18c (1:4 molar ratio M18c to Sx 4 N Δ 36/SNAP23). Percentage of NBD emission (fusion) was plotted against time using software described in section 2.2.3.7. This figure shows a typical result obtained.

Another approach was taken to check if M18c inhibition is also time dependent.

Reconstituted Sx 4 N Δ 36/SNAP23 vesicles were allowed to pre-dock overnight, or not, before addition of His₆-M18c for only 2 h (instead of overnight). Interestingly, results from figure 4.18A shows that M18c inhibited fusion of vesicles that were not allowed to form trans-SNARE complexes by approximately 70 %. In contrast, vesicles that were allowed to pre-dock overnight before 2 h incubation with His₆-M18c did not have their fusion rates altered by M18c addition (figure 4.18B). This result is similar to the result obtained in figure 4.17, which indicates that the formation of the ternary complex formed by Sx 4 N Δ 36/SNAP23/VAMP2 prior to addition of M18c abolishes M18c inhibition. There was essentially no change in the results obtained when comparing M18c incubation overnight with incubation for only 2 h (figures 4.17A and 4.18A respectively).

A



B

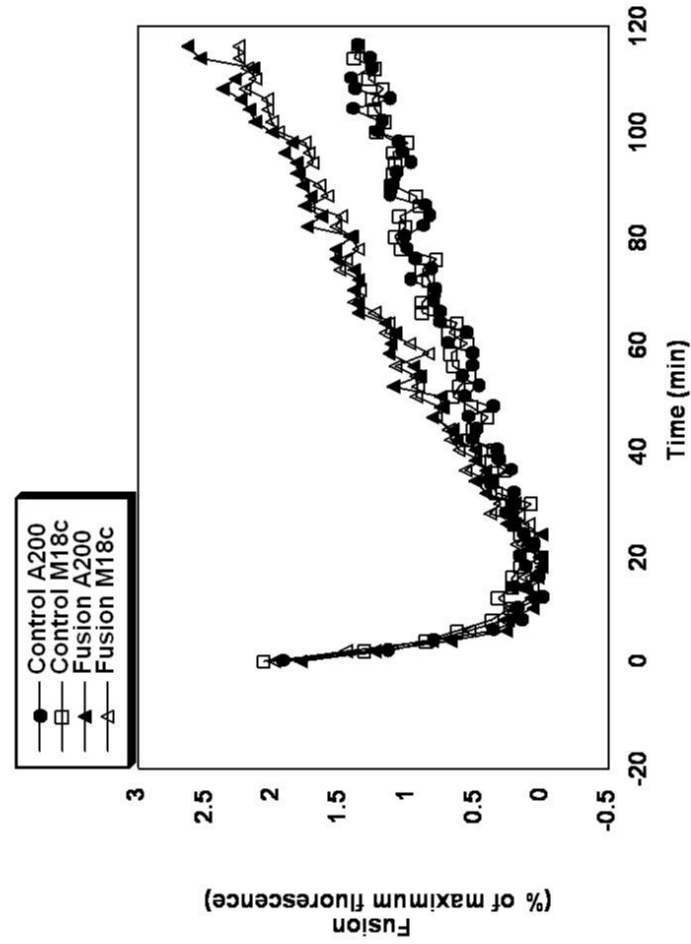


Figure 4.18 *In vitro* fusion of Sx 4 N Δ 36/SNAP23 liposomes with VAMP2 liposomes (pre-docked or not) in the presence or in the absence of His₆-M18c for 2 h

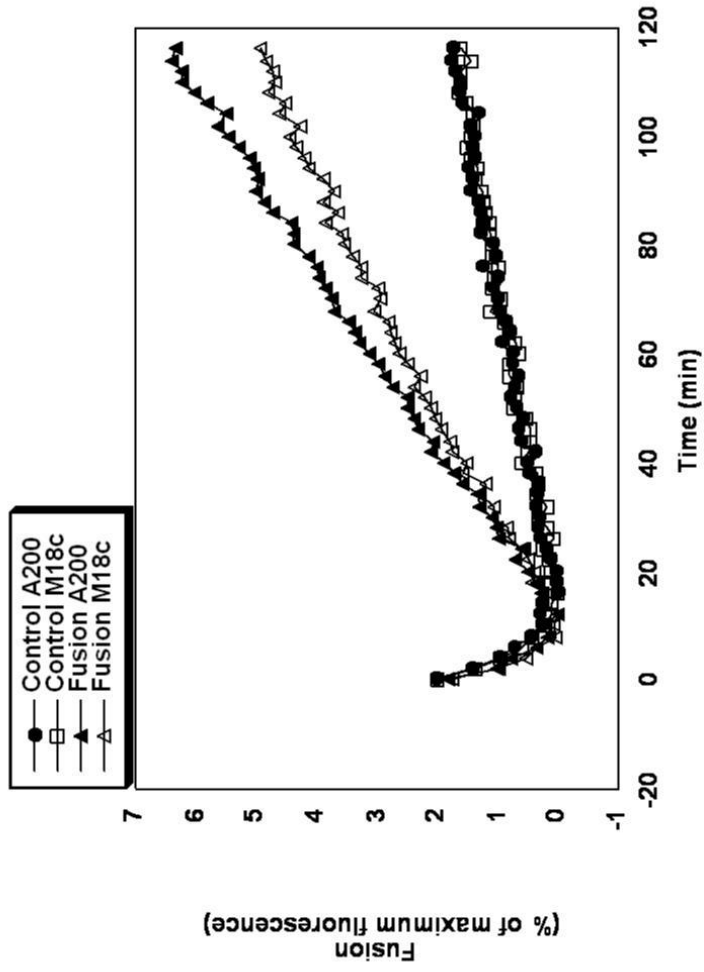
(A) 5 μ l of v- and 45 μ l of t- SNARE liposomes containing Sx 4 N Δ 36/SNAP23 shown in figure 4.15B, were mixed inside a well and incubated at 4 °C with M18c for 2 h at a molar ratio of 4:1 M18c to Sx 4 N Δ 36/SNAP23 (open triangles). In another well, instead of M18c, an equal volume A200 buffer was added (filled triangles). Incubation was continued at 4 °C before the temperature was elevated to 37 °C for fusion. In order to block the formation of trans-SNARE complexes, the cytoplasmic domain of VAMP2 (VAMP2 Δ TMD) was added to the t-complex and incubated for 10 min before the addition of VAMP2 vesicles in the presence and in the absence of M18c (negative controls; open squares and filled circles respectively). (B) In this experiment, 5 μ l of v- and 45 μ l of t- SNARE liposomes were pre-mixed and incubated at 4 °C overnight thus allowing the vesicles to dock. In the following day, M18c was added to the pre-assembled liposomes at a molar ratio of 4:1 M18c to t-SNARE complex and incubation occurred for 2 h at 4 °C (open triangles). For the controls, A200 buffer was added instead of M18c (filled triangles). As negative controls, VAMP2 Δ TMD was added prior to the addition of VAMP2 vesicles to the reactions containing either A200 buffer (filled circles) or M18c (open squares). Fluorescence was measured as described in section 2.2.3.6. The raw data normalised to 100 % detergent signal for A and B is shown in the appendix (figure IV). Graphs A and B show levels of fusion as a percentage of the maximum NBD emission plotted against time in minutes. This figure shows a typical result obtained after performing the experiment twice.

4.3.5.5 Effects of adding M18c into the fusion assays of Sx 4 OPEN/SNAP23 and Sx 4 OPEN N Δ 36/SNAP23 with VAMP2

In this section, the same approach as in section 4.3.5.4 was taken. The only difference was the versions of Sx 4 used. Sx 4 locked in the open conformation and Sx 4 open lacking the 36 amino acids from the N-terminus were reconstituted with SNAP23 to form t-SNARE complexes as shown in figure 4.15. In sets A (figures 4.19, 4.20 and 4.21) vesicles were not allowed to pre-dock while in sets B (figures 4.19, 4.20 and 4.21), vesicles were allowed to pre-dock overnight at 4 °C before addition of 4:1 molar ratio M18c: t-complex.

Figure 4.19, shows that His₆-M18c affects negatively vesicles that were not allowed to form trans-SNARE complexes (approximately 55 %) rather than vesicles that were allowed to pre-dock overnight (approximately 24 % inhibition). This result indicates that the formation of the ternary complex formed by Sx 4 OPEN/SNAP23/VAMP2 prevents M18c inhibition.

B



A

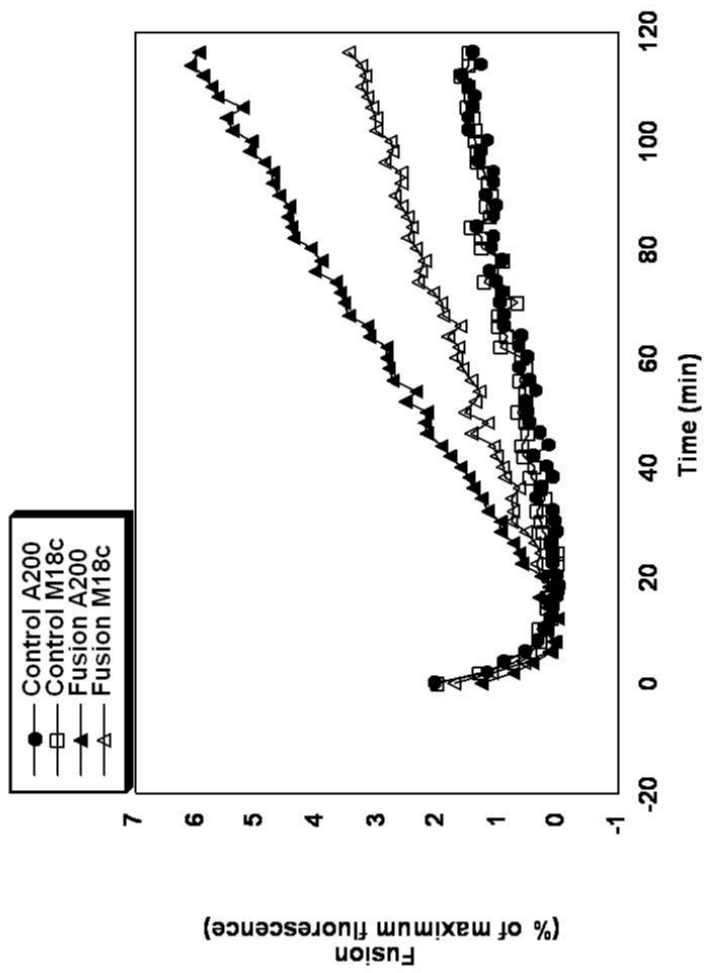
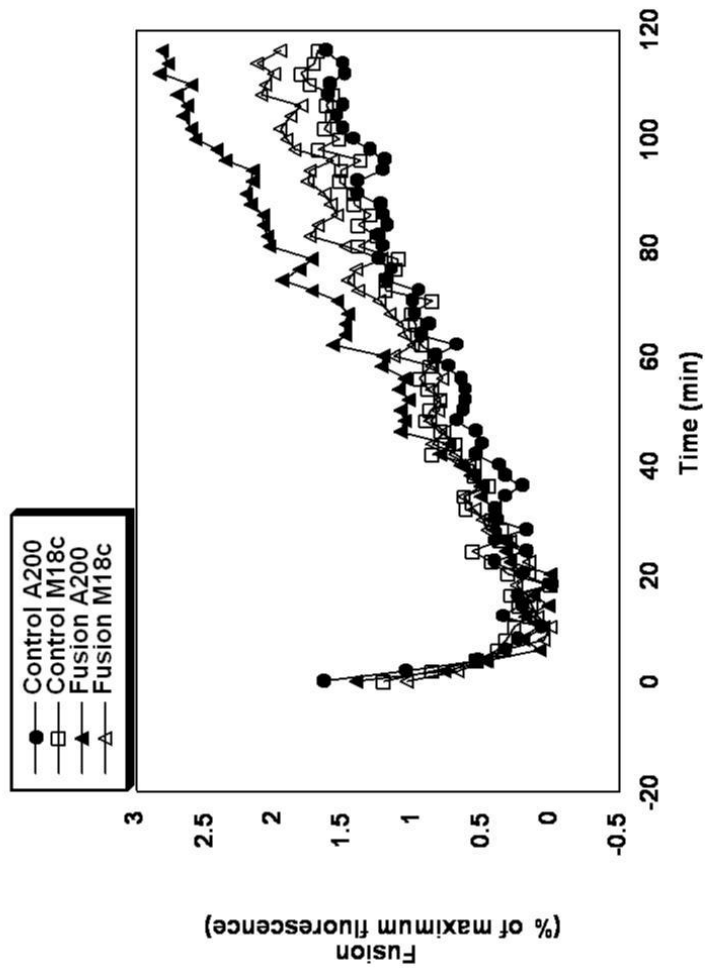


Figure 4.19 *In vitro* fusion of Sx 4 OPEN/SNAP23 with VAMP2 vesicles (pre-docked overnight or not) in the presence and in the absence of M18c

(A) 5 μ l of v- and 45 μ l of t- SNARE liposomes containing Sx 4 OPEN instead of wild-type were mixed inside a well and incubated at 4 °C with M18c overnight at a molar ratio of 4:1 M18c to Sx 4 OPEN/SNAP23 (open triangles). To another well an equal volume of buffer A200 was added instead of M18c (filled triangles). To block the formation of trans-SNARE complexes, the cytoplasmic domain of VAMP2 (VAMP2 Δ TMD) was added to the t-complex and incubated for 10 min before the addition of VAMP2 vesicle in the presence and in the absence of M18c (open squares and filled circles respectively). Fusion was then monitored by placing the 96 well plate in the fluorescence reader set at 37 °C as described in section 2.2.3.6. Top graph correspond to raw fluorescence normalised to percentage of maximum detergent signal (100 %) against time. Lower graph shows levels of fusion determined as a percentage of the 100 % signal also against time. (B) In this experiment, 5 μ l of v- and 45 μ l of t- SNARE liposomes were pre-mixed and incubated at 4 °C overnight thus allowing the trans-SNARE complex to form before addition of M18c. In the following day, M18c was added to the pre-assembled liposomes at a molar ratio of 4:1 M18c to Sx 4 OPEN/SNAP23 and incubation occurred for 2 h at 4 °C (open triangles). For the controls, A200 buffer was added instead of M18c (filled triangles). As negative controls, VAMP2 Δ TMD was added to separate reactions containing either A200 buffer (filled circles) or M18c (open squares). Fusion measurements occurred at 37 °C as described in section 2.2.3.6. The raw data corresponds to raw fluorescence normalised to percentage of maximum detergent signal (100 %) against time (see appendix, figure V). Graphs A and B show levels of fusion determined as a percentage of the 100 % signal also against time.

The removal of the 36 amino acids from the N-terminal region of the OPEN Sx 4 protein did not affect dramatically the results compared to full-length Sx 4 OPEN, the main difference was in the percentage of inhibition when vesicles were allowed to pre-dock before M18c addition (24 % for OP and 0 % for OP N Δ 36). Figure 4.20 shows that M18c inhibits fusion of vesicles that were not allowed pre-dock by approximately 75 % (figure 4.20A). Rates of fusion of vesicles that were allowed to pre-dock overnight (figure 4.20B), were not affected by M18c. This result indicates that the formation of the ternary complex consisting of Sx 4 OPEN N Δ 36/SNAP23/VAMP2 prior to addition of M18c also abolishes M18c inhibition. Deletion of the short N-terminal peptide of Sx 4 OPEN did not affect significantly the results when compared to full length Sx 4 OPEN (figures 4.20 and 4.19 respectively).

A



B

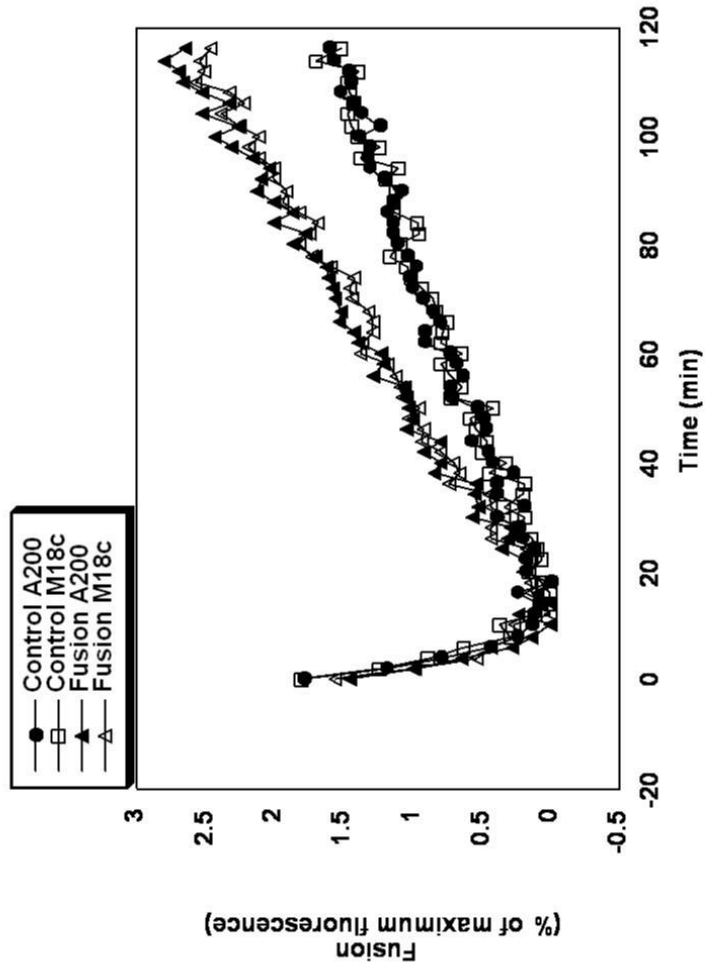


Figure 4.20 *In vitro* fusion of Sx 4 OPEN N Δ 36/SNAP23 with VAMP2 vesicles (pre-docked overnight and not docked) in the presence and in the absence of M18c

In this fusion assay, the same protocol described in figure 4.19 was followed, however instead of using reconstituted t-complexes containing OPEN Sx 4, a shorter version lacking the 36 amino acids from the N-terminus was used instead. Figure 4.15A, shows reconstituted Sx 4 OPEN N Δ 36/SNAP23 and VAMP2 used in this assay. (A) and (B) show levels of fusion as a percentage of the maximum NBD fluorescence emission. In both (A) and (B), filled circles correspond to control with cytoplasmic VAMP2 plus A200 buffer, open squares represent control with cytoplasmic VAMP2 plus M18c (1:4 molar ratio M18c to OPEN Sx 4 N Δ 36/SNAP23), filled triangles correspond to fusion in the presence of A200 buffer and finally open triangles correspond to fusion in the presence of M18c (1:4 molar ratio M18c to OPEN Sx 4 N Δ 36/SNAP23). For fusion reactions, the raw data normalised to 100 % detergent signal for A and B is shown in the appendix (figure VI). Graphs A and B show levels of fusion as a percentage of the maximum NBD emission plotted against time in minutes. This figure shows a typical result obtained after several fusion assays.

Another approach was taken to confirm the findings obtained in figure 4.20. Reconstituted Sx 4 OPEN N Δ 36/SNAP23 from figure 4.15B were allowed to form ternary complexes with VAMP2 vesicles overnight (figure 4.21, set B) or not (figure 4.21, set A) before the addition of M18c for only 2 h in both cases. Again, M18c was added at 4:1 molar ratio M18c: Sx 4 OPEN N Δ 36/SNAP23. Thus, differently to figure 4.20, M18c was not pre-incubated overnight with the t- and v-SNARE vesicles. Figure 4.21A, shows that M18c inhibits fusion of vesicles that were not allowed to pre-dock before M18c addition, since 80 % of inhibition in fusion was observed compared to fusion without M18c. However, M18c addition to vesicles that were allowed to pre-dock overnight (figure 4.21B), were just affected slightly by 18 %. Thus, even 2 h incubation with M18c was enough to inhibit fusion of Sx 4 OPEN N Δ 36/SNAP23/VAMP2 when these vesicles were not pre-docked. This result indicates that the formation of the ternary complex formed by Sx 4 OPEN N Δ 36/SNAP23/VAMP2 prior to addition of M18c abolishes M18c inhibition, and that M18c inhibition is not affected by the removal of the 36 amino acids from Sx 4 OPEN.

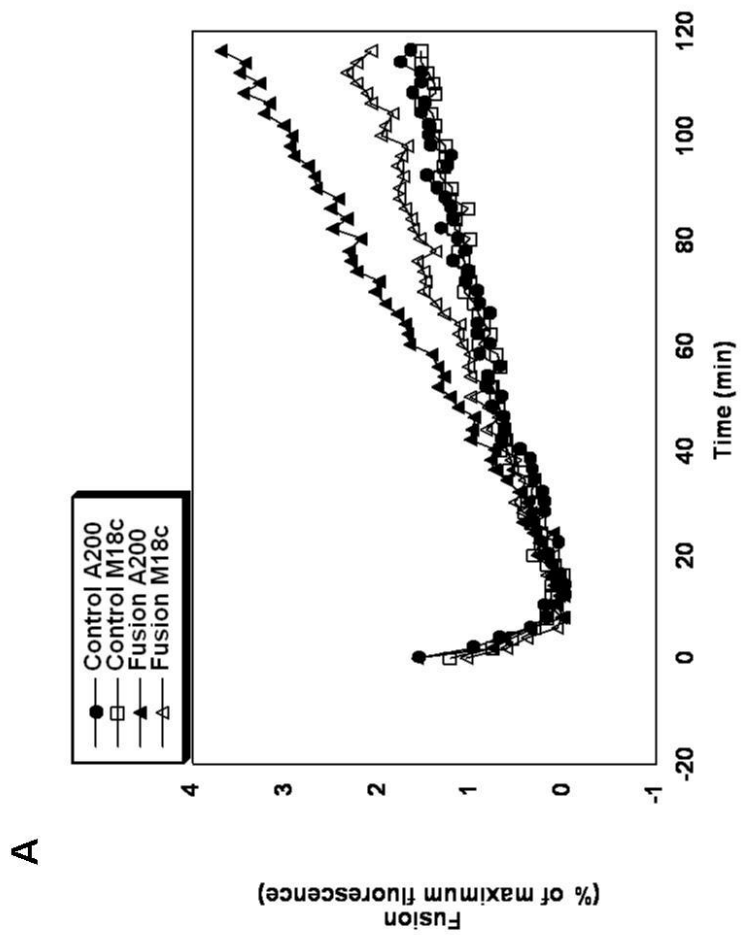
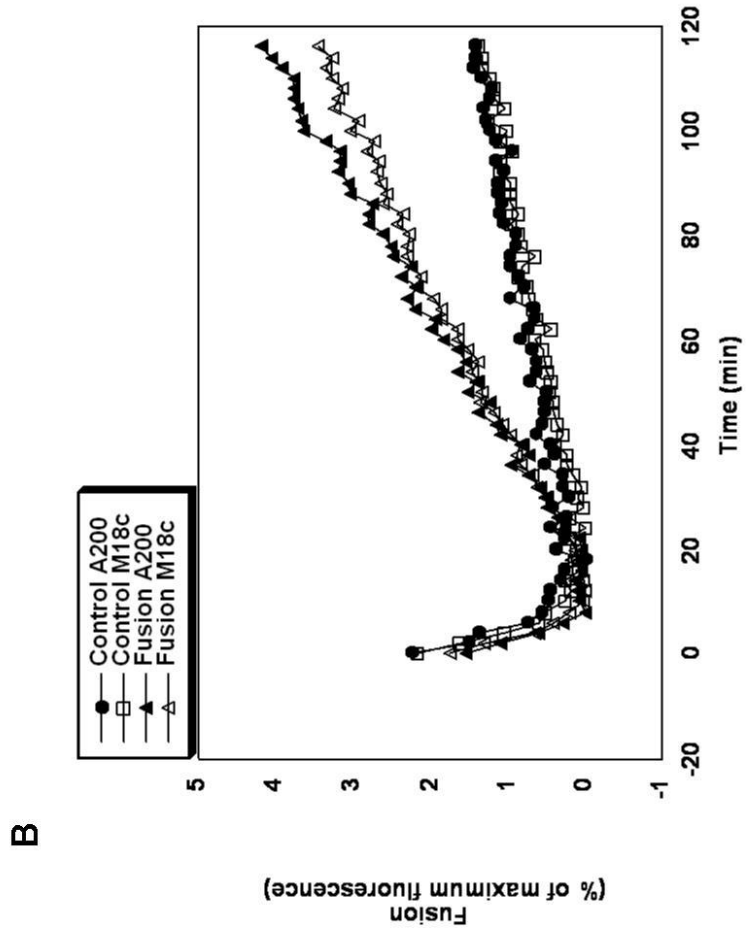


Figure 4.21 *In vitro* fusion of Sx 4 OPEN N Δ 36/SNAP23 with VAMP2 vesicles (pre-docked overnight or not) in the presence and in the absence of M18c for 2 h

(A) 5 μ l of v- and 45 μ l of t- SNARE liposomes containing Sx 4 OPEN N Δ 36/SNAP23 shown in figure 4.15B were mixed inside a well and incubated at 4 °C with M18c for 2 h at a molar ratio of 4:1 M18c to Sx 4 OPEN N Δ 36/SNAP23 (open triangles). In another well, instead of M18c, an equal volume A200 buffer was added (filled triangles). Incubation was continued at 4 °C before the temperature was elevated to 37 °C for fusion at the end of the 2 h. To block the formation of trans-SNARE complexes, the cytoplasmic domain of VAMP2 (VAMP2 Δ TMD) was added to the t-complex and incubated for 10 min before the addition of VAMP2 vesicle in the presence and in the absence of M18c (negative controls, filled circles and open squares). (B) In this experiment, 5 μ l of v- and 45 μ l of t- SNARE liposomes were pre-mixed and incubated at 4 °C overnight thus allowing the trans-SNARE complex to form. In the following day, M18c was added to the pre-assembled liposomes at a molar ratio of 4:1 M18c to Sx 4 OPEN N Δ 36/SNAP23 and incubated for further 2 h at 4 °C (open triangles). For the controls, A200 buffer was added instead of M18c (filled triangles). As negative controls, VAMP2 Δ TMD was added prior to the addition of VAMP2 vesicles to the reactions containing either A200 buffer (filled circles) or M18c (open squares). The raw data normalised to 100 % detergent signal for A and B is shown in the appendix (figure VII). Graphs A and B show levels of fusion as a percentage of the maximum NBD emission plotted against time in minutes. Details on how the measurements are made are described in section 2.2.3.7. This figure shows a typical result obtained after two fusion assays.

Figure 4.22 summarises the results obtained in sections 4.3.5.4 and 4.3.5.5. As can be seen from the charts, the highest percentages of M18c inhibition came from the experiments where M18c was added directly together with the SNARE liposomes before fusion reaction. Lower percentages of inhibition were observed in the fusion assays where the vesicles were allowed to pre-dock before M18c addition. Furthermore, deletion of the 36 amino acids from both wild-type and open forms of Sx 4 did not alter significantly the results.

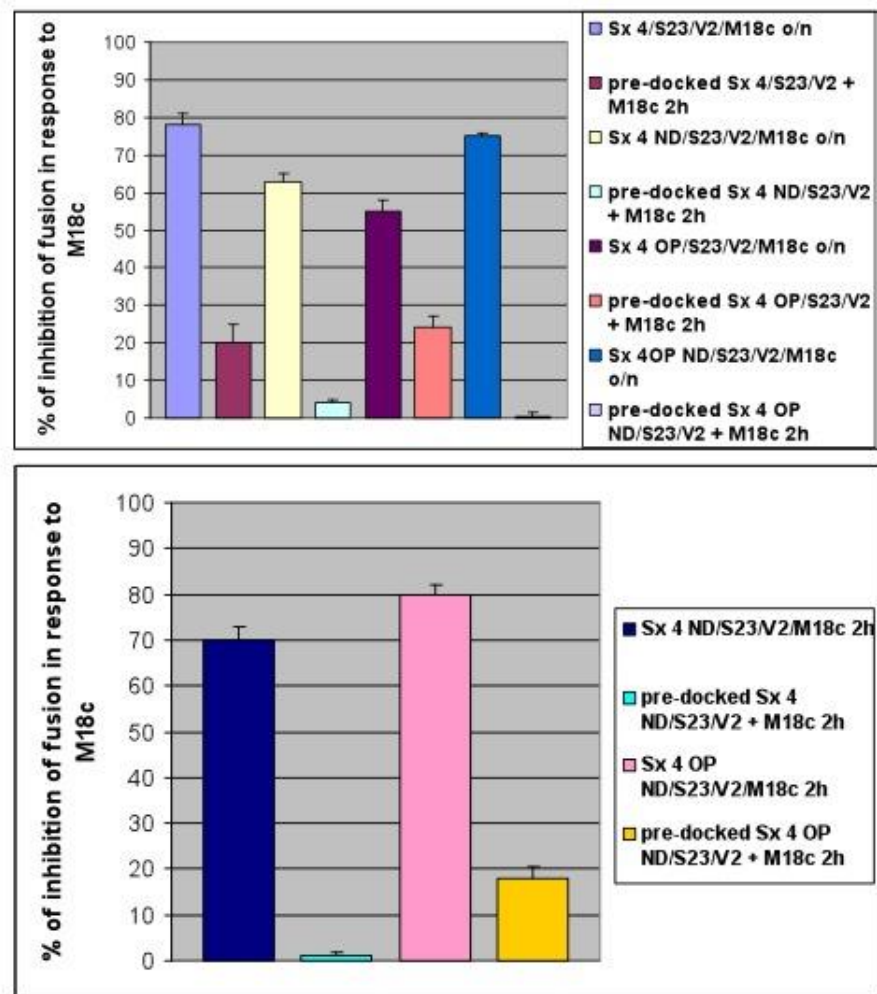


Figure 4.22 Quantifications of the percentages of fusion inhibited by M18c when added at the same time as the SNARE liposomes or added after pre-incubation of SNAREs

The top graph shows the percentages of inhibition by M18c when the different SNARE complexes were allowed, or not, to pre-dock overnight. The lower graph shows the N-delete versions of both wild-type Sx 4 and open Sx 4 pre-incubated overnight before M18c addition or incubated directly with M18c for 2 h before fusion reactions. All percentages were obtained comparing the maximum fusion rate at 120 min in the absence and in the presence of M18c. Error bars represent the standard error of the mean of two independent experiments.

4.4 Discussion

In this chapter a series of experiments were performed to assess the effects of M18c on the rates of fusion between synthetic liposomes containing Sx 4 (wild-type and mutant versions) with VAMP2 liposomes. The highly conserved N-terminal domain of exocytic syntaxins form an autonomously folded 3 helical bundle termed Habc domain, and in the neuronal Sx 1A this domain was shown to be able to fold back onto the SNARE domain generating a “closed” conformation unable to form SNARE complexes (Misura *et al.*, 2000). Mutation of residues L165 and E166 within the hinge region induces this syntaxin to adopt a more “open” conformation (Dulubova *et al.*, 1999). The introduction of a L173A/E174A mutation into the same region in Sx 4 sequence also led to a more “open” form (Aran *et al.*, 2009; D'Andrea-Merrins *et al.*, 2007). Thus, in this chapter, Sx 4 constructs were generated containing the trans-membrane domain in order to reconstitute them into liposomes. These constructs were in the open, open N Δ 36, and N Δ 36 forms. They were reconstituted into liposomes (together with SNAP23) and compared to the wild-type form of Sx 4 in the capability to fuse with VAMP2 vesicles. The fusion reactions were successful as shown in figure 4.12.

Previous studies have shown that SM proteins have the potential to stimulate SNARE-mediated membrane fusion *in vitro* in yeast and neuronal cells (Scott *et al.*, 2004; Shen *et al.*, 2007), but little is known about the effects of M18c on the SNARE proteins involved in GLUT4 fusion. Since we observed that the short N-terminal peptide comprising 36 amino acids of Sx 4 is important for M18c binding (Aran *et al.*, 2009), the Sx 4 constructs generated in this study were reconstituted into liposomes and all versions were tested for fusion with and without M18c.

In these experiments, purified recombinant M18c was added to the liposome fusion assays. Addition of M18c at molar ratios of either 1:1 or 10:1 M18c:wild-type t-SNARE complexes, inhibited liposome fusion catalysed by this SNARE complex in a dose-dependent manner (chapter 4, figure 4.14). Importantly, addition of an equivalent amount of M18a had no effect on fusion (data not shown, Prof James McNew, Rice University, Texas). Then, M18c was added at a molar ratio 4:1 M18c: t-complexes (containing the different versions of Sx 4: wild-type, Sx 4 N Δ 36, Sx 4 OPEN and Sx 4 OPEN N Δ 36). The results showed that deletion of the short N-terminal peptide did not significantly alleviate M18c negative regulation of fusion. This was unexpected, since this mutant lacks the short N-terminal region of Sx 4 which has been shown, through crystallographic studies, to

interact with M18c *via* the pocket mode of binding (Hu *et al.*, 2007). Apart from this, in all fusion reactions where vesicles were allowed to pre-dock at 4 °C, fusion was not dramatically affected by M18c addition (B in figures 4.16, 4.17, 4.18, 4.19, 4.20, 4.21), whereas vesicles that were not allowed to pre-dock and were incubated directly with M18c either overnight or for 2h, were affected (A in figures 4.16, 4.17, 4.18, 4.19, 4.20, 4.21). It was not possible to reconstitute equimolar amounts of M18c together with the different versions of Sx 4/SNAP23 (as seen for the wild-type version in figure 4.14C) for technical reasons.

The negative regulation observed might be happening not only due to the M18c/Sx 4 interaction, but also due to the interaction between M18c and the SNARE motif of VAMP2 shown in chapter 3. Actually, in neuronal cells, M18a was shown to stimulate fusion not only *via* its interaction with Sx 1A, but also *via* its interaction with VAMP2 (Shen *et al.*, 2007). These data also correlates to the finding that in the absence of M18a, a total loss of neurotransmitter release occurs, whereas in the absence of M18c an increase in GLUT4 translocation was observed (Kanda *et al.*, 2005), suggesting that M18c negatively regulates GLUT4 fusion. These data will be further discussed in chapter 6.

In summary, these results indicate that the formation of the ternary complex formed by Sx 4/SNAP23/VAMP2 might be regulated by M18c at least *in vitro*, since other factors might also regulate this process *in vivo*. M18c negatively regulates Sx 4/SNAP23/VAMP2 mediated membrane fusion *in vitro* and this apparently involves other interactions apart from the short N-terminal peptide region in Sx 4.

Chapter 5

5 The consequences of Syntaxin 4 and Munc18c phosphorylation on the regulation of SNARE complex formation

5.1 Introduction

As shown in chapter 4, when recombinant purified, bacterially expressed SNAP23, Sx 4 and VAMP2 are reconstituted into synthetic proteoliposomes, they can mediate fusion. Our studies suggested that non-SNARE proteins such as M18c could negatively affect SNARE-mediated membrane fusion *in vitro*. Nevertheless, other factors might also regulate SNARE-mediated membrane fusion *in vivo*.

In order to maintain normal glucose homeostasis, insulin binds to its heterotetrameric integral-membrane receptor, which in turn triggers a signalling cascade resulting in the translocation and fusion of intracellular GLUT4-containing vesicles with the PM (Olson and Pessin, 1996). This mechanism suggests that factors such as insulin-derived signals might be involved in the regulation of GLUT4 vesicle fusion with the PM. These signals could serve as important regulators of the fusion machinery through phosphorylation of SNARE proteins.

Some studies have reported that SNARE proteins undergo phosphorylation *in vitro*. For example, Sx 4 was shown to be susceptible to phosphorylation by the serine/threonine kinases protein kinase A, casein kinase II, and to a lesser extent by conventional protein kinase C, *in vitro* (Foster *et al.*, 1998). In this study, phosphorylation of Sx 4 by PKA (but not casein kinase II) was shown to affect Sx 4 binding to SNAP23 (Foster *et al.*, 1998). Another study using the yeast two-hybrid system with the PM t-SNARE Sx 4 as bait, has identified a novel human kinase termed SNAK (SNARE kinase), which specifically phosphorylates unassembled SNAP23 (*i.e.* SNAP23 which are not associated with other SNAREs) *in vivo* (Cabaniols *et al.*, 1999). Interestingly, SNAP23 expression and stability were enhanced upon phosphorylation, therefore increasing the assembly of newly synthesized SNAP23 with Sx 4 (Cabaniols *et al.*, 1999).

In 2006, Thurmond's group showed that M18c becomes tyrosine-phosphorylated upon stimulation in both islet β -cells and 3T3-L1 adipocytes (Oh and Thurmond, 2006). Also in 2006, Schmelzle and colleagues, by performing mass spectrometric analyses, have identified tyrosine phosphorylation sites on proteins involved in GLUT4 translocation (Schmelzle *et al.*, 2006). In this study, 3T3-L1 adipocytes were stimulated with insulin for 0, 5, 15 and 45 min. Interestingly, upon 5 min of insulin stimulation Sx 4 increased in phosphorylation by >3-fold and surprisingly M18c showed at least a 10-fold increase in tyrosine phosphorylation. The tyrosine residues that become phosphorylated in response to

insulin are: Y521 on M18c and Y115, Y251 on Sx 4. Interestingly, another group has reported that M18c becomes phosphorylated on residue Y521 in response to platelet-derived growth factor (PDGF) stimulation in skeletal muscle, cultured myotubes, and 3T3-L1 adipocytes (Umahara *et al.*, 2008).

Another potential way in which SM proteins could be regulated is *via* a protein called Doc2 β (Ke *et al.*, 2007). Doc2 proteins are C2 domain-containing proteins which were first identified in the brain (Doc2 α) (Orita *et al.*, 1995) and later found to be ubiquitously expressed (Doc2 β) (Sakaguchi *et al.*, 1995). Doc2 β associates with both M18a in neurons (Verhage *et al.*, 1997) and M18c in islet β -cells and adipocytes suggesting that Doc proteins could regulate M18 interaction with syntaxins (Ke *et al.*, 2007). The association of Doc2 β with M18c was shown to be important for glucose-stimulated insulin secretion (Ke *et al.*, 2007). This data indicates that SM proteins such as M18c might have other “partners” that help in the regulation of syntaxin function.

It is well established that tyrosine phosphorylation plays an important role in insulin signalling, however the exact function of tyrosine phosphorylation in SNARE-mediated membrane fusion remains uncertain. Thus, a more comprehensive study is needed to improve the understanding of how phosphorylation may affect the machinery that leads to glucose uptake in muscle and adipocytes.

5.2 Aims of this chapter

SNARE and SM protein phosphorylation might regulate SNARE-mediated GLUT4 translocation and fusion with the PM (see above). M18c and Sx 4 were shown to become tyrosine phosphorylated in response to insulin, however it is not known if these events are part of the signalling network leading to GLUT4 translocation, or could affect the binding of these proteins to other SNAREs. Thus, an approach consisting of mapping studies, site-directed mutagenesis, pull-down assays and radiolabelling studies were undertaken to establish whether these phosphorylation events impact on SNARE/SM interactions.

5.3 Results

5.3.1 Sx 4 phosphomimetic mutants

The recombinant SNARE proteins expressed in this study were produced in *E.coli*, thus important post-translational modifications that affect mammalian cells could not be assessed unless they were intentionally engineered to produce modifications in the protein of interest. Therefore, to examine whether Sx 4 phosphorylation is able to affect its binding to other proteins, phosphomimetic mutants of tyrosine residues that become phosphorylated in response to insulin were induced. A change to a glutamic acid was an ideal choice, since it is bulky (like tyrosine) and will mimic a phosphorylated residue due to its negative charge.

5.3.1.1 Site-directed mutagenesis and protein purification

Three different mutations were introduced in the Sx 4 sequence using pETDuet-1 Sx 4 as template. The mutations were Y115E, Y251E and Y115E/Y251E (double-mutant). Site-directed mutagenesis was performed as outlined in section 2.2.1.2. Primers were designed taking in consideration melting temperature, length and GC content of the primer. Successful mutation was confirmed by DNA sequencing. Designed primers were as follows (letters in bold refer to original codon and underlined refer to mutated codon):

Sx 4 sequence: 5' CAG AAG GAG GAA GCT GAT GAG AAT **TAC** AAC TCA GTC AAC ACA AGG ATG AAG 3'

Sx 4 Y115E Forward: 5' CAG AAG GAG GAA GCT GAT GAG AAT GAG AAC TCA GTC AAC ACA AGG ATG AAG 3'

Sx 4 Y115E Reverse: 5' CTT CAT CCT TGT GTT GAC TGA GTT CTC ATT CTC ATC AGC TTC CTC CTT CTG 3'

Sx 4 sequence: 5' CTG AGC TCG GCC GAC **TAC** GTG GAA CGT GGG CAA 3'

Sx 4 Y251E Forward: 5' CTG AGC TCG GCC GAC GAG GTG GAA CGT GGG CAA3'

Sx4 Y251E Reverse: 5' TTG CCC ACG TTC CAC CTC GTC GGC CGA GCT CAG 3'

The Sx 4 double mutant was achieved by first generating one mutation (Y115E) and afterwards introducing the second mutation (Y251E) in the Sx 4 Y115E DNA template. The cytosolic domains of Sx 4 Y115E, Y251E and double-mutant were expressed as C-terminally tagged GST fusion proteins from the pETDuet-1 vector. The vector pETDuet-1-Sx 4 was a gift from Dr Fiona Brandie (Glasgow University).

Protein expression was performed in BL21 (DE3) cells as outlined in section 2.2.2.4. Expression was induced using 0.5 mM IPTG, media was incubated overnight at 24 °C and protein purification was achieved as described in section 2.2.2.4. Because these recombinant proteins were made to be used in pull-down assays, they were eluted using 15 mM of reduced glutathione in 50 mM Tris pH 8.0 in order to keep the GST tag. Proteins were dialysed overnight against binding buffer (section 2.1), run on a 12 % SDS-PAGE gel and stained with Coomassie Blue as outlined in sections 2.2.2.1 and 2.2.2.3 respectively. Results from a typical set of purifications are shown in figure 5.1.

As can be seen in figure 5.1, elutions (EL) from each protein purification contained one major band of the expected size (indicated with arrows) corresponding to GST-Sx 4 Y115E (A), GST-Sx 4 Y251E (B) and GST-Sx 4 Y115E/251E (C).

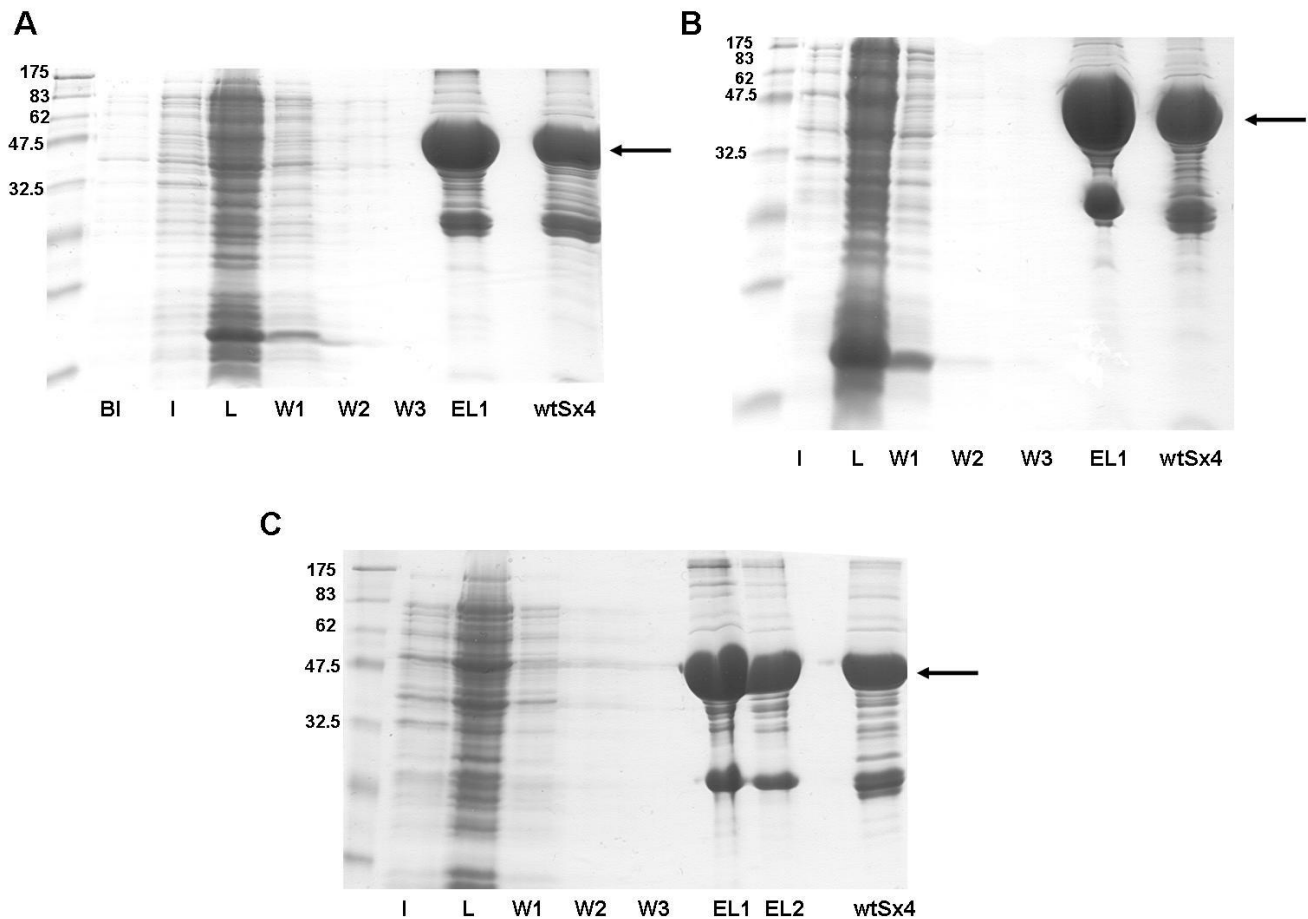


Figure 5.1 Purification of Sx 4 phosphomimetic mutants

The cytosolic domains of Sx 4 Y115E (A), Sx 4 Y251E (B) and the double mutant Sx 4 Y115E/ Y251E (C) were expressed in BL21 (DE3) *E. coli* cells as C-terminally tagged GST fusion proteins coming from the plasmids pETDuet-1 Sx 4 Y115E, pETDuet-1 Sx 4 Y251E and pETDuet-1 Sx 4 Y115E/Y251E respectively. Proteins were purified as described in section 2.2.2.4. The lysate (L) was incubated with glutathione sepharose overnight at 4 °C. After several washes (W1, W2, W3), proteins were eluted using 15 mM of reduced glutathione in 50 mM Tris pH 8.0. Proteins were dialysed overnight against binding buffer (as outlined in section 2.2.2.6), run on a 12 % SDS-PAGE gel and stained with Coomassie Blue as outlined in sections 2.2.2.1 and 2.2.2.3. 10 µl Elutions (EL) were compared to wild-type Sx 4 (wtSx4) sample in A, B and C. Arrows indicate precise position of Sx 4 proteins in the gel. Positions of molecular weight markers are shown. Data from a typical set of purifications are presented, repeated many times with similar results.

5.3.1.2 Circular dichroism of purified syntaxin 4 mutants

Mutations can, sometimes, alter the structure of proteins and these alterations can affect their biological function. To examine whether phosphomimetic mutations affected Sx 4 structure, a comparison between the wild-type and mutant forms of GST-Sx 4 was made using circular dichroism (CD). CD is a form of spectroscopy which relies on the differential absorption of left and right circularly polarised light by optically active elements such as backbone amide bonds, disulphide bonds and aromatic side chains within the protein molecule (Kelly and Price, 2000). It is extremely useful for examining structural integrity since the spectra collected allow information on the secondary structure and, in some cases, the tertiary structure of proteins to be obtained.

CD measurements in the far UV region can give important characteristics of the secondary structure of molecules. The differential absorption occurs below 240 nm and is due principally to the peptide bonds of molecules which can adopt various conformations (α -helix, β -sheets and random coil). CD measurements in the near UV range can be used to obtain information on the tertiary structure of proteins, corresponding to aromatic amino acid contributions (phenylalanine, tyrosine and tryptophan side chains) in the range between 260 to 320 nm. If the aromatic side chains are held rigidly in an asymmetric environment it can be possible to obtain a unique spectral profile which is a very useful tool when comparing wild-type and mutant versions of proteins (Kelly *et al.*, 2005).

Figure 5.2 shows the far UV CD spectra comparing the secondary structures of the cytosolic domains of wild-type GST-Sx 4 with the cytosolic domains of the GST-tagged phosphomimetic mutants. GST-alone was included for comparison since the proteins were GST tagged. CD analysis confirmed that with the exception of the Y115E/Y251E double mutant the overall secondary structure of the Sx 4 mutants are similar which inferred that the mutations did not significantly affect their secondary structures. In the case of the double mutant, the spectral intensity was found to be less than the wild-type which may reflect problems in the reliability of the protein concentration estimation following removal of the tyrosine residues. A small change in secondary structure may have occurred following the replacement of Y115 and Y251 with glutamate residues.

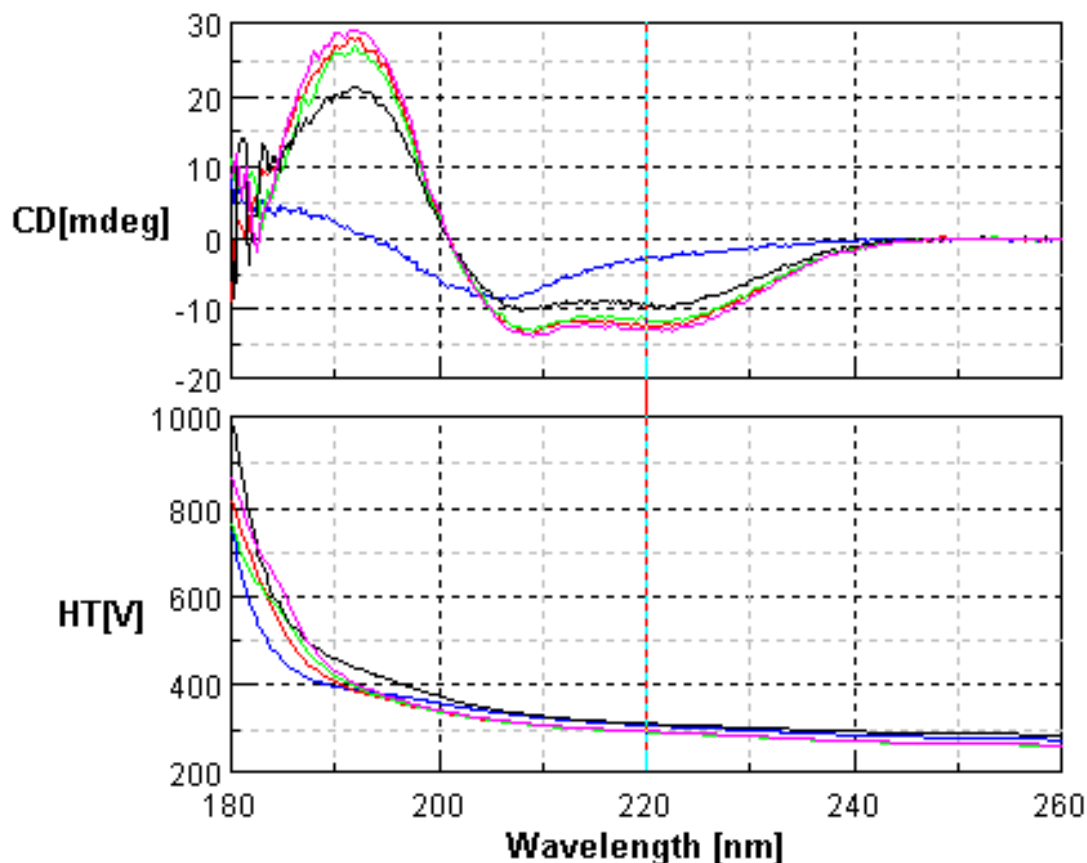


Figure 5.2 Far UV CD spectra of the cytosolic domains of wild-type Sx 4, Y115E, Y251E and Y115E/Y251E

Far UV CD spectra were recorded for the cytosolic domains of recombinant GST (blue), wild type GST- Sx 4 (green), GST-Sx 4 Y115E (pink), GST-Sx 4 Y251E (red) and GST-Sx 4 Y115E/Y251E (black) from 180 nm to 260 nm. HT[V] stands for high tension (*i.e.* the voltage applied to the photomultiplier to keep the current constant). Proteins were diluted to 0.7 mg/ml in 50 mM K_2HPO_4 - KH_2PO_4 pH 7.4. The data shown were obtained from the average of 8 scans. CD measurements were collected on a CD JASCO J-810 spectropolarimeter by Dr Sharon Kelly (University of Glasgow).

Figure 5.3 shows the near UV CD spectra giving an indication of the overall tertiary structures of the wild-type GST-Sx 4 and GST-Sx 4 phosphomimetic mutants. As can be seen in figure 5.3, the overall spectral features of the mutant proteins are similar to the wild-type, suggesting that the aromatic residues are properly buried and the tertiary structural integrity for each protein has been maintained. The small difference observed in the intensity of the peaks is probably due to the removal of tyrosine residues.

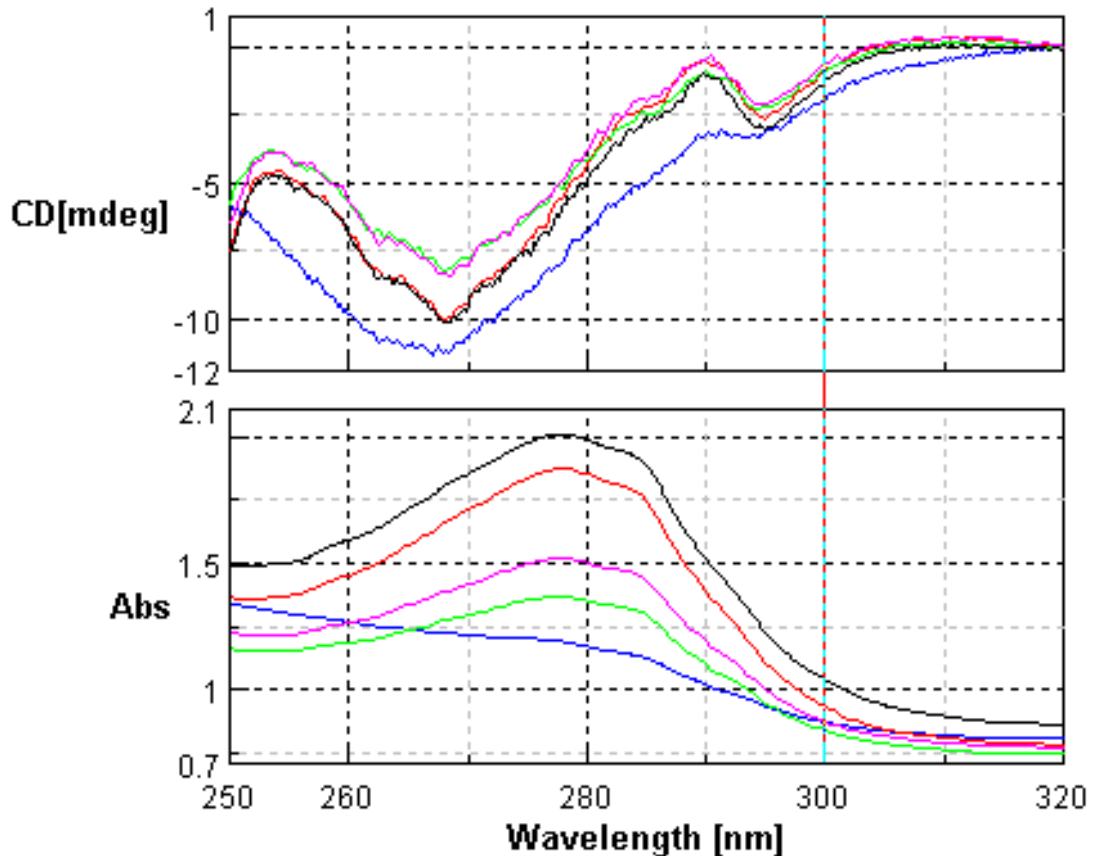


Figure 5.3 Near UV CD spectra of wild-type GST-Sx 4 and Sx 4 Y115E, Sx4 Y251E, and Y115E/Y251E

Near UV CD spectra were recorded for the cytosolic domains of recombinant GST (blue), wild-type GST- Sx 4 (green), GST-Sx 4 Y115E (pink), GST-Sx 4 Y251E (red) and GST-Sx 4 Y115E/Y251E (black) from 250 nm to 320 nm. Proteins were diluted to 1 mg/ml in 50 mM K_2HPO_4 - KH_2PO_4 pH 7.4. The data shown was obtained from the average of 8 scans. CD measurements were collected on a CD JASCO J-810 spectropolarimeter by Dr Sharon Kelly (University of Glasgow).

5.3.1.3 Interaction of Sx 4 phosphomimetic mutants with Munc18c

In order to test whether phosphomimetic mutations could affect Sx 4 binding to M18c, pull-down experiments were carried out in which set amounts of the phosphomimetic GST-Sx 4 recombinant proteins were immobilised on glutathione sepharose beads before incubation with His₆-M18c. GST alone was used as a negative control in the pull-downs.

The result of a typical experiment is shown in figure 5.4.

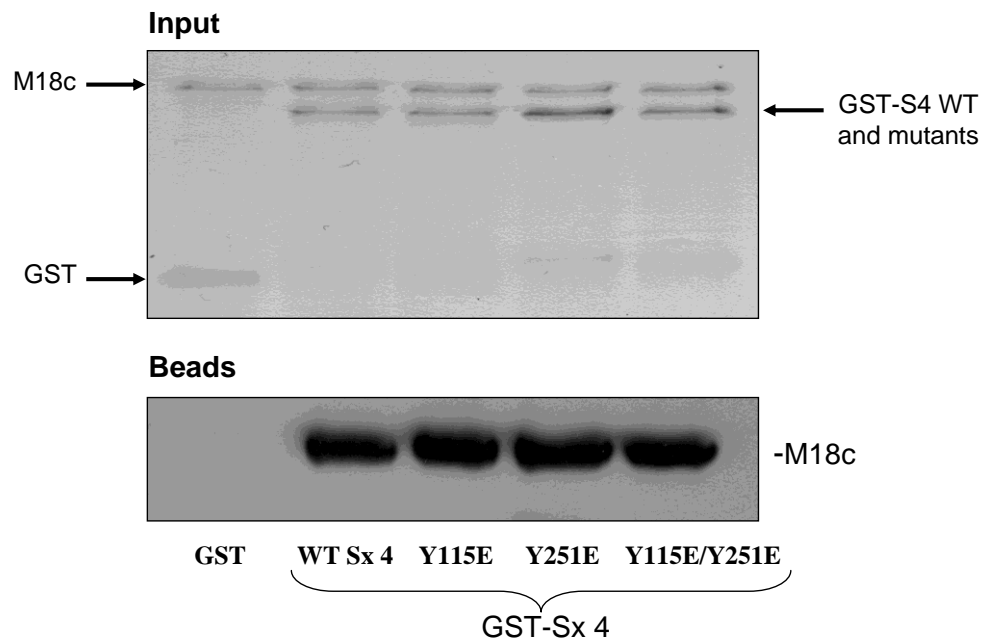


Figure 5.4 Binding of His₆-M18c to GST-Sx 4 wild-type (WT), Sx 4 Y115E, Sx 4 Y251E and Sx 4 Y115E/Y251E

Pull-down assay was performed where 5 µg of recombinant GST, GST fused to the cytosolic domain of wild-type (WT) Sx 4, Sx 4 Y115E, Sx 4 Y251E and Sx 4 Y115E/Y251E were firstly immobilised on glutathione Sepharose for 1.5 h at 4 °C. After 3 washes with binding buffer, beads were incubated overnight at 4 °C with 5 µg of His₆-M18c in a final volume of 500 µl. 4 % of each mixture was removed to assess protein input. Bound proteins were eluted, resolved by 12 % SDS-PAGE and immunoblot analysis was carried out to determine which of the GST proteins His₆-M18c had bound to. Upper panel represents a Coomassie stained gel of the GST-fusion proteins/M18c inputs (4 % of the total input); lower panel shows immunoblot analysis with α-M18c antibody used to determine bound M18c. 50 % of the eluted sample was loaded. This experiment was repeated three times.

As can be seen in figure 5.4, His₆-M18c can still efficiently bind phosphomimetic mutants as well as wild-type GST-Sx 4. In several experiments of this type, we saw no difference in M18c binding to any phosphomimetic mutant compared to wild-type Sx 4. This result indicates that post-translational modifications such as phosphorylation of Sx 4 protein do not affect their interaction with their regulatory protein M18c *in vitro*.

5.3.1.4 Interaction of Sx 4 phosphomimetic mutants with SNAP23

Since phosphomimetic mutations in Sx 4 were not able to confer considerable changes in binding to M18c, it was then investigated whether its interaction with the SNARE protein, SNAP23, was affected. Sx 4 and SNAP23 proteins interact to form a heterodimer at the PM of muscle and adipocytes and this binding is essential for SNARE complex formation. Thus, the interaction between Sx 4 phosphomimetic mutants and SNAP23 was investigated through pull-down studies.

Data obtained from pull-downs, shown in figure 5.5, indicates that phosphomimetic mutations did not affect significantly Sx 4 binding to SNAP23.

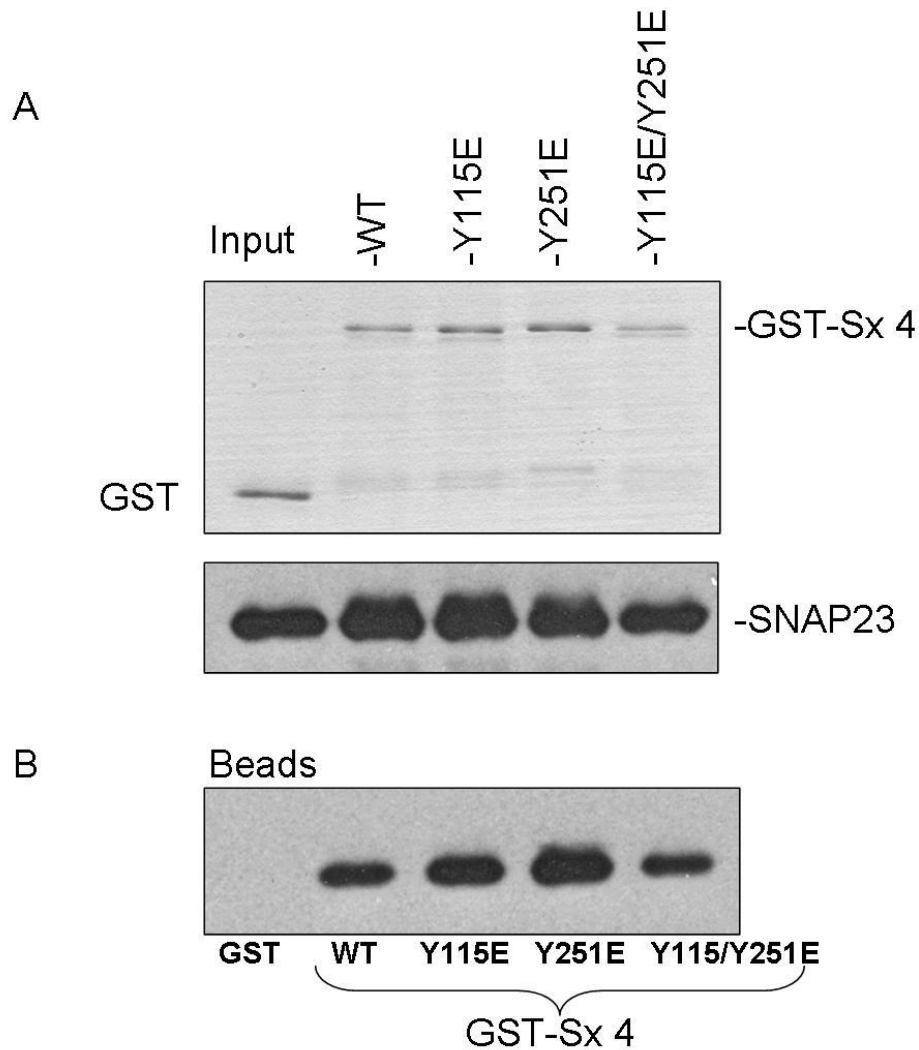


Figure 5.5 Binding of His₆-SNAP23 to GST-Sx 4 wild-type (WT), Sx 4 Y115E, Sx 4 Y251E and Sx 4 Y115E/Y251E

Pull-down assay was performed where 5 µg of recombinant GST, GST fused to the cytosolic domain of wild-type (WT) Sx 4, Sx 4 Y115E, Sx 4 Y251E and Sx 4 Y115E/Y251E were firstly immobilised on glutathione Sepharose for 1.5 h at 4 °C. After 3 washes with binding buffer, beads were incubated overnight at 4 °C with 5 µg of His₆-tagged SNAP23 in a final volume of 500 µl. 4 % of each mixture was removed to assess protein input. After extensive washing, bound proteins were eluted, resolved by SDS-PAGE and immunoblot analysis was carried out to determine which of the GST proteins His₆-SNAP23 had bound to. **(A)** Upper panel represents a Coomassie stained gel of the GST-fusion proteins inputs (2 % of the total input); lower panel shows immunoblot analysis with α-SNAP23 antibody used to determine input of SNAP23 (2 %). **(B)** Final immunoblot analysis with α-SNAP23 antibody used to determine bound SNAP23. Shown is data from a typical experiment, repeated 6 times. No statistical difference in SNAP23 binding to Sx 4 was observed for any of the mutants.

5.3.2 *Munc18c* phosphomimetic mutant Y521E

It was previously shown that the tyrosine residue at position 521 in M18c is specifically phosphorylated upon insulin stimulation (Schmelzle *et al.*, 2006). By using amino acid substitution, the role of tyrosine 521 in binding of Sx 4 was assessed. A glutamate substitution (Y521E), closely mimicking phosphorylated tyrosine, was obtained *via* site-directed mutagenesis.

5.3.2.1 Site-directed mutagenesis and protein purification

The Y521 mutation was introduced into the M18c sequence using pQE30-M18c as template and mutation was performed as outlined in section 2.2.1.2. Primers were designed taking in consideration melting temperature, length and GC content of the primer. Designed primers were as follows (letters in bold refer to original codon and underlined refer to mutated codon):

M18c wt sequence: 5' CAG AAA CCC AGA ACT AAC **TAC** TTA GAG CTG GAC
CGG AAA 3'

M18cY521E Forward: 5' CAG AAA CCC AGA ACT AAC GAG TTA GAG CTG GAC
CGG AAA 3'

M18cY521E Reverse: 5' TTT CCG GTC CAG CTC TAA CTC GTT AGT TCT GGG
TTT CTG 3'.

Successful mutation was confirmed by DNA sequencing.

M18cY521E was expressed and purified similarly to wild-type M18c. His₆-M18cY521E was expressed in M15 *E. coli* cells that also co-expressed the chaperone protein GroEL in order to increase M18cY521E solubility. Low levels of IPTG were used (0.2 mM) and protein expression was induced at 22 °C overnight as these conditions were empirically determined to give better levels of expression. His₆-M18cY521E was purified using Ni-NTA agarose as described in section 2.2.4.

A typical purification is shown in figure 5.6.

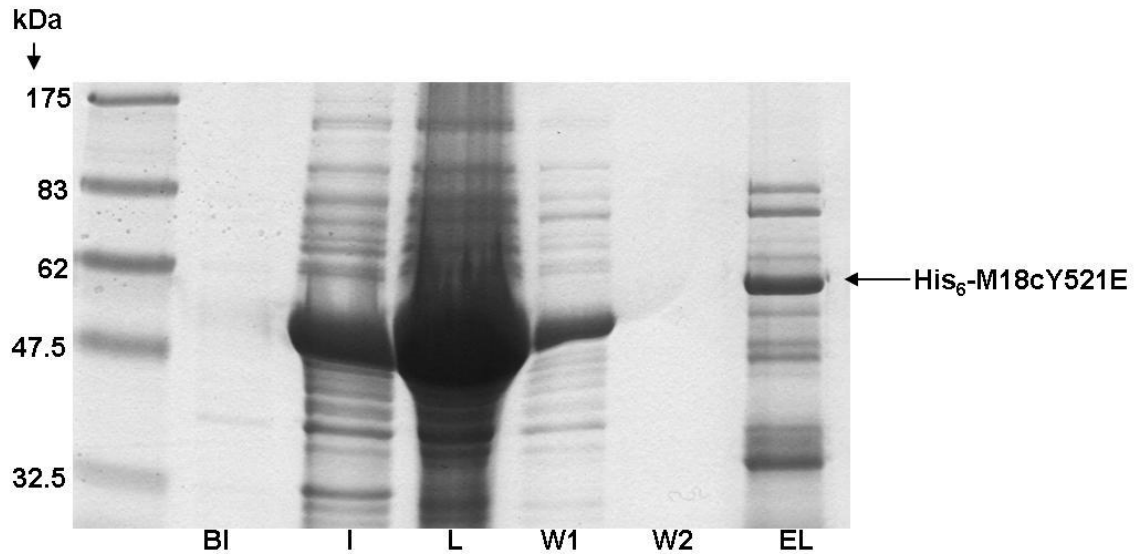


Figure 5.6 M18cY521E protein purification

His₆-M18cY521E was expressed from vector pQE30 in M15 *E. coli* cells expressing the chaperone GroEL. Expression was induced by adding 0.2 mM IPTG to the media and incubation was carried out overnight at 22°C. The figure shows several samples taken during the process of protein purification which were run on a 12 % SDS-PAGE gel and stained with Coomassie Blue as outlined in section 2.2.2.1 and 2.2.2.3 respectively. The positions of the molecular weight markers are shown on the left. The first lane corresponds to a sample before induction (BI) followed by a sample after induction (I), sample from the lysate (L), wash 1 (W1), wash 2 (W2) and fraction eluted (15 µl) using 500 mM imidazole (EL).

From the data presented in figure 5.6, the elution (EL) obtained from the Ni-TA agarose contained one major product of the expected size which corresponds to His₆-M18cY521E. The sample purity could be improved if more washes were applied. In order to further confirm that the elution obtained was really the M18c phosphomimetic mutant, wild-type and mutant M18c were run side by side on a 12 % SDS-PAGE and subjected to immunoblot analysis using antibody against M18c.

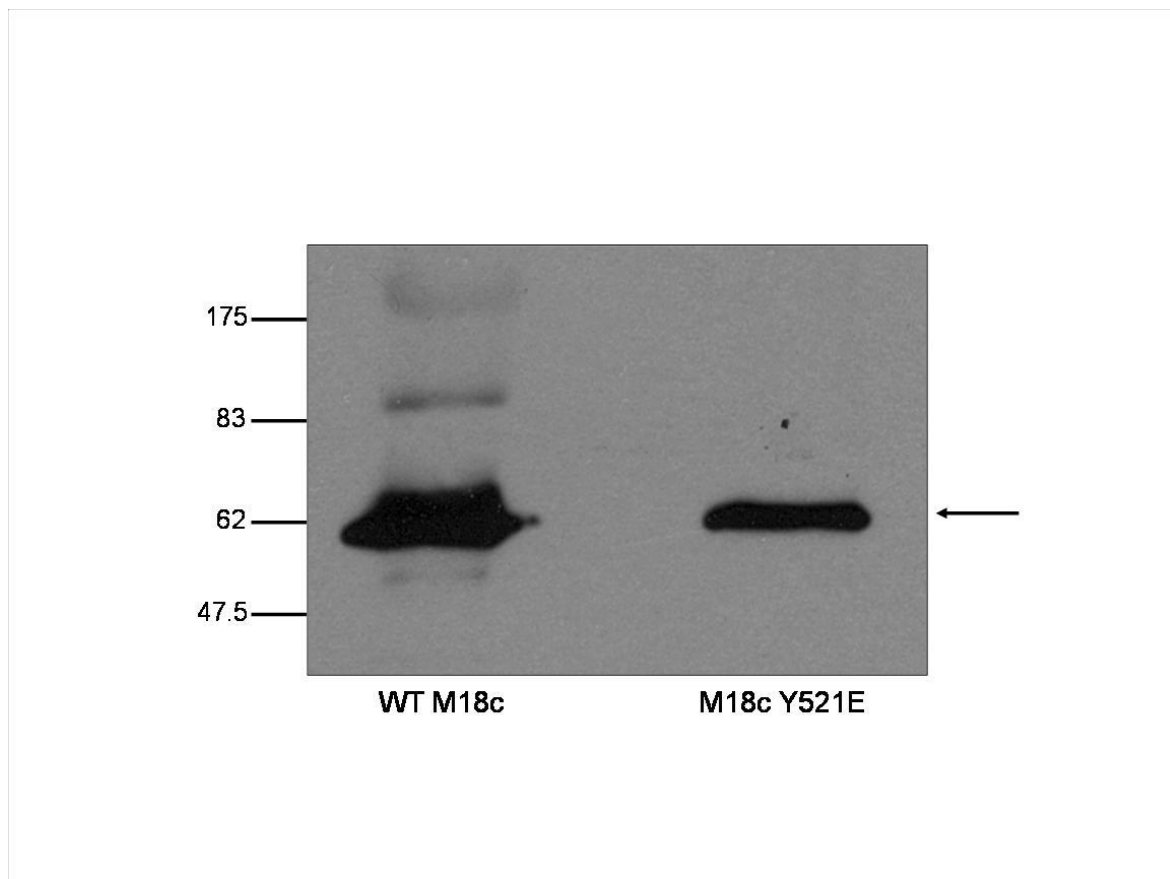


Figure 5.7 Comparison between wild-type M18c and M18cY521E

Similar quantities (approximately 1 μ g each) of recombinant wild-type M18c and M18c Y521E were resolved on a 12 % SDS-PAGE for subsequent immunoblotting with anti-Munc18c antibody. Molecular weight markers are shown on the left. Arrow indicates M18c WT and mutant bands.

As shown in figure 5.7, polyclonal M18c antibody was able to recognise both wild-type and the mutant M18cY521E and both proteins, as expected, run at a similar molecular weight.

5.3.2.2 Circular dichroism analysis of purified His₆-M18cY521E

SM proteins such as M18c are generally poorly expressed or unstable needing to be co-expressed with the chaperone GroEL (Scott *et al.*, 2004). The presence of GroEL, a protein folding chaperone, has been shown to be very useful for improving recombinant proteins solubility and assisting successful folding (Yasukawa *et al.*, 1995). Truncations in M18c can affect their structure due to protein instability (Oh and Thurmond, 2006). In order to assess if the tyrosine mutation to a glutamic acid has affected M18cY521E folding, CD and intrinsic tryptophan fluorescence spectra were performed to compare both wild-type and M18cY521E structures. Near UV CD analysis was not possible due to the low protein concentrations.

Figure 5.8 shows the far UV CD spectra obtained from His₆-M18c (blue), and the mutant His₆-M18cY521E (red). As shown, there is no significant change in the overall secondary structure of the mutant His₆-M18c Y521E when compared to wild-type His₆-M18c. The His₆-M18c (blue) displayed a poor signal to noise ratio below 195 nm due to traces of chloride ions in the buffer.

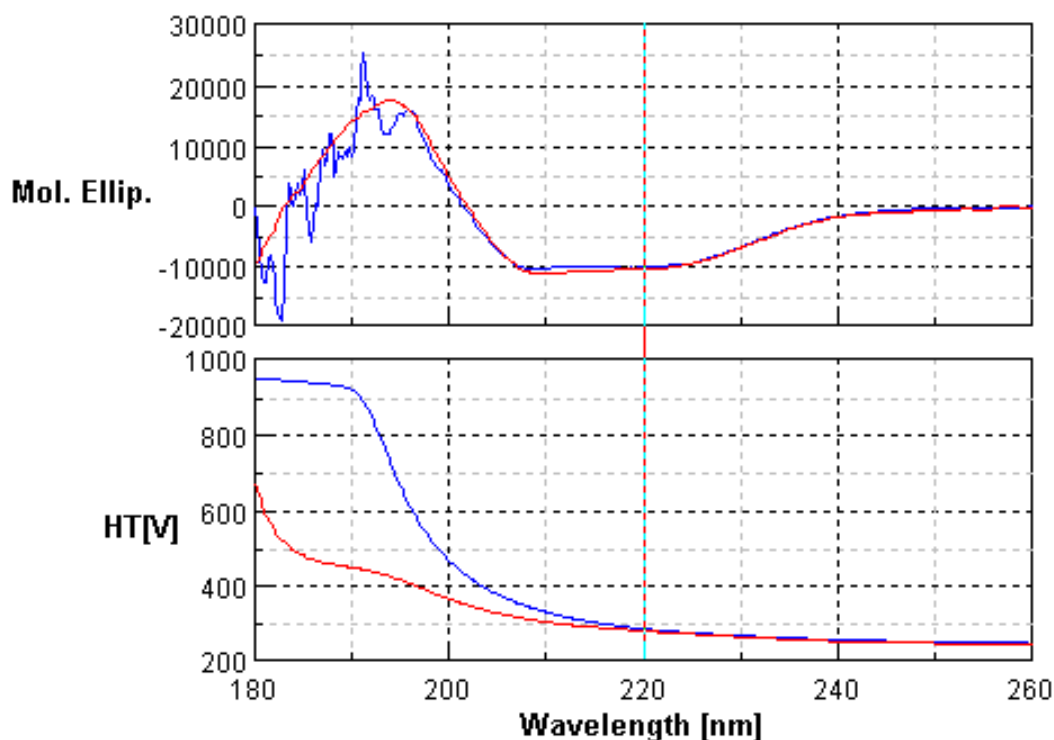


Figure 5.8 Far UV CD spectra of wild-type M18c (blue) and mutant M18cY521E (red)

Far UV CD spectra were recorded for recombinant wild-type His₆-M18c (blue), and the mutant His₆-M18cY521E (red) from 180 nM to 260 nM. Proteins were diluted to 0.5 mg/ml in 50 mM K₂HPO₄- KH₂PO₄ pH 7.4. Top graph shows molar ellipticity and second graph shows HT[V] which stands for high tension (*i.e.* the voltage applied to the photomultiplier to keep the current constant). The data shown was obtained from the average of 8 scans. CD measurements were collected on a CD JASCO J-810 spectropolarimeter by Dr Sharon Kelly (University of Glasgow).

Figure 5.9 represents the fluorescence spectra of the wild-type His₆-M18c compared with mutant His₆-M18c. Near CD UV analysis were not carried out for His₆-M18cY521E since the removal of tyrosine would affect the spectral contributions corresponding to the tyrosine side chains and since near UV CD requires protein concentrations of approximately 1 mg/ml and there was an insufficient concentration of protein for this analysis. Instead, fluorescence spectroscopy was used. Tryptophan emission fluorescence following excitation at 295 nm is dominant over the weaker tyrosine and phenylalanine contributions.

Tryptophan is a very useful intrinsic fluorescent probe which can be used to estimate the nature of the tryptophan environment when excited. This hydrophobic amino acid favours being buried in protein hydrophobic cores. Protein mutations can sometimes affect the tryptophan environment since they could expose the tryptophan to an aqueous or less hydrophobic environment instead of the protein interior. Thus, tryptophan exposure as a result of unfolding would result in a peak which would be shifted to longer wavelengths compared with the wild-type.

The fluorescence spectra of wild-type and mutant forms of M18c allowed the positions of the tryptophan peaks for each protein to be determined. Figure 5.9 shows that the emission spectra obtained following excitation at 295nm gave a peak around 345 nm for wild-type and His₆-M18cY521E suggesting that these proteins have a similar conformation in the region pertaining to the position of the tryptophans. The difference in the levels of fluorescence might indicate fluorescence quenching due to protein concentration or grade of purity of protein in this study.

Such data collectively suggest that His₆-M18cY521E is correctly folded.

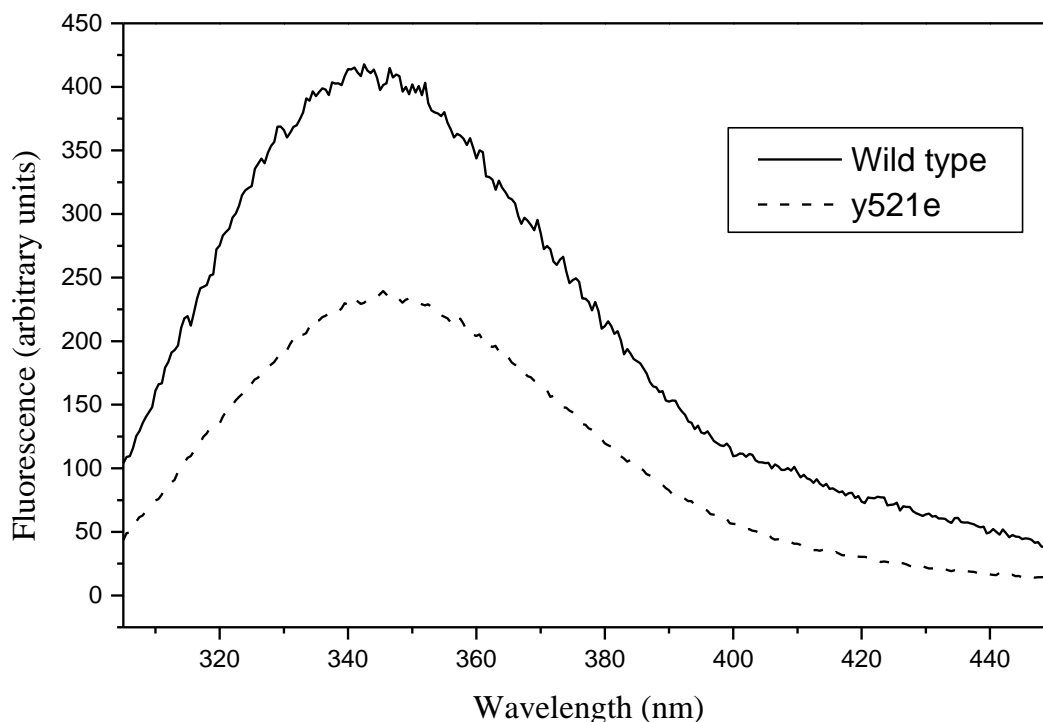


Figure 5.9 Tryptophan fluorescence spectra of His₆-M18c and His₆-M18c Y521E

Emission spectra of His₆-M18c and His₆-M18cY521E following excitation at 295nm. The amount of protein used to obtain the fluorescent spectrum were 0.6 mls of 0.2 mg/ml protein and measurements were performed by Dr Sharon Kelly (University of Glasgow) on a Perkin-Elmer LS 50B fluorometer.

5.3.2.3 Interaction of His₆-M18cY521E with different versions of Sx 4

Glutathione sepharose bound to GST-Sx 4 proteins harbouring the cytosolic domains of the different version of Sx 4, were used to pull down His₆-M18cY521E. C-terminally tagged GST- Sx 4, GST-Sx 4 NΔ36, GST-Sx 4 L173A/E174A, GST-Sx 4 L173A/E174A NΔ36 were purified as described in section 2.2.2.4.

The result of a typical experiment is shown in figure 5.10. While wild-type His₆-M18c was able to bind the different version of Sx 4, the mutant His₆-M18cY521E did not. Less than 10 % of the total His₆-M18cY521E input was shown to bind Sx 4.

After repeating this experiment several times, this data indicates that phosphomimetic mutation in M18c (Y521E) results in abrogation of M18c/Sx 4 interaction.

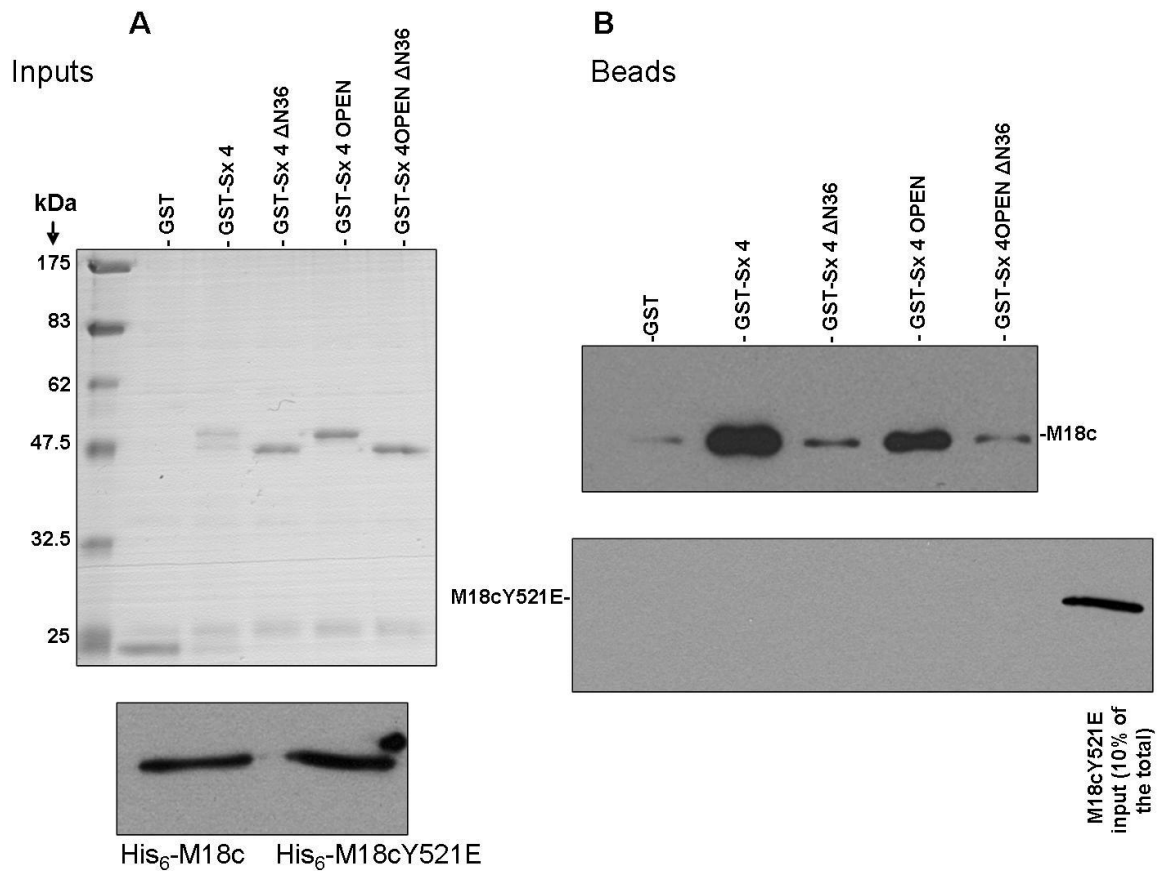


Figure 5.10 Pull-down assay of the different versions of cytosolic GST-Sx4 with both wild-type His₆- M18c and His₆-M18cY521E

Pull-down assay was performed in which 5 μ g of either recombinant GST, or GST fused to the cytosolic domain of WT Sx 4, Sx 4 Δ N36, Sx 4 open and Sx 4 open Δ N36 were firstly immobilised on glutathione Sepharose. Beads were then incubated overnight at 4 $^{\circ}$ C with 1 μ g of His₆-M18cY521E in a final volume of 200 μ l. As a positive control, another set of proteins (GST and GST-Sx 4 wild-type and mutants) were incubated with wild-type 1 μ g His₆-M18c. After extensive washing, bound proteins were eluted using 15 μ l of 1 x sample buffer (containing 20 mM DTT), resolved by SDS-PAGE and immunoblot analysis were carried out to determine which of the GST proteins His₆-M18c and His₆-M18cY521E had bound to. Panel (A) shows protein inputs (7.5 %) for GST and GST-tagged Sx 4 proteins which were purified as described in section 2.2.2.4, were resolved by SDS-PAGE and visualised by staining with Coomassie Blue (A, top panel). 10 % of the M18c input from both wild-type and mutant forms were analysed by SDS-PAGE followed by immunoblot analysis with α -M18c antibody (A, lower panel). Panel (B) shows immunoblot analysis with α -M18c antibody used to determine bound M18c (top panel) and bound M18cY521E (lower panel). This experiment was repeated three times.

5.3.2.4 Interaction of His₆-M18cY521E with GST-VAMP2

Since no interaction was observed of His₆-M18cY521E with cytosolic Sx 4 and we have recently reported that VAMP2 interacts with M18c (chapter 3), the interaction between His₆-M18cY521E with the cytosolic portion of the v-SNARE VAMP2 was assessed.

Recombinant cytosolic N-terminally tagged GST-VAMP2 was purified as described in section 2.2.2.4. Glutathione sepharose bound to either recombinant GST or GST- VAMP2 were used to pull down His₆-M18cY521E.

Similarly to Sx 4, GST-VAMP2 was unable to pull-down His₆-M18cY521E as can be seen in figure 5.11.

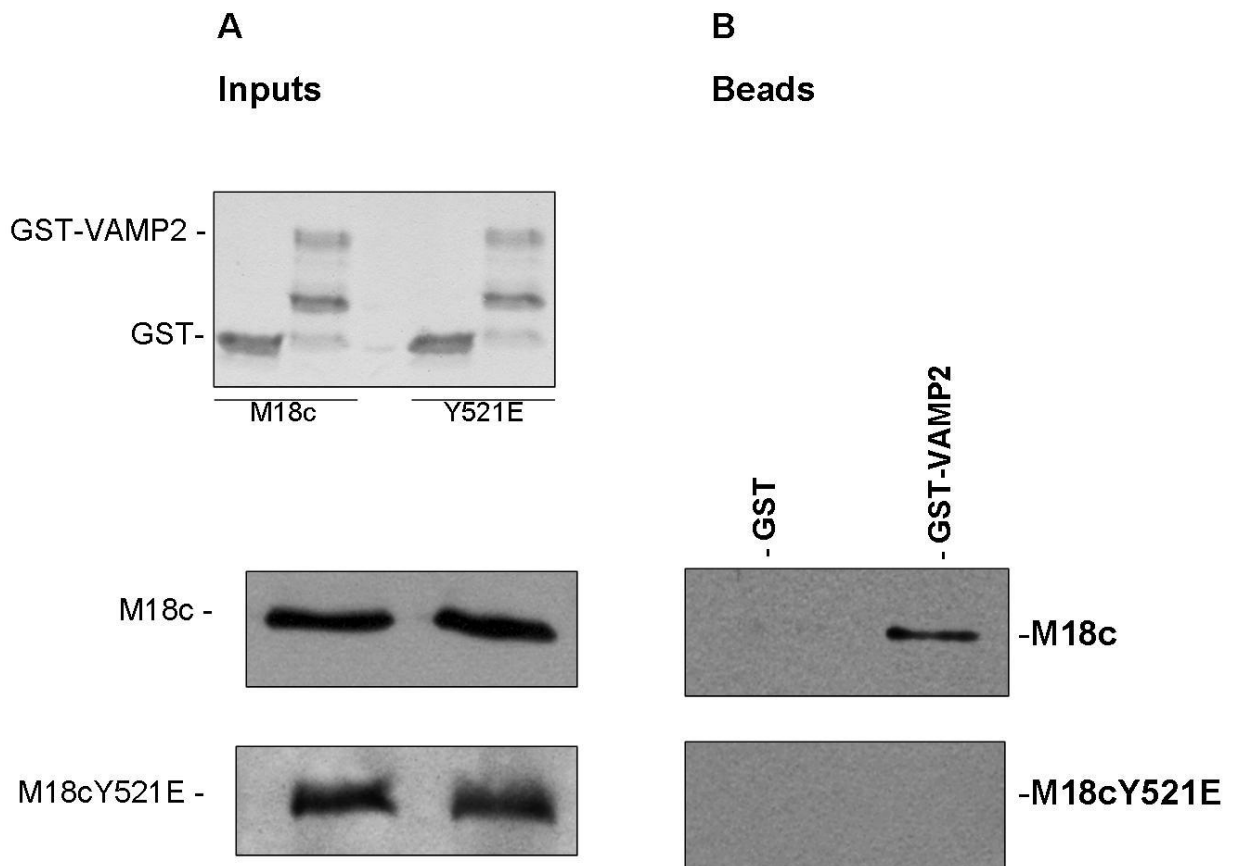


Figure 5.11 GST pull-down of GST-VAMP2 and His₆- M18cY521E

Pull-down assay was performed in which 5 μ g of either recombinant GST, or GST fused to the cytosolic domain of VAMP2 were first immobilised on glutathione sepharose. Beads were then incubated overnight at 4 $^{\circ}$ C with 1 μ g of His₆-M18cY521E and another set of GST and GST-VAMP2 were incubated with 1 μ g wild-type His₆-M18c in a final volume of 200 μ l. After extensive washing, bound proteins were eluted using 15 μ l of 1 x sample buffer (containing 20 mM DTT), resolved by SDS-PAGE and immunoblot analysis were carried out to determine if His₆-M18c and His₆-M18cY521E had both bound to GST-VAMP2. **(A)** Shows protein inputs (7.5 %) for GST and GST-tagged VAMP2 proteins which were purified as described in section 2.2.2.4, were resolved by SDS-PAGE and visualised by staining with Coomassie Blue (A, top panel). 10 % of the M18c input for both wild-type and mutant forms were analysed by SDS-PAGE followed by immunoblot analysis with α -M18c antibody (A, lower panels). **(B)** Shows immunoblot analysis with α -M18c antibody used to determine bound M18c (top panel) and bound M18cY521E (lower panel).

5.3.3 The Recombinant Cytoplasmic Insulin Receptor Kinase (CIRK)

Insulin action results in tyrosine phosphorylation, through the binding of insulin to its receptor which contains a tyrosine kinase domain. This results in autophosphorylation of the receptor which will eventually stimulate phosphorylation of the insulin receptor substrate (IRS) which will carry the signal downstream of the receptor. However, termination of insulin action requires the dephosphorylation of the insulin receptor and IRS.

In order to identify which tyrosine phosphatases were responsible for dephosphorylation of both the insulin receptor and IRS-1, a group of researchers generated a recombinant cytoplasmic domain of the human insulin receptor, which they termed CIRK (Kuhne *et al.*, 1994). This recombinant receptor consists of amino acids 941-1343 of the β subunit of the insulin receptor which contains the intrinsic tyrosine kinase domain. CIRK was expressed and purified from Baculovirus-infected Sf9 cells according to work done by Villalba and colleagues (Villalba *et al.*, 1989).

The generation of CIRK was a very interesting tool to improve the understanding of the insulin action *via* phosphorylation of the insulin receptor and also its consequences among other proteins including SNAREs. Therefore, studies were carried out to analyse if CIRK autophosphorylation could result in phosphorylation of other substrates such as Sx 4 and M18c. CIRK was kindly given to us by Prof Gustav E. Lienhard (Dartmouth University, USA).

Fig 5.12 shows recombinant CIRK running at approximately 47 kDa on a 12 % SDS-PAGE.

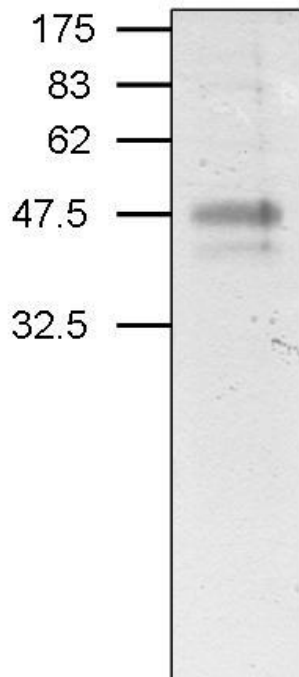


Figure 5.12 SDS-PAGE analysis of recombinant CIRK

CIRK was autophosphorylated as described in section 2.2.5.1. 20 μ l of autophosphorylated CIRK (7.4 μ g) were loaded on a 12 % SDS-PAGE gel followed by Coomassie Blue staining as outlined in sections 1 and 2. Positions of the broad range molecular weight markers are shown.

5.3.3.1 Phosphorylation of M18c and SNARE proteins in response to CIRK

In previous studies, protein kinases were shown to induce phosphorylation in some SNARE proteins and also M18c (see section 5.1). To assess if this was the case for CIRK, this recombinant kinase was firstly autophosphorylated as described in section 2.2.5.1.

Secondly, autophosphorylated CIRK was incubated with M18c and with the t-SNARE complex in a buffer containing ATP, MnCl_2 and $[\gamma\text{-}^{32}\text{P}]\text{ATP}$. After 30 min incubation at 30 $^\circ\text{C}$, samples were subjected to SDS-PAGE, and analysed by autoradiography (as outlined in sections 2.2.5.1 and 2.2.5.2).

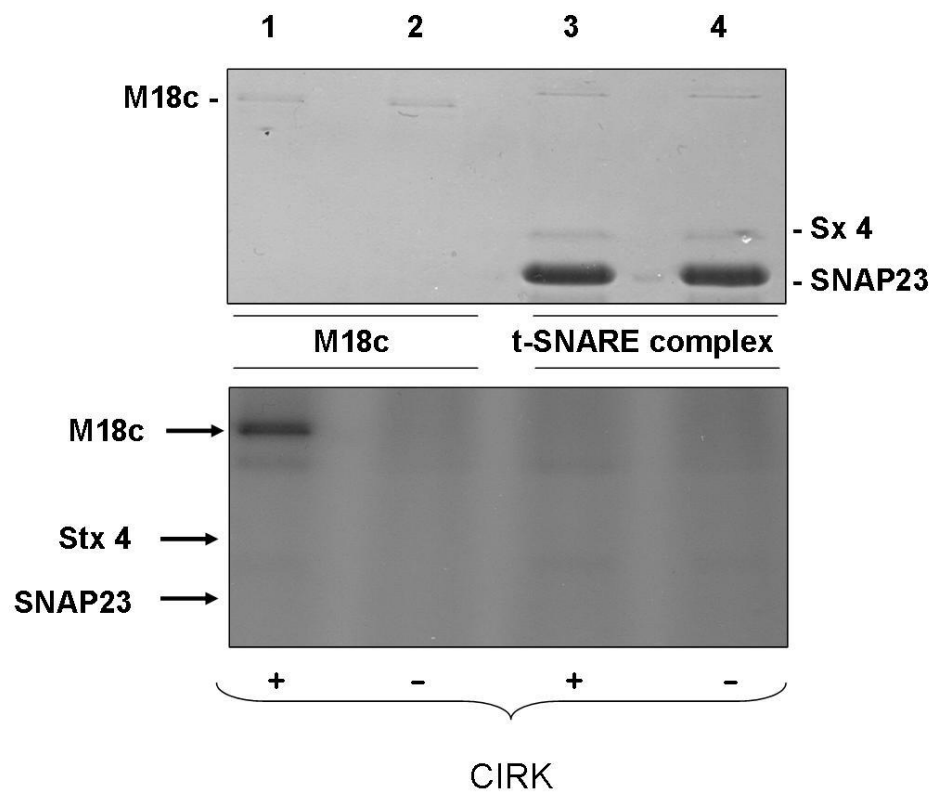


Figure 5.13 Autoradiography studies using M18c and Sx 4/SNAP23 complex which were pre-incubated with CIRK

1 μ g of M18c and Sx4/SNAP23 were incubated with 1 μ l of activated CIRK (370 ng). CIRK activation (autophosphorylation) was achieved as described in section 2.2.5.1. Recombinant proteins plus CIRK were incubated in a buffer containing 50 mM HEPES pH 7.5, 4 mM MnCl_2 , 0.2 mM DTT, 100 μ M ATP and 6 μ Ci [γ - 32 P]ATP. Control samples had no CIRK. Incubation was carried out for 30 min at 30 $^{\circ}$ C. After 30 min, 15 μ l of 4 x sample buffer (containing 20 mM DTT) were added to each tube. Samples were boiled at 65 $^{\circ}$ C for 10 min. Proteins were separated by SDS gel electrophoresis, then the gel was dried and subjected to autoradiography. Upper panel represents a Coomassie stained gel of the total M18c and t-complex inputs (25 μ l samples, \sim 0.5 μ g); lower panel show autoradiography analysis after 72 h exposure (at room temperature).

As shown in figure 5.13, M18c becomes phosphorylated in response to CIRK (Lane 1, lower panel). In contrast, the complex formed by Sx 4 and SNAP23 did not become phosphorylated in response to CIRK (Lane 3, lower panel). As expected, in the absence of CIRK, none of the proteins became phosphorylated (Lanes 2 and 4, lower panel).

Because Sx 4 and SNAP23 form a heterodimer, this could have masked the sites in Sx 4 that become phosphorylated with activated CIRK. In order to further confirm that Sx 4 was not able to become phosphorylated, monomeric Sx 4 was incubated in the presence and in the absence of CIRK. M18c was also incubated with and without CIRK. Because Sx 4 was GST tagged, an extra control was made by incubating recombinant GST in the presence and in the absence of CIRK.

The autoradiography analysis presented in figure 5.14 shows that CIRK was able to phosphorylate both M18c and monomeric Sx 4. However, phosphorylation of M18c seemed greater than Sx 4, as can be seen by the intensity of the band.

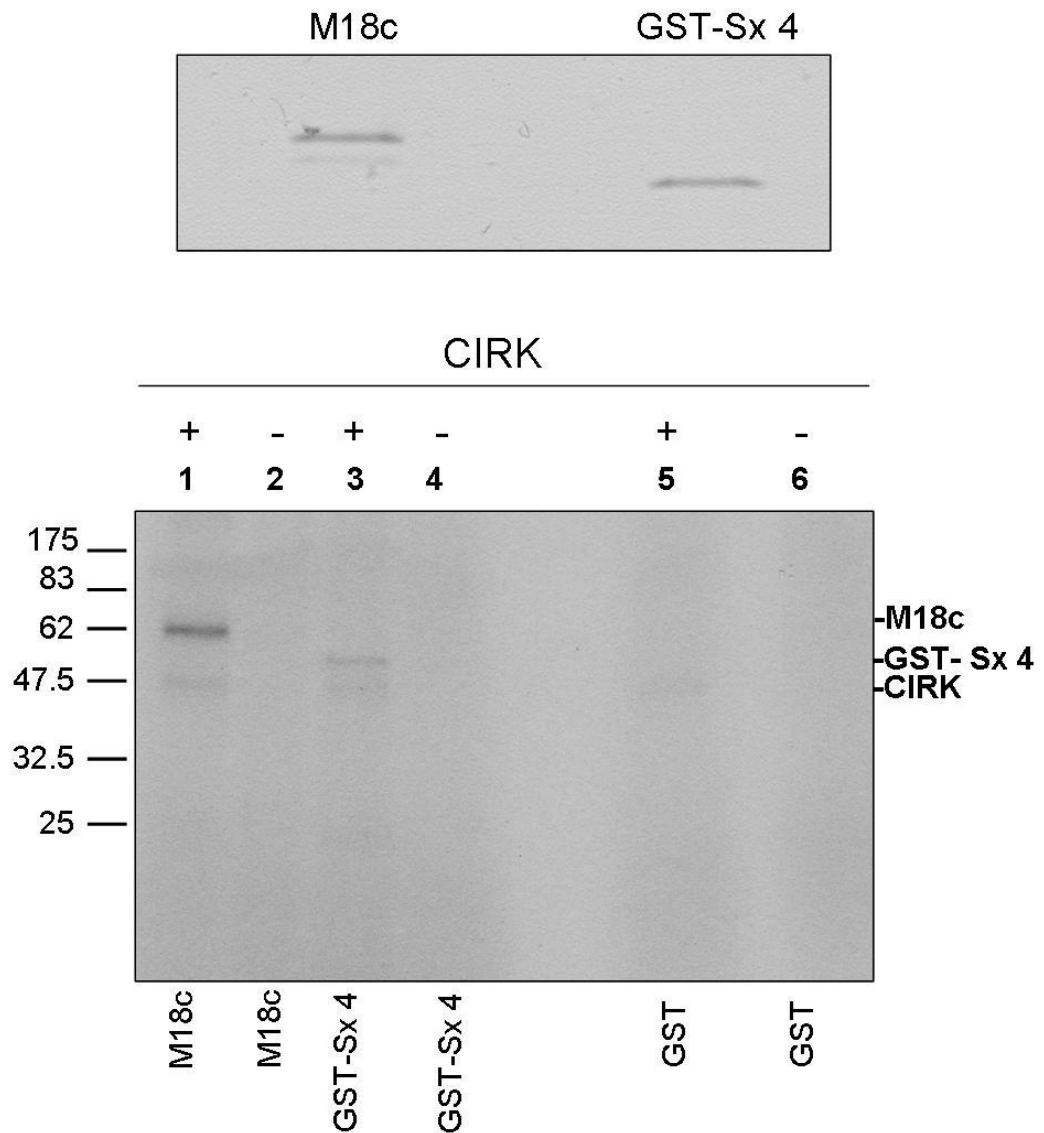


Figure 5.14 M18c and Sx 4 phosphorylation by CIRK

CIRK (370 ng) was incubated with 1 μ g M18c (lane 1; lower panel), 1 μ g GST-Sx 4 (lane 3; lower panel) and with GST alone (lane 5; lower panel). Reactions were carried out as described in sections 2.2.5.2 and 2.2.5.3. As controls, M18c and GST-Sx 4 were incubated without CIRK, whereas GST was incubated with and without CIRK (lanes 2, 4, 5 and 6 respectively; lower panel). GST was incubated separately with CIRK because Sx 4 is GST tagged. Proteins were separated by 12 % SDS gel electrophoresis and the gel was dried and subjected to autoradiography. Upper panel represents a Coomassie blue stained gel of the total amounts of His₆-M18c (left) and GST-Sx 4 (right) used (~ 0.5 μ g samples from each protein); lower panel show autoradiography analysis after 72 h exposure (at room temperature).

5.3.3.2 Stoichiometry of protein phosphorylation in response to CIRK

Since Phosphorus-32 were readily introduced into the M18c and Sx 4 molecules, the stoichiometry of protein phosphorylation could be calculated by measuring the counts per min (cpm) using a Scintillation counter. Cpm gives a good estimate about the number of atoms in a given quantity of radioactive material that has decayed in one min. The cpm of both M18c and Sx 4 were determined by excising the dried gel slices corresponding to each of the proteins, placing them in vials and measuring cpm using a scintillation counter. Knowing the molecular weight of the molecule, the amount of protein loaded and the cpm obtained, it is possible to make an estimate of the percentage of the protein that is phosphorylated.

Under the conditions used in 5.14, Sx 4 and M18c were shown to be phosphorylated by less than 1 %. In order to improve M18c phosphorylation levels, changes were made in the protocol. The time of incubation at 30 °C was increased from 30 min to 150 min and the amount of CIRK was increased 5 times, from 1 µl to 5 µl (from 370 ng to 1.85 µg). Figure 5.15 shows the results of an autoradiography after 48 h exposure. Note the increase in intensity of the M18c band as the amount of CIRK and the time of incubations were prolonged.

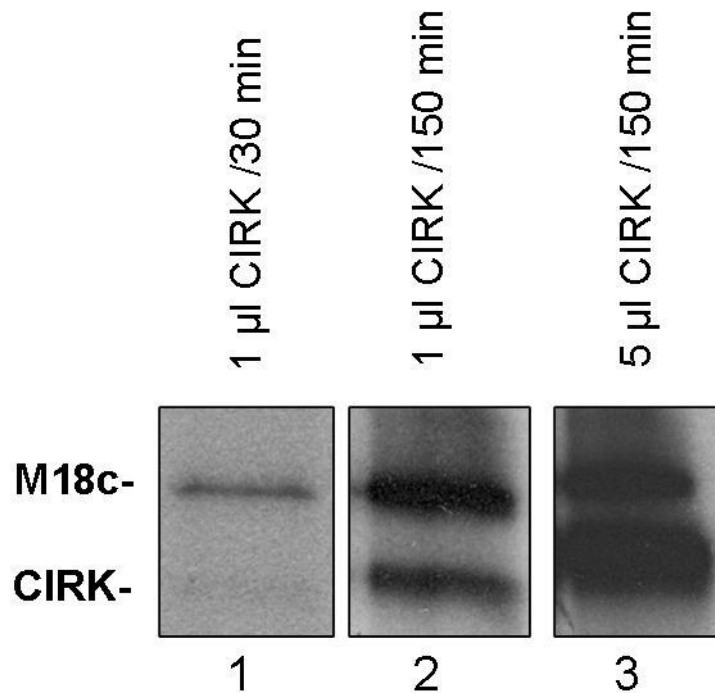


Figure 5.15 M18c phosphorylation by CIRK using different amounts of CIRK and different times of incubation

1 µg of His₆-M18c was incubated with 370 ng CIRK (lanes 1 and 2) for 30 min (lane 1) or 150 min (lane 2), or with 1.85 µg CIRK for 150 min (lane 3), at 30 °C. Reaction mixtures also contained buffer plus radiolabelled ATP as described in section 2.2.5.3. Reactions were stopped by boiling the samples and 25 µl (~ 0.5 µg of His₆-M18c) of each reaction mixture were processed by SDS-PAGE followed by Coomassie Blue staining and autoradiography as indicated in section 2.2.5.3. This figure shows an autoradiography analysis after 48 h exposure (at room temperature).

Figure 5.15 shows that the percentage of M18c phosphorylation is proportional to the amount of CIRK used and to the time of incubation. After 30 min incubation with 370 ng CIRK (lane 1), only ~ 1 % of the M18c molecule became phosphorylated, whereas after 150 min, there was an increase of ~ 16 % in the levels of M18c phosphorylation. By increasing 5 fold the amount of CIRK and keeping the 150 min incubation period (lane 3), ~ 24 % of M18c became phosphorylated. By performing this experiment, it was possible to optimise the conditions to allow maximum phosphorylation of M18c in response to CIRK in order to start the *in vitro* binding assays described in the following sections.

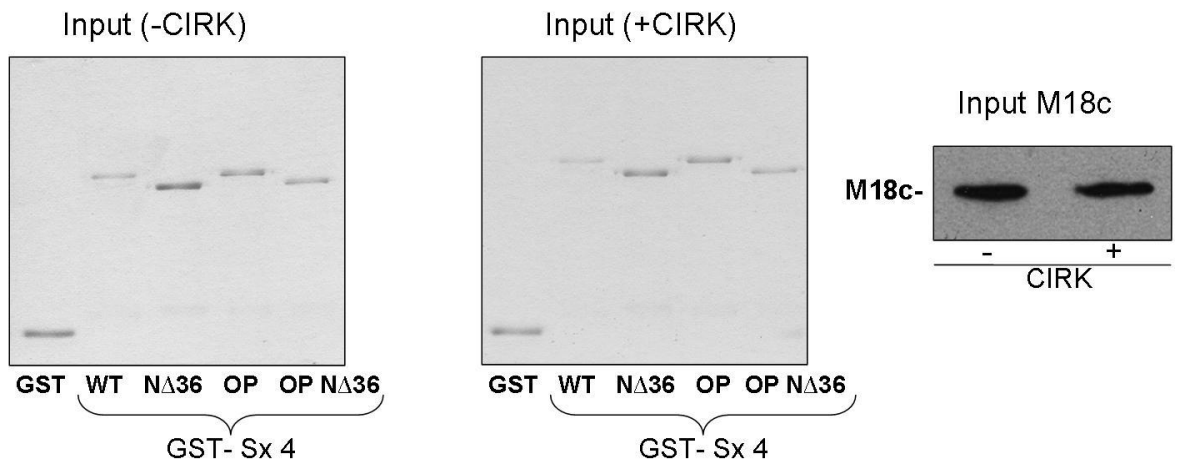
5.3.3.3 Analysis of the interaction between M18c phosphorylated by CIRK and the different versions of Sx 4

The fact that CIRK was able to phosphorylate M18c *in vitro* gave rise to the idea of assessing how this phosphorylation could affect M18c interaction with SNARE proteins such as Sx 4 or VAMP2.

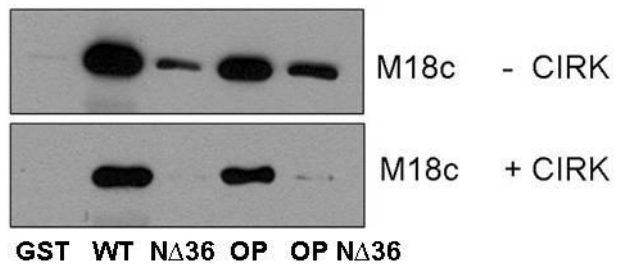
As previously mentioned in chapter 4, M18c is able to bind Sx 4 lacking the short N-terminal peptide, which corresponds to the 36 amino acids of the N-terminus, but at a much lesser extent than wild-type Sx 4 (as outlined in section 4.1.1). M18c is also able to bind the open version of Sx 4 which contains a mutation in the hinge region of Sx 4 (L173A/E174A) (Aran *et al.*, 2009; D'Andrea-Merrins *et al.*, 2007). Thus, pull-down experiments were performed in which a set amount of the different versions of C-terminally tagged Sx 4 were immobilised on glutathione sepharose before overnight incubation with M18c phosphorylated by CIRK. A C-terminal tagged version of Sx 4 was used in order to leave the N-terminal part of Sx 4 available to bind M18c. In order to check if phosphorylated M18c is able to bind the different version of Sx 4 *in vitro*, a pull-down assay was performed.

Figure 5.16B shows an overall decrease in the amounts of His₆-M18c which are able to bind the different versions of GST- Sx 4 plus CIRK versus minus CIRK. So, in order to check if bound His₆-M18c were tyrosine phosphorylated, western blot analysis were carried out using 8 µl of the total 15 µl sample. α-phosphotyrosine antibodies were used to determine if bound M18c was tyrosine phosphorylated or not. The right side of figure 5.16C shows that autophosphorylated CIRK induces His₆-M18c phosphorylation on tyrosine residues. In contrast, the left hand side on figure 5.16C shows the interesting fact that His₆-M18c (+ CIRK), which was bound to wt Sx 4 and Sx 4 open versions on glutathione sepharose (figure 5.16B; lower panel), were not tyrosine phosphorylated. This result indicates that M18c phosphorylated by CIRK loses affinity for Sx 4.

A



B



C

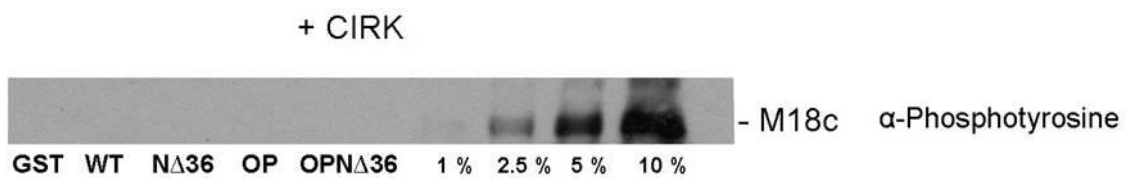


Figure 5.16 M18c phosphorylated by CIRK loses affinity for Sx 4 *in vitro*

Pull-down assay was performed where 1 µg of either recombinant GST, or GST fused to the cytosolic domain of WT Sx 4, Sx 4 NΔ36, Sx 4 open and Sx 4 open NΔ36 were firstly immobilised on glutathione Sepharose. Beads were then incubated overnight at 4 °C with 1 µg of His₆-M18c (already phosphorylated by CIRK) in a final volume of 300 µl. 6 % of each mixture was removed to assess protein input (A). After extensive washing, bound proteins were eluted using 15 µl of 1 x sample buffer (containing 20 mM DTT), resolved by SDS-PAGE and immunoblot analysis were carried out to determine which of the GST-fusion proteins M18c had bound to. Upper panel represents a Coomassie stained gel of the GST-fusion proteins (A, left and middle panels) and M18c inputs (1 % of the total input); panel B shows immunoblot analysis with α-M18c antibody used to determine bound M18c (~ 47 % of the eluted sample was loaded into the gel); panel C shows immunoblot analysis with α-phosphotyrosine antibody used to determine bound proteins which are tyrosine phosphorylated (~ 53 % of the eluted sample was loaded into the gel) and also levels of 1 %, 2.5 %, 5 % and 10 % of total phosphorylated M18c input for comparison. This experiment was repeated 3 times giving similar conclusions.

5.3.3.4 Interaction between Munc18c phosphorylated by CIRK and VAMP2

Results from section 5.3.3.3 show that phosphorylated M18c is not able to interact with Sx 4, *in vitro*. In chapter 3, data has demonstrated that M18c is also able to interact with VAMP2, therefore similar pull-down experiments were carried out to check if CIRK induced phosphorylation of M18c could also result in a decrease of M18c-VAMP2 affinity. A typical result of an experiment of this type is shown in figure 5.17.

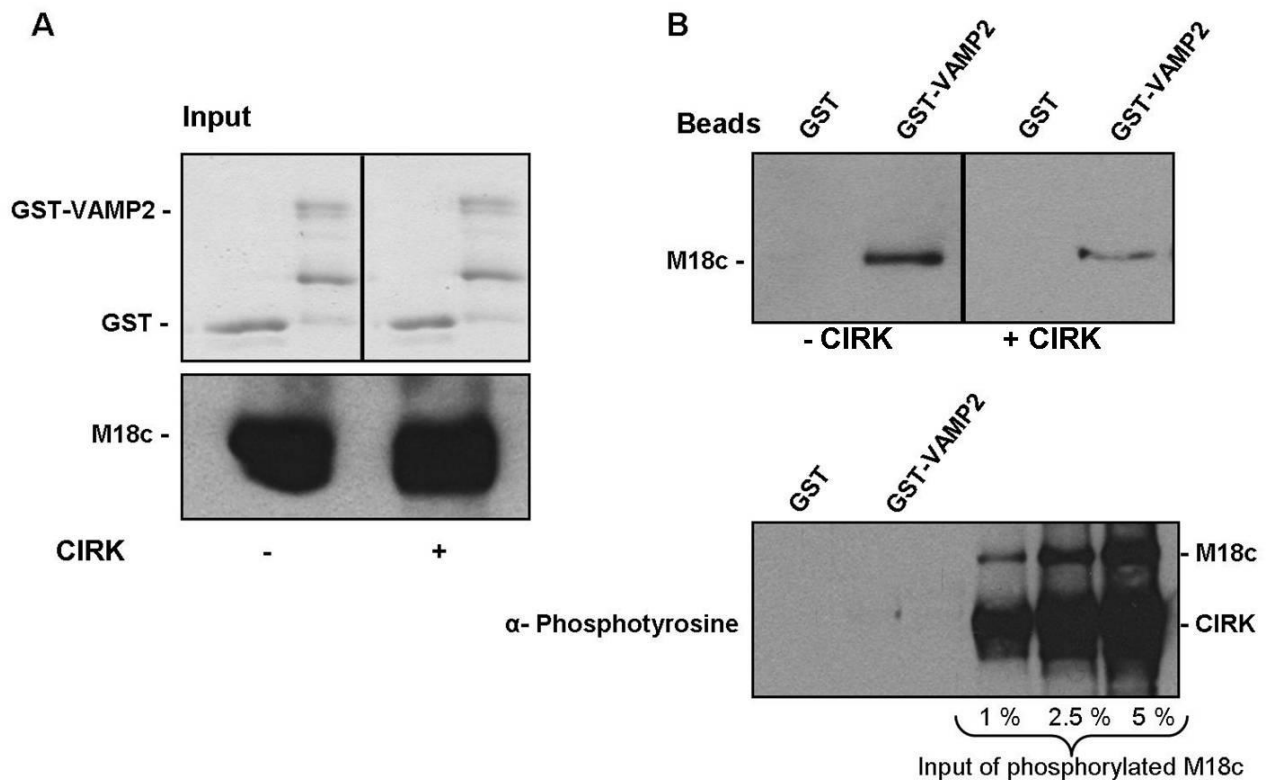


Figure 5.17 Pull-down assay of GST- VAMP2 and M18c phosphorylated by CIRK

Pull-down assay was performed where 1 μ g of either recombinant GST, or GST fused to the cytosolic domain of VAMP2 were immobilised on glutathione Sepharose. Beads were then incubated overnight at 4 $^{\circ}$ C with 1 μ g of His₆-M18c, which has been previously incubated with CIRK, for 150 min and with the control M18c without CIRK. M18c and VAMP2 were incubated in a final volume of 300 μ l. **(A)** upper panel represents a Coomassie stained gel of GST and GST-VAMP2 (6 % of total input) and lower panel represents immunoblot analysis using α -M18c antibody to show 4 % of the total M18c input in the presence and absence of CIRK; **(B)** upper panel shows immunoblot analysis with α -M18c antibody used to determine bound M18c (~ 47 % of the eluted 15 μ l sample was loaded into the gel); lower panel shows immunoblot analysis with α -phosphotyrosine antibody used to determine bound proteins which are tyrosine phosphorylated (~ 53 % of the eluted 15 μ l sample was loaded into the gel). The right side of the blot shows levels of total M18c which are phosphorylated in response to CIRK (1 %, 2.5 %, and 5 % of total phosphorylated M18c input). This experiment was repeated 3 times giving similar conclusions.

Similarly to section 5.3.3.3, figure 5.17 shows that in the presence of CIRK there is an overall decrease in the amounts of His₆-M18c that are able to bind recombinant cytosolic GST-VAMP2 compared to the pull-down of His₆-M18c which are not phosphorylated by CIRK (upper panel B). So, in order to check if bound His₆-M18c were tyrosine phosphorylated, western blot analysis were carried out using 8 μ l of the total 15 μ l eluted sample. The antibody α -phosphotyrosine was used to determine if M18c which was bound

to VAMP2 was tyrosine phosphorylated or not. The lower panel of figure 5.17B shows that autophosphorylated CIRK induces His₆-M18c phosphorylation on tyrosine residues. However, His₆-M18c which was bound to GST-VAMP2, was not tyrosine phosphorylated, as can be seen in the immunoblot with α -phosphotyrosine (figure 5.17B, lower panel). Less than 1 % of bound His₆-M18c was tyrosine phosphorylated, as judged from the immunoblot.

5.3.3.5 Mass spectrometry analysis of M18c phosphorylated by CIRK

In order to determine the amino acid residues from M18c that get phosphorylated upon incubation with CIRK, 1 μ g of recombinant M18c was incubated with CIRK as described in section 5.3.3.1. The sample was then trypsinised and the phosphorylated sites determined by liquid chromatography – electrospray ionisation – mass spectrometry (LC-ESI-MS) and electrospray ionisation – mass spectrometry/mass spectrometry (ESI-MS/MS) using an ABI Qtrap 4000 instrument (all analyses were carried out at the Dundee University Post-genomics facility). As shown in figure 5.18, incubation of M18c with CIRK generated two major $[M-2H]^{2-}$ (doubly charged) quasis molecular ions at m/z 551.3 and 615.3. These ions are absent in the M18c sample that was not incubated with CIRK (figure 5.19), suggesting they represent phosphorylated tryptic peptides. It is worth pointing out that these analyses were carried in negative ion mode and set up only to identify tryptic peptides that release 79 mass units (which corresponds to PO_3^- and suggests the presence of a phosphopeptide). After identification of candidate phosphorylated peptides (figure 5.18), the polarity of the mass spectrometer was switched to positive and the same ions were submitted to ESI-MS/MS in order to determine their amino acid sequences and locate the phosphorylated residue (s). As shown in the figure XVIII (peptide 1) and figure XIX (peptide 2) of the appendix, fragmentation of both ions generated a series of intense $[M-H]^+$ (singly charged) *y*- and *b*-ions, which correspond to the C-terminus and N-terminus, respectively, and where the number refers to the location in the peptide sequence. Such fragments made possible the identification of peptide 1 as T N Yp L E L D R and peptide 2 T N Yp L E L D R K (peptide 2 represents the miscleavage of peptide 1). In both peptides, Tyr was the only residue found phosphorylated, which in the entire M18c amino acidic sequence corresponds to Y521 (see figure X from appendix) and tables I A and B of the appendix (for a summary of the assignments). In summary, these analyses unequivocally demonstrate that M18c is a substrate for CIRK phosphorylation. Furthermore, the only amino acid residue that gets phosphorylated by CIRK appears to be Y521.

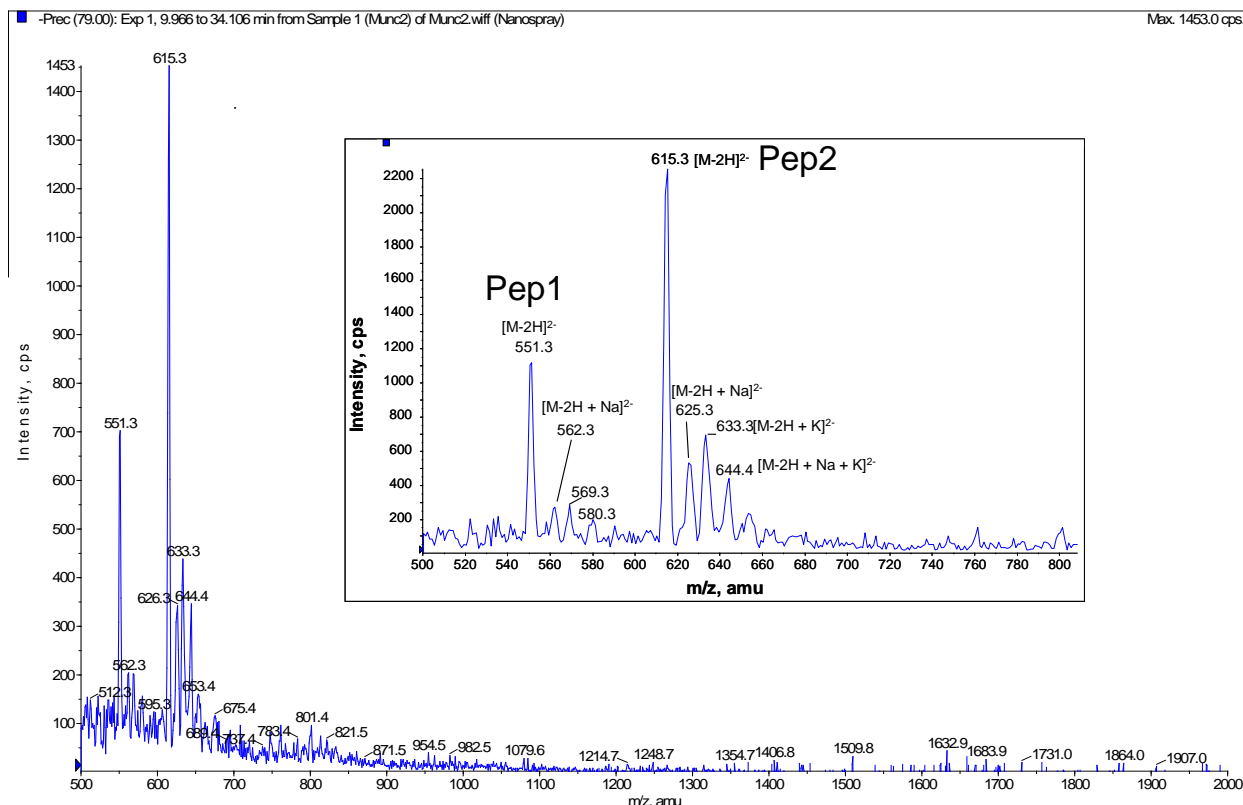


Figure 5.18 Negative-ion ESI-MS of phosphorylated M18c

1 μ g M18c were incubated with CIRK as outlined in sections 2.2.5.2 and 5.3.3.1. The reaction was stopped and the protein trypsinised and analysed by LC-ESI-MS in a Qtrap 400 in negative-ion mode. The spectrum shows only the ions detected by the “precursor ion” scan of 79 mass units, which represents PO_3^- and suggests the presence of a phosphopeptide. The inset shows a detail of the two major $[\text{M}-2\text{H}]^{2-}$ (doubly charged) ions (Peptide 1 and peptide 2). The ions representing both peptides, are each one accompanied by the same peptide but coupled to one or two metal ions (i.e. m/z 562.3, 569.3 and 580.3 (for peptide 1), and m/z 625.3, 633.3 and 644.4 (for peptide 2)).

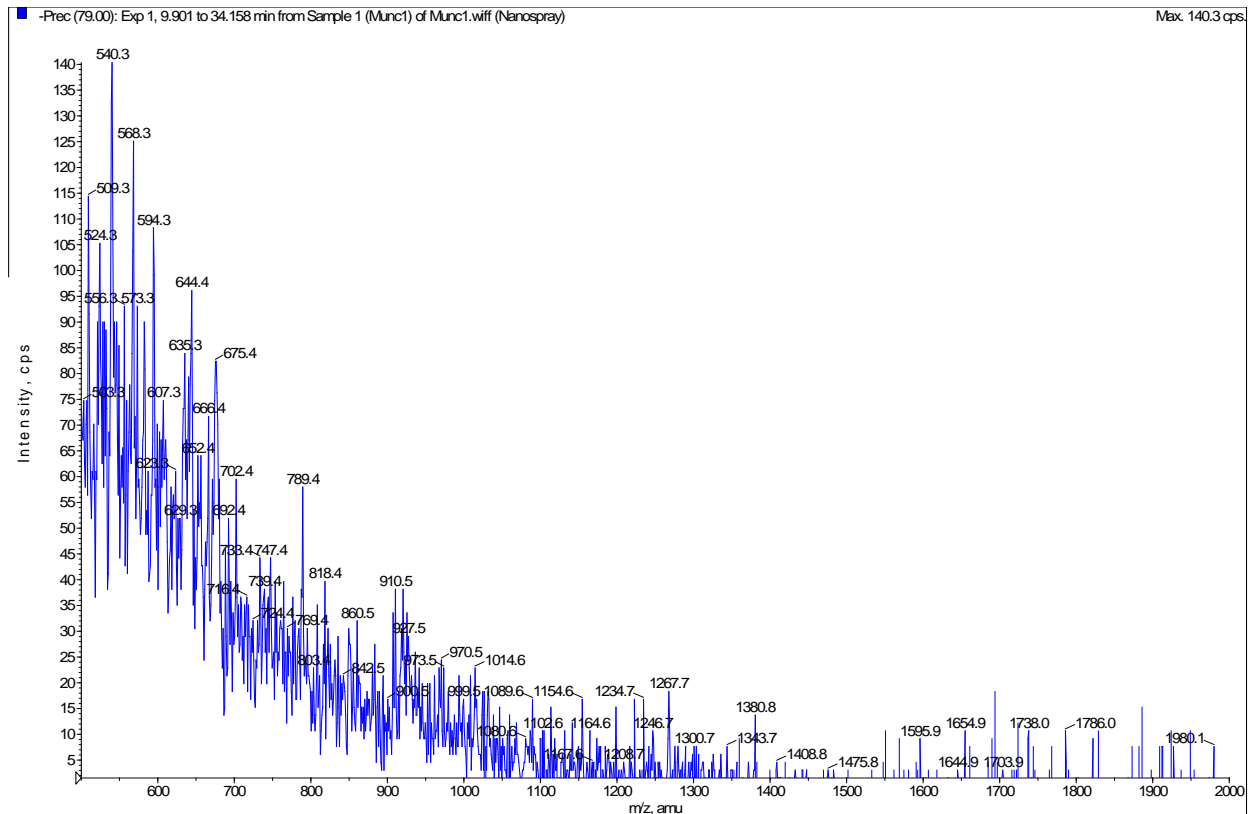


Figure 5.19 Negative-ion ESI-MS of non-phosphorylated M18c

M18c alone was incubated as in figure 5.18 (but without CIRK), trypsinised and the generated peptides analysed by LC-ESI-MS in a Qtrap 400 in negative-ion mode. The spectrum shows only the ions detected by the “precursor ion” scan of 79 mass units. As can be seen, no significant ions were detected.

5.3.4 Phosphorylation of endogenous M18c in response to insulin

The ability of insulin to stimulate tyrosine phosphorylation of endogenous M18c was investigated by incubating 3T3-L1 adipocytes with and without 150 nM insulin for 5 min at 37 °C. The supernatant fraction coming from these cells were incubated with phosphotyrosine agarose for 3 h. Beads were washed and bound proteins were subject to western blot analysis using both anti-M18c and anti-phosphotyrosine antibodies.

The upper panel of figure 5.20 shows that the insulin receptor substrate 1 (IRS1) and the β subunit of the insulin receptor (IR) become tyrosine phosphorylated only in response to insulin as expected. This positive control was performed to confirm that phosphorylation

was indeed occurring in 3T3-L1 adipocytes upon insulin stimulation. The lower panel of figure 5.20 shows that only in the insulin stimulated state M18c becomes phosphorylated.

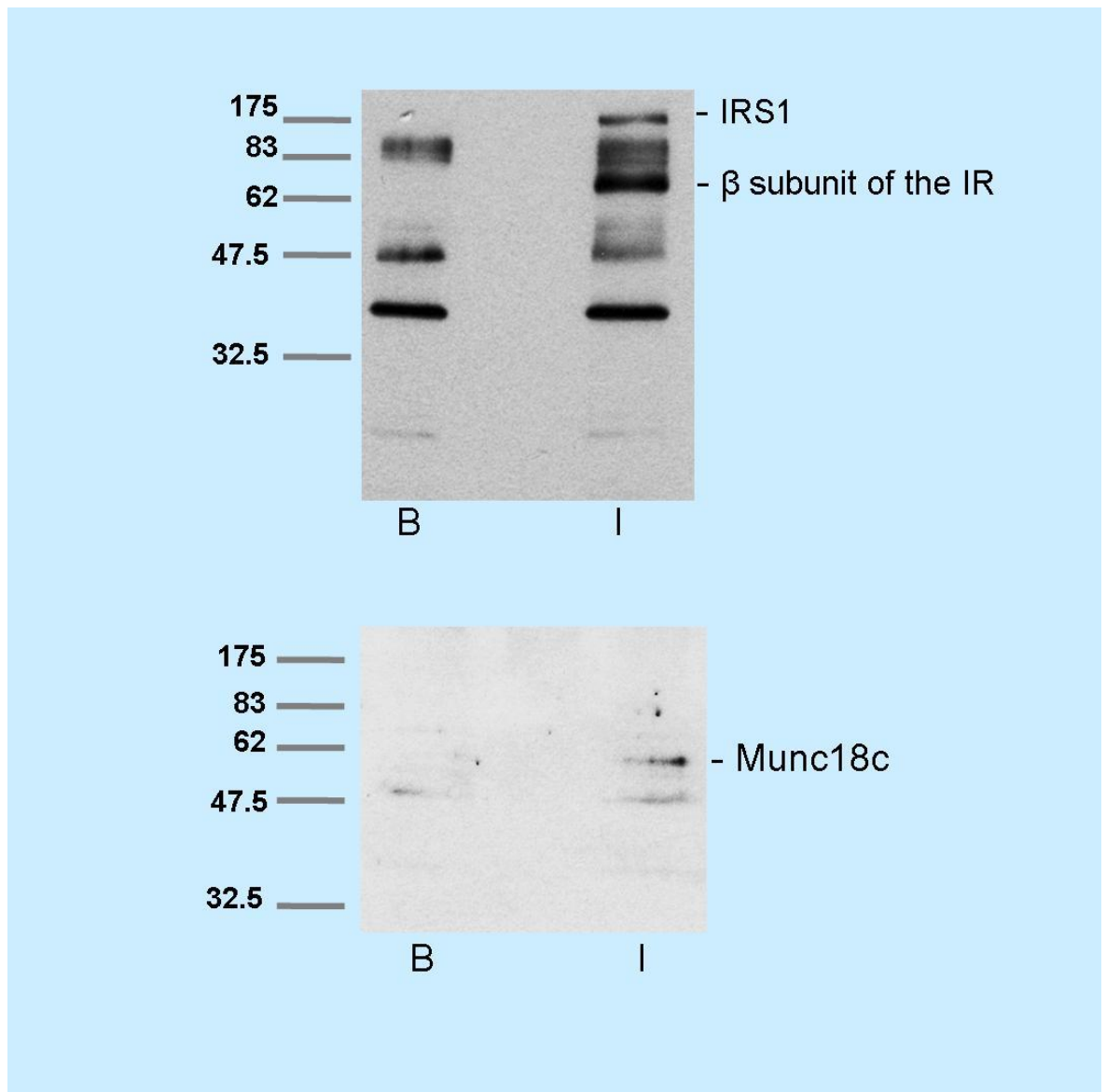


Figure 5.20 Endogenous M18c undergoes insulin-stimulated tyrosine phosphorylation
Cell lysates derived from 3T3-L1 adipocytes which have been previously incubated for 5 min with 150 nM insulin (I) and without insulin (B) at 37 °C, were incubated with anti-phosphotyrosine agarose for 3 h. At the end of the 3 h, beads were washed 3 times with 1 ml buffer (indicated in section 2.2.6). Bound proteins were eluted by boiling the beads in 50 μ l of 1 x sample buffer (containing 20 mM DTT). Bound proteins for both basal (B) and insulin stimulated samples (I) were resolved on a 12 % SDS-PAGE followed by immunoblot analysis with antibodies against phosphotyrosine (top panel) and M18c (lower panel).

5.4 Discussion

The work presented in this chapter aimed to investigate the precise role of phosphorylation in SNARE complex formation. Proteins such as Sx 4 and M18c, which were not previously associated directly with the insulin-signalling network, were found to be phosphorylated on tyrosine residues upon insulin stimulation (Schmelzle *et al.*, 2006). In order to understand the function of these tyrosine phosphorylation sites, site-directed mutagenesis was performed to mimic the phosphorylated form of the residue.

Phosphomimetic mutations in Sx 4 (Y115E, Y251E and Y115E/Y251E) were obtained *via* site-directed mutagenesis and the conformation of Sx 4 before and after mutations were analysed by CD. Far UV CD demonstrated that introduction of phosphomimetic mutations into cytosolic Sx 4 did not cause gross protein misfolding (figure 5.2). The near UV analysis suggests that the double mutant might be slightly less rigid than the wild-type (figure 5.3). However, the environment of the aromatic residues did not change dramatically, suggesting that the overall tertiary structure remained similar to the wild-type. GST-pull downs were then performed to investigate the effects of Sx 4 phosphomimetic mutations on the interaction with both M18c and its SNARE partner SNAP23. Interestingly, these mutations did not affect binding to either M18c or SNAP23 as can be seen in figures 5.4 and 5.5 respectively. These results are in agreement with a previous finding suggesting that Sx 4 residues 118-194 are sufficient for interaction with M18c since these residues contain the Hc α -helix and flexible linker region which control closed to open conformational transitions of syntaxins (Jewell *et al.*, 2008).

The role of tyrosine phosphorylation of Y521 in M18c on its interaction with Sx 4 was also investigated by introducing a phosphomimetic mutation into the murine sequence of His₆-M18c. Recently, studies performed in adipocytes showed that residue Y521 in M18c is the major PDGF receptor-dependent tyrosine phosphorylation site (Umahara *et al.*, 2008) and this residue was also shown to become phosphorylated in response to insulin (Schmelzle *et al.*, 2006; Umahara *et al.*, 2008). In order to mimic the phosphorylated form of the protein, a phosphomimetic mutant of M18c was generated by changing a tyrosine to the negatively charged glutamic acid. After the mutations were successfully obtained, GST pull-downs were carried out to determine whether the mutation could affect binding to different versions of GST tagged Sx 4 including Sx 4 wild-type, Sx 4 Δ 36, Sx 4 L173A/E174A (open Sx 4) and L173A/E174A Δ 36. Interestingly, His₆-M18c mutant was completely unable to bind Sx 4 as can be seen in figure 5.10. A further pull-down was performed to

determine whether the phosphomutant could still bind VAMP2 *in vitro*. We found that His₆-M18cY521E was also not able to interact with GST-VAMP2 (figure 5.11). The disruption of M18c binding to both GST- Sx 4 and GST-VAMP2 were not caused by gross conformational changes in His₆-M18c since the overall structure of His₆-M18cY521E molecule was shown to be preserved by performing CD and fluorescence spectra analysis (figures 5.8 and 5.9 respectively).

The exact manner by which M18c and Sx 4 interact has been rather a mystery than a clear relationship. One model of interaction is based upon the structure of the homologous pair of neuronal proteins Sx 1A/M18a (Misura *et al.*, 2000). In this model, M18a is an arch shaped molecule that binds Sx 1A and “holds” it in a so-called “closed” conformation that is incompetent for fusion (Misura *et al.*, 2000). The other model of interaction suggests that SM proteins bind to the extreme N-terminus of syntaxins. The structure of M18c in complex with the N-terminal peptide of Sx 4 has been described (Hu *et al.*, 2007). Thus, in collaboration with Prof James Milner-White (University of Glasgow), a model was obtained based on previous modelling from M18A/Sx 1A and Sx 4 N-terminal peptide/M18c (Hu *et al.*, 2007; Misura *et al.*, 2000) in order to verify where these residues that become tyrosine phosphorylated are in relation to binding sites, and to assess how their mutations could affect Sx 4/M18c interaction.

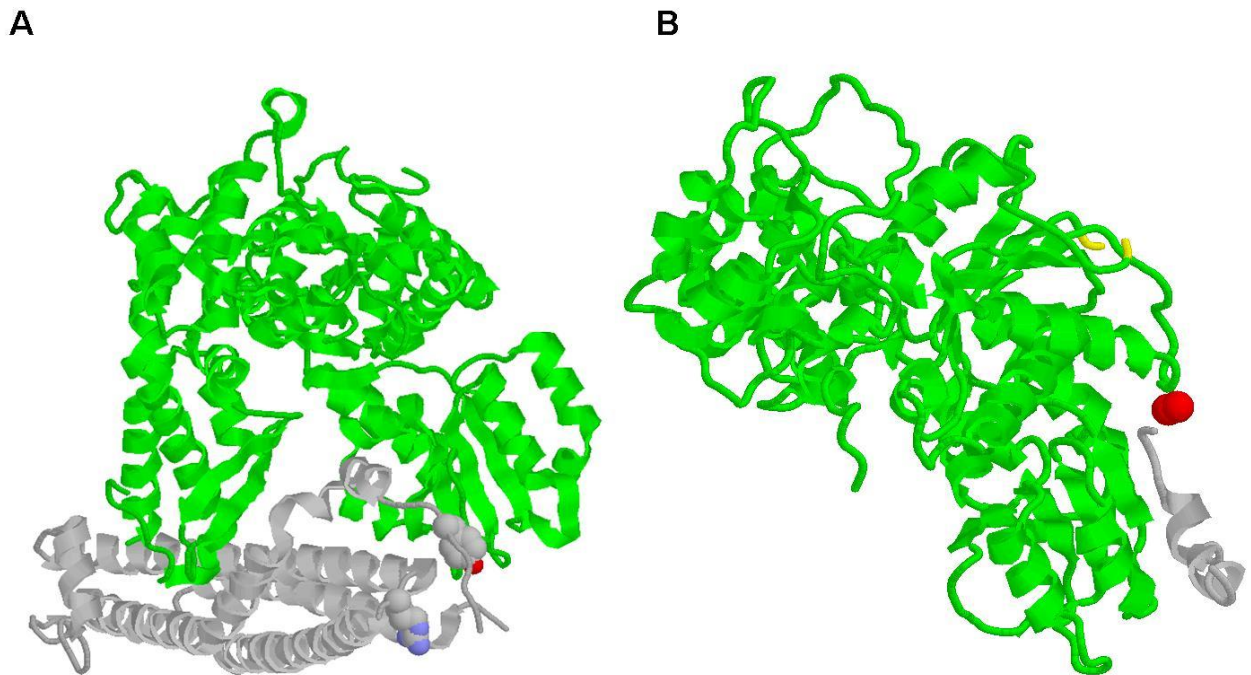


Figure 5.21 Ribbon models of Sx 4 in complex with M18c showing the key residues within Sx 4 and M18c which are targets for phosphorylation

Model (A) shows M18c (green) holding Sx 4 (grey) in a closed conformation. Sx 4 Y115 site is highlighted in red and residue Y251 in blue. Model (B) shows the short N-terminal peptide of Sx 4 (grey) interacting with the outer face of domain I in M18c (green). The part of the M18c sequence containing the Y521 site was unstructured in the model of Hu *et al*, and residues 502 to 526 are absent from their structure. The ends of this region are shown in yellow. Modelling potential structures of this missing region based on the M18A structure suggest that residue Y521 may lie close to the pocket into which the Sx 4 peptide inserts. Y521 is shown in red. Models were obtained based on previously described models and designed by Prof James Milner-White (University of Glasgow) using Rasmol software.

As can be seen in figure 5.21A, residues Y115 and Y251 were confirmed to face away from the sites of Sx 4/M18c interaction indicating that mutations in these residues are not likely to affect binding to M18c. This was confirmed in the pull-down experiments described in sections 5.3.1.3 and 5.3.1.4.

Unfortunately, it is not known exactly where the Y521 site is located in relation to Sx 4 because this region corresponds to an unstructured region (yellow ends in figure 5.21B) being probably part of a flexible region. Therefore, Y521 could not be definitively added to the model. Arguably, it is predicted that this residue might be present around the hydrophobic pocket area present in M18c (described in chapter 1), which would disrupt binding to the open conformation of the Sx 4. Interestingly, both results presented in sections 5.3.2.3 and 5.3.2.4 show that His₆-M18cY521E loses affinity for both GST-Sx 4 and GST-VAMP2. It is uncertain why there is a loss in affinity to GST-VAMP2, however

it is predicted that the Y521E mutation could disrupt binding to Sx 4 especially *via* its open conformation. It would be useful to use Surface Plasmon Resonance to measure and compare the affinities between M18cY521E/Sx 4 and M18cY521E/VAMP2, in isolation.

A second approach was taken to understand how phosphorylated M18c might affect binding to SNARE proteins. A recombinant cytoplasmic insulin receptor kinase (CIRK) was used in order to phosphorylate native M18c. CIRK was shown to be able to phosphorylate M18c and Sx 4 *in vitro* (figures 5.13, 5.14 and 5.15). M18c phosphorylation was greater than Sx 4 phosphorylation which agrees with published data (Schmelzle *et al.*, 2006). When the interaction of His₆-M18c phosphorylated by CIRK with GST-Sx 4 was analysed, although M18c still bound to the beads, none of the phosphorylated M18c bound (figure 5.16). Moreover, His₆-M18c phosphorylated by CIRK was also unable to interact with GST-VAMP2 (figure 5.17). In summary, the experiments performed with CIRK and also with a phosphomimetic version of M18c (Y521E) suggest that phosphorylation affects M18c binding to both GST-Sx 4 and GST-VAMP2.

After obtaining the results that CIRK indeed phosphorylates M18c *in vitro*, phosphorylated and non-phosphorylated forms of M18c were sent to Dundee University in order to perform mass spectrometry analysis to map which residues in recombinant His₆-M18c become phosphorylated by CIRK. Interestingly, only one residue in M18c becomes phosphorylated, which was identified as Y521 (figure 5.18), the same residue identified in previous mass spectrometry analysis of M18c which were phosphorylated in response to insulin and PDGF *in vivo* (Schmelzle *et al.*, 2006; Umahara *et al.*, 2008).

All these data gave rise to the hypothesis that phosphorylation of M18c may displace M18c from Sx 4 and VAMP2 allowing the in-coming vesicles to fuse with the PM. If M18c is not present bound to either VAMP2 or Sx 4 these proteins will be free to form SNARE complexes and consequently drive membrane fusion. Interestingly, work performed with 3T3-L1 adipocytes have shown that over-expression of M18c inhibits insulin-stimulated GLUT4 translocation to the PM (Tamori *et al.*, 1998; Thurmond *et al.*, 1998) and M18c gene knockout in adipocytes results in an increase of GLUT4-containing vesicles fusion with the PM without affecting GLUT4 translocation to the cell periphery (Kanda *et al.*, 2005).

The idea that phosphorylation of M18c on tyrosine residues may regulate membrane fusion has been supported by other studies. Glucose stimulation of pancreatic β -cells was shown

to stimulate tyrosine phosphorylation of M18c at residue Y219 (Oh and Thurmond, 2006) and, as mentioned previously, experiments performed in adipocytes suggested that residue Y521 in M18c is the major PDGF receptor-dependent tyrosine phosphorylation site and it is also phosphorylated by insulin causing the dissociation of M18c from Sx 4 (Umahara *et al.*, 2008). These data support the idea that M18c negatively regulates Sx 4, and that their dissociation is important to allow GLUT4 translocation and fusion with the PM.

The results obtained in this chapter will be further discussed in chapter 6.

Chapter 6

6 Discussion

Defining a conserved mechanism by which SM proteins act in the process of SNARE-mediated membrane fusion has been difficult mostly due to the considerable divergence on the binding modes between different SM/syntaxin pairs. Although SM proteins possess high homology between species, a conserved role could not be determined. In this thesis, attention was mainly focused on the interaction of Sx 4, SNAP23 and VAMP2 with the SM protein M18c. Although, these proteins are known to mediate the insulin-stimulated delivery of GLUT4 vesicles to the PM in muscle and adipose tissue, the regulation of this process is unclear. M18c has been shown to interact strongly with Sx 4 (Tellam *et al.*, 1997). Studies have shown that this interaction is mediated *via* the N-terminal region of Sx 4 (Grusovin *et al.*, 2000) and that the N-terminal 29 amino acids of Sx 4 are necessary for its interaction with M18c (Latham *et al.*, 2006). This binding mode was also observed in the yeast syntaxins Sed5p and Tlg2p and mammalian Sx 1A, and Sx 16 with their respective SM proteins (Bracher and Weissenhorn, 2002; Burkhardt *et al.*, 2008; Carpp *et al.*, 2006; Dulubova *et al.*, 2002; Latham *et al.*, 2006; Yamaguchi *et al.*, 2002). M18c binds the short N-terminal peptide region in Sx 4 when this syntaxin is present in an “open” conformation (Hu *et al.*, 2007) and also binds to binary and ternary SNARE complexes (Latham *et al.*, 2006). A third binding mode is also a possibility which could relate to the neuronal M18a/ closed Sx 1A complex, where the whole Sx 1A Habc domain interacts with M18a (Misura *et al.*, 2000). These different modes of interaction might be related to the regulation of SNARE assembly/disassembly. In neurons, a study using fluorescent fusions of M18a and Sx 1A (wild-type and open versions) visualised in N2A cells, reported that the two modes of interaction are spatially distinct, where Sx 1A binds M18a predominantly in intracellular locations avoiding any unspecific interaction with the Sx 1A trafficking to the PM (Rickman *et al.*, 2007). And upon arrival at the PM, the syntaxin would change conformation from closed to open in order to participate in SNARE complexes, while M18a could still be bound *via* the short N-terminal peptide of Sx 1A (Rickman *et al.*, 2007). Thus, the different modes of interaction between SM and syntaxin proteins might represent different regulatory steps in the SNARE cycle.

In chapter 1, pull-down assays provided evidence that M18c binds directly to the v-SNARE VAMP2, which has not been previously identified (Brandie *et al.*, 2008). In addition, competition binding experiments showed that Sx 4 was able to displace VAMP2 from M18c (figure 3.3 and 3.5B), whereas VAMP2 was not able to displace Sx 4 from M18c, *in vitro* (figure 3.4 and 3.5A). These results agreed with studies performed in yeast, where some v-SNAREs were shown to bind SM proteins *in vitro* (Carpp *et al.*, 2006; Peng and Gallwitz, 2004). A hypothetical model would be that in the basal state, M18c could

retain Sx 4 in order to inhibit constant SNARE complex formation. Upon stimulation, M18c could direct VAMP2-containing vesicles to the PM in order to interact with Sx 4. M18c would then release VAMP2 to allow it to interact with Sx 4, however Sx 4 could still bind M18c *via* a different conformation (probably through its short N-terminal peptide). Because Sx 4 seems to bind M18c into two different conformations (Aran *et al.*, 2009; D'Andrea-Merrins *et al.*, 2007) and VAMP2 *via* its SNARE motif only, this could explain why VAMP2 is displaced easier from M18c than Sx 4. Other possibility is that both proteins (Sx 4 and VAMP2) can bind to the same region in M18c, thus explaining why one (probably with the most affinity) can displace the other. Unfortunately, there was not enough time to perform careful and detailed investigation on whether M18c could bridge VAMP2 and Sx 4 interaction as proposed by the “bridging hypothesis” (Peng and Gallwitz, 2004). Although the observation that Sx 4 binding disrupts the M18c/VAMP2 interaction does not agree with this hypothesis, in cells other factors might work in concert to allow this possibility. Nevertheless, it would be very useful to use Surface Plasmon Resonance to measure and compare the affinities between M18c/Sx 4 and M18c/VAMP2, in isolation.

Membrane fusion within the cells must be regulated precisely in order to maintain the integrity of the different cellular organelles and the formation of specific SNARE complexes. In order to understand more about this process, the *in vitro* fusion assay was an important tool used in this study. This assay was previously shown to be very useful to determine that SNARE proteins are necessary and sufficient to drive membrane fusion *in vitro* (Weber *et al.*, 1998). Previously in the lab, Dr Fiona Brandie has shown that by reconstituting Sx 4/SNAP23 and VAMP2 (all produced as recombinant proteins in *E. coli*) into two separate population of synthetic liposomes, fusion occurs (Brandie *et al.*, 2008). This result was further confirmed in chapter 4, where these proteins were also shown to be sufficient to drive membrane fusion *in vitro* (chapter 4, fig 4.12A). Although, *in vitro*, fusion was shown to occur depending only on the t- and v-SNAREs complex formation, *in vivo* other factors are important for the regulation SNARE-mediated membrane fusion. Thus, the effects of the SM protein M18c on SNARE-mediated membrane fusion catalysed by Sx 4/SNAP23 and VAMP2 were investigated. We found that M18c inhibited liposome fusion catalysed by this SNARE complex in a dose-dependent manner (chapter 4, figure 4.14B). In order to define how M18c causes inhibition of fusion, several approaches were taken including the generation of different Sx 4 constructs (all containing the trans-membrane domain). They were Sx 4 N Δ 36, Sx 4 OPEN and Sx 4 OPEN N Δ 36. Fusion was successful for all different versions (Figure 4.12). The fusion rates between the different

SNARE complexes could not be precisely compared since the amount of reconstituted proteins vary. Then, the different complexes were either allowed to pre-incubate at 4 °C before M18c addition or they were incubated directly with M18c without pre-incubation of the vesicles. By performing these experiments, M18c was shown to inhibit SNARE-mediated membrane fusion *in vitro* when pre-incubated with the v- and t- SNAREs prior to fusion (by 55-80 %; figure 4.22). However, M18c did not inhibit significantly SNARE-mediated membrane fusion *in vitro*, when the v- and t-SNARE liposomes were allowed to pre-dock before M18c addition (inhibition varied between 0 to 24 %; figure 4.22). Note that these sets of fusion experiments, in the presence and in the absence of M18c, were performed twice to confirm the results and the percentages reported represent the means of the two experiments, which exhibited good agreement. Furthermore, it was not possible to reconstitute equimolar amounts of the different t-complexes together with M18c (such as in figure 4.14C) due to the low levels of the purified complexes.

The involvement of the Sx 4 N-peptide in the inhibitory activity of M18c was tested in these *in vitro* fusion experiments. Surprisingly, even when the N-terminal 36 residues of Sx 4 were removed (in both wt and open forms), the inhibitory effect of M18c was not abolished (figures 4.17, 4.18, 4.20 and 4.21). In fact, regulation of SNARE complex formation was shown to be dependent on the association of M18c with both the C- and N-terminus of Sx 4 (D'Andrea-Merrins *et al.*, 2007), thus M18c could still be able to bind other regions on Sx 4 sequence resulting in inhibition of fusion. This was further confirmed in another study where significant binding between M18c and a truncated version of Sx 4 (missing the first 40 amino acids) was observed (ter Beest *et al.*, 2005). Furthermore, in the neuronal Sx 1A, the Habc domain was shown to act as an inhibitor of fusion and deletion of this region accelerated the fusion rates mediated by neuronal SNAREs (Fix *et al.*, 2004). A similar event could be happening to Sx 4, thus the removal of the whole N-terminal domain of Sx 4 (*i.e.* the Habc domain and the short N-terminal peptide) would be a good control to test whether M18c inhibits fusion *via* the Sx 4 N-terminal region.

Another explanation for M18c negative regulation could come from the fact that upon SNARE complex formation, the binding sites on Sx 4 that could be exposed to interact with M18c are making contacts with Sx 4 cognate SNARE proteins, thus inhibiting M18c binding and consequently allowing complex formation. However, when M18c is added together with the Sx 4/SNAP23/VAMP2 liposomes, the high affinity interaction between M18c/Sx 4 could inhibit SNARE complex formation. Also, Prof James McNew has

observed that the position of the tag on the SM protein might influence the fusion process positively or negatively (Rodkey *et al.*, 2008). Since the M18c construct used in these experiments was N-terminally tagged, a new construct could be generated containing the His tag at the C-terminus of the protein in order to test it in the *in vitro* fusion assay using the Sx 4 constructs originated in this thesis. Furthermore, M18c negative regulation on the assays performed in chapter 4, could be also related to data presented in chapter 1. M18c was shown to bind VAMP2 *in vitro* and this interaction occurred *via* the SNARE motif on the v-SNARE. Since the SNARE motif is the region responsible for mediating SNARE complex assembly (Paumet *et al.*, 2004), M18c when added directly to the *in vitro* fusion assay (before pre-docking of the SNAREs), might associate with the SNARE motif in VAMP2, thus inhibiting SNARE complex formation and consequently fusion.

Interestingly, M18a was shown to stimulate Sx 1A/SNAP25/VAMP2 membrane fusion *in vitro* not only *via* Sx 1A but also *via* interaction with VAMP2, since mutations in VAMP2 were shown to abolish the stimulatory effect of M18a (Shen *et al.*, 2007). *In vitro* fusion studies performed in our lab have shown that VAMP2 was also important. However, Dr Fiona Brandie observed that inhibition *via* VAMP2 was less inhibitory than *via* the t-SNARE complex by reconstituting either the t-complex or VAMP2 liposomes with M18c (unpublished). This might be due to the strong interaction formed between Sx 4 and M18c. The idea that M18c could act as a regulatory protein controlling the process of SNARE complex assembly could be tested by mixing the SNARE proteins with M18c and checking if SDS-resistant complexes can be formed over time. This technique has been used in the past to show that the neuronal SNARE proteins form stable complexes which are SDS resistant (Hayashi *et al.*, 1994). Recently, the functional effect of the Sx 1A short N-terminal peptide in controlling SNARE complex assembly was also tested using this method (Burkhardt *et al.*, 2008). Thus, M18c could be pre-incubated either with Sx 4 alone or the t-complex or VAMP2 alone (before addition of the other SNAREs) or it could be mixed together with all the three different SNAREs to observe if SDS-resistant complexes are formed. These would be *in vitro* approaches, nevertheless, *in vivo*, SNARE-mediated membrane fusion of GLUT4 vesicles are subjected by several levels of control including cell signalling cascades.

The fusion between GLUT4 vesicles with the PM was shown to be regulated by insulin (Koumanov *et al.*, 2005). Insulin stimulation leads to activation of the insulin receptor by increasing its tyrosine kinase activity. The insulin receptor autophosphorylates and causes phosphorylation of several substrates including some SNARE proteins involved in GLUT4 translocation. At the PM, GLUT4 acts to clear glucose from the blood. Failure in this

process can lead to insulin resistance and Type 2 Diabetes (Saltiel, 2001). In chapter 5, the role of phosphorylation on the trafficking machinery that leads to GLUT4 externalisation, was studied. Two tyrosine sites in Sx 4 (Y115, Y251) and one site in M18c (Y521) were shown to become phosphorylated in response to insulin (Schmelzle *et al.*, 2006). Thus, phosphomimetic mutants of both proteins were generated in order to perform pull-down assays to analyse their interactions with their respective SNARE partners. Phosphomimetic mutations in Sx 4 (Y115E, Y251E and double mutant) did not affect their interactions with both M18c and SNAP23 (figures 5.4 and 5.5 respectively), whereas the mutation Y521E in M18c, abolished binding to both Sx 4 and VAMP2 (figures 5.10 and 5.11 respectively). These results were not due to protein misfolding, since CD analysis demonstrated that all the mutants were properly folded (see figures 5.2, 5.3 and 5.8, 5.9). Another study demonstrated that, in adipocytes, insulin and PDGF stimulation causes M18c phosphorylation also on residue Y521 (Umahara *et al.*, 2008). This was further confirmed after incubating 3T3-L1 adipocytes for 5 min with insulin, which resulted in M18c tyrosine phosphorylation, as can be seen in figure 5.18.

In addition, another approach was taken to confirm phosphorylation of M18c. The use of a recombinant cytoplasmic tyrosine kinase domain of the insulin receptor (CIRK) has proven that M18c and Sx 4 indeed become phosphorylated on tyrosine residues *in vitro*, as can be seen in figures 5.13, 5.14 and 5.15. Mass spectrometry analysis indicated that the residue in M18c that becomes tyrosine phosphorylated in response to CIRK is Y521 (figure 5.18). Pull-down assays analysing the interaction of His₆-M18c phosphorylated by CIRK with both cytosolic GST-Sx 4 and GST-VAMP2 were performed and demonstrated that, although M18c was still able to bind to the beads, none of the phosphorylated M18c bound (figure 5.16 and 5.17). Thus, these CIRK experiments confirmed that phosphorylation affects M18c binding to both GST-Sx 4 and GST-VAMP2, *in vitro*.

It is uncertain why Sx 4 phosphorylation did not affect its binding to other SNAREs. An option could be that Sx 4 phosphorylation could stabilise t-SNARE complex formation promoting fusion, whereas phosphorylation of M18c seems to inhibit binding to both VAMP2 and Sx 4, thus inhibiting M18c negative effect on fusion. This agrees with studies which suggested that M18c needs to be dissociated from Sx 4 in order to allow GLUT4 fusion with the PM in response to insulin (Araki *et al.*, 1997; Kanda *et al.*, 2005; Thurmond *et al.*, 2000; Umahara *et al.*, 2008). Therefore, phosphorylation could be an important post-translational modification in the process of SNARE-mediated membrane fusion. It could influence the activity and conformation of M18c *in vivo*. There is a

possibility that M18c is not completely dissociated from Sx 4 upon phosphorylation *in vivo*, however phosphorylation might change the conformation by which these proteins interact. It would be interesting to test if the mutant M18cY521E would still be able to affect negatively the *in vitro* fusion assay catalysed by Sx 4/SNAP23/VAMP2. However, it was not possible to perform this experiment due to the poor expression of M18cY521E and the lack of time to optimise the conditions to purify high levels of the protein.

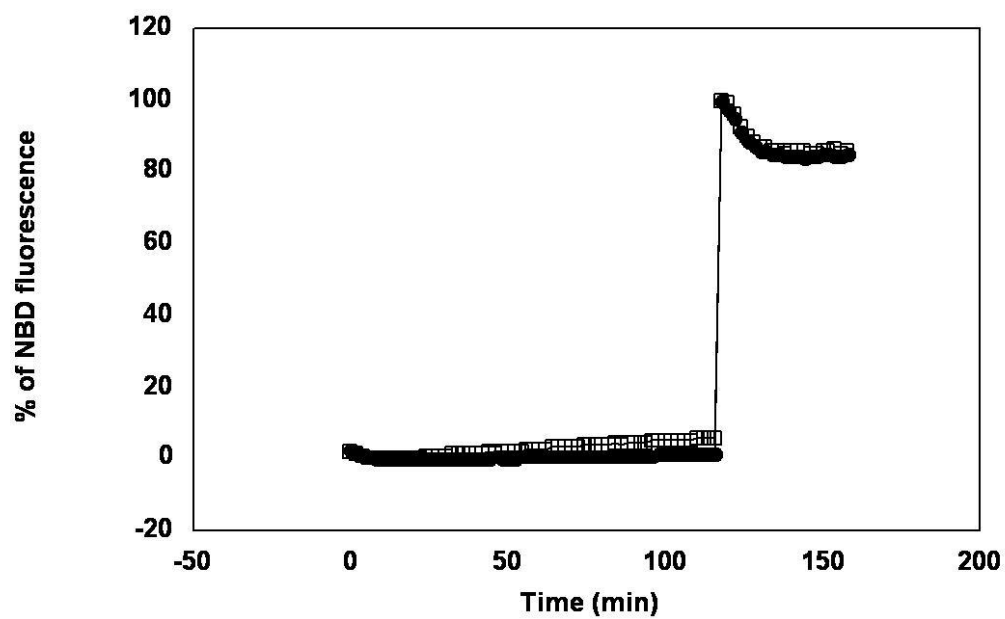
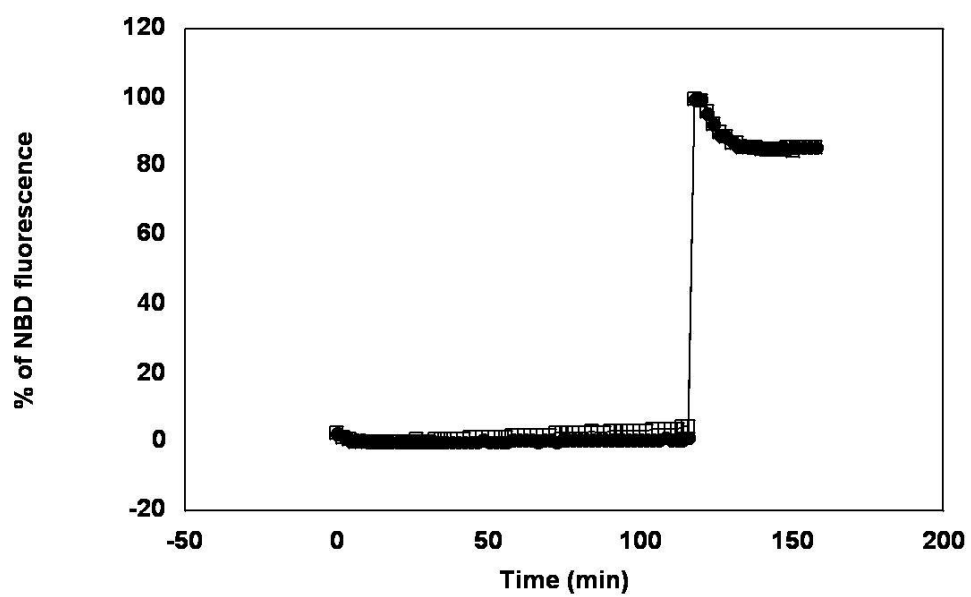
Others have expressed the M18c mutant Y521A in adipocytes (Umahara *et al.*, 2008). However, in these experiments both the mutant and the wild-type form of M18c inhibited GLUT4 translocation to a similar degree (Umahara *et al.*, 2008). However, these experiments were performed in cells expressing endogenous M18c, which could generate competition between mutant and wild-type forms. Thus, a phospho-resistant (Y521A) and a phosphomimetic mutant (Y521E) should be examined separately in adipocytes. Expressing wild-type M18c, M18cY521A or Y521E at levels approaching those of endogenous M18c in 3T3-L1 adipocytes, in which endogenous M18c is depleted using siRNA, will be a good experiment to assess the effects of phosphorylation on GLUT4 trafficking *in vivo*. These experiments are now being performed in collaboration with Prof Jeffrey E. Pessin (Albert Einstein College of Medicine, New York, USA).

In summary, a reasonable model for the Sx 4/M18c interaction would be that when monomeric Sx 4 is in the basal state, M18c is able to inhibit complex formation by binding to the closed conformation of this syntaxin. Then, upon stimulus, a conformational change in Sx 4 could occur. Due to the different modes of binding between these two proteins, M18c would be able to re-associate with Sx 4 when the latter is in an open conformation, thus allowing SNARE complex formation. In this state, the possibility that M18c could also remain bound to the SNARE complexes should not be excluded. The trigger factor for this conformational change in the process of GLUT4 translocation, could be attributed to the hormone insulin, which would affect protein-protein interactions *via* phosphorylation of several substrates including M18c and SNARE proteins. Nevertheless, it is important to mention that other Sx 4 interacting proteins, such as synip and tomosyn (Min *et al.*, 1999; Widberg *et al.*, 2003), might also influence SNARE complex assembly. In addition, the interaction of M18c with its novel partner Doc2 β could also be important, since this association was shown to release M18c inhibition over Sx 4 to facilitate exocytosis (Ke *et al.*, 2007). Understanding how GLUT4 trafficking events are controlled at the molecular level will bring new tools for the treatment of the global epidemic of insulin-resistance and Type 2 diabetes.

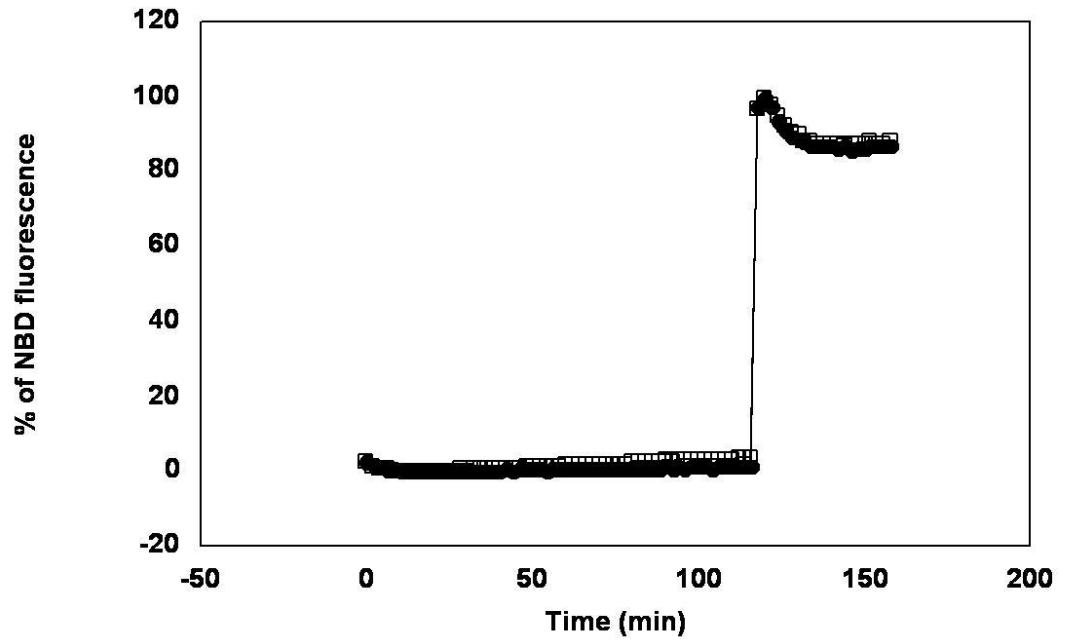
The findings presented in this thesis provided new insights into the mechanism by which SM functions in muscle and adipose tissue. However, which other factors might influence and regulate the fusion facilitated by Sx 4/SNAP23 and VAMP2 needs further investigation.

Appendix

Supplementary figures for chapter 4:

A**B**

C



D

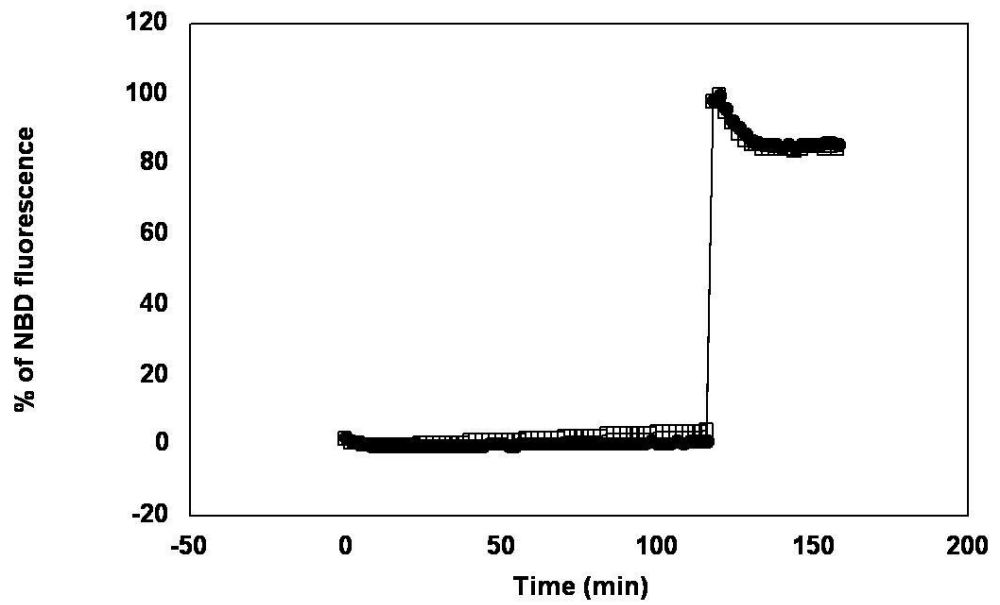
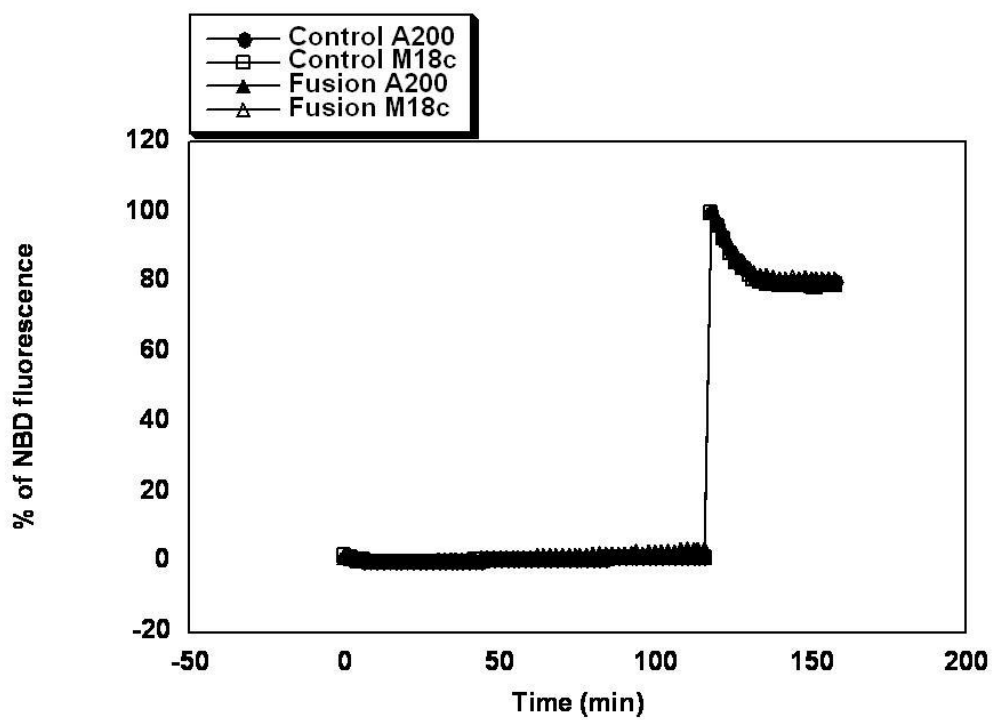


Figure I (chapter 4, figure 4.12) Raw fluorescence data from *in vitro* fusion assays of liposomes containing either full-length Sx 4/SNAP23 (A) or Sx 4 N Δ 36/SNAP23 (B) or Sx 4 OPEN/SNAP23 (C) or Sx 4 OPEN N Δ 36/SNAP23 (D) with liposomes containing VAMP2

These are supplement figures related to figure 4.12 (chapter 4). A graphing and analysis programme called KaleidaGraph (Synergy Software) was used in order to analyse the data obtained from the Fluorescence reader after fusion assays where 5 μ l of fluorescently labelled donor VAMP2 liposomes were mixed with 45 μ l of unlabelled acceptor t-complexes being either wild-type (A) or Sx 4 N Δ 36/SNAP23 (B) or Sx 4 OPEN/SNAP23 (C) or Sx 4 OPEN N Δ 36/SNAP23 (D). Raw fluorescence was normalised to maximum detergent signal (100 %) and plotted against time in minutes (graphs A, B, C and D).

A



B

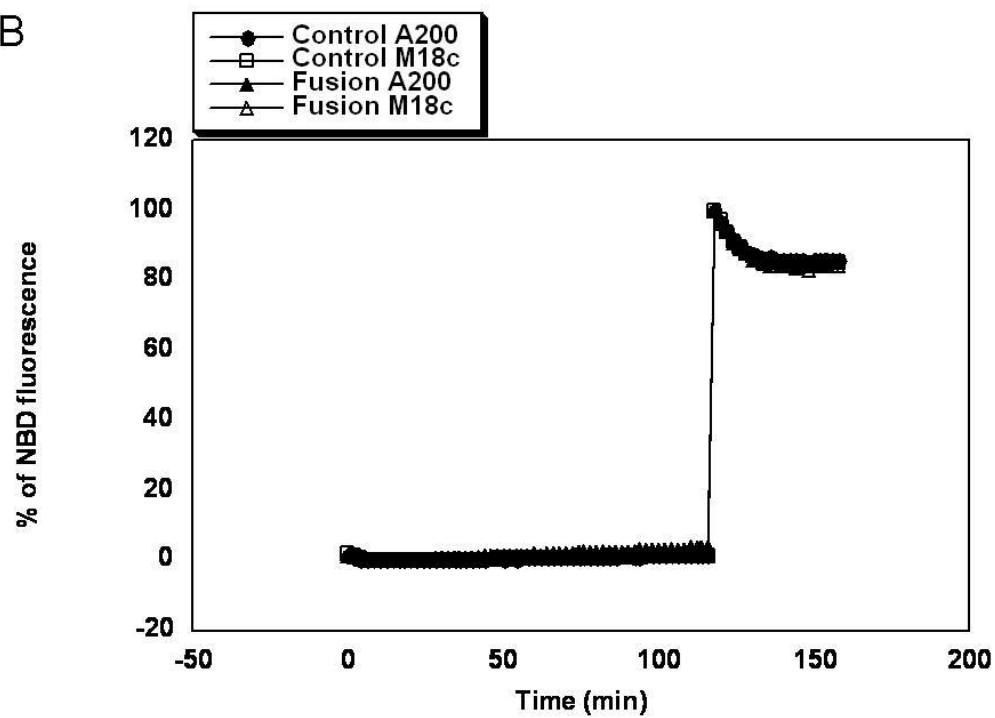
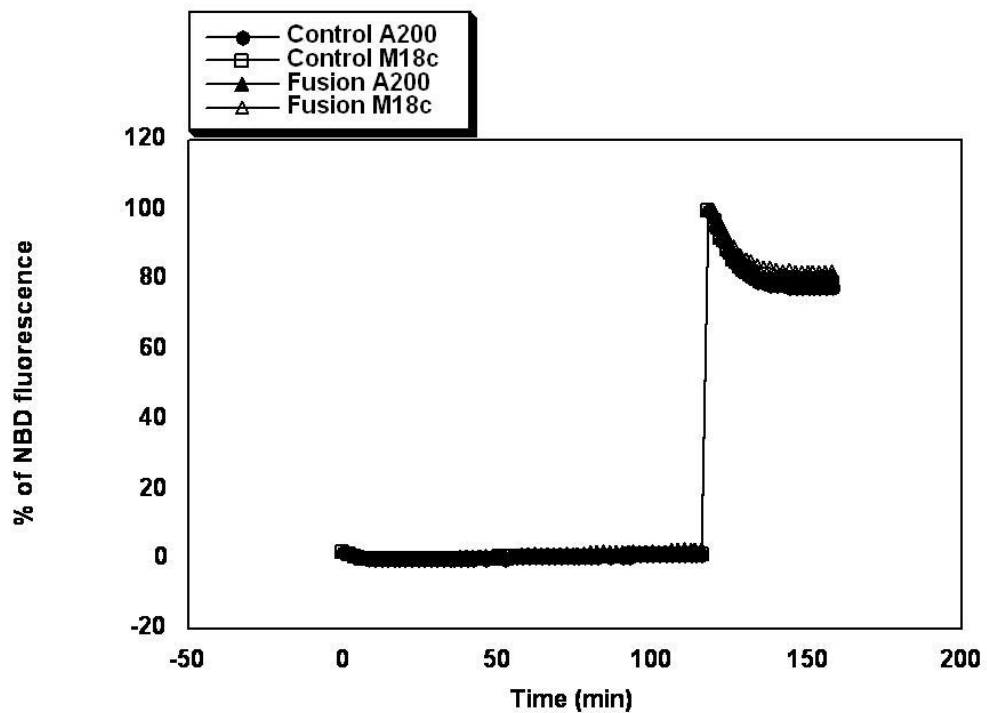


Figure II (chapter 4, figure 4.16) Raw fluorescence data from *in vitro* fusion of wild-type Sx 4/SNAP23 with VAMP2 vesicles (pre-docked and not docked) in the presence and in the absence of His₆-M18c

This fusion assay was described as outlined in figure 4.16. Raw data is shown normalised to 100 % detergent signal for A and B. **(A)** The liposomes were pre-incubated overnight with M18c. **(B)** The liposomes were NOT pre-incubated overnight with M18c, instead they were pre-docked overnight and incubated with M18c for 2 h before fusion at 37 °C.

A



B

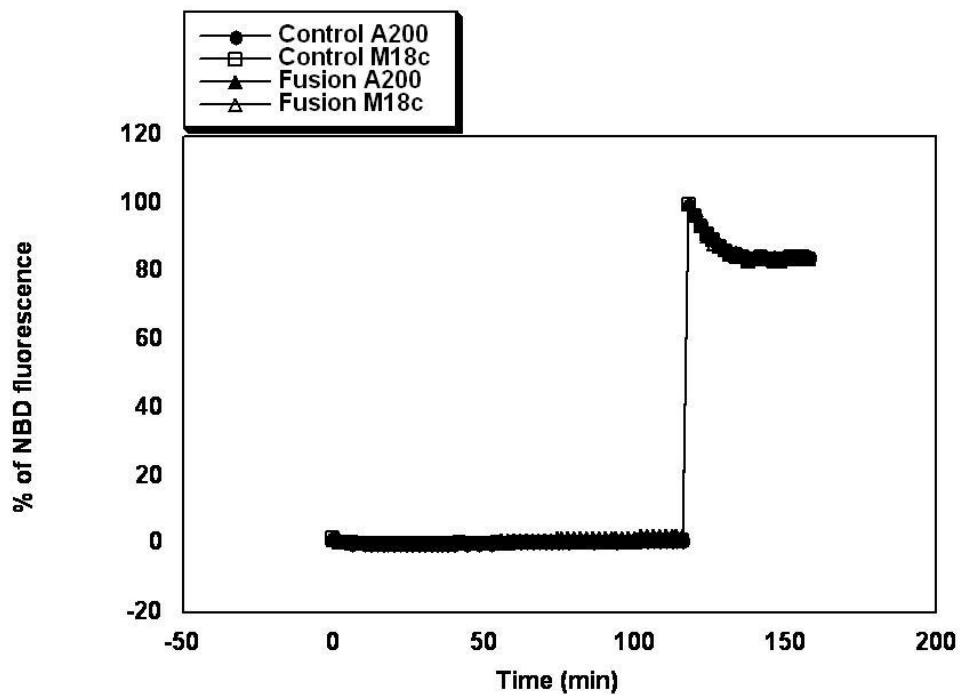
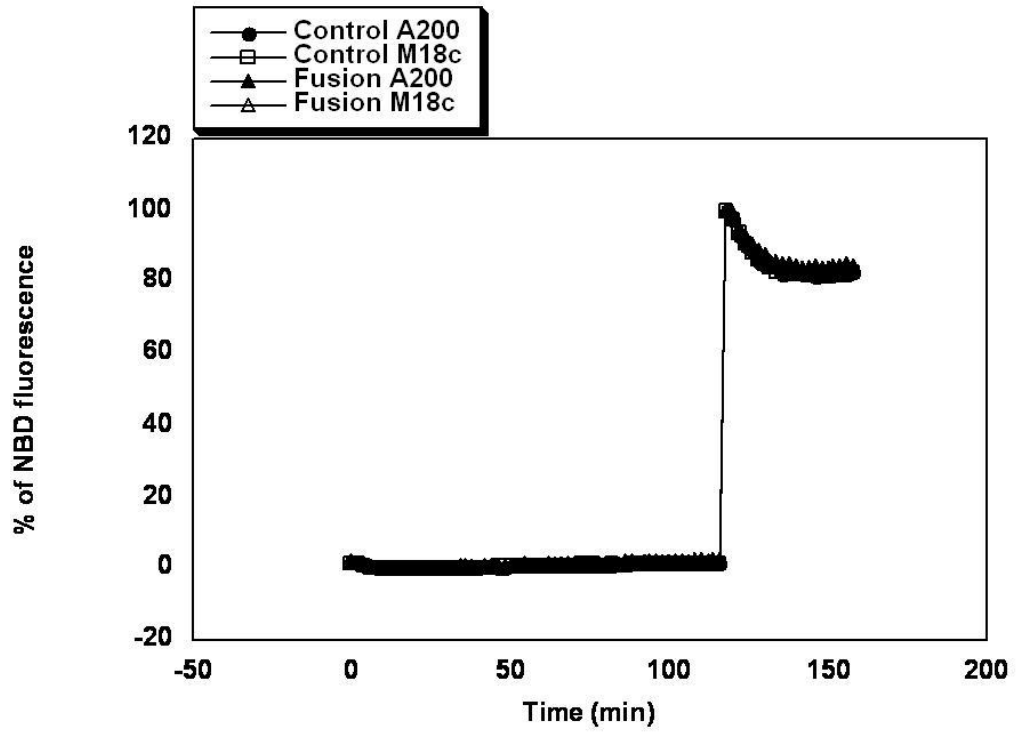


Figure III (chapter 4, figure 4.17) Raw fluorescence data from *in vitro* fusion of Sx 4 N Δ 36/SNAP23 with VAMP2 vesicles (pre-docked overnight or not) in the presence and in the absence of His₆-M18c

This fusion assay was described as outlined in figure 4.17. Raw data is shown normalised to 100 % detergent signal for A and B. **(A)** The liposomes were pre-incubated overnight with M18c. **(B)** The liposomes were NOT pre-incubated overnight with M18c, instead they were pre-docked overnight and incubated with M18c for 2 h before fusion took place.

A



B

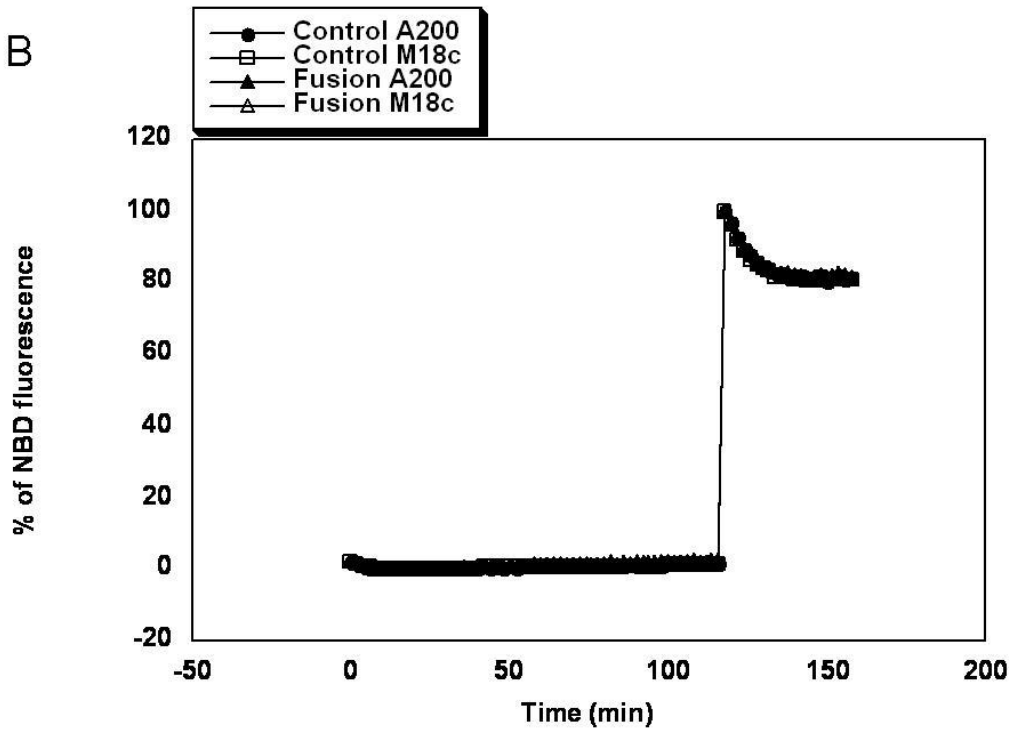
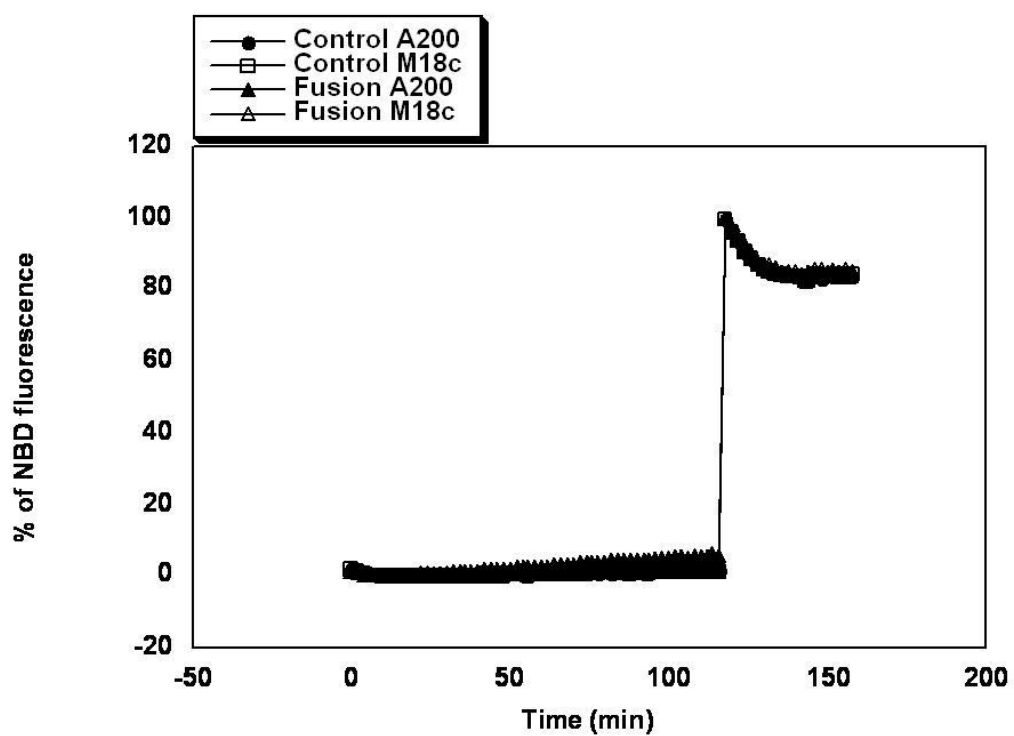


Figure IV (chapter 4, figure 4.18) Raw fluorescence data from *in vitro* fusion of Sx 4 N Δ 36/SNAP23 liposomes with VAMP2 liposomes (pre-docked or not) in the presence or in the absence of His₆-M18c for only 2 h

This fusion assay was described as outlined in figure 4.18. Raw data is shown normalised to 100 % detergent signal for A and B. **(A)** v- and t-liposomes were pre-incubated for 2 h with M18c. **(B)** v- and t-liposomes were allowed to pre-dock before incubation with M18c for 2 h.

A



B

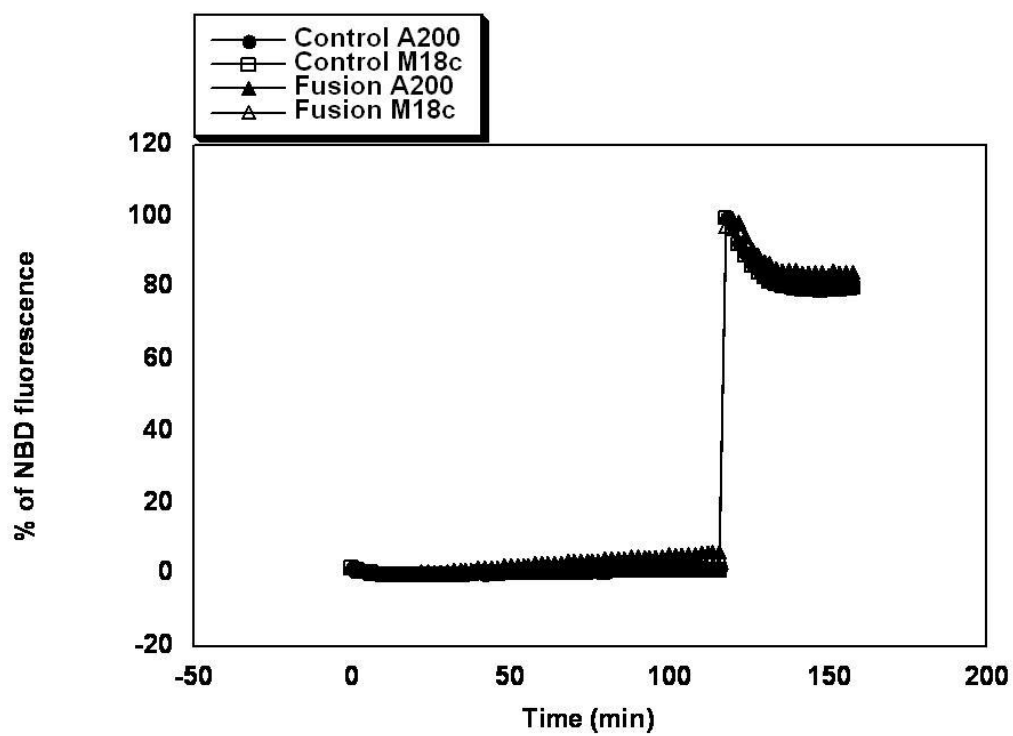
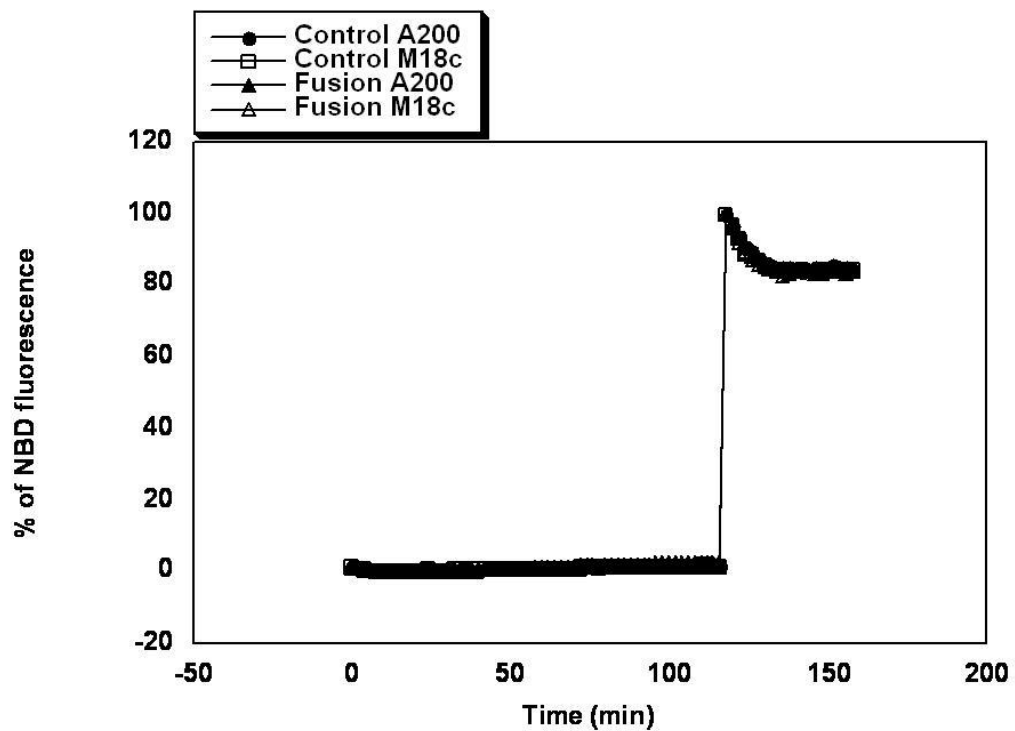


Figure V (chapter 4, figure 4.19) Raw fluorescence data from *in vitro* fusion of Sx 4 OPEN/SNAP23 with VAMP2 vesicles (pre-docked overnight and not docked) in the presence and in the absence of M18c

This fusion assay was described as outlined in figure 4.19. Raw data is shown normalised to 100 % detergent signal for A and B. **(A)** v- and t-liposomes were pre-incubated overnight with M18c. **(B)** v- and t-liposomes were NOT pre-incubated overnight with M18c, instead they were pre-docked overnight and incubated with M18c for 2 h before fusion took place.

A



B

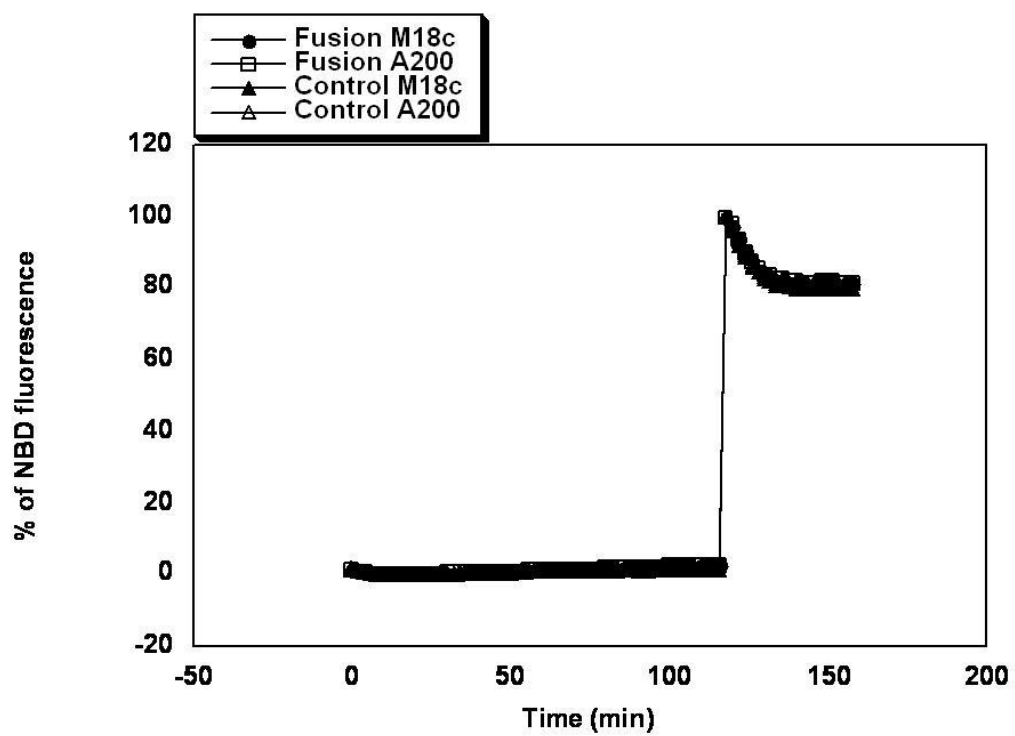
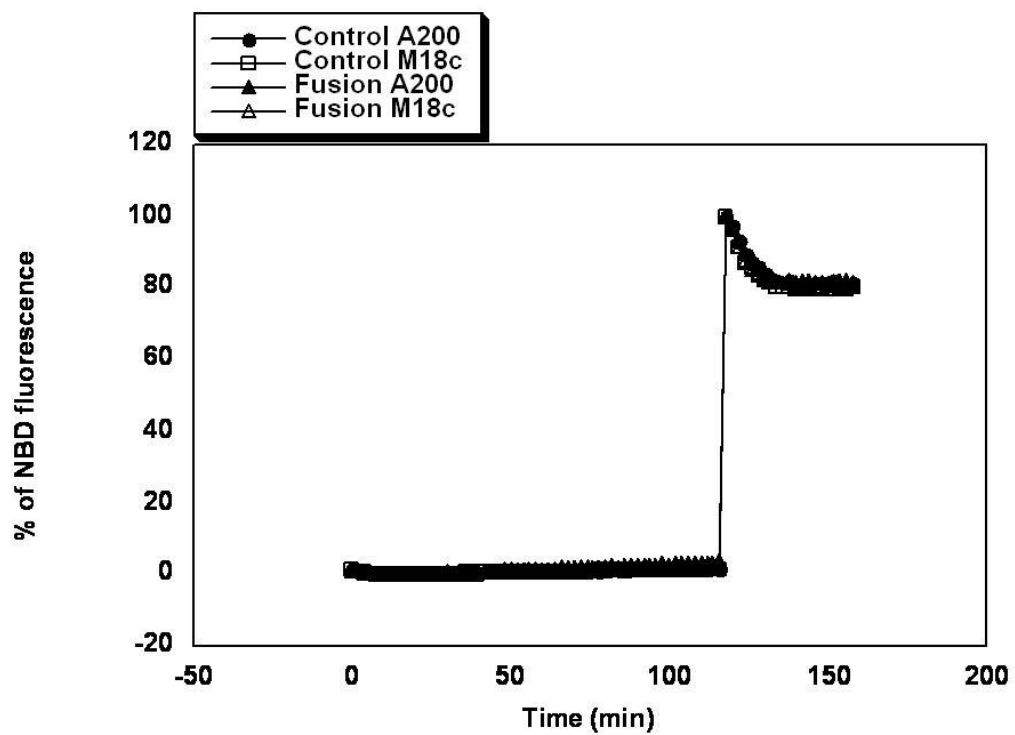


Figure VI (chapter 4, figure 4.20) Raw fluorescence data *in vitro* fusion of Sx 4 OPEN N Δ 36/SNAP23 with VAMP2 vesicles (pre-docked overnight and not docked) in the presence and in the absence of M18c

This fusion assay was described as outlined in figure 4.16. Raw data is shown normalised to 100 % detergent signal for A and B. **(A)** v- and t- liposomes were pre-incubated overnight with M18c. **(B)** v- and t- liposomes were NOT pre-incubated overnight with M18c, instead they were pre-docked overnight and incubated with M18c for 2 h before fusion.

A



B

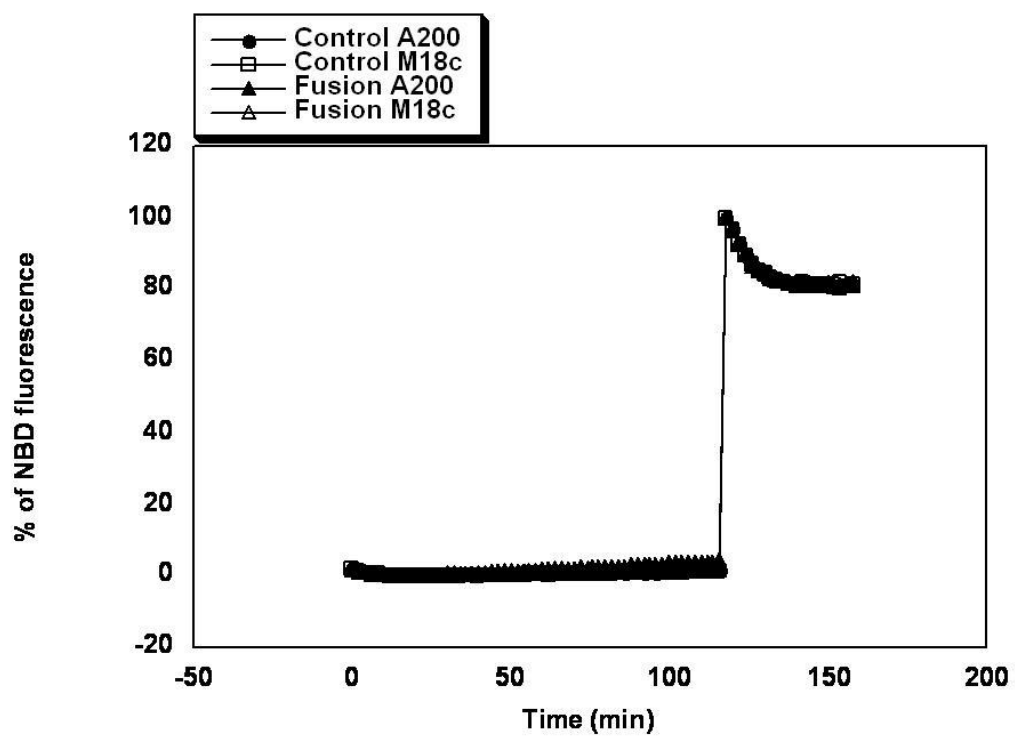


Figure VII (chapter 4, figure 4.21) Raw fluorescent data from *in vitro* fusion of Sx 4 OPEN N Δ 36/SNAP23 with VAMP2 vesicles (pre-docked overnight or not) in the presence and in the absence of M18c for 2 h

This fusion assay was described as outlined in figure 4.21. Raw data is shown normalised to 100 % detergent signal for A and B. (A) The liposomes were pre-incubated for 2 h with M18c. (B) The liposomes were allowed to pre-doc before incubation with M18c for 2 h.

Supplementary figures for chapter 5:

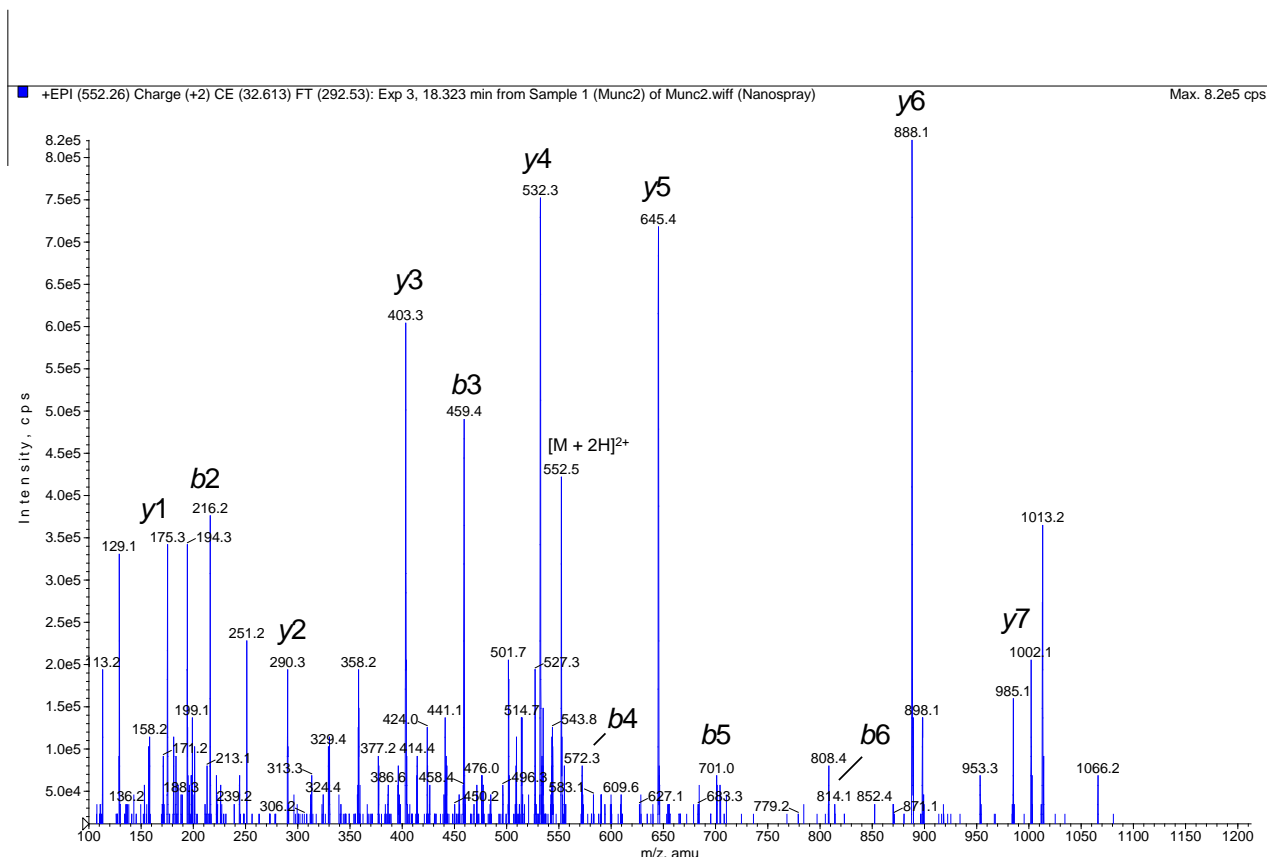


Figure VIII Positive-ion ESI-MS/MS of Peptide 1 (residues Thr 519- Arg 526)

Several fragment (*b* and *y*) ions were observed as indicated. The *b*₃ and *y*₆ fragment ions indicate that Y521 is phosphorylated. The sequence of phosphorylated peptide 1 is shown in figure X.

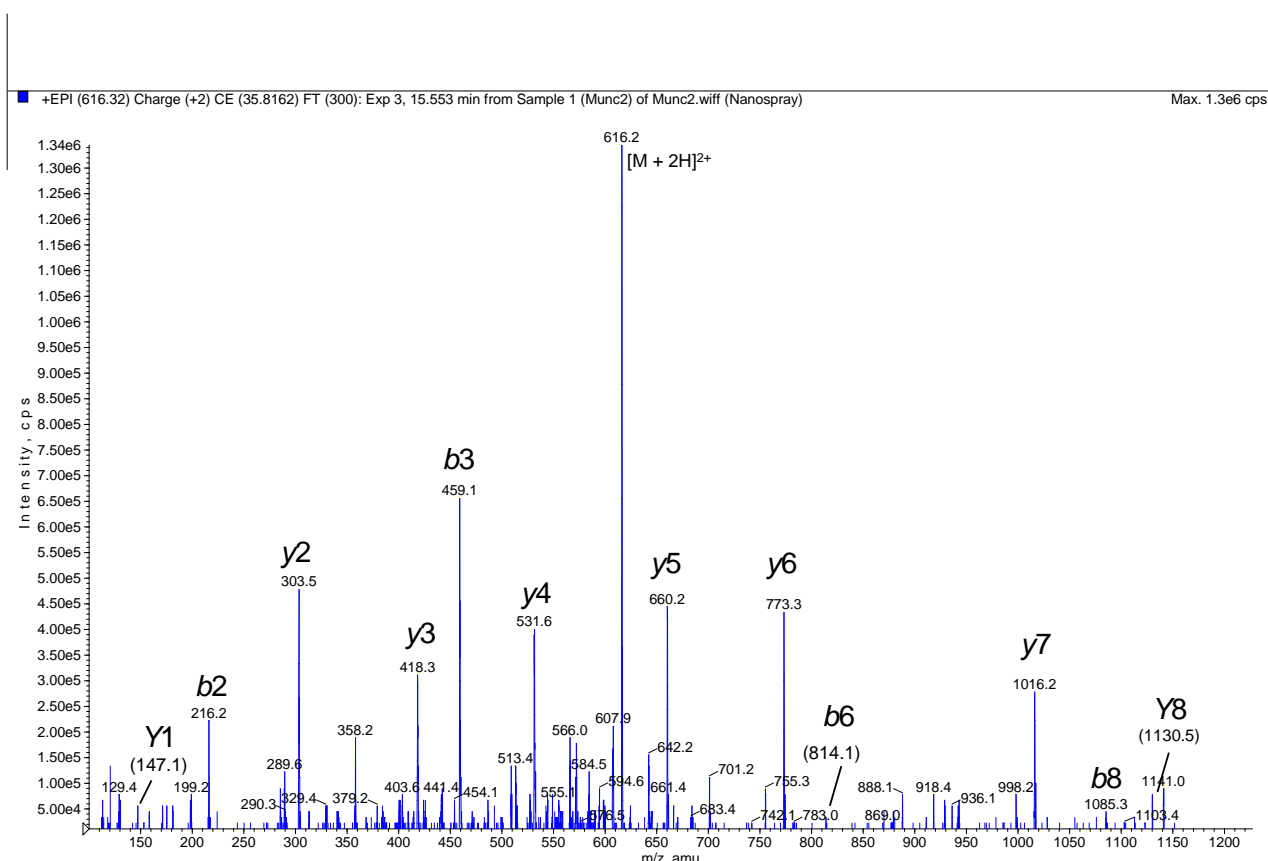


Figure IX Positive-ion ESI-MS/MS spectrum of the phosphorylated peptide 2 (residues Thr 519-Lys 527) of M18c

Several fragment (*b* and *y*) ions were observed as indicated. The *b*₃ and *y*₇ fragment ions indicate that Y521 is phosphorylated. The sequence of phosphorylated peptide 2 is shown in figure X.

Peptide 1:

<i>b</i> -ions		1	2	3	4	5	6	7	8
NH-	T	N	Y_p	L	E	L	D	R	-OH
<i>y</i> -ions	8	7	6	5	4	3	2	1	

Peptide 2:

<i>b</i> -ions		1	2	3	4	5	6	7	8	9
NH-	T	N	Y_p	L	E	L	D	R	K	-OH
<i>y</i> -ions	9	8	7	6	5	4	3	2	1	

Figure X Sequences of the phosphorylated tryptic peptides 1 and 2 from M18c

A

<i>y</i>-ions (<i>m/z</i>)^a		<i>b</i>-ions (<i>m/z</i>)^a	
Theoretical^a	Experimental	Theoretical	Experimental
175.1 (<i>y</i> 1)	175.3	120.1 (<i>b</i> 1)	ND ^b
290.2 (<i>y</i> 2)	290.3	216.1 (<i>b</i> 2)	216.2
403.2 (<i>y</i> 3)	403.3	459.1 (<i>b</i> 3)	459.4
532.3 (<i>y</i> 4)	532.3	572.2 (<i>b</i> 4)	572.3
645.4 (<i>y</i> 5)	645.4	701.3 (<i>b</i> 5)	701.0
888.4 (<i>y</i> 6)	888.1	814.4 (<i>b</i> 6)	814.1
1002.4 (<i>y</i> 7)	1002.1	929.4 (<i>b</i> 7)	ND

^a[M-H]⁻ quase molecular ions.^bNot detected

B

<i>y</i>-ions (<i>m/z</i>)^a		<i>b</i>-ions (<i>m/z</i>)^a	
Theoretical^a	Experimental	Theoretical	Experimental
147.1 (<i>y</i> 1)	147.1	120.1 (<i>b</i> 1)	ND ^b
303.2 (<i>y</i> 2)	303.5	216.1 (<i>b</i> 2)	216.2
418.2 (<i>y</i> 3)	418.3	459.1 (<i>b</i> 3)	459.1
531.3 (<i>y</i> 4)	531.6	572.2 (<i>b</i> 4)	572.3
660.4 (<i>y</i> 5)	660.2	701.3 (<i>b</i> 5)	701.0
773.5 (<i>y</i> 6)	773.3	814.4 (<i>b</i> 6)	814.1
1016.5 (<i>y</i> 7)	1016.2	929.4 (<i>b</i> 7)	ND
1130.5 (<i>y</i> 8)	1130.5	1085.5 (<i>b</i> 8)	1085.3

^a[M-H]⁻ quase molecular ions.^bNot detected

Table I Summary of the peptides identified after fragmentation of peptide 1 9A) (*m/z* 551.3) and peptide 2 (B) (*m/z* 615.3).

References

- Advani, R.J., Yang, B., Prekeris, R., Lee, K.C., Klumperman, J. and Scheller, R.H. (1999) VAMP-7 mediates vesicular transport from endosomes to lysosomes. *J Cell Biol*, **146**, 765-776.
- Aledo, J.C., Lavoie, L., Volchuk, A., Keller, S.R., Klip, A. and Hundal, H.S. (1997) Identification and characterization of two distinct intracellular GLUT4 pools in rat skeletal muscle: evidence for an endosomal and an insulin-sensitive GLUT4 compartment. *Biochem J*, **325 (Pt 3)**, 727-732.
- Alessi, D.R., James, S.R., Downes, C.P., Holmes, A.B., Gaffney, P.R., Reese, C.B. and Cohen, P. (1997) Characterization of a 3-phosphoinositide-dependent protein kinase which phosphorylates and activates protein kinase B α . *Curr Biol*, **7**, 261-269.
- Antonin, W., Fasshauer, D., Becker, S., Jahn, R. and Schneider, T.R. (2002) Crystal structure of the endosomal SNARE complex reveals common structural principles of all SNAREs. *Nat Struct Biol*, **9**, 107-111.
- Araki, S., Tamori, Y., Kawanishi, M., Shinoda, H., Masugi, J., Mori, H., Niki, T., Okazawa, H., Kubota, T. and Kasuga, M. (1997) Inhibition of the binding of SNAP-23 to syntaxin 4 by Munc18c. *Biochem Biophys Res Commun*, **234**, 257-262.
- Aran, V., Brandie, F.M., Boyd, A.R., Kantidakis, T., Rideout, E.J., Kelly, S.M., Gould, G.W. and Bryant, N. (2009) Characterisation of two distinct binding modes between Syntaxin 4 and Munc18c. *Biochem J*.
- Baba, T., Sakisaka, T., Mochida, S. and Takai, Y. (2005) PKA-catalyzed phosphorylation of tomosyn and its implication in Ca²⁺-dependent exocytosis of neurotransmitter. *J Cell Biol*, **170**, 1113-1125.
- Banerji, M.A. (2002) Impaired beta-cell and alpha-cell function in African-American children with type 2 diabetes mellitus--"Flatbush diabetes". *J Pediatr Endocrinol Metab*, **15 Suppl 1**, 493-501.
- Baumann, C.A., Ribon, V., Kanzaki, M., Thurmond, D.C., Mora, S., Shigematsu, S., Bickel, P.E., Pessin, J.E. and Saltiel, A.R. (2000) CAP defines a second signalling pathway required for insulin-stimulated glucose transport. *Nature*, **407**, 202-207.
- Beckers, C.J., Block, M.R., Glick, B.S., Rothman, J.E. and Balch, W.E. (1989) Vesicular transport between the endoplasmic reticulum and the Golgi stack requires the NEM-sensitive fusion protein. *Nature*, **339**, 397-398.
- Bell, G.I., Murray, J.C., Nakamura, Y., Kayano, T., Eddy, R.L., Fan, Y.S., Byers, M.G. and Shows, T.B. (1989) Polymorphic human insulin-responsive glucose-transporter gene on chromosome 17p13. *Diabetes*, **38**, 1072-1075.
- Bennett, M.K., Calakos, N. and Scheller, R.H. (1992) Syntaxin: a synaptic protein implicated in docking of synaptic vesicles at presynaptic active zones. *Science*, **257**, 255-259.
- Bennett, M.K., Garcia-Ararras, J.E., Elferink, L.A., Peterson, K., Fleming, A.M., Hazuka, C.D. and Scheller, R.H. (1993) The syntaxin family of vesicular transport receptors. *Cell*, **74**, 863-873.
- Birnbaum, M.J. (1989) Identification of a novel gene encoding an insulin-responsive glucose transporter protein. *Cell*, **57**, 305-315.
- Bock, J.B., Lin, R.C. and Scheller, R.H. (1996) A new syntaxin family member implicated in targeting of intracellular transport vesicles. *J Biol Chem*, **271**, 17961-17965.
- Bock, J.B., Matern, H.T., Peden, A.A. and Scheller, R.H. (2001) A genomic perspective on membrane compartment organization. *Nature*, **409**, 839-841.
- Bracher, A. and Weissenhorn, W. (2002) Structural basis for the Golgi membrane recruitment of Sly1p by Sed5p. *Embo J*, **21**, 6114-6124.

- Brandie, F.M., Aran, V., Verma, A., McNew, J.A., Bryant, N.J. and Gould, G.W. (2008) Negative regulation of syntaxin4/SNAP-23/VAMP2-mediated membrane fusion by Munc18c *in vitro*. *PLoS ONE*, **3**, e4074.
- Brenner, S. (1974) The genetics of *Caenorhabditis elegans*. *Genetics*, **77**, 71-94.
- Bryant, N.J., Govers, R. and James, D.E. (2002) Regulated transport of the glucose transporter GLUT4. *Nat Rev Mol Cell Biol*, **3**, 267-277.
- Bryant, N.J. and James, D.E. (2003) The Sec1p/Munc18 (SM) protein, Vps45p, cycles on and off membranes during vesicle transport. *J Cell Biol*, **161**, 691-696.
- Burkhardt, P., Hattendorf, D.A., Weis, W.I. and Fasshauer, D. (2008) Munc18a controls SNARE assembly through its interaction with the syntaxin N-peptide. *Embo J*, **27**, 923-933.
- Cabaniols, J.P., Ravichandran, V. and Roche, P.A. (1999) Phosphorylation of SNAP-23 by the novel kinase SNAK regulates t-SNARE complex assembly. *Mol Biol Cell*, **10**, 4033-4041.
- Cain, C.C., Trimble, W.S. and Lienhard, G.E. (1992) Members of the VAMP family of synaptic vesicle proteins are components of glucose transporter-containing vesicles from rat adipocytes. *J Biol Chem*, **267**, 11681-11684.
- Carpp, L.N., Ciuffo, L.F., Shanks, S.G., Boyd, A. and Bryant, N.J. (2006) The Sec1p/Munc18 protein Vps45p binds its cognate SNARE proteins via two distinct modes. *J Cell Biol*, **173**, 927-936.
- Charron, M.J., Brosius, F.C., 3rd, Alper, S.L. and Lodish, H.F. (1989) A glucose transport protein expressed predominately in insulin-responsive tissues. *Proc Natl Acad Sci U S A*, **86**, 2535-2539.
- Cheatham, B., Vlahos, C.J., Cheatham, L., Wang, L., Blenis, J. and Kahn, C.R. (1994) Phosphatidylinositol 3-kinase activation is required for insulin stimulation of pp70 S6 kinase, DNA synthesis, and glucose transporter translocation. *Mol Cell Biol*, **14**, 4902-4911.
- Cheatham, B., Volchuk, A., Kahn, C.R., Wang, L., Rhodes, C.J. and Klip, A. (1996) Insulin-stimulated translocation of GLUT4 glucose transporters requires SNARE-complex proteins. *Proc Natl Acad Sci U S A*, **93**, 15169-15173.
- Chen, Y.A. and Scheller, R.H. (2001) SNARE-mediated membrane fusion. *Nat Rev Mol Cell Biol*, **2**, 98-106.
- Chernomordik, L.V. and Kozlov, M.M. (2005) Membrane hemifusion: crossing a chasm in two leaps. *Cell*, **123**, 375-382.
- Cheviet, S., Bezzi, P., Ivarsson, R., Renstrom, E., Viertl, D., Kasas, S., Catsicas, S. and Regazzi, R. (2006) Tomosyn-1 is involved in a post-docking event required for pancreatic beta-cell exocytosis. *J Cell Sci*, **119**, 2912-2920.
- Chiang, S.H., Baumann, C.A., Kanzaki, M., Thurmond, D.C., Watson, R.T., Neudauer, C.L., Macara, I.G., Pessin, J.E. and Saltiel, A.R. (2001) Insulin-stimulated GLUT4 translocation requires the CAP-dependent activation of TC10. *Nature*, **410**, 944-948.
- Clary, D.O., Griff, I.C. and Rothman, J.E. (1990) SNAPs, a family of NSF attachment proteins involved in intracellular membrane fusion in animals and yeast. *Cell*, **61**, 709-721.
- Cowles, C.R., Emr, S.D. and Horazdovsky, B.F. (1994) Mutations in the VPS45 gene, a SEC1 homologue, result in vacuolar protein sorting defects and accumulation of membrane vesicles. *J Cell Sci*, **107 (Pt 12)**, 3449-3459.
- Cushman, S.W. and Wardzala, L.J. (1980) Potential mechanism of insulin action on glucose transport in the isolated rat adipose cell. Apparent translocation of intracellular transport systems to the plasma membrane. *J Biol Chem*, **255**, 4758-4762.

- D'Andrea-Merrins, M., Chang, L., Lam, A.D., Ernst, S.A. and Stuenkel, E.L. (2007) Munc18c interaction with syntaxin 4 monomers and SNARE complex intermediates in GLUT4 vesicle trafficking. *J Biol Chem*, **282**, 16553-16566.
- Diaz, R., Mayorga, L.S., Weidman, P.J., Rothman, J.E. and Stahl, P.D. (1989) Vesicle fusion following receptor-mediated endocytosis requires a protein active in Golgi transport. *Nature*, **339**, 398-400.
- Dirac-Svejstrup, A.B., Sumizawa, T. and Pfeffer, S.R. (1997) Identification of a GDI displacement factor that releases endosomal Rab GTPases from Rab-GDI. *Embo J*, **16**, 465-472.
- Dulubova, I., Khvotchev, M., Liu, S., Huryeva, I., Sudhof, T.C. and Rizo, J. (2007) Munc18-1 binds directly to the neuronal SNARE complex. *Proc Natl Acad Sci U S A*, **104**, 2697-2702.
- Dulubova, I., Sugita, S., Hill, S., Hosaka, M., Fernandez, I., Sudhof, T.C. and Rizo, J. (1999) A conformational switch in syntaxin during exocytosis: role of munc18. *Embo J*, **18**, 4372-4382.
- Dulubova, I., Yamaguchi, T., Arac, D., Li, H., Huryeva, I., Min, S.W., Rizo, J. and Sudhof, T.C. (2003) Convergence and divergence in the mechanism of SNARE binding by Sec1/Munc18-like proteins. *Proc Natl Acad Sci U S A*, **100**, 32-37.
- Dulubova, I., Yamaguchi, T., Gao, Y., Min, S.W., Huryeva, I., Sudhof, T.C. and Rizo, J. (2002) How Tlg2p/syntaxin 16 'snares' Vps45. *Embo J*, **21**, 3620-3631.
- Dybbs, M., Ngai, J. and Kaplan, J.M. (2005) Using microarrays to facilitate positional cloning: identification of tomosyn as an inhibitor of neurosecretion. *PLoS Genet*, **1**, 6-16.
- Ewart, M.A., Clarke, M., Kane, S., Chamberlain, L.H. and Gould, G.W. (2005) Evidence for a role of the exocyst in insulin-stimulated Glut4 trafficking in 3T3-L1 adipocytes. *J Biol Chem*, **280**, 3812-3816.
- Fasshauer, D., Otto, H., Eliason, W.K., Jahn, R. and Brunger, A.T. (1997) Structural changes are associated with soluble N-ethylmaleimide-sensitive fusion protein attachment protein receptor complex formation. *J Biol Chem*, **272**, 28036-28041.
- Fasshauer, D., Sutton, R.B., Brunger, A.T. and Jahn, R. (1998) Conserved structural features of the synaptic fusion complex: SNARE proteins reclassified as Q- and R-SNAREs. *Proc Natl Acad Sci U S A*, **95**, 15781-15786.
- Fernandez, I., Ubach, J., Dulubova, I., Zhang, X., Sudhof, T.C. and Rizo, J. (1998) Three-dimensional structure of an evolutionarily conserved N-terminal domain of syntaxin 1A. *Cell*, **94**, 841-849.
- Fiebig, K.M., Rice, L.M., Pollock, E. and Brunger, A.T. (1999) Folding intermediates of SNARE complex assembly. *Nat Struct Biol*, **6**, 117-123.
- Fix, M., Melia, T.J., Jaiswal, J.K., Rappoport, J.Z., You, D., Sollner, T.H., Rothman, J.E. and Simon, S.M. (2004) Imaging single membrane fusion events mediated by SNARE proteins. *Proc Natl Acad Sci U S A*, **101**, 7311-7316.
- Foster, L.J., Yeung, B., Mohtashami, M., Ross, K., Trimble, W.S. and Klip, A. (1998) Binary interactions of the SNARE proteins syntaxin-4, SNAP23, and VAMP-2 and their regulation by phosphorylation. *Biochemistry*, **37**, 11089-11096.
- Fujita, Y., Sasaki, T., Fukui, K., Kotani, H., Kimura, T., Hata, Y., Sudhof, T.C., Scheller, R.H. and Takai, Y. (1996) Phosphorylation of Munc-18/n-Sec1/rbSec1 by protein kinase C: its implication in regulating the interaction of Munc-18/n-Sec1/rbSec1 with syntaxin. *J Biol Chem*, **271**, 7265-7268.
- Fujita, Y., Shirataki, H., Sakisaka, T., Asakura, T., Ohya, T., Kotani, H., Yokoyama, S., Nishioka, H., Matsuura, Y., Mizoguchi, A., Scheller, R.H. and Takai, Y. (1998) Tomosyn: a syntaxin-1-binding protein that forms a novel complex in the neurotransmitter release process. *Neuron*, **20**, 905-915.
- Fukuda, M. (2008) Membrane traffic in the secretory pathway: Regulation of secretory vesicle traffic by Rab small GTPases. *Cell Mol Life Sci*, **65**, 2801-2813.

- Gagescu, R. (2000) SNARE hypothesis 2000. *Nat Rev Mol Cell Biol*, **1**, 5.
- Gerber, S.H., Rah, J.C., Min, S.W., Liu, X., de Wit, H., Dulubova, I., Meyer, A.C., Rizo, J., Arancillo, M., Hammer, R.E., Verhage, M., Rosenmund, C. and Sudhof, T.C. (2008) Conformational switch of syntaxin-1 controls synaptic vesicle fusion. *Science*, **321**, 1507-1510.
- Glick, B.S. and Rothman, J.E. (1987) Possible role for fatty acyl-coenzyme A in intracellular protein transport. *Nature*, **326**, 309-312.
- Gould, G.W., Brant, A.M., Kahn, B.B., Shepherd, P.R., McCoid, S.C. and Gibbs, E.M. (1992) Expression of the brain-type glucose transporter is restricted to brain and neuronal cells in mice. *Diabetologia*, **35**, 304-309.
- Grusovin, J., Stoichevska, V., Gough, K.H., Nunan, K., Ward, C.W. and Macaulay, S.L. (2000) Definition of a minimal munc18c domain that interacts with syntaxin 4. *Biochem J*, **350 Pt 3**, 741-746.
- Gual, P., Le Marchand-Brustel, Y. and Tanti, J.F. (2005) Positive and negative regulation of insulin signaling through IRS-1 phosphorylation. *Biochimie*, **87**, 99-109.
- Harrison, S.D., Broadie, K., van de Goor, J. and Rubin, G.M. (1994) Mutations in the *Drosophila* Rop gene suggest a function in general secretion and synaptic transmission. *Neuron*, **13**, 555-566.
- Hashiramoto, M. and James, D.E. (2000) Characterization of insulin-responsive GLUT4 storage vesicles isolated from 3T3-L1 adipocytes. *Mol Cell Biol*, **20**, 416-427.
- Hata, Y., Slaughter, C.A. and Sudhof, T.C. (1993) Synaptic vesicle fusion complex contains unc-18 homologue bound to syntaxin. *Nature*, **366**, 347-351.
- Hayashi, T., McMahon, H., Yamasaki, S., Binz, T., Hata, Y., Sudhof, T.C. and Niemann, H. (1994) Synaptic vesicle membrane fusion complex: action of clostridial neurotoxins on assembly. *Embo J*, **13**, 5051-5061.
- Hayashi, T., Yamasaki, S., Nauenburg, S., Binz, T. and Niemann, H. (1995) Disassembly of the reconstituted synaptic vesicle membrane fusion complex *in vitro*. *Embo J*, **14**, 2317-2325.
- Hirshman, M.F., Goodyear, L.J., Wardzala, L.J., Horton, E.D. and Horton, E.S. (1990) Identification of an intracellular pool of glucose transporters from basal and insulin-stimulated rat skeletal muscle. *J Biol Chem*, **265**, 987-991.
- Hohl, T.M., Parlati, F., Wimmer, C., Rothman, J.E., Sollner, T.H. and Engelhardt, H. (1998) Arrangement of subunits in 20 S particles consisting of NSF, SNAPs, and SNARE complexes. *Mol Cell*, **2**, 539-548.
- Holt, M., Varoqueaux, F., Wiederhold, K., Takamori, S., Urlaub, H., Fasshauer, D. and Jahn, R. (2006) Identification of SNAP-47, a novel Qbc-SNARE with ubiquitous expression. *J Biol Chem*, **281**, 17076-17083.
- Hong, W. (2005) SNAREs and traffic. *Biochim Biophys Acta*, **1744**, 493-517.
- Hu, S.H., Gee, C.L., Latham, C.F., Rowlinson, S.W., Rova, U., Jones, A., Halliday, J.A., Bryant, N.J., James, D.E. and Martin, J.L. (2003) Recombinant expression of Munc18c in a baculovirus system and interaction with syntaxin4. *Protein Expr Purif*, **31**, 305-310.
- Hu, S.H., Latham, C.F., Gee, C.L., James, D.E. and Martin, J.L. (2007) Structure of the Munc18c/Syntaxin4 N-peptide complex defines universal features of the N-peptide binding mode of Sec1/Munc18 proteins. *Proc Natl Acad Sci U S A*, **104**, 8773-8778.
- Hua, Y. and Scheller, R.H. (2001) Three SNARE complexes cooperate to mediate membrane fusion. *Proc Natl Acad Sci U S A*, **98**, 8065-8070.
- Inoue, M., Chang, L., Hwang, J., Chiang, S.H. and Saltiel, A.R. (2003) The exocyst complex is required for targeting of Glut4 to the plasma membrane by insulin. *Nature*, **422**, 629-633.

- Ishikura, S., Bilan, P.J. and Klip, A. (2007) Rabs 8A and 14 are targets of the insulin-regulated Rab-GAP AS160 regulating GLUT4 traffic in muscle cells. *Biochem Biophys Res Commun*, **353**, 1074-1079.
- James, D.E., Brown, R., Navarro, J. and Pilch, P.F. (1988) Insulin-regulatable tissues express a unique insulin-sensitive glucose transport protein. *Nature*, **333**, 183-185.
- James, D.E., Strube, M. and Mueckler, M. (1989) Molecular cloning and characterization of an insulin-regulatable glucose transporter. *Nature*, **338**, 83-87.
- Jewell, J.L., Oh, E., Bennett, S.M., Meroueh, S.O. and Thurmond, D.C. (2008) The tyrosine phosphorylation of Munc18c induces a switch in binding specificity from Syntaxin 4 to Doc2beta. *J Biol Chem*.
- Joost, H.G. and Thorens, B. (2001) The extended GLUT-family of sugar/polyol transport facilitators: nomenclature, sequence characteristics, and potential function of its novel members (review). *Mol Membr Biol*, **18**, 247-256.
- Kaestner, K.H., Christy, R.J., McLenithan, J.C., Braiterman, L.T., Cornelius, P., Pekala, P.H. and Lane, M.D. (1989) Sequence, tissue distribution, and differential expression of mRNA for a putative insulin-responsive glucose transporter in mouse 3T3-L1 adipocytes. *Proc Natl Acad Sci U S A*, **86**, 3150-3154.
- Kahn, S.E., Hull, R.L. and Utzschneider, K.M. (2006) Mechanisms linking obesity to insulin resistance and type 2 diabetes. *Nature*, **444**, 840-846.
- Kanda, H., Tamori, Y., Shinoda, H., Yoshikawa, M., Sakaue, M., Udagawa, J., Otani, H., Tashiro, F., Miyazaki, J. and Kasuga, M. (2005) Adipocytes from Munc18c-null mice show increased sensitivity to insulin-stimulated GLUT4 externalization. *J Clin Invest*, **115**, 291-301.
- Kandror, K.V. and Pilch, P.F. (1996) Compartmentalization of protein traffic in insulin-sensitive cells. *Am J Physiol*, **271**, E1-14.
- Kane, S., Sano, H., Liu, S.C., Asara, J.M., Lane, W.S., Garner, C.C. and Lienhard, G.E. (2002) A method to identify serine kinase substrates. Akt phosphorylates a novel adipocyte protein with a Rab GTPase-activating protein (GAP) domain. *J Biol Chem*, **277**, 22115-22118.
- Katz, E.B., Stenbit, A.E., Hatton, K., DePinho, R. and Charron, M.J. (1995) Cardiac and adipose tissue abnormalities but not diabetes in mice deficient in GLUT4. *Nature*, **377**, 151-155.
- Kawanishi, M., Tamori, Y., Okazawa, H., Araki, S., Shinoda, H. and Kasuga, M. (2000) Role of SNAP23 in insulin-induced translocation of GLUT4 in 3T3-L1 adipocytes. Mediation of complex formation between syntaxin4 and VAMP2. *J Biol Chem*, **275**, 8240-8247.
- Kayano, T., Fukumoto, H., Eddy, R.L., Fan, Y.S., Byers, M.G., Shows, T.B. and Bell, G.I. (1988) Evidence for a family of human glucose transporter-like proteins. Sequence and gene localization of a protein expressed in fetal skeletal muscle and other tissues. *J Biol Chem*, **263**, 15245-15248.
- Ke, B., Oh, E. and Thurmond, D.C. (2007) Doc2beta is a novel Munc18c-interacting partner and positive effector of syntaxin 4-mediated exocytosis. *J Biol Chem*, **282**, 21786-21797.
- Kee, Y., Yoo, J.S., Hazuka, C.D., Peterson, K.E., Hsu, S.C. and Scheller, R.H. (1997) Subunit structure of the mammalian exocyst complex. *Proc Natl Acad Sci U S A*, **94**, 14438-14443.
- Kelly, S.M., Jess, T.J. and Price, N.C. (2005) How to study proteins by circular dichroism. *Biochim Biophys Acta*, **1751**, 119-139.
- Kelly, S.M. and Price, N.C. (2000) The use of circular dichroism in the investigation of protein structure and function. *Curr Protein Pept Sci*, **1**, 349-384.
- Khan, A.H., Thurmond, D.C., Yang, C., Ceresa, B.P., Sigmund, C.D. and Pessin, J.E. (2001) Munc18c regulates insulin-stimulated glut4 translocation to the transverse tubules in skeletal muscle. *J Biol Chem*, **276**, 4063-4069.

- Khvotchev, M., Dulubova, I., Sun, J., Dai, H., Rizo, J. and Sudhof, T.C. (2007) Dual modes of Munc18-1/SNARE interactions are coupled by functionally critical binding to syntaxin-1 N terminus. *J Neurosci*, **27**, 12147-12155.
- Klip, A., Ramlal, T., Bilan, P.J., Cartee, G.D., Gulve, E.A. and Holloszy, J.O. (1990) Recruitment of GLUT-4 glucose transporters by insulin in diabetic rat skeletal muscle. *Biochem Biophys Res Commun*, **172**, 728-736.
- Kohn, A.D., Barthel, A., Kovacina, K.S., Boge, A., Wallach, B., Summers, S.A., Birnbaum, M.J., Scott, P.H., Lawrence, J.C., Jr. and Roth, R.A. (1998) Construction and characterization of a conditionally active version of the serine/threonine kinase Akt. *J Biol Chem*, **273**, 11937-11943.
- Kohn, A.D., Summers, S.A., Birnbaum, M.J. and Roth, R.A. (1996) Expression of a constitutively active Akt Ser/Thr kinase in 3T3-L1 adipocytes stimulates glucose uptake and glucose transporter 4 translocation. *J Biol Chem*, **271**, 31372-31378.
- Koumanov, F., Jin, B., Yang, J. and Holman, G.D. (2005) Insulin signaling meets vesicle traffic of GLUT4 at a plasma-membrane-activated fusion step. *Cell Metab*, **2**, 179-189.
- Kuhne, M.R., Zhao, Z., Rowles, J., Lavan, B.E., Shen, S.H., Fischer, E.H. and Lienhard, G.E. (1994) Dephosphorylation of insulin receptor substrate 1 by the tyrosine phosphatase PTP2C. *J Biol Chem*, **269**, 15833-15837.
- Laage, R., Rohde, J., Brosig, B. and Langosch, D. (2000) A conserved membrane-spanning amino acid motif drives homomeric and supports heteromeric assembly of presynaptic SNARE proteins. *J Biol Chem*, **275**, 17481-17487.
- Lane, S.R. and Liu, Y. (1997) Characterization of the palmitoylation domain of SNAP-25. *J Neurochem*, **69**, 1864-1869.
- Larance, M., Ramm, G., Stockli, J., van Dam, E.M., Winata, S., Wasinger, V., Simpson, F., Graham, M., Junutula, J.R., Guilhaus, M. and James, D.E. (2005) Characterization of the role of the Rab GTPase-activating protein AS160 in insulin-regulated GLUT4 trafficking. *J Biol Chem*, **280**, 37803-37813.
- Latham, C.F., Lopez, J.A., Hu, S.H., Gee, C.L., Westbury, E., Blair, D.H., Armishaw, C.J., Alewood, P.F., Bryant, N.J., James, D.E. and Martin, J.L. (2006) Molecular dissection of the Munc18c/syntaxin4 interaction: implications for regulation of membrane trafficking. *Traffic*, **7**, 1408-1419.
- Leibiger, I.B. and Berggren, P.O. (2008) Insulin signaling in the pancreatic beta-cell. *Annu Rev Nutr*, **28**, 233-251.
- Leysens, N., Murray, J.C. and Bell, G.I. (1989) A KpnI polymorphism for the human insulin-responsive glucose transporter gene (GLUT4) on chromosome 17. *Nucleic Acids Res*, **17**, 3621.
- Li, D., Randhawa, V.K., Patel, N., Hayashi, M. and Klip, A. (2001) Hyperosmolarity reduces GLUT4 endocytosis and increases its exocytosis from a VAMP2-independent pool in l6 muscle cells. *J Biol Chem*, **276**, 22883-22891.
- Lin, R.C. and Scheller, R.H. (2000) Mechanisms of synaptic vesicle exocytosis. *Annu Rev Cell Dev Biol*, **16**, 19-49.
- Littleton, J.T., Chapman, E.R., Kreber, R., Garment, M.B., Carlson, S.D. and Ganetzky, B. (1998) Temperature-sensitive paralytic mutations demonstrate that synaptic exocytosis requires SNARE complex assembly and disassembly. *Neuron*, **21**, 401-413.
- Livingstone, C., James, D.E., Rice, J.E., Hanpeter, D. and Gould, G.W. (1996) Compartment ablation analysis of the insulin-responsive glucose transporter (GLUT4) in 3T3-L1 adipocytes. *Biochem J*, **315** (Pt 2), 487-495.
- Malhotra, V., Orci, L., Glick, B.S., Block, M.R. and Rothman, J.E. (1988) Role of an N-ethylmaleimide-sensitive transport component in promoting fusion of transport vesicles with cisternae of the Golgi stack. *Cell*, **54**, 221-227.

- Martin, L.B., Shewan, A., Millar, C.A., Gould, G.W. and James, D.E. (1998) Vesicle-associated membrane protein 2 plays a specific role in the insulin-dependent trafficking of the facilitative glucose transporter GLUT4 in 3T3-L1 adipocytes. *J Biol Chem*, **273**, 1444-1452.
- Martin, S., Tellam, J., Livingstone, C., Slot, J.W., Gould, G.W. and James, D.E. (1996) The glucose transporter (GLUT-4) and vesicle-associated membrane protein-2 (VAMP-2) are segregated from recycling endosomes in insulin-sensitive cells. *J Cell Biol*, **134**, 625-635.
- Marz, K.E., Lauer, J.M. and Hanson, P.I. (2003) Defining the SNARE complex binding surface of alpha-SNAP: implications for SNARE complex disassembly. *J Biol Chem*, **278**, 27000-27008.
- McNew, J.A., Parlati, F., Fukuda, R., Johnston, R.J., Paz, K., Paumet, F., Sollner, T.H. and Rothman, J.E. (2000) Compartmental specificity of cellular membrane fusion encoded in SNARE proteins. *Nature*, **407**, 153-159.
- Miinea, C.P., Sano, H., Kane, S., Sano, E., Fukuda, M., Peranen, J., Lane, W.S. and Lienhard, G.E. (2005) AS160, the Akt substrate regulating GLUT4 translocation, has a functional Rab GTPase-activating protein domain. *Biochem J*, **391**, 87-93.
- Min, J., Okada, S., Kanzaki, M., Elmendorf, J.S., Coker, K.J., Ceresa, B.P., Syu, L.J., Noda, Y., Saltiel, A.R. and Pessin, J.E. (1999) Synip: a novel insulin-regulated syntaxin 4-binding protein mediating GLUT4 translocation in adipocytes. *Mol Cell*, **3**, 751-760.
- Misura, K.M., Scheller, R.H. and Weis, W.I. (2000) Three-dimensional structure of the neuronal-Sec1-syntaxin 1a complex. *Nature*, **404**, 355-362.
- Mitra, P., Zheng, X. and Czech, M.P. (2004) RNAi-based analysis of CAP, Cbl, and CrkII function in the regulation of GLUT4 by insulin. *J Biol Chem*, **279**, 37431-37435.
- Mueckler, M. (1994) Facilitative glucose transporters. *Eur J Biochem*, **219**, 713-725.
- Nagamatsu, S., Kornhauser, J.M., Burant, C.F., Seino, S., Mayo, K.E. and Bell, G.I. (1992) Glucose transporter expression in brain. cDNA sequence of mouse GLUT3, the brain facilitative glucose transporter isoform, and identification of sites of expression by in situ hybridization. *J Biol Chem*, **267**, 467-472.
- Novick, P., Medkova, M., Dong, G., Hutagalung, A., Reinisch, K. and Grosshans, B. (2006) Interactions between Rabs, tethers, SNAREs and their regulators in exocytosis. *Biochem Soc Trans*, **34**, 683-686.
- Novick, P. and Schekman, R. (1979) Secretion and cell-surface growth are blocked in a temperature-sensitive mutant of *Saccharomyces cerevisiae*. *Proc Natl Acad Sci U S A*, **76**, 1858-1862.
- Novick, P. and Zerial, M. (1997) The diversity of Rab proteins in vesicle transport. *Curr Opin Cell Biol*, **9**, 496-504.
- Oh, E., Spurlin, B.A., Pessin, J.E. and Thurmond, D.C. (2005) Munc18c heterozygous knockout mice display increased susceptibility for severe glucose intolerance. *Diabetes*, **54**, 638-647.
- Oh, E. and Thurmond, D.C. (2006) The stimulus-induced tyrosine phosphorylation of Munc18c facilitates vesicle exocytosis. *J Biol Chem*, **281**, 17624-17634.
- Okada, S., Ohshima, K., Uehara, Y., Shimizu, H., Hashimoto, K., Yamada, M. and Mori, M. (2007) Synip phosphorylation is required for insulin-stimulated Glut4 translocation. *Biochem Biophys Res Commun*, **356**, 102-106.
- Okada, T., Kawano, Y., Sakakibara, T., Hazeki, O. and Ui, M. (1994) Essential role of phosphatidylinositol 3-kinase in insulin-induced glucose transport and antilipolysis in rat adipocytes. Studies with a selective inhibitor wortmannin. *J Biol Chem*, **269**, 3568-3573.
- Olson, A.L. and Pessin, J.E. (1996) Structure, function, and regulation of the mammalian facilitative glucose transporter gene family. *Annu Rev Nutr*, **16**, 235-256.

- Orita, S., Sasaki, T., Naito, A., Komuro, R., Ohtsuka, T., Maeda, M., Suzuki, H., Igarashi, H. and Takai, Y. (1995) Doc2: a novel brain protein having two repeated C2-like domains. *Biochem Biophys Res Commun*, **206**, 439-448.
- Oyler, G.A., Higgins, G.A., Hart, R.A., Battenberg, E., Billingsley, M., Bloom, F.E. and Wilson, M.C. (1989) The identification of a novel synaptosomal-associated protein, SNAP-25, differentially expressed by neuronal subpopulations. *J Cell Biol*, **109**, 3039-3052.
- Palade, G. (1975) Intracellular aspects of the process of protein synthesis. *Science*, **189**, 347-358.
- Paumet, F., Rahimian, V. and Rothman, J.E. (2004) The specificity of SNARE-dependent fusion is encoded in the SNARE motif. *Proc Natl Acad Sci U S A*, **101**, 3376-3380.
- Peng, R. and Gallwitz, D. (2002) Sly1 protein bound to Golgi syntaxin Sed5p allows assembly and contributes to specificity of SNARE fusion complexes. *J Cell Biol*, **157**, 645-655.
- Peng, R. and Gallwitz, D. (2004) Multiple SNARE interactions of an SM protein: Sed5p/Sly1p binding is dispensable for transport. *Embo J*, **23**, 3939-3949.
- Pevsner, J., Hsu, S.C., Braun, J.E., Calakos, N., Ting, A.E., Bennett, M.K. and Scheller, R.H. (1994a) Specificity and regulation of a synaptic vesicle docking complex. *Neuron*, **13**, 353-361.
- Pevsner, J., Hsu, S.C. and Scheller, R.H. (1994b) n-Sec1: a neural-specific syntaxin-binding protein. *Proc Natl Acad Sci U S A*, **91**, 1445-1449.
- Pfeffer, S. and Aivazian, D. (2004) Targeting Rab GTPases to distinct membrane compartments. *Nat Rev Mol Cell Biol*, **5**, 886-896.
- Pfeffer, S.R., Dirac-Svejstrup, A.B. and Soldati, T. (1995) Rab GDP dissociation inhibitor: putting rab GTPases in the right place. *J Biol Chem*, **270**, 17057-17059.
- Pobbati, A.V., Razeto, A., Boddener, M., Becker, S. and Fasshauer, D. (2004) Structural basis for the inhibitory role of tomosyn in exocytosis. *J Biol Chem*, **279**, 47192-47200.
- Poirier, M.A., Hao, J.C., Malkus, P.N., Chan, C., Moore, M.F., King, D.S. and Bennett, M.K. (1998a) Protease resistance of syntaxin.SNAP-25.VAMP complexes. Implications for assembly and structure. *J Biol Chem*, **273**, 11370-11377.
- Poirier, M.A., Xiao, W., Macosko, J.C., Chan, C., Shin, Y.K. and Bennett, M.K. (1998b) The synaptic SNARE complex is a parallel four-stranded helical bundle. *Nat Struct Biol*, **5**, 765-769.
- Ramm, G., Slot, J.W., James, D.E. and Stoorvogel, W. (2000) Insulin recruits GLUT4 from specialized VAMP2-carrying vesicles as well as from the dynamic endosomal/trans-Golgi network in rat adipocytes. *Mol Biol Cell*, **11**, 4079-4091.
- Ravichandran, V., Chawla, A. and Roche, P.A. (1996) Identification of a novel syntaxin- and synaptobrevin/VAMP-binding protein, SNAP-23, expressed in non-neuronal tissues. *J Biol Chem*, **271**, 13300-13303.
- Rea, S., Martin, L.B., McIntosh, S., Macaulay, S.L., Ramsdale, T., Baldini, G. and James, D.E. (1998) Syndet, an adipocyte target SNARE involved in the insulin-induced translocation of GLUT4 to the cell surface. *J Biol Chem*, **273**, 18784-18792.
- Ribon, V., Printen, J.A., Hoffman, N.G., Kay, B.K. and Saltiel, A.R. (1998) A novel, multifunctional c-Cbl binding protein in insulin receptor signaling in 3T3-L1 adipocytes. *Mol Cell Biol*, **18**, 872-879.
- Ribon, V. and Saltiel, A.R. (1997) Insulin stimulates tyrosine phosphorylation of the proto-oncogene product of c-Cbl in 3T3-L1 adipocytes. *Biochem J*, **324 (Pt 3)**, 839-845.
- Rickman, C., Hu, K., Carroll, J. and Davletov, B. (2005) Self-assembly of SNARE fusion proteins into star-shaped oligomers. *Biochem J*, **388**, 75-79.
- Rickman, C., Medine, C.N., Bergmann, A. and Duncan, R.R. (2007) Functionally and spatially distinct modes of munc18-syntaxin 1 interaction. *J Biol Chem*, **282**, 12097-12103.

- Rodkey, T.L., Liu, S., Barry, M. and McNew, J.A. (2008) Munc18a scaffolds SNARE assembly to promote membrane fusion. *Mol Biol Cell*, **19**, 5422-5434.
- Rodnick, K.J., Slot, J.W., Studelska, D.R., Hanpeter, D.E., Robinson, L.J., Geuze, H.J. and James, D.E. (1992) Immunocytochemical and biochemical studies of GLUT4 in rat skeletal muscle. *J Biol Chem*, **267**, 6278-6285.
- Saito, T., Okada, S., Yamada, E., Ohshima, K., Shimizu, H., Shimomura, K., Sato, M., Pessin, J.E. and Mori, M. (2003) Syntaxin 4 and Synip (syntaxin 4 interacting protein) regulate insulin secretion in the pancreatic beta HC-9 cell. *J Biol Chem*, **278**, 36718-36725.
- Sakaguchi, G., Orita, S., Maeda, M., Igarashi, H. and Takai, Y. (1995) Molecular cloning of an isoform of Doc2 having two C2-like domains. *Biochem Biophys Res Commun*, **217**, 1053-1061.
- Saltiel, A.R. (2001) New perspectives into the molecular pathogenesis and treatment of type 2 diabetes. *Cell*, **104**, 517-529.
- Salzberg, A., Cohen, N., Halachmi, N., Kimchie, Z. and Lev, Z. (1993) The Drosophila Ras2 and Rop gene pair: a dual homology with a yeast Ras-like gene and a suppressor of its loss-of-function phenotype. *Development*, **117**, 1309-1319.
- Sano, H., Eguez, L., Teruel, M.N., Fukuda, M., Chuang, T.D., Chavez, J.A., Lienhard, G.E. and McGraw, T.E. (2007) Rab10, a target of the AS160 Rab GAP, is required for insulin-stimulated translocation of GLUT4 to the adipocyte plasma membrane. *Cell Metab*, **5**, 293-303.
- Sano, H., Kane, S., Sano, E. and Lienhard, G.E. (2005) Synip phosphorylation does not regulate insulin-stimulated GLUT4 translocation. *Biochem Biophys Res Commun*, **332**, 880-884.
- Sano, H., Kane, S., Sano, E., Miinea, C.P., Asara, J.M., Lane, W.S., Garner, C.W. and Lienhard, G.E. (2003) Insulin-stimulated phosphorylation of a Rab GTPase-activating protein regulates GLUT4 translocation. *J Biol Chem*, **278**, 14599-14602.
- Satoh, S., Nishimura, H., Clark, A.E., Kozka, I.J., Vannucci, S.J., Simpson, I.A., Quon, M.J., Cushman, S.W. and Holman, G.D. (1993) Use of bismannose photolabel to elucidate insulin-regulated GLUT4 subcellular trafficking kinetics in rat adipose cells. Evidence that exocytosis is a critical site of hormone action. *J Biol Chem*, **268**, 17820-17829.
- Schmelzle, K., Kane, S., Gridley, S., Lienhard, G.E. and White, F.M. (2006) Temporal dynamics of tyrosine phosphorylation in insulin signaling. *Diabetes*, **55**, 2171-2179.
- Schuetz, C.G., Hatsuzawa, K., Margittai, M., Stein, A., Riedel, D., Kuster, P., Konig, M., Seidel, C. and Jahn, R. (2004) Determinants of liposome fusion mediated by synaptic SNARE proteins. *Proc Natl Acad Sci U S A*, **101**, 2858-2863.
- Scott, B.L., Van Komen, J.S., Irshad, H., Liu, S., Wilson, K.A. and McNew, J.A. (2004) Sec1p directly stimulates SNARE-mediated membrane fusion *in vitro*. *J Cell Biol*, **167**, 75-85.
- Shen, J., Tareste, D.C., Paumet, F., Rothman, J.E. and Melia, T.J. (2007) Selective activation of cognate SNAREpins by Sec1/Munc18 proteins. *Cell*, **128**, 183-195.
- Shisheva, A., Chinni, S.R. and DeMarco, C. (1999) General role of GDP dissociation inhibitor 2 in membrane release of Rab proteins: modulations of its functional interactions by *in vitro* and *in vivo* structural modifications. *Biochemistry*, **38**, 11711-11721.
- Sieber, J.J., Willig, K.I., Heintzmann, R., Hell, S.W. and Lang, T. (2006) The SNARE motif is essential for the formation of syntaxin clusters in the plasma membrane. *Biophys J*, **90**, 2843-2851.
- Slot, J.W., Geuze, H.J., Gigengack, S., James, D.E. and Lienhard, G.E. (1991a) Translocation of the glucose transporter GLUT4 in cardiac myocytes of the rat. *Proc Natl Acad Sci U S A*, **88**, 7815-7819.

- Slot, J.W., Geuze, H.J., Gigengack, S., Lienhard, G.E. and James, D.E. (1991b) Immunolocalization of the insulin regulatable glucose transporter in brown adipose tissue of the rat. *J Cell Biol*, **113**, 123-135.
- Sollner, T., Bennett, M.K., Whiteheart, S.W., Scheller, R.H. and Rothman, J.E. (1993a) A protein assembly-disassembly pathway *in vitro* that may correspond to sequential steps of synaptic vesicle docking, activation, and fusion. *Cell*, **75**, 409-418.
- Sollner, T., Whiteheart, S.W., Brunner, M., Erdjument-Bromage, H., Geromanos, S., Tempst, P. and Rothman, J.E. (1993b) SNAP receptors implicated in vesicle targeting and fusion. *Nature*, **362**, 318-324.
- Spurlin, B.A., Thomas, R.M., Nevins, A.K., Kim, H.J., Kim, Y.J., Noh, H.L., Shulman, G.I., Kim, J.K. and Thurmond, D.C. (2003) Insulin resistance in tetracycline-repressible Munc18c transgenic mice. *Diabetes*, **52**, 1910-1917.
- St-Denis, J.F., Cabaniols, J.P., Cushman, S.W. and Roche, P.A. (1999) SNAP-23 participates in SNARE complex assembly in rat adipose cells. *Biochem J*, **338** (Pt 3), 709-715.
- Steggmaier, M., Yang, B., Yoo, J.S., Huang, B., Shen, M., Yu, S., Luo, Y. and Scheller, R.H. (1998) Three novel proteins of the syntaxin/SNAP-25 family. *J Biol Chem*, **273**, 34171-34179.
- Stenbit, A.E., Tsao, T.S., Li, J., Burcelin, R., Geenen, D.L., Factor, S.M., Houseknecht, K., Katz, E.B. and Charron, M.J. (1997) GLUT4 heterozygous knockout mice develop muscle insulin resistance and diabetes. *Nat Med*, **3**, 1096-1101.
- Stern, M.P. (2000) Strategies and prospects for finding insulin resistance genes. *J Clin Invest*, **106**, 323-327.
- Struck, D.K., Hoekstra, D. and Pagano, R.E. (1981) Use of resonance energy transfer to monitor membrane fusion. *Biochemistry*, **20**, 4093-4099.
- Sutton, R.B., Fasshauer, D., Jahn, R. and Brunger, A.T. (1998) Crystal structure of a SNARE complex involved in synaptic exocytosis at 2.4 Å resolution. *Nature*, **395**, 347-353.
- Suzuki, K. and Kono, T. (1980) Evidence that insulin causes translocation of glucose transport activity to the plasma membrane from an intracellular storage site. *Proc Natl Acad Sci U S A*, **77**, 2542-2545.
- Tamori, Y., Kawanishi, M., Niki, T., Shinoda, H., Araki, S., Okazawa, H. and Kasuga, M. (1998) Inhibition of insulin-induced GLUT4 translocation by Munc18c through interaction with syntaxin4 in 3T3-L1 adipocytes. *J Biol Chem*, **273**, 19740-19746.
- Tellam, J.T., Macaulay, S.L., McIntosh, S., Hewish, D.R., Ward, C.W. and James, D.E. (1997) Characterization of Munc-18c and syntaxin-4 in 3T3-L1 adipocytes. Putative role in insulin-dependent movement of GLUT-4. *J Biol Chem*, **272**, 6179-6186.
- Tellam, J.T., McIntosh, S. and James, D.E. (1995) Molecular identification of two novel Munc-18 isoforms expressed in non-neuronal tissues. *J Biol Chem*, **270**, 5857-5863.
- Teng, F.Y., Wang, Y. and Tang, B.L. (2001) The syntaxins. *Genome Biol*, **2**, REVIEWS3012.
- ter Beest, M.B., Chapin, S.J., Avrahami, D. and Mostov, K.E. (2005) The role of syntaxins in the specificity of vesicle targeting in polarized epithelial cells. *Mol Biol Cell*, **16**, 5784-5792.
- TerBush, D.R., Maurice, T., Roth, D. and Novick, P. (1996) The Exocyst is a multiprotein complex required for exocytosis in *Saccharomyces cerevisiae*. *Embo J*, **15**, 6483-6494.
- TerBush, D.R. and Novick, P. (1995) Sec6, Sec8, and Sec15 are components of a multisubunit complex which localizes to small bud tips in *Saccharomyces cerevisiae*. *J Cell Biol*, **130**, 299-312.

- Thorens, B. (1992) Molecular and cellular physiology of GLUT-2, a high-Km facilitated diffusion glucose transporter. *Int Rev Cytol*, **137**, 209-238.
- Thurmond, D.C., Ceresa, B.P., Okada, S., Elmendorf, J.S., Coker, K. and Pessin, J.E. (1998) Regulation of insulin-stimulated GLUT4 translocation by Munc18c in 3T3L1 adipocytes. *J Biol Chem*, **273**, 33876-33883.
- Thurmond, D.C., Kanzaki, M., Khan, A.H. and Pessin, J.E. (2000) Munc18c function is required for insulin-stimulated plasma membrane fusion of GLUT4 and insulin-responsive amino peptidase storage vesicles. *Mol Cell Biol*, **20**, 379-388.
- Tian, W., Ma, C., Liu, Y. and Xu, T. (2008) An efficient co-expression and purification system for the complex of Stx4 and C-terminal domain of Synip. *Biochem Biophys Res Commun*, **371**, 366-370.
- Trimble, W.S., Cowan, D.M. and Scheller, R.H. (1988) VAMP-1: a synaptic vesicle-associated integral membrane protein. *Proc Natl Acad Sci U S A*, **85**, 4538-4542.
- Umahara, M., Okada, S., Yamada, E., Saito, T., Ohshima, K., Hashimoto, K., Yamada, M., Shimizu, H., Pessin, J.E. and Mori, M. (2008) Tyrosine phosphorylation of Munc18c regulates platelet-derived growth factor-stimulated glucose transporter 4 translocation in 3T3L1 adipocytes. *Endocrinology*, **149**, 40-49.
- van Vliet, C., Thomas, E.C., Merino-Trigo, A., Teasdale, R.D. and Gleeson, P.A. (2003) Intracellular sorting and transport of proteins. *Prog Biophys Mol Biol*, **83**, 1-45.
- Verhage, M., de Vries, K.J., Roshol, H., Burbach, J.P., Gispen, W.H. and Sudhof, T.C. (1997) DOC2 proteins in rat brain: complementary distribution and proposed function as vesicular adapter proteins in early stages of secretion. *Neuron*, **18**, 453-461.
- Verhage, M., Maia, A.S., Plomp, J.J., Brussaard, A.B., Heeroma, J.H., Vermeer, H., Toonen, R.F., Hammer, R.E., van den Berg, T.K., Missler, M., Geuze, H.J. and Sudhof, T.C. (2000) Synaptic assembly of the brain in the absence of neurotransmitter secretion. *Science*, **287**, 864-869.
- Villalba, M., Wenthe, S.R., Russell, D.S., Ahn, J.C., Reichelderfer, C.F. and Rosen, O.M. (1989) Another version of the human insulin receptor kinase domain: expression, purification, and characterization. *Proc Natl Acad Sci U S A*, **86**, 7848-7852.
- Vogel, K. and Roche, P.A. (1999) SNAP-23 and SNAP-25 are palmitoylated in vivo. *Biochem Biophys Res Commun*, **258**, 407-410.
- Volchuk, A., Sargeant, R., Sumitani, S., Liu, Z., He, L. and Klip, A. (1995) Cellubrevin is a resident protein of insulin-sensitive GLUT4 glucose transporter vesicles in 3T3-L1 adipocytes. *J Biol Chem*, **270**, 8233-8240.
- Volchuk, A., Wang, Q., Ewart, H.S., Liu, Z., He, L., Bennett, M.K. and Klip, A. (1996) Syntaxin 4 in 3T3-L1 adipocytes: regulation by insulin and participation in insulin-dependent glucose transport. *Mol Biol Cell*, **7**, 1075-1082.
- Vollenweider, P., Martin, S.S., Haruta, T., Morris, A.J., Nelson, J.G., Cormont, M., Le Marchand-Brustel, Y., Rose, D.W. and Olefsky, J.M. (1997) The small guanosine triphosphate-binding protein Rab4 is involved in insulin-induced GLUT4 translocation and actin filament rearrangement in 3T3-L1 cells. *Endocrinology*, **138**, 4941-4949.
- Watanabe, T., Smith, M.M., Robinson, F.W. and Kono, T. (1984) Insulin action on glucose transport in cardiac muscle. *J Biol Chem*, **259**, 13117-13122.
- Watson, R.T. and Pessin, J.E. (2001) Subcellular compartmentalization and trafficking of the insulin-responsive glucose transporter, GLUT4. *Exp Cell Res*, **271**, 75-83.
- Watson, R.T., Shigematsu, S., Chiang, S.H., Mora, S., Kanzaki, M., Macara, I.G., Saltiel, A.R. and Pessin, J.E. (2001) Lipid raft microdomain compartmentalization of TC10 is required for insulin signaling and GLUT4 translocation. *J Cell Biol*, **154**, 829-840.

- Weber, T., Zemelman, B.V., McNew, J.A., Westermann, B., Gmachl, M., Parlati, F., Sollner, T.H. and Rothman, J.E. (1998) SNAREpins: minimal machinery for membrane fusion. *Cell*, **92**, 759-772.
- Widberg, C.H., Bryant, N.J., Girotti, M., Rea, S. and James, D.E. (2003) Tomosyn interacts with the t-SNAREs syntaxin4 and SNAP23 and plays a role in insulin-stimulated GLUT4 translocation. *J Biol Chem*, **278**, 35093-35101.
- Williams, D. and Pessin, J.E. (2008) Mapping of R-SNARE function at distinct intracellular GLUT4 trafficking steps in adipocytes. *J Cell Biol*, **180**, 375-387.
- Wimmer, C., Hohl, T.M., Hughes, C.A., Muller, S.A., Sollner, T.H., Engel, A. and Rothman, J.E. (2001) Molecular mass, stoichiometry, and assembly of 20 S particles. *J Biol Chem*, **276**, 29091-29097.
- Wong, S.H., Xu, Y., Zhang, T. and Hong, W. (1998) Syntaxin 7, a novel syntaxin member associated with the early endosomal compartment. *J Biol Chem*, **273**, 375-380.
- Xu, Y., Zhang, F., Su, Z., McNew, J.A. and Shin, Y.K. (2005) Hemifusion in SNARE-mediated membrane fusion. *Nat Struct Mol Biol*, **12**, 417-422.
- Yamada, E., Okada, S., Saito, T., Ohshima, K., Sato, M., Tsuchiya, T., Uehara, Y., Shimizu, H. and Mori, M. (2005) Akt2 phosphorylates Synip to regulate docking and fusion of GLUT4-containing vesicles. *J Cell Biol*, **168**, 921-928.
- Yamaguchi, T., Dulubova, I., Min, S.W., Chen, X., Rizo, J. and Sudhof, T.C. (2002) Sly1 binds to Golgi and ER syntaxins via a conserved N-terminal peptide motif. *Dev Cell*, **2**, 295-305.
- Yang, B., Steegmaier, M., Gonzalez, L.C., Jr. and Scheller, R.H. (2000) nSec1 binds a closed conformation of syntaxin1A. *J Cell Biol*, **148**, 247-252.
- Yang, C., Coker, K.J., Kim, J.K., Mora, S., Thurmond, D.C., Davis, A.C., Yang, B., Williamson, R.A., Shulman, G.I. and Pessin, J.E. (2001) Syntaxin 4 heterozygous knockout mice develop muscle insulin resistance. *J Clin Invest*, **107**, 1311-1318.
- Yasukawa, T., Kanei-Ishii, C., Maekawa, T., Fujimoto, J., Yamamoto, T. and Ishii, S. (1995) Increase of solubility of foreign proteins in Escherichia coli by coproduction of the bacterial thioredoxin. *J Biol Chem*, **270**, 25328-25331.
- Yokoyama, S., Shirataki, H., Sakisaka, T. and Takai, Y. (1999) Three splicing variants of tomosyn and identification of their syntaxin-binding region. *Biochem Biophys Res Commun*, **256**, 218-222.
- Zeigerer, A., McBrayer, M.K. and McGraw, T.E. (2004) Insulin stimulation of GLUT4 exocytosis, but not its inhibition of endocytosis, is dependent on RabGAP AS160. *Mol Biol Cell*, **15**, 4406-4415.
- Zeng, Q., Subramaniam, V.N., Wong, S.H., Tang, B.L., Parton, R.G., Rea, S., James, D.E. and Hong, W. (1998) A novel synaptobrevin/VAMP homologous protein (VAMP5) is increased during *in vitro* myogenesis and present in the plasma membrane. *Mol Biol Cell*, **9**, 2423-2437.
- Zerial, M. and McBride, H. (2001) Rab proteins as membrane organizers. *Nat Rev Mol Cell Biol*, **2**, 107-117.
- Zhang, F., Chen, Y., Su, Z. and Shin, Y.K. (2004) SNARE assembly and membrane fusion, a kinetic analysis. *J Biol Chem*, **279**, 38668-38672.
- Zimmet, P., Alberti, K.G. and Shaw, J. (2001) Global and societal implications of the diabetes epidemic. *Nature*, **414**, 782-787.

Publications

- Aran, V., Brandie, F.M., Boyd, A.R., Kantidakis, T., Rideout, E.J., Kelly, S.M., Gould, G.W. and Bryant, N. (2009) Characterisation of two distinct binding modes between Syntaxin 4 and Munc18c. *Biochem J*.
- Brandie, F.M., Aran, V., Verma, A., McNew, J.A., Bryant, N.J. and Gould, G.W. (2008) Negative regulation of syntaxin4/SNAP-23/VAMP2-mediated membrane fusion by Munc18c *in vitro*. *PLoS ONE*, **3**, e4074.